



**HAL**  
open science

# Design optimization of CSO CWS Key processes and development of a modelling toolkit

Tamás Gábor Pálffy

► **To cite this version:**

Tamás Gábor Pálffy. Design optimization of CSO CWS Key processes and development of a modelling toolkit. Environmental Engineering. Université de Lyon, 2016. English. NNT : 2016LYSEI156 . tel-02605997v2

**HAL Id: tel-02605997**

**<https://theses.hal.science/tel-02605997v2>**

Submitted on 7 Feb 2019

**HAL** is a multi-disciplinary open access archive for the deposit and dissemination of scientific research documents, whether they are published or not. The documents may come from teaching and research institutions in France or abroad, or from public or private research centers.

L'archive ouverte pluridisciplinaire **HAL**, est destinée au dépôt et à la diffusion de documents scientifiques de niveau recherche, publiés ou non, émanant des établissements d'enseignement et de recherche français ou étrangers, des laboratoires publics ou privés.



**INSA**

N°d'ordre NNT : 2016LYSEI156



**THESE de DOCTORAT DE L'UNIVERSITE DE LYON**  
Réalisée au sein de l'Irstea Lyon

Ecole Doctorale N° 206  
« Chimie, Procédés, Environnement » de Lyon  
Spécialité Sciences de l'Environnement Industriel et Urbain

Soutenue publiquement le 20 Décembre 2016 par

**TAMÁS GÁBOR PÁLFY**

---

**OPTIMISATION DU DIMENSIONNEMENT  
DES FILTRES PLANTES POUR LE TRAITEMENT  
DES SURVERSES DE DÉVERSOIR D'ORAGE**

MECHANISMES CLEFS ET DEVELOPPEMENT D'UN OUTILS D'AIDE AU  
DIMENSIONNEMENT

---

**Design optimization of CSO CWS**  
Key processes and development of a modelling toolkit

© Tamás Gábor Pálffy

Soutenance devant le jury composé de

---

Pascal MOLLE	HDR, Ingénieur de recherche, MALY, IRSTEA Lyon	Co-directeur de thèse
Rémy GOURDON	Professeur, Laboratoire DEEP, INSA Lyon	Co-Directeur de thèse
Günter LANGERGRABER	Priv.-Doc., SIG, Univ. of Natural Resources and Life Sciences, Vienna, Austria	Rapporteur
Diederik ROUSSEAU	Professeur, Ghent University, Ghent, Belgium	Rapporteur
Stéphane TROESCH	Responsable Recherche et Développement, Epur Nature s.a.r.l	Examineur
Ulrich DITTMER	Arbeitsbereichsleiter, ISWA, University of Stuttgart, Germany	Examineur
Jaime NIVALA	Senior Research Engineer, Helmholtz Center Leipzig (UFZ)	Examineur
Sylvie GILLOT	Directrice de Recherche, MALY, IRSTEA Lyon	Président

---



**Département FEDORA – INSA Lyon - Ecoles Doctorales – Quinquennal 2016-2020**

<b>SIGLE</b>	<b>ECOLE DOCTORALE</b>	<b>NOM ET COORDONNEES DU RESPONSABLE</b>
<b>CHIMIE</b>	<b>CHIMIE DE LYON</b> <a href="http://www.edchimie-lyon.fr">http://www.edchimie-lyon.fr</a>  Sec : Renée EL MELHEM Bat Blaise Pascal 3 <sup>e</sup> etage secretariat@edchimie-lyon.fr Insa : R. GOURDON	<b>M. Stéphane DANIELE</b> Institut de Recherches sur la Catalyse et l'Environnement de Lyon IRCELYON-UMR 5256 Équipe CDFA 2 avenue Albert Einstein 69626 Villeurbanne cedex <a href="mailto:directeur@edchimie-lyon.fr">directeur@edchimie-lyon.fr</a>
<b>E.E.A.</b>	<b>ELECTRONIQUE, ELECTROTECHNIQUE, AUTOMATIQUE</b> <a href="http://edeea.ec-lyon.fr">http://edeea.ec-lyon.fr</a>  Sec : M.C. HAVGOUDOUKIAN <a href="mailto:Ecole-Doctorale.eea@ec-lyon.fr">Ecole-Doctorale.eea@ec-lyon.fr</a>	<b>M. Gérard SCORLETTI</b> Ecole Centrale de Lyon 36 avenue Guy de Collongue 69134 ECULLY Tél : 04.72.18 60.97 Fax : 04 78 43 37 17 <a href="mailto:Gerard.scorletti@ec-lyon.fr">Gerard.scorletti@ec-lyon.fr</a>
<b>E2M2</b>	<b>EVOLUTION, ECOSYSTEME, MICROBIOLOGIE, MODELISATION</b> <a href="http://e2m2.universite-lyon.fr">http://e2m2.universite-lyon.fr</a>  Sec : Sylvie ROBERJOT Bât Atrium - UCB Lyon 1 04.72.44.83.62 Insa : H. CHARLES <a href="mailto:secretariat.e2m2@univ-lyon1.fr">secretariat.e2m2@univ-lyon1.fr</a>	<b>M. Fabrice CORDEY</b> CNRS UMR 5276 Lab. de géologie de Lyon Université Claude Bernard Lyon 1 Bât Géode 2 rue Raphaël Dubois 69622 VILLEURBANNE Cédex Tél : 06.07.53.89.13 <a href="mailto:cordev@univ-lyon1.fr">cordev@univ-lyon1.fr</a>
<b>EDISS</b>	<b>INTERDISCIPLINAIRE SCIENCES-SANTE</b> <a href="http://www.ediss-lyon.fr">http://www.ediss-lyon.fr</a>  Sec : Sylvie ROBERJOT Bât Atrium - UCB Lyon 1 04.72.44.83.62 Insa : M. LAGARDE <a href="mailto:secretariat.ediss@univ-lyon1.fr">secretariat.ediss@univ-lyon1.fr</a>	<b>Mme Emmanuelle CANET-SOULAS</b> INSERM U1060, CarMeN lab, Univ. Lyon 1 Bâtiment IMBL 11 avenue Jean Capelle INSA de Lyon 696621 Villeurbanne Tél : 04.72.68.49.09 Fax :04 72 68 49 16 <a href="mailto:Emmanuelle.canet@univ-lyon1.fr">Emmanuelle.canet@univ-lyon1.fr</a>
<b>INFOMATHS</b>	<b>INFORMATIQUE ET MATHEMATIQUES</b> <a href="http://infomaths.univ-lyon1.fr">http://infomaths.univ-lyon1.fr</a>  Sec : Renée EL MELHEM Bat Blaise Pascal 3 <sup>e</sup> etage <a href="mailto:infomaths@univ-lyon1.fr">infomaths@univ-lyon1.fr</a>	<b>Mme Sylvie CALABRETTO</b> LIRIS – INSA de Lyon Bat Blaise Pascal 7 avenue Jean Capelle 69622 VILLEURBANNE Cedex Tél : 04.72. 43. 80. 46 Fax 04 72 43 16 87 <a href="mailto:Sylvie.calabretto@insa-lyon.fr">Sylvie.calabretto@insa-lyon.fr</a>
<b>Matériaux</b>	<b>MATERIAUX DE LYON</b> <a href="http://ed34.universite-lyon.fr">http://ed34.universite-lyon.fr</a>  Sec : M. LABOUNE PM : 71.70 –Fax : 87.12 Bat. Direction <a href="mailto:Ed.materiaux@insa-lyon.fr">Ed.materiaux@insa-lyon.fr</a>	<b>M. Jean-Yves BUFFIERE</b> INSA de Lyon MATEIS Bâtiment Saint Exupéry 7 avenue Jean Capelle 69621 VILLEURBANNE Cedex Tél : 04.72.43 71.70 Fax 04 72 43 85 28 <a href="mailto:jean-yves.buffiere@insa-lyon.fr">jean-yves.buffiere@insa-lyon.fr</a>
<b>MEGA</b>	<b>MECANIQUE,ENERGETIQUE,GENIE CIVIL,ACOUSTIQUE</b> <a href="http://mega.universite-lyon.fr">http://mega.universite-lyon.fr</a>  Sec : M. LABOUNE PM : 71.70 –Fax : 87.12 Bat. Direction <a href="mailto:mega@insa-lyon.fr">mega@insa-lyon.fr</a>	<b>M. Philippe BOISSE</b> INSA de Lyon Laboratoire LAMCOS Bâtiment Jacquard 25 bis avenue Jean Capelle 69621 VILLEURBANNE Cedex Tél : 04.72 .43.71.70 Fax : 04 72 43 72 37 <a href="mailto:Philippe.boisse@insa-lyon.fr">Philippe.boisse@insa-lyon.fr</a>
<b>ScSo</b>	<b>ScSo*</b> <a href="http://recherche.univ-lyon2.fr/scso/">http://recherche.univ-lyon2.fr/scso/</a>  Sec : Viviane POLSINELLI Brigitte DUBOIS Insa : J.Y. TOUSSAINT Tél : 04 78 69 72 76 <a href="mailto:viviane.polsinelli@univ-lyon2.fr">viviane.polsinelli@univ-lyon2.fr</a>	<b>M. Christian MONTES</b> Université Lyon 2 86 rue Pasteur 69365 LYON Cedex 07 <a href="mailto:Christian.montes@univ-lyon2.fr">Christian.montes@univ-lyon2.fr</a>

\*ScSo : Histoire, Géographie, Aménagement, Urbanisme, Archéologie, Science politique, Sociologie, Anthropologie





# **DESIGN OPTIMIZATION OF CSO CWS KEY PROCESSES AND DEVELOPMENT OF A MODELLING TOOLKIT**

by

**TAMÁS GÁBOR PÁLFY**

This thesis has been prepared in the frames of a CIFRE (industrial contracts for training through research) funded by the French Ministry of Higher Education and Research.

© 2016, Tamás Gábor Pálffy



***“Ma whero ma pango ka oti ai te mahi.”***

With red and black is the work complete.

Avec rouge et noir est du travail complet.

A munka pirossal és feketével készül.

Mit Rot und Schwarz ist die Arbeit fertig.



## Abstract

Constructed wetlands for combined sewer overflow treatment (CSO CWs) are vertical flow filters in France. They effectively remove pollutants and mitigate hydraulic peaks, which protects natural waters. They receive unsettled flows with stochastic return periods, volumes and concentrations, making design optimization difficult. In the presented work, design is targeted from two sides. First, the scientific basis is laid down for the design-support software Orage. The tool is model-based and as such, it considers the stochasticity of CSOs site-specifically. Its core model has been calibrated and then verified by a range of tests. Simulations fit to measured data from a full-scale CSO site (Marcy l'Etoile). The goodness of fit is evaluated visually and statistically. Model robustness has been confirmed by a sensitivity analysis (Morris method). After this, the iterative shell has been parameterized and tested (the software element doing automatic optimization). The design proposals of the tool have been found realistic. The other approach to target optimization has been a detailed field research at Marcy l'Etoile. The site at Marcy l'Etoile has been monitored for three years, using automatic samplers and online probes. The filling of the porous media at event start proves and explains short-circuiting behaviour. Adsorption capacities have been quantified for pozzolana and a sand and zeolite mixture. A temperature-dependent equation is calibrated to calculate nitrification rate. System efficiency is high for target pollutants (TSS, COD, NH<sub>4</sub>-N). Design, operational and environmental factors have been analysed to seek potential effects on removal performance and sludge accumulation. Additionally, PAHs and metals are indicated for a few selected events. The field results were essential to calibrate Orage and to see options for design improvements. The understanding of CSO CWs and the development of Orage was promoted also by simulating lab-scale columns using the process-based model package HYDRUS / CW2D.

**Keywords:** constructed wetland, combined sewer overflow, Orage, design-support modelling, dynamic design, CW2D, stormwater treatment





## Résumé

En France les filtres plantés à écoulement vertical sont utilisés pour le traitement des surverses de déversoir d'orage (CSO en anglais). Ils sont efficaces pour le traitement des polluants ainsi que pour assurer un rôle de tampon hydraulique permettant de protéger les milieux hydriques superficiels. Ils ont la particularité de recevoir des effluents bruts dont la fréquence, l'intensité, la durée et les concentrations sont stochastiques. En conséquence de quoi l'optimisation du dimensionnement est particulièrement délicate. Dans ce travail, le dimensionnement est abordé suivant deux approches. D'une part en définissant les processus clefs pour une optimisation du dimensionnement et, d'autre part, en construisant un modèle dynamique simplifié (Orage) permettant de prendre en compte, sur le long terme, le caractère stochastique des événements et les contraintes locales. Le cœur du modèle a été calibré et validé sur une large gamme d'évènements mesurés sur un site en taille réelle (site de Marcy l'Etoile). La qualité de la calibration a été validé aussi bien visuellement que statistiquement et la robustesse du modèle étudiée par une analyse de sensibilité (méthode de Morris). L'optimisation automatique du dimensionnement a nécessité la réalisation d'une boucle itérative également paramétrée et testée dans le cadre du site de Marcy l'Etoile et pour des cas théoriques. Les dimensionnements proposés ont été estimés réalistes. La définition des processus clefs du système de traitement, et le développement du modèle simplifié, a également été possible grâce à la simulation d'expérimentations sur colonnes par un modèle mécaniste (HYDRUS / CW2D). La paramétrisation des processus du modèle simplifié a été réalisée sur la base d'expérimentations détaillées sur le site de Marcy l'Etoile. Le site a été suivi pendant trois ans aussi bien par des prélèvements automatiques, des traçages, que des mesures en lignes (hydraulique, azote, teneur en eau). Parmi les processus calibrés, nous retiendrons i) l'importance du niveau de saturation de la base du filtre au début d'un événement vis-à-vis des court circuits hydrauliques, ii) la définition des capacités d'adsorption de l'azote ammoniacale de différents matériaux (pouzzolane, mélange de sable et de zéolite) et iii), la définition des cinétiques de nitrification suivant la température et quantité d'azote ammoniacal adsorbé. Si les performances de l'ouvrage sont hautes pour les paramètres majeurs (MES, DCO, N-NH<sub>4</sub>), l'impact du dimensionnement, de la gestion et des facteurs environnementaux sur les performances et l'accumulation de boue a été étudié. De plus, quelques suivis ont été réalisés sur les métaux et les HAP. Ces mesures ont permis non seulement de calibrer le logiciel Orage mais aussi de proposer des modifications pour l'amélioration du dimensionnement.

**Mots clés:** Filtres plantés, surverse de déversoir d'orage, Orage, outils d'aide au dimensionnement, dimensionnement dynamique, CW2D, traitement des eaux de temps de pluie



# Table of contents

<b>ABSTRACT</b> .....	<b>IX</b>
<b>RESUME</b> .....	<b>XI</b>
<b>TABLE OF CONTENTS</b> .....	<b>XIII</b>
<b>LIST OF TABLES</b> .....	<b>XV</b>
<b>LIST OF FIGURES</b> .....	<b>XVII</b>
<b>ABBREVIATIONS</b> .....	<b>XXI</b>
<b>RESUME ETENDU</b> .....	<b>XXIII</b>
<b>1 GENERAL INTRODUCTION</b> .....	<b>1</b>
<b>2 SYNTHESIS OF RELATED LITERATURE</b> .....	<b>5</b>
2.1 TERMINOLOGY .....	5
2.2 THE CHARACTERISTICS OF COMBINED SEWER OVERFLOW .....	6
2.3 LEGISLATIVE CONTEXT.....	9
2.4 VERTICAL FLOW CONSTRUCTED WETLANDS FOR CSO TREATMENT.....	9
2.4.1 <i>Structural and operational traits of CSO CWs</i> .....	9
2.4.2 <i>Removal processes and efficiency</i> .....	12
2.4.3 <i>Overview of CSO CW practice in Europe</i> .....	13
2.5 NUMERICAL MODELS OF CSO CWS.....	14
2.5.1 <i>General considerations</i> .....	14
2.5.2 <i>Finite element modelling of CSO CWS</i> .....	15
2.5.3 <i>Design-support modelling of CSO CWS</i> .....	15
<b>3 SETUP OF FIELD EXPERIMENTS AND MODEL BUILDING</b> .....	<b>17</b>
3.1 PIONEER FULL-SCALE APPLICATION OF THE FRENCH CSO CW: MARCY L'ETOILE .....	17
3.1.1 <i>Wetland layout (Meyer et al. 2013, EPUR 2012)</i> .....	17
3.1.2 <i>Operation</i> .....	18
3.2 MONITORING TARGETS AND EQUIPMENT .....	18
3.2.1 <i>Monitoring of flows and water level</i> .....	18
3.2.2 <i>Monitoring of pollutant concentrations</i> .....	20
3.2.3 <i>Targeting specific processes of filter functionality</i> .....	21
3.3 MODEL-BASED DESIGN TOOLKIT: ORAGE .....	24
3.3.1 <i>General purpose and structure</i> .....	24
3.3.2 <i>The toolkit frame</i> .....	26
3.3.3 <i>Iterative shell</i> .....	30
3.3.4 <i>Core model</i> .....	31
<b>4 USING PROCESS-BASED MODELS TO SIMULATE CSO CWS</b> .....	<b>34</b>
4.1 CONTEXT AND HIGHLIGHTS .....	35
FULL PAPER – SIMULATION OF CONSTRUCTED WETLANDS TREATING COMBINED SEWER OVERFLOW USING HYDRUS / CW2D .....	36
4.2 KEY FINDINGS OF THE PAPER IN THIS SECTION .....	50
<b>5 ORAGE: MODEL-BASED AND SITE-SPECIFIC OPTIMIZATION OF CSO CWS</b> .....	<b>52</b>
5.1 CONTEXT AND HIGHLIGHTS .....	53
MANUSCRIPT – DESIGN OPTIMIZATION OF CSO CONSTRUCTED WETLANDS: MODELLING FILTER PERFORMANCE .....	54
MANUSCRIPT – DESIGN OPTIMIZATION OF CSO CONSTRUCTED WETLANDS: MODEL-BASED OPTIMIZATION	73
5.2 KEY FINDINGS OF THE TWO MANUSCRIPTS IN THIS SECTION .....	88

<b>6</b>	<b>PERFORMANCE AND PROCESS DYNAMICS OF THE FIRST FULL-SCALE CSO CW IN FRANCE.....</b>	<b>90</b>
6.1	CONTEXT AND HIGHLIGHTS .....	91
	MANUSCRIPT – FILLING HYDRAULICS AND NITROGEN DYNAMICS IN FULL-SCALE CSO CWS .....	92
	MANUSCRIPT – EFFICIENCY OF A FULL-SCALE CSO CW FOR MAJOR- AND MICROPOLLUTANTS .....	107
6.2	KEY FINDINGS OF THE TWO MANUSCRIPTS IN THIS SECTION.....	124
<b>7</b>	<b>DESIGN PROPOSALS AND FINAL CONCLUSIONS .....</b>	<b>125</b>
7.1	PROPOSALS FOR DESIGN PRACTICE .....	125
7.1.1	<i>Minimizing hydraulic short-circuits.....</i>	<i>125</i>
7.1.2	<i>Inlet distribution .....</i>	<i>125</i>
7.1.3	<i>Cross-connection structure.....</i>	<i>126</i>
7.1.4	<i>Overflows.....</i>	<i>126</i>
7.2	CONCLUSIONS AND OUTLOOK .....	126
7.2.1	<i>Process-based modelling of CSO CWs .....</i>	<i>126</i>
7.2.2	<i>Orange in practice .....</i>	<i>127</i>
7.2.3	<i>Filter performance and compact filters .....</i>	<i>127</i>
7.2.4	<i>Second stage for denitrification.....</i>	<i>128</i>
<b>8</b>	<b>ACKNOWLEDGEMENTS .....</b>	<b>129</b>
<b>9</b>	<b>REFERENCES .....</b>	<b>131</b>
	<b>ANNEXES.....</b>	<b>139</b>
	ANNEX A: .....	141
	<i>Program overview .....</i>	<i>143</i>
	<i>Data pre-processing .....</i>	<i>144</i>
	<i>Iterative shell.....</i>	<i>145</i>
	<i>Core model .....</i>	<i>147</i>
	ANNEX B:.....	149
	ANNEX C:.....	161
	ANNEX D: .....	165
	<b>RESEARCH OUTPUT OF THE AUTHOR.....</b>	<b>171</b>

## List of Tables

TABLE 1: TYPICAL RANGES OF CSO AND SSO CONCENTRATIONS. VALUES ARE AVERAGE EMCs OF MULTIPLE EVENTS AND SITES. RANGES REPRESENT THE SMALLEST AND LARGEST VALUE FOUND IN THE LISTED LITERATURE: A) SMULLEN ET AL. (1999); B) KADLEC AND WALLACE (2009); C) FOURNEL (2012); D) SZTRUHAR ET AL. (2002); E) PASSERAT ET AL. (2011); F) ZGHEIB ET AL. (2012) G) SCHULZ ET AL (1994); H) GASPERI ET AL. (2012). *:TKN. ....	8
TABLE 2: REMOVAL RATES OF DIFFERENT TECHNOLOGIES FOR CSO AND SSO TREATMENT. VALUES ARE BASED ON MEASURED EMCs OR THE EQUIVALENT MASS REMOVAL BY EVENT. SOURCES ARE A: EPA 1999A; B: EPA 1999B; C: KADLEC AND WALLACE (2009); D: EPA 1999C; E: WALDHOF 2008; F: PINNEKAMP 2013; G: FRECHEN 2013.....	13
TABLE 3: INFLOW CONCENTRATIONS AT MARCY L'ETOILE. THE VALUES ARE COMPARED TO CSO CONCENTRATIONS FROM THE FOLLOWING LITERATURE: C) FOURNEL (2012); D) SZTRUHÁR ET AL. (2002); E) PASSERAT ET AL. (2011); G) SCHULZ ET AL (1994); H) GASPERI ET AL (2012). VALUES ARE AVERAGE EMCs OF MULTIPLE EVENTS AND SITES. RANGES REPRESENT THE SMALLEST AND LARGEST VALUE FOUND IN THE LISTED LITERATURE. ....	20
TABLE 4: MEAN VOLUME COVERED BY A COMPOSITE SAMPLE, BY EVENT. THE NUMBER OF SAMPLES IS GIVEN BY FILTER SIDE WHERE THE OUTFLOW HAS BEEN SAMPLED ACCORDINGLY, E.G. 9+9 (SAND AND ZEOLITE FILTER AND POZZOLANA FILTER, RESPECTIVELY).....	21
TABLE 5: CLIMATE REGIONS IN ORAGE .....	26
TABLE 6: IMPERVIOUSNESS CATEGORY SELECTION IN ORAGE.....	27
TABLE 7: USER INPUT IN ORAGE.....	27
TABLE 8: QUALITY OF FLOWS IN THE INTERNAL TABLES OF ORAGE. AS CONCENTRATIONS ARE VARIABLE, HIGH CONCENTRATIONS WERE SELECTED FROM THE LITERATURE TO STAY ON THE SAFE SIDE WITH THE APPLICABILITY TEST: H: HENZE AND COMEAU (2008), A: SMULLEN ET AL. (1999); F: ZGHEIB ET AL. (2012).....	28
TABLE 9: CHARACTERISTICS OF THE SINGLE EVENTS (1–4) AND THE EVENT SERIES (5) USED FOR VALIDATION	41
TABLE 10: SETTINGS OF THE CALIBRATION PROCESS TARGETING TO REMOVE THE INITIAL COD PEAK AND TO REACH AN OVERALL GOOD FIT. ....	43
TABLE 11: PARAMETERS OF HYDRUS/CW2D ADJUSTED FOR SIMULATION OF CSO CWS COMPARED TO THE ORIGINAL VALUES IN MEYER (2011) AND THE EFFECT AND RATIONALIZATION OF THE ADJUSTMENTS. ....	44
TABLE 12: NUMERICAL EVALUATION OF THE GOODNESS OF FIT. <b>GREEN: GOOD FIT</b> , OCHRE: MODERATE FIT, <i>PINK: WEAK FIT</i> . THE OUTLINES MARK THE CRUCIAL VALUE ON WHICH THE CATEGORIZATION WAS BASED. ....	48
TABLE 13: SIMULATION SERIES CONSISTING OF FOUR CONSECUTIVE LOADS (EVENT #16-19) AND EVENT #14..	63
TABLE 14: RANGES FOR GOODNESS OF FIT-BASED SENSITIVITY ANALYSIS. ....	65
TABLE 15: SHORT-CIRCUITING TIMES AS THE FUNCTION OF FILTER AREA AT AN OUTFLOW RATE FIXED TO 0.108 m <sup>3</sup> /m <sup>2</sup> /h.....	65
TABLE 16: ANALYSIS OF THE MODEL ACCURACY FOR THE CLOSED EVENT SERIES.....	67
TABLE 17: PREDICTED PERFORMANCE AS THE FUNCTION OF FILTER MEDIA. THE FILTER DESIGN WAS OTHERWISE IDENTICAL TO THE FULL-SCALE CSO CW AT MARCY L'ETOILE. ....	84
TABLE 18: PROPOSED DESIGNS IN FUNCTION OF EFFLUENT LIMITS (FILTER DEPTH: 0.6 METRES). INPUT: 1.5 YEARS MEASURED DATA FROM THE CSO CW AT MARCY-L'ETOILE AND HAD HIGH NH <sub>4</sub> -N CONCENTRATIONS (MEAN AROUND 15 MG/L). S: ADSORPTION CALIBRATED TO A SAND 0-4 MM, D <sub>10</sub> : 0.43 MM; D <sub>60</sub> : 1.89 MM BASED ON THE WORK OF FOURNEL (2012).....	85
TABLE 19: GENERAL CHARACTERISTICS OF THE CSO CW AT MARCY L'ETOILE .....	95
TABLE 20: PARAMETERS AT THE MULTIVARIATE INTERPOLATION OF VOLUMETRIC WATER CONTENT FOR INVERSE DISTANCE WEIGHTING.....	96
TABLE 21: OVERLOAD EVENTS AT MARCY L'ETOILE .....	98
TABLE 22: INTER-EVENTS OF THE THREE NITRIFICATION RATE CAMPAIGNS (REST PERIODS BEFORE THE LOADS). ....	99
TABLE 23: HYDRAULIC LOADS BY FILTER SIDE AT THE CSO CW AT MARCY L'ETOILE. S: SIDE WITH SAND AND ZEOLITE; P: SIDE WITH POZZOLANA.....	112

TABLE 24: INLET METAL CONCENTRATIONS AT MARCY L'ETOILE. METAL CONCENTRATIONS UNDER THE QUANTIFICATION LIMIT: "-".	117
TABLE 25: OVERALL REMOVAL EFFICIENCIES FOR METALS.	117
TABLE 26: OUTLET PAH CONCENTRATIONS AT MARCY L'ETOILE.	117
TABLE 27: PRIORITY SUBSTANCES AND EQS VALUES IN THE EUROPEAN WATER FRAMEWORK DIRECTIVE...	118
TABLE 28: FRENCH REGULATION FOR 3 PAHS AND 6 METALS CONCERNING SLUDGE RECOVERY COMPARED TO THE VALUES FOUND AT MARCY L'ETOILE.	122

## List of Figures

FIG. 1: KNOWLEDGE BASE AND KEY STEPS TOWARDS THE OBJECTIVES (BLUE BOXES). ARROWS WITH TWO HEADS INDICATE WHERE THE PROCESS NEEDED FLEXIBILITY AND ALLOW TWO-DIRECTIONAL EXCHANGE BETWEEN STEPS. ....	4
FIG. 2: CLASSIFICATION OF CONSTRUCTED WETLANDS FOR STORMWATER TREATMENT. *: FOR THE ITALIAN SYSTEM SEE MEYER ET AL. 2013; **: FOR THE GERMAN RSFs SEE UHL AND DITTMER 2005.....	5
FIG. 3: ALTERNATION OF INTRA-EVENT (BLUE) AND INTER-EVENT (OCHRE) PERIODS. THE PERIODS ARE WELL DISCERNIBLE BASED ON THE STAGE IN THE CSO CW (BLUE SERIES). ....	10
FIG. 4: THE FIVE STATES OF A CSO CW. THE CLASSICAL ALTERNATION OF INTRA- AND INTER-EVENT PERIODS CAN BE BROKEN DOWN FURTHER AS SHOWN BY STAGES 1A-1B AND 2-4, RESPECTIVELY. ....	11
FIG. 5: THE GERMAN, FRENCH AND ITALIAN WETLAND SYSTEMS FOR CSO TREATMENT. PANEL A: OVERVIEW OF THE TREATMENT CHAIN. PANEL B: CROSS-SECTION OF THE VF CW IN THE TREATMENT CHAIN.....	14
FIG. 6: HYDRAULICS IN RSF_SIM: TIS MODEL (BASED ON MEYER AND DITTMER, 2015). THE OUTFLOW STRUCTURE COMES WITH AN ORIFICE WHICH THROTTLES THE FLOW. THIS FEATURE IS REPRESENTED BY A CONSTANT IN THE MODEL, ENABLING A HIGH LEVEL OF SIMPLIFICATION IN THE HYDRAULICS, I.E. TO MODEL THE SYSTEM ACCURATELY AS TIS. ....	16
FIG. 7: THE ROUTING OF FLOWS TOWARDS, INTO AND FROM THE FILTER AT MARCY L'ETOILE. POINT [1] MARKS THE CSO STRUCTURE AND THE GREEN RECTANGLES THE TWO FILTERS WITH THE WALL BETWEEN THEM. ....	17
FIG. 8: CROSS-SECTION OF THE FILTER AT MARCY L'ETOILE. UNITS ARE GIVEN IN METRES.....	18
FIG. 9: ANNUAL HYDRAULIC LOADS ON THE FILTER SIDES. F1: SAND (0.48 M) WITH ZEOLITE (0.12 M); F2: 0.6 M POZZOLANA. ....	19
FIG. 10: MEASURED CORRELATION OF PRESSURE HEAD – ORIFICE FLOW. PRESSURE PROBES WERE INSTALLED IN THE OUTFLOW STRUCTURE.....	20
FIG. 11: CORRELATION OF PROBE MEASUREMENTS AND LABORATORY ANALYSIS. THE CORRELATIONS WERE SET BY EVENT, BASED ON THE COMPOSITE SAMPLES TAKEN FROM THE OUTFLOW AND THREE GRAB SAMPLES THICKENED BY $\text{NH}_4\text{Cl}$ AND $\text{Ca}(\text{NO}_3)_2$ . ....	22
FIG. 12: TRIPLE-WIRE TDR PROBE AND IN-HOUSE CALIBRATION (PANEL A AND B, RESPECTIVELY). NOTE THE TWO DIFFERENT FILTER MATERIALS ON PANEL B: POZZOLANA (LEFT) AND SAND AND ZEOLITE MIXTURE IN A RATIO OF 4:1 (RIGHT).....	23
FIG. 13: CORRELATION OF THE DIELECTRIC CONSTANT ( $\epsilon$ ) AND SOIL WATER CONTENT ( $\theta$ ) FOR THE FILTER MATERIALS. ....	24
FIG. 14: THE STRUCTURE OF ORAGE. THE TOOLKIT FRAME SERVES FOR INPUT AND OUTPUT (USER INTERFACE) AS WELL AS DATA PRE-PROCESSING AND ANALYSIS AND RELIES ON THE ITERATIVE SHELL TO CALL THE CORE MODEL REPETITIVELY UNTIL OPTIMIZATION IS REACHED.....	25
FIG. 15: DAILY DRY WEATHER FLOW PATTERN FOR THE DECISION SUPPORT FUNCTION (2000 PE). ....	28
FIG. 16: AN EXAMPLE OF ADJUSTED CSO FLOWS AND CONCENTRATIONS AFTER DATA PRE-PROCESSING (APPLICABILITY TEST ONLY). NOTE THAT CONCENTRATIONS GOT DILUTED AT ALL SEVEN OVERFLOWS BUT ALSO IN CASES WHEN THE PRECIPITATION WAS TOO LITTLE TO GENERATE CSO. ....	29
FIG. 17: THE HYDRAULIC MODEL IN ORAGE. RED ARROWS SHOW POSSIBLE FLOW DIRECTIONS. THE NUMBERED TANKS ARE: 1: COMMON BASIN; 2: REACTORS REPRESENTING THE VOLUME FROM THE FILTER TO THE WALL; 3: PROCESS LAYERS; 4: PERMANENTLY SATURATED DRAINAGE LAYER. P: PRIMARY FILTER SIDE; S: SECONDARY FILTER SIDE. THE TANKS OF THE SECONDARY SIDE HAVE ZERO VOLUMES AND NO FLOWS IF MODELLING SINGLE-SIDED FILTERS (FOR SSO). IF 2P AND 2S ARE FULL, THE INFLOW IS DISTRIBUTED BETWEEN TANKS 1 AND THE EMPTY SPACE IN 2P AND 2S WHICH IS LEFT BY THE CONSTANT OUTFLOW AT EVERY TIME STEP. ....	32
FIG. 18: THREE EXAMPLES OF POLLUTANT REMOVAL CORRELATIONS FOR <i>COD</i> (UNCALIBRATED). CORRELATIONS ARE DEPENDENT FROM THE PREVIOUS INTER-EVENT PERIOD AND ARE DEFINED BY FIVE PARAMETERS: $K$ : BACKGROUND CONCENTRATION, $H_1$ : SLOPE OF THE FIRST STAGE, $H_2$ : SLOPE OF THE SECOND STAGE, $C1$ AND $C2$ : THRESHOLD CONCENTRATIONS BETWEEN $K$ , $H_1$ AND $H_2$ . ....	32



FIG. 19: SECTION DRAFT OF THE PHYSICAL COLUMNS (BASED ON MEYER, 2011). $D = 19$ CM. THE LEFT SIDE TO THE SYMMETRY AXIS IS SWAPPED TO THE LEFT HALF OF THE FINITE ELEMENT MESH USED IN THE SIMULATIONS. ....	40
FIG. 20: BIOMASS (BM) DEVELOPMENT AND VERTICAL DISTRIBUTION AT EQUILIBRIUM. SIMULATED CONCENTRATIONS DURING 160 DAYS OF INOCULATION (LEFT) AND COMPARISON OF THE FINAL DISTRIBUTION AT DAY 160 WITH DNA, RNA AND ATP MEASUREMENTS (WOŹNIAK 2007) ALONG THE VERTICAL PROFILE OF THE FILTER (RIGHT). ....	45
FIG. 21: CALIBRATION RESULTS ON COD AND $\text{NH}_4\text{-N}$ . THE RED DOTTED LINE MARKS THE OUTFLOW RATE GETTING LOWER THAN THE FLOW LIMITATION. ....	45
FIG. 22: VALIDATION RESULTS FROM DOMAINS WITH DIFFERENT FLOW LIMITATIONS. TOP: $0.01 \text{ L/s/m}^2$ , BOTTOM: $0.03 \text{ L/s/m}^2$ , LEFT: COD AND COD FRACTIONS, RIGHT: $\text{NH}_4\text{N}$ . ....	46
FIG. 23: MODEL VALIDATION WITH A SERIES OF FIVE CONSECUTIVE LOADINGS, ES32-36. SIMULATION IS CONTINUOUS BUT MEASUREMENTS WERE MADE DURING THE INTRA-EVENT PERIODS EXCLUSIVELY. ....	47
FIG. 24: COMPARISON OF MEASURED AND SIMULATED FLUSH OF $\text{NO}_3\text{-N}$ OF FIVE CONSECUTIVE LOADINGS, ES32-36. ....	47
FIG. 25: SCHEMATIC CROSS-SECTION AND FLOWS IN CSO CWS. ....	57
FIG. 26: THE SEVEN TANKS AND POSSIBLE VOLUMETRIC EXCHANGES IN THE CORE MODEL. ....	58
FIG. 27: RESULTS IN RSF_SIM: MASS REMOVAL PERCENTAGE ERROR CAN BE DECREASED IF CONSIDERING THE LENGTH OF INTER-EVENT PERIODS. TRANSLUCENT SYMBOLS: ERROR IN PREDICTIONS BEFORE; OPAQUE SYMBOLS: AFTER. FIGURE BASED ON MEYER AND DITTMER (2015). ....	60
FIG. 28: BROKEN-STICK ISOTHERM AND ITS PARAMETERS, COMPARED TO A FREUNDLICH ISOTHERM. $A_1$ : SLOPE BELOW THRESHOLD DISSOLVED PHASE CONCENTRATION $C_1$ ; $A_2$ : DECREASED SLOPE ABOVE $C_1$ . ....	60
FIG. 29: SHORT-CIRCUITING CONDITIONS WITH INCREASING (LEFT) AND DECREASING (RIGHT) INFILTRATION AREA. A POTENTIAL VALUE FOR $H_E$ IS SHOWN. ....	61
FIG. 30: COMPARISON CHART OF MEASURED AND SIMULATED HYDRAULICS OF THE SINGLE LOAD (EVENT #14). WATER LEVEL IS GIVEN BY FILTER SIDE, OUTFLOWS ARE LUMPED. ....	66
FIG. 31: MEASURED AND SIMULATED COD (LEFT) AND $\text{NH}_4\text{-N}$ (RIGHT) CONCENTRATIONS OF THE SINGLE LOAD (EVENT #14). ....	66
FIG. 32: MEASURED AND SIMULATED COD (LEFT) AND $\text{NH}_4\text{-N}$ (RIGHT) CONCENTRATIONS OF THE EVENT SERIES (EXCLUDING EVENT #14). INTRA-EVENT PERIODS ARE CROPPED FOR BETTER VISIBILITY. THE SHORT-CIRCUITING CONSTANT (PARAMETER $K_2$ ) WAS SELECTED DELIBERATELY LOW TO GENERATE HIGH $\text{NH}_4\text{N}$ SPIKES AND SEE FUNCTIONALITY. ....	68
FIG. 33: SENSITIVITY ANALYSIS RESULTS FOR COD. REMOVAL PERFORMANCE PARAMETERS $K$ , $Nu_1$ , $C_2$ AND $Nu_2$ HAD THE MOST EFFECT. THE MODEL WAS ROBUST AGAINST ALL OTHER PARAMETERS ESPECIALLY IN THE CASE OF 6/24H PEAK_MA_CC. ....	69
FIG. 34: SENSITIVITY ANALYSIS RESULTS FOR $\text{NH}_4\text{N}$ : EXTREME SHORT-CIRCUITING DURATIONS IN OVERSCALED FILTERS. PARAMETERS IMPACTING THE LONGEVITY OF SHORT-CIRCUITING ( $H_E$ , $F_{LIMIT\_BASE}$ AND $A_{TOT}$ ) HAD THE MOST SIGNIFICANT EFFECT AND ADSORPTION CAPACITIES WERE LESS IMPORTANT. ....	70
FIG. 35: SENSITIVITY ANALYSIS RESULTS FOR $\text{NH}_4\text{N}$ : HYDRAULICALLY OPTIMIZED RANGE FOR FILTER AREAS. ADSORPTION CAPACITY ( $A_1$ ) AND THE AVAILABLE MASS OF THE MATERIAL ( $D_{FILT}$ ) WERE FOUND TO BE THE MOST SIGNIFICANT. ....	71
FIG. 36: WATER LEVELS IN A FULL-SCALE CSO CW. FILTER OPERATION CAN BE CHARACTERIZED BY THE STOCHASTIC ALTERNATION OF INTRA-EVENT (LOADED; BLUE) AND INTER-EVENT (UNLOADED, OCHRE) PERIODS. ....	75
FIG. 37: ILLUSTRATION OF THE OPTIMIZATION APPROACH FOR $\text{NH}_4\text{N}$ . THE FICTIVE STEPS WERE THE FOLLOWING: 1) CALLING THE CORE ON THREE DIFFERENT MATERIALS FROM THE DATABASE, UNTIL $P(A_{MAX})$ GETS BELOW THE TARGET RANGE (RIGHT); 2) A SIMULATION SHOWING THAT $P(A_{MIN})$ WOULD BE UNSATISFYING (TOP LEFT); 3) THE FIRST LINEAR INTERPOLATION IDENTIFIES $A_1$ AS A POSSIBLE SOLUTION BUT CALLING THE CORE WITH $A_1$ SHOWS THAT $P(A_1)$ IS ABOVE THE TOLERANCE RANGE; SO, $A_1$ BECAME THE NEW $A_{MIN}$ ; 4) THE LINEAR INTERPOLATION AND SIMULATION IS REPEATED TWO MORE TIMES ( $A_2$ AND $A_3$ ) – $P(A_3)$ IS FOUND TO BE IN THE TARGET RANGE AROUND THE LEGISLATIVE THRESHOLD SO IT IS ACCEPTED AS SOLUTION. ....	78
FIG. 38: HYDRAULIC OPTIMIZATION CUTS SMALL FILTER AREAS (ILLUSTRATION). OTHERWISE, EVEN WITH NEGLIGIBLE REMOVAL, SUCH AREAS MIGHT HAVE OFFERED AN UNWANTED SOLUTION AT ALLOWING	

LEGISLATIVE THRESHOLDS ON NH <sub>4</sub> -N CONCENTRATIONS. THE PARAMETER <i>H_MAX</i> PLAYS A KEY ROLE IN DETERMINING <i>A_MIN</i> AND THEREFORE ITS VALUE HAD TO BE FIXED. IT WAS DONE BASED ON N=20 SIMULATION SERIES (FULL <i>PEAK_MA_CC</i> CURVES).....	80
FIG. 39: EVOLUTION OF <i>PEAK_MA_CC</i> (BLACK LINE) IN THE FUNCTION OF FILTER AREA. EACH POINT REPRESENTS ONE SIMULATION. SIMULATIONS CAN BE SEPARATED INTO FOUR DISTINCTIVE REGIONS: 1) SMALL FILTER AREAS WITH NO TREATMENT AND POTENTIAL RISK OF CLOGGING; 2) IDEAL OPTIMIZATION RANGE; 3) RANGE DOMINATED BY A CONCENTRATION INCREASE DUE TO EXCESSIVE SHORT-CIRCUITING; 4) RANGE OF EXCESSIVE DILUTION BY PERMANENT WATER IN THE FILTER. NOTE HOW ALSO THE ANNUAL HYDRAULIC LOAD (CONTINUOUS GREEN LINE) AND THE SHARE OF SHORT-CIRCUITING TIME STEPS (ORANGE DASHED LINE) CHANGES WITH THE AREA.....	81
FIG. 40: <i>PEAK_MA_CC</i> AS THE FUNCTION OF SHORT-CIRCUITING (N=20 SIMULATION SERIES).....	82
FIG. 41: HYDRAULIC LOAD AS THE FUNCTION OF SHORT-CIRCUITING (N=20 SIMULATION SERIES). THE FLOW PATTERN WAS TYPICAL SSO WITH LOADS FROM THE INTERNAL INFLOW SERIES OF ORAGE. WHISKERS MARK 5 <sup>TH</sup> AND 95 <sup>TH</sup> PERCENTILE.....	82
FIG. 42: HYDRAULIC LOAD AT <i>A_MIN</i> (N=20 SIMULATION SERIES). THE FLOW PATTERN WAS TYPICAL SSO WITH LOADS FROM THE INTERNAL INFLOW SERIES OF ORAGE. WHISKERS MARK 5 <sup>TH</sup> AND 95 <sup>TH</sup> PERCENTILE. ....	83
FIG. 43: VERIFICATION OF THE ITERATIVE SHELL OF ORAGE. EACH ARROW BASE/HEAD REPRESENTS ONE OF THE THIRTY-SIX SIMULATIONS. SERIES 1: FIRST OPTIMIZATION FOR NH <sub>4</sub> -N REMOVAL; SERIES 2: OPTIMIZATION FOR COD REMOVAL; SERIES 3: FINAL OPTIMIZATION FOR NH <sub>4</sub> -N REMOVAL. AREAS: A1=500 M <sup>2</sup> ( <i>A_MAX</i> ); A2=472 M <sup>2</sup> (SOLUTION OF SERIES 1); A3=461 M <sup>2</sup> (SOLUTION OF SERIES 2); B=187 M <sup>2</sup> ( <i>A_MIN</i> ); C=315 M <sup>2</sup> (FINAL SOLUTION OF SERIES 3).....	84
FIG. 44: CSO CWS IN FRANCE COME WITH TWIN FILTER SIDES AND PERMANENTLY SATURATED DRAINAGE LAYER.....	94
FIG. 45: CROSS-SECTION AND INTERNAL STRUCTURE OF THE CSO CW AT MARCY L'ETOILE, FRANCE.....	95
FIG. 46: POSITION OF THE EIGHTEEN TDR PROBES ALONG THE LONGITUDINAL FILTER SECTION (CELLS ARE 5 CM VERTICALLY AND 25 CM HORIZONTALLY). FRAMED CELLS REPRESENT THE PROBES. SQUARES FILLED WITH 'x' REPRESENT EXTRA POINTS WHERE THE WATER CONTENT WAS KNOWN TO BE SATURATED DURING LOADING (DRAINAGE LAYER AND INLET POINT AT THE TOP). THE BROWN STRIP MARKS THE COMPOST AND SLUDGE COVER. ....	96
FIG. 47: NORMALIZATION OF SHORT-CIRCUITING PEAKS. A BREAKTHROUGH WOULD BE COMPLETE IF THE EFFLUENT CONCENTRATION WAS EQUAL TO THE INFLOW CONCENTRATION. BY THE TIME THE SATURATION IS COMPLETE (FILTER SURFACE AT 100 CM LEVEL) THE PEAK WAS ALWAYS OVER JUST LIKE ON THIS EXAMPLE REPRESENTING THE STRONGEST OBSERVED PEAK.....	97
FIG. 48: THE SHORT-CIRCUITING PHENOMENA OF CSO CWS. WHEN LOADS BEGIN, THE FLOW IS LIMITED CLOSE TO THE INLET POINT (PANELS B TO D; TOP LEFT). WITH INCREASING WATER LEVEL, MORE FILTER MEDIA GETS WATER-CONTACTED (PANELS E-F) UNTIL SATURATION IS REACHED (PANEL G). THIS LATEST ENSURES MAXIMIZED PERFORMANCE AND IS CONSIDERED AS NORMAL OPERATION (NEAR PLUG-FLOW).....	100
FIG. 49: TRACER CONCENTRATION (URANINE) AT THE OUTLET. THE ARROWS NEAR THE ORIGIN MARK TRACER INJECTIONS. THE BOXES AT THE PEAKS WRITE THE DELAY [IN HOURS] SINCE THE CORRESPONDING INJECTION. THE WATER LEVEL REACHED THE FILTER SURFACE AT 100 CM. ....	100
FIG. 50: THE STRENGTH OF NH <sub>4</sub> -N BREAKTHROUGH DUE TO SHORT-CIRCUITING IN THE FUNCTION OF PRESSURE HEAD AT COMMENCING LOAD. THE BLUE SERIES REPRESENT THE THREE PERIOD MOVING AVERAGE. BASED ON THE VISUAL INTERPRETATION OF THE TREND, THERE IS LITTLE ROOM FOR FURTHER DETERIORATION OR IMPROVEMENT BELOW 25 CM AND ABOVE 45 CM, RESPECTIVELY. ....	101
FIG. 51: BREAKTHROUGH CURVE AND ADSORPTION CAPACITIES BASED ON BOTH FILTER SIDES (E14).....	101
FIG. 52: BREAKTHROUGH CURVE AND ADSORPTION CAPACITIES BY FILTER SIDE (E30). FP: PRIMARY FILTER SIDE; FS: SECONDARY FILTER SIDE. ....	102
FIG. 53: CUMULATIVE MASSES OF ADSORBED NITROGEN (NH <sub>4</sub> -N) AND RELEASED NITROGEN (NO <sub>3</sub> -N). THE ARROWS MARK THE RESIDUAL MASS IN THE FILTER AT THE END OF EACH INTER-EVENT. INTRA-EVENT INCREMENTS ARE LINEAR INTERPOLATIONS BASED ON THE BEGINNING AND END OF EVENTS. ....	103
FIG. 54: NITRIFICATION RATE AS FUNCTION OF TEMPERATURE AND ADSORBED MASS. THE SURFACE GIVEN BY EQ. 1 WAS FITTED TO FIELD MEASUREMENTS (RED POINTS). THE EQUATION WAS USED TO SIMULATE NITRIFICATION (STRAIGHT BLACK SECTIONS FOR THE NINE INTER-EVENTS) BASED ON THE MEASURED	

ADSORBED MASS (HIGHER END) AT THE MEAN OF INTER-EVENT TEMPERATURES. THE MEANS OF SIMULATED RATES WERE MARKED BY THE BLACK POINTS.....	104
FIG. 55: COMPLETENESS OF THE NITRATE FLUSH AS THE FUNCTION OF THE HYDRAULIC LOAD FOR N=19 FLUSH PEAKS. FOR THE INTERPRETATION, THE MEDIAN EVENT NEEDED ABOUT 0.95 METRES OF LOAD UNTIL THE FLUSH WAS COMPLETE. ....	105
FIG. 56: THE LAYOUT OF THE CSO CW AT MARCY L'ETOILE. ....	109
FIG. 57: CROSS-SECTION OF THE CSO CW AT MARCY L'ETOILE. NOTE THE DIFFERENT FILTER MATERIALS IN F1 AND F2 (SAND AND ZEOLITE AND POZZOLANA, RESPECTIVELY) .....	109
FIG. 58: NUMBER OF EVENTS BY FILTER SIDE PRIORITY .....	110
FIG. 59: SLUDGE SAMPLING PATHS. NOTE THAT COMPOST WAS AVOIDED TO BE TAKEN WITH THE SAMPLES (BOTTOM LEFT CORNER).....	111
FIG. 60: ANNUAL HYDRAULIC LOADS IN THE MONITORING PERIOD.....	112
FIG. 61: IN-AND OUTLET EMCs AND MASS REMOVAL PERFORMANCES (H) FOR THE MAJOR POLLUTANTS. WHISKERS REPRESENT THE 10 <sup>TH</sup> AND 90 <sup>TH</sup> PERCENTILE. N: NUMBER OF EVENTS. ....	113
FIG. 62: IN-AND OUTLET EMCs AND MASS REMOVAL PERFORMANCE (H) FOR DISSOLVED POLLUTANTS. E: ENTIRE FILTER, P: POZZOLANA FILTER SIDE, S: SAND FILTER SIDE, N: NUMBER OF EVENTS.....	114
FIG. 63: IN-AND OUTLET EMCs AND MASS REMOVAL PERFORMANCES (H) FOR SOLIDS AND ORGANICS BY LOAD. LEFT: EVENTS BELOW, AND RIGHT, EVENTS ABOVE THE DESIGN LOAD (2.3 M). N: NUMBER OF EVENTS. ....	115
FIG. 64: IN-AND OUTLET EMCs AND MASS REMOVAL PERFORMANCES (H) FOR NUTRIENTS BY LOAD. LEFT: EVENTS BELOW, AND RIGHT, EVENTS ABOVE THE DESIGN LOAD (2.3 M). N: NUMBER OF EVENTS. ....	115
FIG. 65: RESULT OF THE PCA ON COD REMOVAL (N=24).....	116
FIG. 66: PREDICTIONS IN FUNCTION OF MEASURED EFFLUENT COD CONCENTRATIONS.....	116
FIG. 67: IN- AND OUTLET CONCENTRATIONS AND REMOVAL EFFICIENCIES FOR PAHs. THE CONCENTRATION OF OTHER COMPOUNDS WAS TOO CLOSE TO THE QUANTIFICATION LIMIT TO CALCULATE REMOVAL PERFORMANCES.....	118
FIG. 68: SLUDGE BLANKET MAP AFTER THREE YEARS OF OPERATION. ABOVE AND BELOW: AFTER HEAVY LOADS (8 M <sup>3</sup> /M <sup>2</sup> AND 12 M <sup>3</sup> /M <sup>2</sup> ) SEPARATED BY A ONE-MONTH INTER-EVENT. ....	119
FIG. 69: CHANGES IN THE SLUDGE VOLUME AFTER A HEAVY LOAD. THE CHANGE IS THE INTEGRATED EFFECT OF A LONG INTER-EVENT PERIOD (1 MONTH, DECOMPOSITION) AND THE LOAD (ABOUT 12 M <sup>3</sup> /M <sup>2</sup> , ACCUMULATION).....	120
FIG. 70: DRY AND VOLATILE ORGANIC MATTER CONTENT OF THE SLUDGE. ....	120
FIG. 71: PAHs IN THE SLUDGE OF MARCY L'ETOILE.....	121
FIG. 72: METALS IN THE SLUDGE OF MARCY L'ETOILE.....	121

## Abbreviations

ASM.....	Activated Sludge Model, see Henze et al. (2000)
BMP.....	Best Management Practice
<i>COD</i> .....	Model component in Orage, represents COD
<i>COD_tot</i> .....	Total COD
<i>COD_S</i> .....	Dissolved COD fraction
<i>COD_X</i> .....	Particulate COD fraction
CSO .....	Combined Sewer Overflow
CSO CW .....	Constructed Wetland for Combined Sewer Overflow Treatment
CST.....	Combined Sewer Tank
CW.....	Constructed Wetland
CW2D.....	biokinetic model, see Langergraber (2005)
EMC.....	Event Mean Concentration
ET .....	Evapotranspiration
FWS.....	Free Water Surface (equals SF)
HF .....	Horizontal Flow
<i>NH4N</i> .....	Model component in Orage, represents NH <sub>4</sub> -N
PE.....	Population Equivalent
<i>Peak_MA_cc</i> .....	Concentration variable in Orage, optimized to the legislative threshold
PET .....	Potential Evapotranspiration
RSF.....	Retention Soil Filter (German standard of CSO CWs)
SF.....	Surface Flow
SSF.....	SubSurface Flow
SSO.....	Separate Sewer Outlet
SSO CW .....	Constructed Wetland treating Separate Sewer Outlet
TDR.....	Time Domain Reflectometry
TIS.....	Tank-In-Series (hydraulic model)
<i>TSS</i> .....	Model component in Orage, represents TSS
VF.....	Vertical Flow
WFD .....	Water Framework Directive (EC 2000/60)
WWTP.....	Wastewater Treatment Plant (refers to any classical facility)

The abbreviations in the attached articles and manuscripts are resolved in the text and are not listed here. Model parameters and variables are written in *italic*.



# Résumé étendu

## 1 Introduction générale

L'eau couvre 71% de la surface de la Terre. Si l'eau n'est pas rare, 99.3% est stockée dans les mers et océans ou sous forme de glace. Les eaux douces se répartissent les 0.7% restant, principalement sous forme d'eau souterraine ou de nappes phréatiques (Moss, 2010). Les eaux douces ne sont pas seulement essentielles mais un patrimoine précieux qu'il faut gérer avec sagesse pour faire face aux challenges que représente d'une population grandissante et les effets indésirables de l'activité humaine.

Un de ces effets est lié à l'urbanisation. De l'ordre de 54 % de la population mondiale vivait en milieu urbain en 2014. Cette valeur est sujette à s'accroître encore, passant de 30% en 1950 à 66% en 2050. En Europe elle est de 73% et seulement l'Afrique et l'Asie restent globalement rurales – avec la prédiction d'un équilibre critique en 2050 (UN 2014). L'extension de l'urbanisation et la croissance de la population est synonyme d'un accroissement des émissions et d'une extension des surfaces imperméabilisées comparé aux zones rurales. D'un côté, les surfaces imperméabilisées induisent des volumes de ruissellements accrus lors de précipitations ainsi que des débits plus importants provoquant des chocs hydrauliques sur les milieux aquatiques des bassins versants. D'un autre côté, les précipitations lavent l'atmosphère et les surfaces de polluants accumulés. En conclusion, notre environnement anthropique altère les caractéristiques des ruissellements naturels aussi bien sur l'hydraulique que la qualité des bassins versants et impacte les eaux naturelles. Pour ces raisons, la gestion des eaux urbaines de temps de pluie est d'une importance grandissante avec l'imperméabilisation et l'urbanisation en général (Loperfido et al. 2014, Fournel 2012, Walsch et al. 2005, Chocat et al. 1994).

C'est la Directive Cadre sur l'Eau (DCE 2000), dans l'Union Européenne, qui définit un cadre, transposé à l'échelle locale, pour atteindre le bon état écologique des milieux. Elle a été transposée à la législation française par l'Act no. 2004-338 et l'Act no. 2006-1772. Bien que de pratique courante de déverser les surverses de déversoir d'orage directement dans le milieu récepteur, la nouvelle législation impose de limiter les déversements d'eaux brutes des réseaux unitaires sans traitement. L'objectif étant de protéger le milieu récepteur.

Les rejets urbains de temps de pluie posent de sérieux problèmes sur les milieux comme l'érosion, la sédimentation de particules, des inondations, des changements de températures du milieu, une chute des teneurs en oxygène, des apports de nutriment et donc l'eutrophisation des milieux, l'accumulation de toxiques et peuvent donc conduire à une réduction de la biodiversité et des changements physiologiques dans les communautés benthiques (Marsalek 1998). Les déversements peuvent engendrer des flux supérieurs à ceux rejetés par les stations d'épuration sur plusieurs polluants comme la DCO, les matières en suspension (MES), les métaux et des charges importantes en ammonium (Kadlec and Wallace 2009). Pour atteindre les objectifs de qualité à l'échelle régional et locale, des pratiques de bonnes gestions (Best Management Practices – BMPs) sont utilisées comme des techniques de traitement, de mesures ou de contrôle, pour minimiser ou éviter les problèmes liés aux eaux pluviales (Muthukrishnan et al. 2006). BMPs peuvent être aussi bien centralisées que difuses, ces dernières étant privilégiées, et de nouvelles tendances émergent (Loperfido et al. 2014). Ce travail de thèse se focalise sur une de ces techniques : les filtres plantés à écoulement vertical pour le traitement des surverses de déversoir d'orage (CSO) dans le contexte français. Faisant partie d'un projet de plus grande ampleur (projet ADEPTE) touchant également au

traitement des eaux pluviales strictes, le logiciel d'aide au dimensionnement développé dans le cadre de ce travail de recherche répond également à la problématique des eaux pluviales strictes. Les filtres plantés à écoulement vertical pour le traitement des surverses de DO sont mis en place entre un déversoir d'orage d'un réseau d'assainissement et le milieu récepteur. Ils trouvent leur intérêt lorsque le réseau est saturé en temps de pluie et que les techniques de réduction des intrusions d'eaux pluviales dans le réseau ne sont pas (plus) efficaces.

25 % des réseaux sont unitaires collectant ainsi des eaux pluviales (SoeS 2011) en France. Les débits générés en temps de pluie, lorsqu'excédants les capacités des réseaux (ou de la station de traitement) sont généralement déversés directement dans le milieu récepteur. La directive 91/271/CEE demande à limiter les pollutions liées aux pluies d'orage. A ce titre, l'article 4 de la directive eaux résiduaires urbaines stipule : « les eaux urbaines résiduaires qui pénètrent dans les systèmes de collecte sont soumises, avant d'être rejetées, à un traitement secondaire ou équivalent » et l'art. R.2224-11 du Code Général des Collectivités Territoriales prévoit que : « Les eaux entrant dans un système de collecte des eaux usées doivent, sauf dans le cas de situations inhabituelles, être soumises à un traitement avant d'être rejetées dans le milieu naturel ». Les eaux de surverses de déversoir d'orage doivent donc être traitées avant d'être rejetées dans le milieu. Les paramètres auxquels s'applique le traitement sont similaires à ceux fixés pour l'unité de traitement de l'agglomération et peuvent donc aussi bien concerner la DCO, DBO, MES que l'azote ou le phosphore. De même on retiendra l'intérêt de tamponner hydrauliquement les rejets pour éviter les problèmes d'érosion et de remise en suspension de sédiment dans le milieu. Les filtres plantés de roseaux à écoulement vertical sont mis en avant pour leurs performances de traitement (Mungasavalli and Viraraghavan 2006). Leur efficacité pour différent type d'effluent a été démontré (Kadlec and Wallace 2009). Lorsque bien dimensionnés ils permettent aussi bien une filtration physique, biologique et chimique qu'un rôle de tampon hydraulique. Ils sont par conséquent capables d'éliminer une large gamme de polluants particuliers et dissous (Uhl and Dittmer 2005).

Plusieurs projets de recherche ont été conduit à Irstea (Institut national de recherche en sciences et technologies pour l'environnement et l'agriculture) dans l'objectif d'optimiser le dimensionnement des filtres à écoulement vertical pour le traitement des surverses de déversoir d'orage. Le premier projet (SEGTEUP - Fournel 2012) avait pour objectif d'adapter le dimensionnement des filtres Allemands développés pour cette application. Le concept Allemand met en œuvre un bassin de décantation suivi d'un filtre plantés (nommé « *Retentionsbodenfilter* » - RSF). Utilisés depuis de nombreuses années (Uhl and Dittmer 2005), l'expérience Allemande a été mixée avec l'expérience françaises sur le traitement des eaux usées domestiques brutes (Molle et al. 2005) pour tester des pilotes de filtres plantés traitant les surverse de DO sans décantation primaire (Pilotes de 20 m<sup>2</sup> plantés de *Phragmites australis*). Plusieurs matériaux et conceptions ont été testés et suivis pour aboutir à la réalisation d'un système en taille réelle.

A la suite du projet SEGTEUP, le projet ADEPTE (*Aide au Dimensionnement pour la gestion des Eaux Pluviales par Traitement Extensif*), en collaboration avec différent partenaires, avait pour objectifs de valider les règles de dimensionnement et de développer un logiciel d'aide au dimensionnement nommé Orage (librement disponible à partir de 2017). Aussi bien destinés aux surverses de DO qu'aux eaux pluviales strictes, l'outil permet de définir les surfaces, matériaux et profondeurs à mettre en œuvre pour garantir un niveau de rejet précis. Les travaux du projet ADEPTE se sont déroulés dans quatre contextes climatiques différents en France :

- I. Marcy l'Etoile (Surverses de DO) : Situé dans l'agglomération Lyonnaise en climat semi-continentale. Premier filtre en France pour cette application et innovant dans de nombreux



aspects lié à son dimensionnement. Il a été le lieu des expérimentations intensives menées dans le cadre de ce travail de thèse.

- II. Leuville-sur-Orge/Saint Germain les Arpajon (pluvial stricte): Situé au sud de Paris, ce filtre planté à écoulement vertical est représentatif d'un climat océanique de transition.
- III. Moulins les Metz (pluvial stricte): ce filtre planté à écoulement vertical, situé au sud du Luxembourg, correspond à un climat semi continental de transition.
- IV. Périgny (pluvial stricte): Il s'agit ici d'un filtre à écoulement horizontal en climat océanique.

Le travail mené dans le cadre de cette thèse s'est focalisé sur la construction du modèle simplifié d'aide au dimensionnement en se basant sur des expérimentations menées sur le site de Marcy l'Etoile. Les objectifs principaux étaient :

- Vérifier l'applicabilité du modèle Hydrus/CW2D pour le traitement des surverses de DO afin de mieux déterminer les processus clés à mettre en œuvre dans un modèle simplifié dédié au traitement des surverses de DO pour l'aide au dimensionnement (le logiciel Orage).
- Créer les bases du modèle simplifié dans l'objectif de préciser les surfaces, matériaux et profondeurs à mettre en œuvre. La première étape a été de définir les processus et les choix conceptuels du modèle pour représenter l'hydraulique et l'évolution des concentrations (MES, DCO, NH<sub>4</sub>, NO<sub>3</sub>) dans le temps. La seconde étape a été de formuler la boucle d'optimisation de manière à optimiser le temps de calcul. L'optimisation pour les eaux pluviales strictes, compte tenu des faibles concentrations en polluant en sortie, concerne principalement une optimisation hydraulique.
- Calibrer et valider le modèle d'aide au dimensionnement sur la base du suivi du site expérimental de Marcy l'étoile ainsi que les résultats du projet SEGTEUP sur des pilotes de taille semi-industrielle. Le suivi à concerner aussi bien l'hydraulique que les performances de traitement sur les paramètres DCO, MES et formes azotées. Le traitement de l'azote étant représenté sous deux étapes successives par adsorption et nitrification.
- Proposer des voies d'amélioration pour le dimensionnement et la gestion des filtres actuellement proposés pour le traitement des surverses de DO.

Le travail de thèse est présenté sous forme d'articles successifs (5) et divisé en quatre parties. Les paramètres de calage du modèle sont présentés de manière à respecter une certaine confidentialité dans le cadre du projet ADEPTE.

La partie 1 (Chapitre 1) est une synthèse générale de la revue bibliographique. Les filtres plantés de roseaux pour le traitement des surverses de DO sont présentés ainsi que la terminologie des différentes configurations. De même, une revue de la modélisation de ces ouvrages est présentée. Ce chapitre donne une vue d'ensemble du contexte général de ce travail (modélisation et expérimentations) pour une meilleure compréhension du travail réalisé.

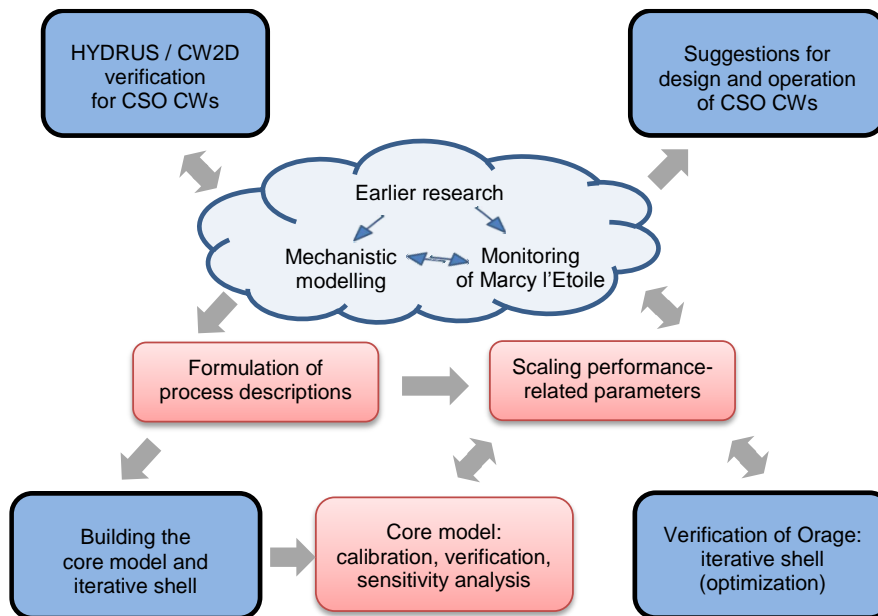


Figure 1: acquisition de connaissances et étapes clés du travail de thèse vis-à-vis des objectifs (cadres bleus). Les doubles flèches indiquent des liens de va et vient entre les différentes étapes.

La partie 2 (Chapitre 3) intitulée « dispositif expérimental et construction du modèle » discute les méthodologies mises en places aussi bien sur le site expérimental que les étapes et les méthodes mises en œuvres pour le développement, la calibration et la vérification du modèle. Ce chapitre a pour objectif de présenter l'ensemble de la démarche ainsi que les composantes clés du modèle (processus et optimisation) en lien avec les suivis de performances ou suivis spécifiques de calibration du site de Marcy l'étoile. Bien que présentés dans des articles individuels, compte tenu des liens entre les différentes étapes, ils sont présentés ici de manière conjointe. Le chapitre est divisé en plusieurs parties, deux dédiées au suivi expérimental et un dédié au modèle simplifié, tout en faisant référence aux liens entre les différents travaux.

La partie 3 (Chapitres 4 à 6) présente les articles issus de ce travail. Elle est divisée en sous-chapitres représentant les différentes étapes du travail sous forme d'articles. Une partie générale introductive ainsi qu'un résumé général synthétise les travaux de chaque article. Ils abordent les étapes présentés dans la Fig. 1.

La partie 4 (chapitre 7) résume les principales avancées du travail de thèse et apporte également des suggestions pour améliorer le dimensionnement et la gestion des filtres plantés pour le traitement des surverses de DO. Les nouvelles questions de recherches et de modélisation, issues de ce travail, sont également présentées pour donner des indications pour les futures recherches dans le domaine.

## 2 Synthèse de la revue bibliographique

### 2.1 Terminologie

Les zones humides artificielles (Constructed wetlands : CWs en anglais) sont des ouvrages issus de l'ingénierie écologique qui utilise les processus naturels liés à l'activité microbienne, les plantes et les matériaux constituant du filtre qui accueillent cette activité biologique (Vymazal 2007). Largement étudiés ces dernières décennies, ils représentent une famille de procédés de conception différente. Suivant l'hydraulique des systèmes, ils peuvent être à écoulement surfacique

(Surface flow – SF) ou d’écoulement sous-surface (subsurface flow – SSF : ce sont des filtres). Suivant la direction de l’écoulement, les SSF peuvent être divisés en plusieurs type de filtres : des filtres à écoulement horizontal (HF) ou des filtres à écoulement vertical (VF). Dans ces derniers types de filtres, les écoulements peuvent être librement drainés, variablement saturés ou saturés. Lorsque saturés, ils peuvent être à écoulement ascendant ou descendant. Les CWs peuvent avoir un large domaine d’application que ce soit pour des eaux usées domestiques, industrielles, des eaux pluviales, des boues ... (Kadlec and Wallace 2009, Fonder and Headley 2013). La Fig. 2 présente les types de systèmes utilisés pour des eaux urbaines de temps de pluie suivant le type de réseau et la direction des écoulements. Ce travail de thèse s’attache à étudier les filtres à écoulement vertical variablement saturés tel que conçus en France suivant les règles de l’art actuelles. Ils se réfèrent à la terminologie VF CWs.

STORMWATER TREATMENT			
CONSTRUCTED WETLANDS	separate sewers		combined sewers
	SF	stormwater ponds retention ponds	FWS wetland (only as part of a treatment chain)*
	VF	biofilters	CSO CWs
		RSFs** VF CWs for stormwater	
SSF	HF	HFCWs for stormwater	-

Figure 2: Classification des CWs pour les eaux urbaines de temps de pluie. \*: pour le système Italien voir Meyer et al. 2013; \*\*: pour le système Allemand voir Uhl and Dittmer 2005.

Les eaux de temps pluie génèrent, souvent lors d’évènement pluvieux intenses, de grands volumes de ruissellement. Les stations d’épuration, a l’exutoire d’un réseau unitaire, peuvent généralement accepter des volumes de l’ordre de 3 fois le débit de temps sec (le lagunage naturel et les filtres plantés de roseaux pouvant accepter des volumes supérieurs) si aucun bassin d’orage n’est mis en place (ce ratio est de 2 à 7 fois le débits de temps sec en Allemagne (Uhl and Dittmer 2005). De même, les capacités hydrauliques des réseaux unitaires peuvent être dépassée générant des surverses, un des principaux contributeurs de dégradation des milieux aquatiques en zone urbanisés (Chocat et al., 1994; Walsh et al., 2005).

## 2.2 Caractéristiques des surverses de déversoirs d’orage

Les caractéristiques des surverses de DO sont grandement impactées par les activités humaines. Cinq grandes sources de contamination peuvent être citées (Paren-Rouault and Boisson 2007, Gromaire 1998, Dechesne 2002, Mourad 2005, Fournel 2012):

1. *Retombées atmosphérique de temps de pluie,*
2. *Lessivage urbain,*
3. *Ruissellement des toitures,*
4. *Eaux parasites,*
5. *La contribution des eaux usées (spécifique aux réseaux unitaires).*

Les polluants majeurs peuvent être répartis en trois groupes (Fournel 2012) :i) particulaire (MES, MVS); ii) polluants organiques (DCO, DBO<sub>5</sub>, COT, COD et COV comme certains HAP, et

l'azote et le phosphore organique); iii) pollution ionique ( $\text{NH}_4\text{-N}$ ,  $\text{NO}_3\text{-N}$ ,  $\text{NO}_2\text{-N}$ ,  $\text{PO}_4\text{-P}$ , les métaux, sels antigels). Les concentrations des eaux urbaines de temps de pluie dépendent du temps. Les pollutogrammes permettent de suivre cette évolution au sein d'un évènement. Ces variations, mises en évidence par de nombreuses mesures sur des évènements et sites différents, et l'évolution des mesures en ligne, ont conduit à la nécessité de développer des calculs statistiques évolués pour bien définir les propriétés d'évolution des polluants. Les concentrations moyennes d'un évènement, proportionnelles au débit, (EMC) ont été largement utilisées : le Table 1 présente les différences entre surverses de DO et eaux pluviales strictes de plusieurs sites.

Tableau 1: gamme de concentrations (EMC) typiques de surverses de DO (CSO) et d'eau pluviales strictes (SSO) de plusieurs sites. Les gammes représentent les plus petites et plus grandes valeurs trouvées dans la littérature. a) Smullen et al. (1999); b) Kadlec and Wallace (2009); c) Fournel (2012); d) Sztruhár et al. (2002); e) Passerat et al. (2011); f) Zgheib et al. (2012) g) Schulz et al (1994); h) Gasperi et al. (2012). \*:TKN.

Paramètres	unités	SSO [EMC]	CSO [EMC]
MES	mg/L	78.4 <sup>a</sup> -106 <sup>f</sup>	85 <sup>c</sup> -430 <sup>d</sup>
DBO <sub>5</sub>	mg O <sub>2</sub> /L	14.1 <sup>a</sup>	35 <sup>c</sup> -135 <sup>h</sup>
DCO_tot	mg O <sub>2</sub> /L	52.8 <sup>a</sup> -89 <sup>f</sup>	99 <sup>c</sup> -445 <sup>d</sup>
NT	mg/L	2.4 <sup>a</sup>	3.6 <sup>c</sup> -16.8 <sup>d</sup>
NH <sub>4</sub> -N	mg/L	2.8 <sup>f</sup>	2.0 <sup>c</sup> -9.9 <sup>h</sup>
PT	mg/L	0.3 <sup>a</sup> -0.9 <sup>f</sup>	1.3 <sup>c</sup> -3.5 <sup>h</sup>
Cu	µg/L	13.5 <sup>a</sup> -55.0 <sup>f</sup>	250 <sup>g</sup>
Pb	µg/L	27.0 <sup>f</sup> -67.5 <sup>a</sup>	250 <sup>g</sup>
Zn	µg/L	162 <sup>a</sup> -270 <sup>f</sup>	570 <sup>d</sup> -1020 <sup>g</sup>
Coliformes fécaux	1000 CFU/ml	1.5 <sup>b</sup>	1.3 <sup>d</sup> -76 <sup>e</sup>

### 2.3 Les filtres à écoulement vertical pour le traitement des surverses de DO

De nombreux systèmes existent pour le traitement des eaux urbaines de temps de pluie. Les choix techniques doivent être réalisés spécifiquement à chaque site, en cherchant la complémentarité des techniques, plutôt que leur concurrence, en gardant en tête l'objectif proposé par Geoff et al. (2016) : La préservation ou la restauration du milieu récepteur.

Le travail de recherche mené dans le cadre de cette thèse se focalise sur le modèle français de filtre à écoulement vertical pour le traitement des surverses de DO. Ce système comporte différents compartiments, qui ont chacun une fonction. Ils sont présentés sur la Figure 3:

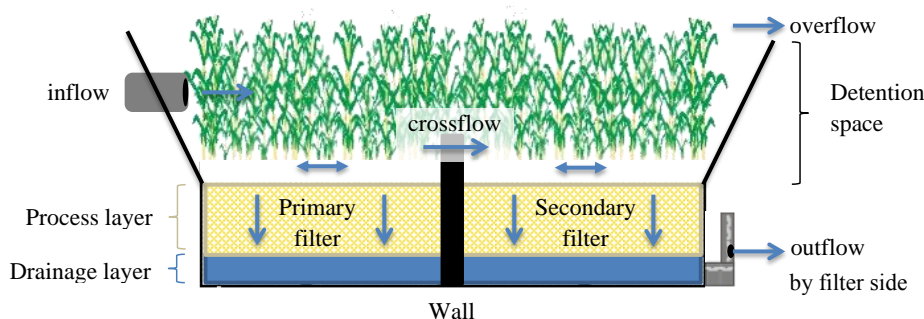


Figure 3: coupe schématique d'un filtre à écoulement vertical pour le traitement des surverses de DO.

Les eaux de temps pluie arrivent sur le filtre de manière stochastique aussi bien en ce qui concerne les volumes, les concentrations, les débits et leur fréquence. On peut qualifier deux

grandes périodes : des périodes d'alimentation pendant les épisodes pluvieux et des périodes sèches entre deux événements. Dittmer (2006) précise que ces périodes ne sont pas régies par les mêmes mécanismes épuratoires. La Fig. 3 présente l'alternance entre les périodes d'alimentation et sèches sur la base d'un suivi du niveau de saturation d'un filtre.

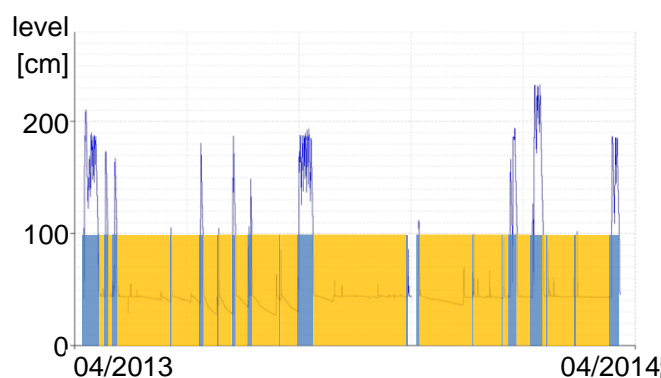


Figure 4: Alternation of intra-event (blue) and inter-event (ochre) periods. The periods are well discernible based on the stage in the CSO CW (blue series).

Les périodes « sèches » permettent au système de se régénérer entre deux événements pluvieux. Le terme « sèche » est une mauvaise interprétation du milieu qui reste constamment humide en réalité même après le drainage de l'eau gravitaire. La porosité étant non saturée, les processus aérobies dominent et permettent notamment la nitrification. Des périodes trop longues sans aucune alimentation va générer un manque de nutriment qui peut affecter négativement les performances sur le paramètre DCO (Dittmer 2006).

AU démarrage d'un épisode pluvieux, le milieu est non saturé et la limitation de débit de fuite n'a pas encore d'effet. Excepté dans le cas de faibles débits de surverses, c'est une période courte où l'infiltration des eaux est localisée proche des points d'alimentation : seule une petite partie du filtre est effectivement utilisée. Ce phénomène correspond à un passage préférentiel. En condition normal de fonctionnement, lorsque le filtre est saturé, l'écoulement est du type piston grâce à la limitation du débit de fuite (Dittmer 2006). Un flaquage de surface a lieu de quelques heures à quelques jours suivant l'intensité et la durée de l'épisode pluvieux. Après l'épisode pluvieux, le filtre se draine en quelques heures.

Les mécanismes de traitement des polluants se basent sur les interactions solide-liquide-biomasse à l'image de l'ensemble des CWs. La limitation du débit de fuite est une contrainte hydraulique plus forte que la perméabilité du milieu. Les valeurs ciblées sont de 0.036-0.180 m<sup>3</sup>/m<sup>2</sup>/h soit de 0.01-0.05 L/s/m<sup>2</sup> (Meyer 2011). Cela permet d'assurer un certain temps de séjour dans le milieu.

Les mécanismes épuratoires sont différents suivant que l'on soit dans une phase d'alimentation ou entre deux événements. Pendant les phases d'alimentation les particules solides sont filtrées par le milieu conduisant à la formation d'une couche de dépôt en surface. Cette couche de dépôt peut créer un problème de colmatage sur le long terme (ou si le système est mal dimensionné). D'un autre côté, elle permet i) une protection contre le séchage du milieu, le froid et l'érosion du milieu, ii) d'accroître les capacité d'adsorption, iii) de créer un milieu favorable aux organismes vivant par le maintien d'une certaine humidité et présence de nutriments et iv) favorise la distribution de l'eau au démarrage des événements pluvieux. La couche de dépôt et le milieu filtrant seront appeler couche de filtration dans le reste du document, à moins que la distinction soit faite. La surface développée de cette couche de filtration est le lieu d'une adsorption, phénomène

prépondérant pour la rétention de l'azote ammoniacal. L'activité biologique pendant les épisodes pluvieux permettra d'abattre la DCO dissoute (COD<sub>S</sub>). Compte tenu de la saturation du milieu, les processus pendant les événements pluvieux sont principalement considérés comme anaérobiques ou anoxiques. Lorsque le filtre se draine gravitairement, l'air revient dans le milieu les processus aérobies deviennent prépondérants. L'azote adsorbé peut être nitrifié permettant de libérer les sites d'adsorption et provoquant un lessivage de nitrate à l'évènement pluvieux suivant. Les conditions aérobies et d'humidité favorisent la minéralisation de la matière organique, phénomène important pour la couche de dépôt de surface (Dittmer et al. 2005, Uhl and Dittmer 2005, Meyer 2011, Dittmer and Schmitt 2011, Dittmer et al. 2016).

L'alternance des processus entre les phases d'alimentation et de repos, bien que les performances sont évaluées généralement sur les périodes d'alimentation, permet de réaliser le lien qu'on chacune des phases sur l'autre. Les performances moyennes à l'échelle d'un évènement pour différentes technologies sont présentées dans le Table 2 (RSFs sont des filtres plantés à écoulement vertical, technologie très répandue en Allemagne. Ils sont proches du système développé en France).

Tableau 2: Performances de traitement de différentes technologies (CSO et SSO). treatment. Sources : EPA 1999a; b: EPA 1999b; c: Kadlec and Wallace (2009); d: EPA 1999c; e: Waldhoff 2008; f: Pinnekamp 2013; g: Frechen 2013

Paramètres	Filtres à sable <sup>a</sup>	Performances de traitement [%]		
		Bioretention <sup>b</sup>	Lag à macrophytes	RSFs
MES	70	90	68 <sup>c</sup>	93 <sup>e</sup>
DBO <sub>5</sub>	70			
DCO <sub>tot</sub>				86 <sup>e</sup>
COT	48	90	34 <sup>d</sup>	62 <sup>f</sup>
NT <sub>S</sub>				
NT	21		30 <sup>c</sup>	
NTK	46	68-80		
NH <sub>4</sub> -N			31 <sup>c</sup>	83 <sup>e</sup>
NO <sub>3</sub> -N	0		45 <sup>c</sup>	
PT	33	70-83	41 <sup>c</sup>	80 <sup>e</sup>
Cu		93-98	49 <sup>c</sup>	78 <sup>g</sup>
Pb	45	93-98	74 <sup>c</sup>	64 <sup>&lt;g</sup>
Zn	45	93-98	60 <sup>c</sup>	62 <sup>&lt;g</sup>
Coliformes fécaux	76	90	77 <sup>d</sup>	90 <sup>e</sup>

## 2.4 Modèles numériques appliqués aux CSO CWs

Les règles de dimensionnement classiquement utilisées pour les filtres plantés ne peuvent être utilisées pour les eaux urbaines de temps de pluie en général en raison de leur caractère stochastique. Si les modèles numériques semblent intéressants pour mieux comprendre les processus des filtres alimentés par des eaux urbaines de temps de pluie, la modélisation apparaît comme délicate également pour le dimensionnement également en raison du caractère stochastique des événements pluvieux et l'impact des changements des conditions du filtre sur les processus épuratoires.

Les modèles existants utilisés ou développés pour cette problématique sont de deux types :

- i) Modèles mécanistiques pour une meilleure compréhension des mécanismes ;
- ii) Modèles d'aide à la décision pour optimiser le dimensionnement.

Comme décrit par Meyer et al. (2015), tous les modèles sont d'intérêt mais pour des objectifs différents. Les modèles mécanistiques sont souvent complexe d'utilisation. Ils apportent des informations scientifiques d'importance mais ne sont pas aisés à utiliser pour le dimensionnement. Hydrus (© PC-Progress s.r.o., Šimůnek et al., 2011), développé pour des questions scientifiques, avec le module CW2D (pour les CW en général, Langergraber and Šimůnek, 2012). Bien qu'il n'ait pas été développé pour des eaux urbaines de temps de pluie, il a été testé pour la simulation de l'hydraulique et des performances de filtre pour le traitement des surverses de DO (Langergraber and Šimůnek, 2005). Les recherches se sont focalisé à déterminer les limites de son application aux surverse de DO progressivement par Heinrichs et al. (2007; 2009), Meyer (2011) puis Meyer et al. (2013) en se focalisant principalement sur le calage du  $\text{NH}_4\text{-N}$ . Malgré cela, une biomasse stable n'a pas pu être représentée posant des problèmes sur la prédiction de la DCO. Cette croissance non limitée de biomasse ne permet pas de réaliser des simulations de long terme. Cette lacune laisse la place pour de futures recherches.

Les modèles d'aide au dimensionnement sont des modèles simplifiés développés suite à un besoin de l'ingénierie d'avoir des modèles pratiques d'utilisation pour le dimensionnement (Meyer et al 2015). Le premier modèle simplifié développé pour les filtres à écoulement vertical pour le traitement des surverses de DO provient de l'expérience Allemande sur les « Retention Soil Filters ». Le premier modèle (RSF\_Disc, Dittmer 2006) a été implémenté dans le logiciel KOSMO simulant les réseaux (Schmitt and Dittmer 2007). RSF\_Disc a servi de base au développement du modèle RSF\_Sim (Meyer and Dittmer 2015) avec lequel les concentrations de sortie ont été bien représentées sur des systèmes à échelle réelle (Tondera et al. 2013). L'hydraulique est représentée par des réacteurs parfaitement mélangés en série (Figure 5) en représentant plusieurs polluants (MES, DCO et  $\text{NH}_4\text{-N}$ ) et en modélisant de manière séparée la DCO dissoute et particulaire.

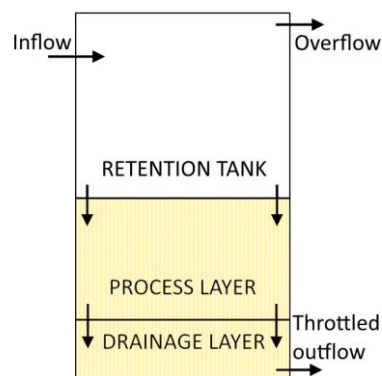


Figure 5: Hydraulique de RSF\_Sim: réacteurs parfaitement mélangés (basé sur Meyer and Dittmer, 2015).

### 3 Résumé : Dispositif expérimental et construction du modèle

#### 3.1 Premier filtre taille réelle pour le traitement des surverse de DO en France: Marcy l'Etoile

Le premier filtre planté pour le traitement des surverses de DO (Figure 6) a été réalisé en 2012 à Marcy l'Etoile. Le dimensionnement est basé sur la nécessité de traiter les eaux d'une pluie de période de retour d'un an ( $1160 \text{ m}^3$ ) d'un bassin versant de 98 ha comportant principalement un habitat résidentiel. Le débit de temps sec des habitations et de quelques sources industrielles est de 9 600 EH. Le débit de fuite est calibré par un orifice unique, pour chaque filtre, sur un tuyau vertical sur des valeurs ajustables entre 0.008 or 0.016  $\text{L/s/m}^2$ . La hauteur verticale de l'orifice permet de régler la hauteur de la couche saturée de fond de filtre. Lors d'évènements extrêmes, un



by-pass de surface a lieu sur un déversoir trapézoïdal à 2.1 m de la surface du filtre. La Figure 7 représente une coupe du filtre.

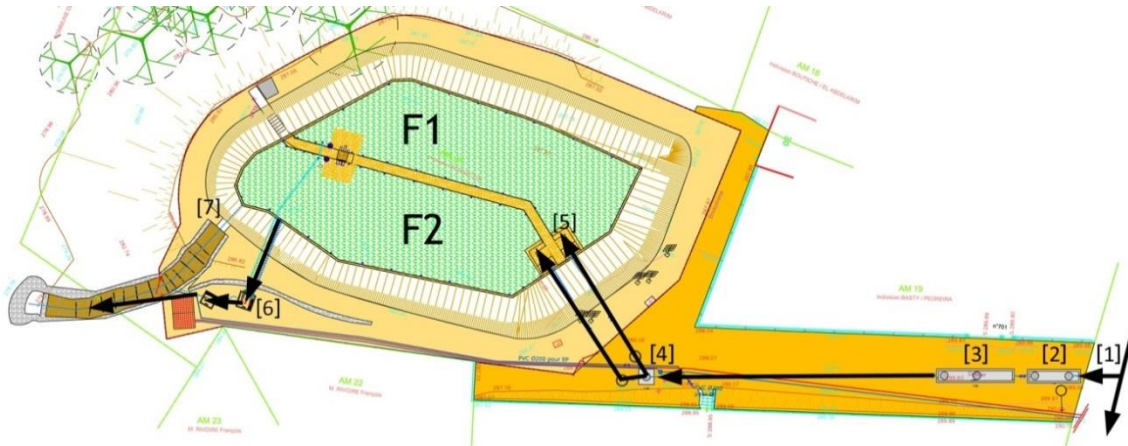


Figure 6: Parcours de l'eau dans le filtre de Marcy l'Etoile. [1]: Déversoir d'orage; [2]: piège à sable; [3]: canal venturi; [4]: alternance des filtres; [5]: points d'alimentation; [6]: dispositif de sortie; [7]: by-pass. La section jaune entre les filtres F1 et F2 représente le mur de séparation entre les filtres.

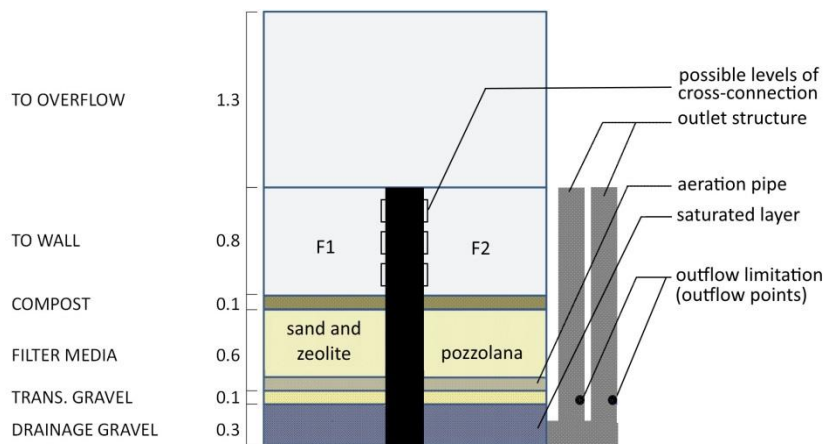


Figure 7: Coupe vertical du filtre de Marcy l'Etoile. La seule différence entre les filtres F1 et F2 est le type de matériau de filtration.

### 3.2 Objectifs de suivi et instrumentation

Le suivi expérimental a débuté après un an de fonctionnement de l'ouvrage. La surverse réglable du DO, permet de pouvoir s'affranchir (ou non) du déversement quotidien d'eau industrielle. Ces eaux industrielles, d'un volume important, avaient heureusement des caractéristiques similaires de celles d'une surverses de DO (gamme haute) permettant de pouvoir également simuler des évènements réguliers pour étudier les limites du système. Les débits et volumes d'entrée étaient mesuré par la mise en place d'une sonde ultra son sur le canal venturi. Le niveau de saturation et de flaquage des filtres était mesuré par une sonde pression (STS ATM.1ST/N/T) dans chacun des filtres. En sortie un débitmètre électro magnétique (Krohne Waterflux 3070) permettait la mesure de débit de drainage des deux filtres à la fois. Pendant les périodes de suivis intensifs, des sondes dans les canalisations de mise en charge de sortie, après corrélation débit hauteur, permettaient d'avoir le débit de drainage individuel de chaque filtre.

Des préleveurs automatiques réfrigérés (Lange Bühler 2000/1027) ont été installé en entrée et sorties des filtres avec un prélèvement proportionnel au débit. L'échantillonnage individuel de

chaque filtre en sortie à été mis en place à partir du 15<sup>ème</sup> évènement mesuré. La stratégie d'échantillonnage est présentée dans le tableau 3 et les EMCs dans le tableau 4.

Tableau 3: Volume prélevé moyen par évènements. Le nombre d'échantillons est présenté par filtres par ex. 9+9 (mélange sable/zéolite et pouzzolane respectivement).

Evènement	Volume [m <sup>3</sup> ]	Echantillons entrée/sortie	Volume moyen entrée/sortie [m <sup>3</sup> ]	Evènement	Volume [m <sup>3</sup> ]	Echantillons entrée/sortie	Volume moyen entrée/sortie [m <sup>3</sup> ]
1	3000	-	-	17	491	2/6+7	246/38
2	300	2/6	150/50	18	448	3/9+8	149/26
3	280	5/4	56/70	19	793	1/14+14	793/28
4	300	5/4	60/75	20	747	2/8+8	374/47
5	2900	28/26	104/112	21	650	4/8+9	163/38
6	1200	1/6	1200/200	22	360	1/8+8	360/23
7	2800	10/18	280/156	23	742	1/10+10	742/37
8	1300	7/11	186/118	24	1321	4/9+9	330/73
9	537	4/14	134/38	25	1011	2/11+8	506/53
10	1020	4/6	255/170	26	1080	6/9+8	180/17
11	1665	9/16	185/104	27	1493	4/10+11	373/71
12	1380	6/11	230/125	28	1496	6/9+9	249/83
13	7500	16/23	469/326	29	1774	5/8+8	355/111
14	5600	13/23	431/243	30	3990	4/6+6	998/333
15	1607	7/9+9	229/89	31	6400	6/9+9	1067/356
16	290	1/5+5	290/29				

Tableau 4: Concentrations d'entrée à Marcy l'Etoile. Les valeurs sont comparées à des concentrations mesurées sur des surverses de DO de la littérature suivante : c) Fournel (2012); d) Sztruhár et al. (2002); e) Passerat et al. (2011); g) Schulz et al (1994); h) Gasperi et al (2012). Valeur moyennes à l'échelle de l'évènement (EMCs) de plusieurs site et évènements. L'écart représente les plus petites et plus grandes EMC de la littérature.

Paramètres	Unités	CSO [EMC]	Marcy l'Etoile [EMC]*
MES	mg/L	85 <sup>c</sup> -430 <sup>d</sup>	220
DBO <sub>5</sub>	mg O <sub>2</sub> /L	35 <sup>c</sup> -135 <sup>h</sup>	76
DCO_tot	mg O <sub>2</sub> /L	99 <sup>c</sup> -445 <sup>d</sup>	220
NT	mg/L	3.6 <sup>c</sup> -16.8 <sup>d</sup>	
NTK	mg/L	22 <sup>h</sup>	21,6
NH4-N	mg/L	2.0 <sup>c</sup> -9.9 <sup>h</sup>	13,8
PT	mg/L	1.3 <sup>c</sup> -3.5 <sup>h</sup>	9,6
PO4-P			6,5
Cu	µg/L	250 <sup>g</sup>	32.5
Pb	µg/L	250 <sup>g</sup>	3.3
Zn	µg/L	570 <sup>d</sup> -1020 <sup>g</sup>	109
Coliformes fécaux	1000 CFU/ml	1.3 <sup>d</sup> -76 <sup>e</sup>	

En plus du suivi des performances globales, le suivi expérimental avait les objectifs suivant :

*Etude de l'hydraulique et des passages préférentiels* : L'étude de l'effet de dilution lors des passages préférentiels et des temps de passage à différents niveaux de saturation a été réalisé par des traçages hydrauliques avec plusieurs injections de traceur. Un fluorimètre (GGUN-FL 932) a été installé en sortie pour une mesure en continu du retour du traceur. Le contrôle du débit d'entrée a été réalisé en pompant l'eau stocké dans le filtre non utilisé de manière à assurer un temps de saturation progressif et cohérent avec les injections du traceur. La fluorescéine a été injectée, en

contrôlant les doses, en trois fois pour générer des pics de sortie à différents niveaux de saturation du filtre.

*Suivi fin des bilans en azote et impact des courts circuits hydrauliques.* Ces objectifs ont été suivis par la mesure en ligne des teneur en nitrate et azote ammoniacal (WTW Varion). Pour l'azote ammoniacal, l'objectif était de suivre aussi bien l'impact des courts circuits hydraulique sur la rétention ainsi que les courbes de percés du filtre pour des charges importantes en azote. En cas d'impact important des courts-circuits, ces mesures devaient permettre de pouvoir adapter le dimensionnement pour en limiter les causes. Les sondes étaient calibrées et contrôlées par des prélèvements analysés au laboratoire à chaque évènement.

*Mesure de la teneur en eau dans le filtre.* La teneur en eau dans le milieu poreux a été mesurée par l'intermédiaire de sondes TDR afin d'avoir une indication sur l'hétérogénéité spatiale et temporelle des écoulements. Des sondes de 30 cm, triple broches, ont été mises en place ; 6 sondes Campbell Scientific CS610 et 12 réalisées à l'Université Catholique de Louvain la Neuve (Belgique). Les mesures ont été réalisé sur un pas de temps de la minute sur un axe longitudinal et à différentes profondeurs, après calibration sur le milieu de Marcy l'Etoile.

*Evaluation des vitesses de nitrification.* La détermination des vitesses de nitrification a été étudiée en réalisant des bilans masses sur l'azote sur une succession maîtrisée d'évènements (grâce aux eaux industrielles). Les évènements ont été enchainés à différentes saisons (effet température) en mettant en œuvre différents temps de repos entre deux évènements.

### **3.3 Modèle d'aide au dimensionnement : Orage**

L'objectif du modèle est de faciliter le dimensionnement des ouvrages. Le logiciel Orage, développé dans le cadre de ce travail, permet de déterminer le matériau (et sa profondeur, ainsi que la surface du filtre sur la base d'une simulation d'une longue série de données d'évènement pluvieux (suivant la période de retour recherchée). Il se compose de trois programmes majeurs (Figure 8) :

- i) Structure de l'outil : une interface utilisateur permet de pouvoir rentrer des données spécifiques au site d'étude et réalise un premier traitement des données ainsi qu'une analyse statistique basique et une représentation graphique des données;
- ii) Un programme itératif réalise l'optimization automatique du dimensionnement et appelée régulièrement le Coeur du modèle pour la simulation des processus. L'optimisation se fait en adaptant le matériau utilisé, la surface du filtre et pour différents polluants (NH<sub>4</sub>-N, DCO et MES). L'optimisation vise un dimensionnement qui satisfait les concentrations limites de sorties fixées tout en utilisant le matériau le moins couteux et la surface la plus faible;
- iii) Le modèle des processus. Le modèle effectue des simulations de séries de données de long terme et calcul un niveau de concentration de sortie moyennée (*Peak\_MA\_cc*) pour chaque polluant, directement comparable aux niveaux de rejet fixés.

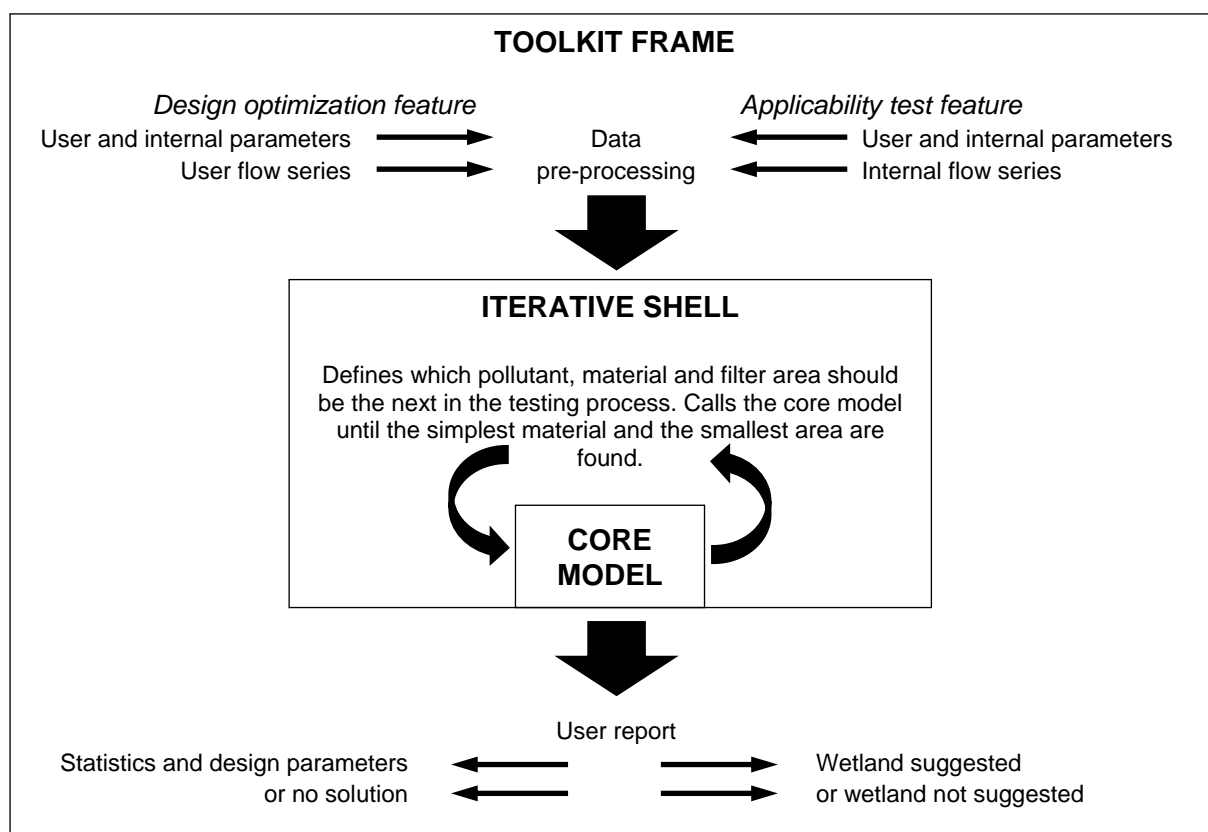


Figure 8: Structure d'Orage.

Le Tableau 5: Données d'entrée d'Orage résume les données d'entrée du logiciel. Si les débits d'entrée sont fournis par l'utilisateur, un format est précisé et les informations de concentrations (précises/réalistes) doivent être données également pour un pas de temps compris entre 6 et 15 minutes.

Tableau 5: Données d'entrée d'Orage

Données d'entrée nécessaires	Fonction du logiciel	
	Aide au dimensionnement	Test d'applicabilité
Débits d'entrée propres au site	X	
Type d'eau (CSO/SSO)	X	X
Surface disponible [m <sup>2</sup> ]	X	X
Région climatique (5)	X	X
Bassin versant [ha]		X
Coefficient d'imperméabilisation [%]		X
Population [EH]		(X)
Capacité hydraulique maximal du réseau [m <sup>3</sup> /h]		(X)
Volume à traiter (charge de dimensionnement) [m <sup>3</sup> ]	X	X
Niveaux de rejet à respecter :		
Débit max admissible par le cours d'eau [m <sup>3</sup> /h]	X	X
NH4-N [mg/L]	X	X
DCO [mg/L]	X	X
MES [mg/L]	X	X

Une fois l'optimisation réalisée, Orage renseigne différentes informations d'entrée et de sortie sous forme de statistiques et de graphiques pour aider l'utilisateur dans l'interprétation des résultats. De plus les indications suivantes, relatives au dimensionnement, sont fournies :

- Surface du filtre [m<sup>2</sup>];
- Matériau de filtration (sable grossier, sable fin, pouzzolane, trois différents mélanges de zéolite et de sable);
- Profondeur de la couche de filtration [m];
- Le plus grand temps de flaquage attendu [h];
- La charge hydraulique annuelle [m];
- Le volume de stockage en surface de filtre nécessaire [m<sup>3</sup>]

Ces aspects seront détaillés et discutés dans différents chapitres dans ce document.

## **4 Résumé du chapitre 4 – l'utilisation de modèle mécanistique pour simuler les filtres plantés traitant les surverses de DO**

### **4.1 Contexte et faits marquants**

Cet article discute des limitations à résoudre pour l'utilisation du modèle mécaniste Hydrus/CW2D pour la simulation des filtres plantés traitant les surverses de DO sur la base d'expérimentations en colonnes de laboratoire issues d'un travail de thèse Allemande. Des précédentes limitations avaient été décrites par Henrichs et al. 2007, 2009; Meyer 2011 and Meyer et al. 2013. Notre travail avait également pour objectif de préciser les points importants dans la simulation des performances sur de longue durée et détailler les processus clés. L'objectif était de poser les bases pour le développement du modèle simplifié Orage. Le travail pouvait aussi permettre d'identifier de nouvelles limites du modèle mécaniste et les besoins futurs.

- Nous avons simulé des filtres plantés pour le traitement des surverse de DO dans Hydrus/CW2D.
- Nous avons calibré le modèle biocinétique sur la base d'expérimentations en colonnes.
- Nous avons obtenu une biomasse quasiment stable et un bon calage sur la base d'un événement ou d'une série d'événements.
- Les précédentes limitations ont été résolues et la validation sur des systèmes pleine échelle peut être maintenant réalisée.

### **4.2 Résumé – Simulation des filtres plantés pour le traitement des surverses de DO avec HYDRUS / CW2D**

Constructed Wetlands 2D (CW2D) est un modèle biocinétique décrivant la dynamique microbienne et les processus de transformation et de dégradation des polluants dans les filtres plantés de roseaux. Le couplage de CW2D et d'Hydrus (©PC Progress s.r.o.) a été testé pour des applications de filtres traitant les surverses de DO. Le caractère stochastique des événements pluvieux, et la limitation de débit de fuite induit des conditions de saturation (événements pluvieux) et de non saturation (entre les événements) aléatoires. Le besoin de vérification de l'aptitude de ce modèle à simuler les filtres provient de ces changements drastiques de conditions de fonctionnement. Des précédentes études ont défini les paramètres clés sur lequel il était important de travailler pour diminuer les limitations du modèle, comme les paramètres biocinétiques, le

fractionnement de la DCO entre rapidement et lentement biodégradable et les formes inertes ou encore l'adsorption de la DCO inerte.

Les nouveaux paramétrages utilisés ont permis d'obtenir des conditions de biomasse stables. Ils ont été utilisés pour simuler des résultats obtenus sur une précédente expérimentation en colonnes de laboratoire allant d'une simulation d'un évènement à une série d'évènements. La qualité de calage a été étudiée par une méthode appropriée avec de bon résultat pour la DCO et le NH<sub>4</sub>-N. le calage des nitrates n'était pas recherché.

### **4.3 Principaux apports**

L'utilisation d'Hudrus / CW2D a permis de simuler les performances de traitement de surverses de DO, sur la base de colonnes de laboratoire, pour les paramètres DCO et NH<sub>4</sub>-N sur de courtes séries. Les précédentes limitations ont pu être écartées, par un ajustement des paramètres biocinétiques, et la dynamique de la biomasse a pu être quasiment stabilisée. Aucun pic de DCO au début des évènements n'est observé.

L'état d'équilibre, après une période d'inoculation, varie par la suite suivant les cycles d'alimentation et de repos. Ces cycles jouent un rôle majeur sur le taux de biomasse au sein du système. La stabilité à long terme reste à confirmer. Cette variation de l'activité bactérienne, suivant les cycles, et donc un point important à prendre en compte dans la construction du modèle simplifié sur des simulations de long terme.

Si la validation du modèle mécaniste reste à faire sur des systèmes de taille réelle, l'outil peut potentiellement être utilisé pour de l'ingénierie. Cela requiert cependant une formation professionnelle poussée et des temps de simulation importants (plusieurs heures). Le passage à la confrontation du modèle à des taille réelle nécessitera un ajustement des paramètres, d'autant plus sur le système développé en France qui reçoit des eaux usées brutes, contrairement aux expérimentations de colonnes.

## **5 Résumé du chapitre 5 - Orage: modèle validation et apports sur l'optimisation du dimensionnement des ouvrages.**

### **5.1 Contexte et faits marquants**

Ce chapitre est composé de deux articles présentant le modèle orage. Ils comportent chacun le terme « *Orage: a design-optimization modelling tool for CSO CWs* » car ils présentent l'outil Orage. Cet outil a été développé pour l'ingénierie pour dimensionner les ouvrages de traitement en prenant en compte le caractère stochastique des évènements pluvieux. Il comporte trois principales composantes. La première est le cœur du modèle qui est présenté, testé et comparé aux données de taille réelle dans le premier article (le terme « core model » est ajouté au titre). Les deux autres composantes sont la boucle itérative d'optimisation et la structure de l'outil. Elles sont présentées, testées et optimisées dans le deuxième article (le terme « iterative shell » est ajouté au titre).

Les faits marquants du premier article sont :

- Le développement d'un modèle simplifié permettant de prendre en compte la présence de filtres en parallèle,
- La présentation de la pertinence du modèle,
- La calibration à un évènement unique de grande ampleur,
- La mise en évidence de la robustesse du modèle via la simulation d'une série d'évènement pluvieux et d'une analyse de sensibilité.

Les faits marquants du deuxième article sont :

- Le développement d'un outil d'optimisation du dimensionnement des ouvrages,
- L'optimisation de la boucle itérative automatique,
- Les paramètres clés de l'optimisation ont été fixés,
- Le test de la boucle itérative et son réalisme en termes de prédictions,
- Les performances sur le NH<sub>4</sub>-N peuvent être tenues, même pour des charges importantes tout en évitant le colmatage.

## **5.2 Résumé – Orage : outil d'aide au dimensionnement des filtres plantés de Roseaux pour le traitement des eaux urbaines de temps de pluie. Cœur du modèle.**

Les filtres plantés de roseaux pour le traitement des surverses de DO sont développés en France sous un mode à écoulement vertical avec une limitation du débit de fuite. En permettant un tampon hydraulique et un traitement des polluants, ils permettent de réduire l'impact des déversements sur le milieu récepteur. Compte tenu du caractère stochastique des évènements pluvieux, le dimensionnement de ces ouvrages nécessite une approche dynamique, autorisée par l'usage de modèles. C'est à cet effet que le modèle Orage a été développé. Il comprend un module lié au processus (le cœur du modèle) ainsi qu'une boucle itérative pour l'optimisation, le tout intégré dans une interface utilisateur. L'optimisation permet de proposer une surface de filtre, un matériau de filtration ainsi que la profondeur de ce matériau. L'optimisation se réalise en prenant en compte les caractéristiques spécifiques du site d'étude, dont une chronique de déversement. Le cœur du modèle simule l'hydraulique et la dynamique des MES, de la DCO et du NH<sub>4</sub>-N. Un premier calage manuel sur un évènement, confronté par la suite à une série d'évènements a permis d'observer la pertinence du modèle. Une analyse de sensibilité a été réalisée pour identifier les paramètres clés nécessaires à caler par des mesures in situ pour affiner la calibration.

## **5.3 Résumé – Orage: outil d'aide au dimensionnement des filtres plantés de Roseaux pour le traitement des eaux urbaines de temps de pluie. Boucle d'optimisation.**

Les filtres plantés de roseaux pour le traitement des surverses de DO sont développés en France sous un mode à écoulement vertical avec une limitation du débit de fuite. L'outil d'aide au dimensionnement (Orage) facilite le dimensionnement en optimisant la surface de filtre, le matériau de filtration ainsi que sa profondeur. L'optimisation se base sur des données propres au site, dont une série de déversements. La boucle d'itération appelle le cœur du modèle de manière répétée pour chaque dimensionnement testé. Pour chaque simulation, débits et concentrations de sortie sont simulés et comparés aux limites de rejets à respecter demandées par l'utilisateur. La boucle a été

testée sur des chroniques de pluie réelles et simulées pour fixer les paramètres d'optimisation afin de répondre à une grande variété de cas. L'approche d'optimisation a été vérifiée en utilisant les données d'un cas réel et ce pour différents niveaux de rejets. L'usage de la zéolite permet une meilleure nitrification pour des charges supérieures à celles classiquement utilisées dans les recommandations actuelles mais nécessite d'être vigilant sur la problématique de colmatage.

## 5.4 Principales avancées

Le cœur du modèle a été testé par de nombreuses approches, y compris des tests statistiques pour évaluer la pertinence du calage. Il a été montré robuste par une analyse de sensibilité et la simulation de séries d'évènements en utilisant des paramètres calés sur un seul évènement. La précision du modèle est modérée à bonne. Elle nécessitera d'être confrontée à plus de données issues de conditions réelles.

La précision et la robustesse du modèle sont deux facteurs importants pour une optimisation du dimensionnement fiable. L'intégration du modèle dans la boucle d'optimisation a montré une fiabilité des optimisations.

L'optimisation des paramètres hydraulique en utilisant des débit de réseaux séparatif d'eaux pluviales et des concentrations en polluants de réseau unitaire (cas défavorable) a montré que des filtres compacts (surface de filtre inférieur à la surface de stockage) permettent de respecter des niveaux bas en azote ammoniacal. Dans ce cas la question d'un possible colmatage à long terme doit se poser.

Dans le cas de filtres surdimensionnés, plusieurs ajustements seraient nécessaires pour une meilleure efficacité d'optimisation. Une approche a été réalisée pour minimiser les court-circuits hydrauliques engendrés par un surdimensionnement mais des données issues de déversoirs d'orage de réseau unitaire seraient nécessaires pour confirmer la méthodologie. D'une manière générale, la boucle d'optimisation a été validée et vérifiée sur le site de Marcy l'Etoile.

## 6 Résumé du chapitre : Performances processus du filtre plantés à écoulement vertical.

### 6.1 Contexte et faits marquants

Le site de Marcy l'étoile est le premier filtre de ce type en France. Il a été suivi pendant trois ans en termes de débits et de performances épuratoires par l'intermédiaire de mesures en lignes et de prélèvement proportionnels au débit. Deux évènements pluvieux de plusieurs jours ont été également évalués en termes de HAP et de métaux. Cela a permis d'évaluer les performances de l'ouvrage. De même, des campagnes de mesures spécifiques ont été réalisées pour préciser la dynamique des processus pour nourrir la construction du modèle. Les processus étudiés avaient pour objectifs de préciser i) l'hydraulique du système à différents niveau de saturation (court-circuits hydrauliques), ii) la dynamique de l'azote (adsorption/nitrification) et iii) l'accumulation des boues en surface de l'ouvrage. Les résultats sont présentés dans ce chapitre en deux articles intitulés « dynamique de l'azote et évolution de l'hydraulique d'un filtre plantés à écoulement vertical pour le traitement des surverses de DO » et « performances épuratoires sur les paramètres majeurs et micropolluants d'un filtre plantés à écoulement vertical pour le traitement des surverses de DO ». Leur quantification était nécessaire pour la calibration du modèle Orage.

Faits marquants sur la dynamique des processus :



- La dynamique des processus a été étudiée sur un système en taille réelle,
- La dynamique de saturation, lors d'évènements pluvieux, a été étudiée suivant une section verticale et longitudinale par rapport au point d'alimentation,
- Les capacités d'adsorption de l'azote ammoniacale ont été évaluées pour la pouzzolane et le mélange zéolite/sable,
- Les vitesses de nitrification et les relargages de nitrates ont été quantifiés et formulés.
- Des propositions d'amélioration du dimensionnement ont été proposées ainsi que des pistes pour de futures recherches.

Faits marquants sur les performances épuratoires et l'accumulation des boues :

- Le premier filtre taille réelle en France a été intensément étudié,
- Un grand nombre d'évènements pluvieux ont été suivis sur les trois ans,
- Une cartographie du dépôt de boues a été réalisée et analysée pour les métaux et HAP,
- Une analyse statistique a permis de mettre en évidence les paramètres clés impactants les performances sur la DCO
- Des recherches supplémentaires sont nécessaires pour une meilleure compréhension du comportement des micropolluants dans le système.

## **6.2 Résumé de l'article – dynamique de l'azote et évolution de l'hydraulique d'un filtre plantés à écoulement vertical pour le traitement des surverses de DO**

L'objectif des filtres plantés à écoulement vertical pour le traitement des surverses de DO est de pouvoir traiter des charges ponctuelles, et rapides, de caractère stochastique. Le premier filtre en taille réelle réalisé en France a été suivi pendant trois ans par l'intermédiaire de prélèvements proportionnels au débit et de mesures en ligne. La teneur en eau dans le milieu a été étudié, par des sondes TDR, suivant différents profils, sur une section longitudinale par rapport au point d'alimentation. L'étude de l'hydraulique a également été complétée par des traçages hydrauliques à différents niveaux de saturation au cours d'un évènement. Ils permettent de mettre en évidence l'impact du niveau de saturation de départ sur l'ampleur des court-circuits hydrauliques. Couplés à des mesures en lignes de  $\text{NH}_4\text{-N}$ , des propositions de dimensionnement ont été faite pour diminuer leur ampleur. LA dynamique de l'azote a été étudiée en réalisant des alimentations répétées du filtre à différentes occurrences et par des bilans massiques. Les capacités d'adsorption évaluées sur la pouzzolane et le mélange zéolite/sable ont été quantifiées similaire au niveau des filtres, mais leur volume dans chaque filtre n'est pas le même. En conséquence de quoi, leur capacité intrinsèque ont pu être évaluée. La vitesse de nitrification a pu être mise en équation dépendant de deux facteurs que sont la température et la masse de  $\text{NH}_4\text{-N}$  adsorbé sur le matériau. Elle permet de pouvoir représenter la masse d'azote nitrifiée pendant les périodes « sèches ». LA vitesse de nitrification double tous les 5.7 °C. Ces résultats ont permis d'affiner la calibration du modèle. Enfin, l'étude de la dynamique de lessivage des nitrates en début d'évènement pluvieux permet de donner de spistes de dimensionnement d'un deuxième étage de traitement pour viser des objectifs d'azote global.

### **6.3 Résumé de l'article – performances épuratoires sur les paramètres majeurs et micropolluants d'un filtre plantés à écoulement vertical pour le traitement des surverses de DO**

Les performances sur les paramètres majeurs, métaux et HAP ont été évalués sur un système en taille réelle pendant trois ans. Les performances sont globalement hautes (97% en MES, 80% en DCO et 72% en NH<sub>4</sub>-N) même si les charges appliquées ont été parfois largement supérieures au charges de dimensionnement : l'objectif était de voir les limites de l'ouvrage. Sur les deux matériaux testés (pouzzolane et mélange Zéolite/sable) des performances similaires ont été mesurées.

Les facteurs environnementaux ont été étudiés pour expliqués les variations observées sur les performances du paramètres DCO. On a pu montrer que les paramètres le plus impactants sont la teneur en DCO dissoute en entrée ainsi que la durée et l'évapotranspiration moyenne de la période de repos précédant un épisode pluvieux. Cette période de repos peut fragiliser la biomasse et impacter les rendements par la suite.

Enfin, le suivi des boues a permis de calculer la vitesse d'accumulation moyenne ainsi que leur régression pendant les périodes sèches.

### **6.4 Principales avancées**

Le suivi de la dynamique des processus a permis de confirmer les processus et de paramétrer le modèle Orage.

Les cour-circuits hydrauliques impactent le niveau de rejet en azote ammoniacal, ce qui peut être une problématique pour des long et petits déversements (ou dans le cas d'ouvrages surdimensionnés). Ceci peut arriver malgré une capacité d'adsorption importante du matériau utilisé. Les possibilités de limitation de l'ampleur de ces court-circuits ont été proposées :

- a) La mise ne place d'une couche de saturation permanente de 40 cm en fond de filtre,
- b) La mise ne place d'un double orifice de régulation du débit de fuite. Un petit orifice au niveau de la couche de saturation de fond et un plus gros au-dessus pour accélérer la saturation du filtre au début de l'évènement pluvieux.
- c) Maximiser la distribution du dépôt de boues en surface et mettre en oeuvre une connection entre les filtres au niveau du dépôt de boue.

Le mélange zéolite/sable et la pouzzolane sont tous deux efficaces pour l'adsorption de l'azote ammoniacal. La mise en œuvre de matériaux de forte capacité d'adsorption permet de réduire considérablement la surface du filtre. Cependant, il ne faut pas négliger dans ce cas l'augmentation du dépôt de boue qui pourrait à terme conduire à un colmatage de l'ouvrage. Ce colmatage n'a pas pu être mis en évidence sur le site de Marcy l'Etoile. Cette thématique mérite d'être poursuivie dans des recherches futures. Une autre problématique liée aux filtres compacts pourrait être la saturation progressive des sites d'adsorption en raison de périodes de repos plus courtes et donc une moindre nitrification. Le modèle Orage permet d'étudier cette problématique.

Enfin, les flux de nitrates en début d'épisode pluvieux sont lessivés dans le cadre du premier mètre d'eau s'évacuant du filtre. La recherche d'objectif de dénitrification sur un deuxième étage de traitement nécessiterait alors de se focaliser uniquement sur ce premier mètre mais pose la question d'une source de carbone compte tenu des concentration en DCO en sortie d'ouvrage.

En ce qui concerne les performances du filtre, la robustesse de ce dernier a pu être mise en évidence par la stabilité des rejets. Pour des événements en dessous de la charge nominale (2.3 m) les niveaux sont bons (97% en TSS, 80% en COD and 85% en NH<sub>4</sub>-N). La chute des n'a été observé que pour des charges extrêmes d'une charge de 12m (cela représente pour le site de Marcy, une pluie de période de retours de deux ans). La pouzzolane est une alternative envisageable à la zéolite lorsque disponible localement.

La concentration en DCO de sortie peut être estimée sur la base de la concentration dissoute en DCO, la durée de la période de repos précédente et l'évapotranspiration de cette période de repos ( $R=0.62$ ). En termes de micropolluants, le système est efficace à la fois pour certains HAP (benzo(a)pyrene, phenanthrene, naphthalene) que des métaux (Al, Ti, Cr and Ba). Cependant, des études supplémentaires et plus fines (suivis plus régulier, mesures de pH, redox ...) sont nécessaires pour mieux appréhender le devenir des micropolluants dans ces ouvrages. Ce que l'on retiendra est que le niveau de concentration dans les boues, actuellement, n'empêche pas une valorisation des boues en agriculture. L'accumulation des boues est localisée proche des points d'alimentation et le filtre utilisé en « secondaire » ne reçoit plus de boues. En conséquence de quoi le niveau de connexion sur le filtre secondaire peut être abaissé pour minimiser les longues périodes de repos qui fragilisent la biomasse.

## **7 Apports pour le dimensionnement et conclusions générales**

### **7.1 Apports pour le dimensionnement**

#### **7.1.1 Diminution des court-circuits hydrauliques**

Le suivi des niveaux de saturation en début d'évènement couplés à la mesure en ligne de l'azote ammoniacal de sortie a permis de mettre en évidence l'impact des court-circuits sur les niveaux de rejet. Ceux-ci sont dus à une infiltration localisée proche des points d'alimentation et peut, dans le cas de faibles évènements pluvieux, durer longtemps et affecter les performances significativement. Le dimensionnement peut être amélioré pour limiter ces effets.

En premier lieu, la structure de sortie peut intégrer deux orifices de sortie pour réguler le débit de fuite. L'objectif étant de saturer plus rapidement le filtre au début d'épisode pluvieux afin d'utiliser l'ensemble du filtre en terme d'hydraulique. L'orifice inférieur doit être calibré à un niveau inférieur au débit de fuite de dimensionnement, pour favoriser la saturation, et l'orifice supérieur calibré de manière à ce que les deux orifices drainent au débit de fuite voulu pour traiter rapidement les volumes importants de manière à autoriser le drainage rapide et la régénération du filtre. Le positionnement de l'orifice du bas peut être positionné à 40 cm du fond pour permettre une réserve en eau pour les périodes de repos et minimiser les court-circuits. L'orifice du haut pourrait être positionné au niveau de la surface du filtre. L'eau stockée dans la porosité ne représentant qu'une petite fraction du volume à traiter (par ex. 60 cm de matériau avec une porosité de 33% ne stocke que 20 cm d'eau). Un ratio de débits de fuites, entre les deux orifices, de 1:2 est proposé. Il induirait, pour une hauteur de flaquage de 1 m, un accroissement de l'ordre de 2,5 heures du drainage. De même cela permettrait d'améliorer le relargage de nitrates en début d'épisode pluvieux.

Un autre moyen de minimiser les court-circuits et de mettre en œuvre une hauteur de saturation permanente de fond à une hauteur comprises entre 0.3 et 0.5 m. En plus de permettre une limitation du séchage du filtre en période de repos, les mesures et simulation réalisées par Orage ont montrées que ces hauteurs permettent de limiter l'effet des court-circuits sur le niveau de rejet en

azote ammoniacal. Ces valeurs ont donc été introduites dans orage pour le dimensionnement suivant que les climats soient arides ou non. On notera que le système d'aération doit se situer au-dessus de cette zone de saturation permanente pour favoriser l'oxygénation et éviter la remobilisation du phosphore ou des métaux.

### **7.1.2 Système de distribution d'entrée**

LE système de distribution des eaux d'entrée est aussi un point impactant l'ampleur des court-circuits. La mise en place d'un seul point d'alimentation peut non seulement favoriser des effets de bords mais aussi ne permet pas une bonne distribution des boues et des eaux. Sur Marcy l'Etoile, aucun dépôt de boues n'est observé à l'extrémité du filtre. Une réflexion sur une meilleure distribution des eaux doit donc être réalisée et, dans le cas d'un seul point, préférentiellement positionné au centre du filtre.

L'usage de plusieurs points de distribution est préférable, que ce soit pour de petits ou grands filtres (Marcy l'Etoile possède un point pour 250 m<sup>2</sup> de filtre), afin d'améliorer la distribution des eaux et des boues. L'infiltration des eaux est limitée par le dépôt organique de surface jusqu'à ce que le filtre soit saturé. Une alimentation par un canal de déversement sur une largeur de filtre peut être une solution par exemple pour améliorer la distribution, comme il est parfois réalisé en Allemagne, mais les potentiels effets de bords mériteraient d'être étudiés.

### **7.1.3 Connection hydraulique entre les filtres**

La connexion hydraulique entre les filtres de Marcy l'Etoile permet une alimentation du filtre secondaire en eaux décantées (Le filtre secondaire ne reçoit que de l'ordre de 15 % des MES d'entrée). En conséquence de quoi, aucune boue n'est observée au niveau des points de connexions. L'infiltration est donc rapide à ce niveau et favorise les court-circuits hydrauliques. Pour minimiser l'effet et mieux répartir les eaux, la connexion pourrait être réalisée là où le dépôt organique est présent, donc proche des points d'alimentation.

Il est également important de ne pas mettre en place de gabions d'entrée qui diminuent la profondeur effective de la couche de filtration comme il a été réalisé à Marcy l'Etoile. Si les gabions d'entrée, nécessaires pour briser l'énergie cinétique de l'eau, s'enfoncent dans la profondeur du filtre, ils induisent automatiquement un court-circuit hydraulique. Ils doivent donc être positionnés en surface ou avoir un fond étanche.

L'alternance des filtres a pour objectif de créer des périodes de repos plus longues entre les événements pluvieux pour minéraliser le dépôt organique. En revanche, dans le cas d'un nombre important de petits événements pluvieux, des périodes de repos longues vont également affecter la biomasse et, par conséquent, les performances épuratoires. Dans la mesure où nous avons observé que les eaux déversées sur le filtre secondaire n'apportent pas beaucoup de MES, des déversements plus fréquents ne devraient pas trop affecter la dynamique de la boue mais favoriser les performances épuratoires. La hauteur de 80 cm mise en place à Marcy l'Etoile semble être satisfaisante à cet effet.

### **7.1.4 By-pass de surface**

Les by-pass de surface transportent de faibles concentrations en MES dans la mesure où ils n'apparaissent que pour des événements extrêmes et une décantation a lieu (visible également sur la DCO NK et PT lié à la partie particulaire). Il semble donc intéressant de mettre une structure de sortie dont l'objectif est uniquement d'arrêter les potentiels macro-déchets.

## 7.2 Conclusions et perspectives

### 7.2.1 Modélisation mécaniste des filtres pour le traitement des surverses de DO

La modélisation par Hydrus/CW2D a permis de représenter correctement les performances de traitement sur la DCO et  $\text{NH}_4\text{-N}$  sur des chroniques courtes et moyennes en ayant une quasi stabilité de la biomasse épuratrice. Il est cependant nécessaire d'avoir une validation de la modélisation sur des ouvrages de pleine échelle, en conditions réelles. De même, son utilisation pour le système français (eaux usées brutes) pose d'autres questions qu'il est nécessaire d'étudier pour transférer ce modèle vers l'ingénierie. Quoi qu'il en soit l'usage de ce modèle nécessite une formation poussée et des temps de calculs importants pour de longues chroniques de débits.

### 7.2.2 Le modèle Orage

Le cœur du modèle orage (processus) est robuste et l'optimisation automatique a été vérifiée. La boucle d'optimisation donne des dimensionnements réalistes lorsque utilisé sur les données de Marcy l'Etoile. La précision du modèle, par un affinage des paramètres de calage, pourra être accrue sur la base de futurs suivis sur des sites réels différents. Pour cela des suivis poussés seront nécessaires. Il s'agira de travailler sur le calage des paramètres liés aux matériaux, aux facteurs influençant les performances sur la DCO et l'optimisation hydraulique. Des études supplémentaires permettront de comparer directement les prédictions du modèle Orage aux mesures. Pour une bonne utilisation, une formation des ingénieurs, décideurs sera nécessaire, même si l'outil est simple d'utilisation.

### 7.2.3 Performances des filtres et compacité.

En ce qui concerne les performances du filtre, la robustesse de ce dernier a pu être mise en évidence par la stabilité des rejets. Pour des événements en dessous de la charge nominale (2.3 m, N=19) les niveaux sont bons (97% en TSS, 80% en COD and 85% en  $\text{NH}_4\text{-N}$ ). Aussi bien la pouzzolane, que le mélange zéolite/sable, ont montrés une forte capacité à l'adsorption de l'azote ammoniacal. Les autres polluants majeurs n'ont que peu d'impact sur le dimensionnement de la surface du filtre. Compte tenu des capacités d'adsorption mesurées, les filtres peuvent engendrer un stockage des eaux (effet tapon hydraulique) supérieur à la surface du filtre nécessaire pour la partie traitement. Cela engendrerait des charges hydrauliques importantes et supérieures à la pratique actuelle. Le risque serait alors de colmater prématurément le filtre. Des recherches supplémentaires sont nécessaires pour bien quantifier l'impact de charges hydrauliques et organiques importantes. Les charges hydrauliques testées pourraient induire des valeurs jusqu'à 250 m/an. Des solutions également pour limiter le déversement des particules solides des réseaux pourraient être étudiées également afin de dimensionner des filtres sur des charges hydrauliques importantes.

La régénération du filtre en saison froide est inférieure à celle attendue. La vitesse de nitrification double tous les 5.7 °C. Cela signifie que les capacités d'adsorption pourraient être limitées en saison froide et nécessiteraient de longues périodes de repos difficiles à mettre en œuvre en hiver. Cela est donc un aspect supplémentaire, avec le colmatage, qui pourrait limiter l'usage de filtres compacts. Le modèle Orage prend en compte ce phénomène dans l'optimisation du dimensionnement.

La concentration en DCO en sortie d'ouvrage peut être estimée en fonction de la DCO dissoute d'entrée et la période de repos précédente (durée, évapotranspiration) sur la base d'une corrélation linéaire établie dans le projet ( $R=0.62$ ). Valable en concentration moyenne sur l'évènement

pluvieux, des recherches futures sont nécessaires pour mieux appréhender ces variations au sein même d'un évènement pluvieux.

Il a été montré également que les filtres plantés permettent de retenir efficacement certains micropolluants de type HAP (benzo(a)pyrene, phenanthrene, naphthalene) et métaux (Al, Ti, Cr and Ba). Cependant, des études plus fines sont nécessaires pour améliorer la compréhension des processus et appréhender les performances de ce type de substances.

#### **7.2.4 Pistes pour la dénitrification**

Il a été montré que le relargage des nitrates est lié à la charge hydraulique qui passe au travers du filtre. La plus-part des nitrates est relargué au début de l'évènement pluvieux sur le premier mètre de charge hydraulique. En conséquence de quoi, seul le traitement de ce premier mètre serait nécessaire pour viser un traitement complet de l'azote global à l'échelle de l'évènement. Cependant cela pose la question de la source de carbone associé au temps de séjour dans un ouvrage secondaire pour garantir un niveau stable. Ceci doit être étudié dans le futur. La confirmation de ce mètre de charge qui relargue les nitrate poussent en faveur de la réalisation de filtres compacts de manière à minimiser les volumes à traiter et donc l'emprise des ouvrages.



## 1 General introduction

Water is covering about 71% of the surface of Earth. Water is not scarce but 99.3% is stored in the seas and oceans or in ice caps and glaciers. Freshwater resources are sharing the other 0.7% of the total in the classical sense, dominated by groundwater (Moss, 2010). Freshwater is not only essential but it is a precious asset to be managed wisely facing the challenges caused by an increasing population and unwanted effects of human activities.

One effect of these human activities is related to urbanization. Globally, 54 per cent of people were living in urban areas in 2014. The global value is predicted to increase further, from 30 per cent in 1950 to 66 per cent in 2050. In Europe, this value is 73 per cent and only Africa and Asia remain mostly rural – with the prediction of a balance pronouncedly tipping by 2050 (UN 2014). Urban sprawl and population increase mean increased emissions, the sprawl of the impermeable surfaces and a changed material use compared to the rural setting. On one hand, sealed surfaces trigger larger runoff volumes at precipitation events with a more pointed, taller discharge curve, creating a hydraulic shock on the often minor natural water bodies of the effected watershed. On the other hand, everything weathers with time, and precipitation tends to wash or solve out pollutants not only from the surfaces but also from the atmosphere of urban areas. In summary, our built environment alters natural runoff characteristics by changing hydraulics and water quality in the watershed which put an adverse impact on natural waters. For these reasons, managing urban stormwater is increasing in significance with the increasing area of sealed land and urbanization in general (Loperfido et al. 2014, Fournel 2012, Walsch et al. 2005, Chocat et al. 1994).

It is the Water Framework Directive (WFD 2000) in the European Union which creates an agenda for water management down to the community level. Its main goal is to improve the quality of deteriorated water bodies or maintain good status of others. The directive is implemented in the national legislation of France via Act no. 2004-338 and Act no. 2006-1772. Although it has been a common practice to release excessive flows originating from urban runoff which exceed the capacity of the municipal wastewater treatment plants (WWTP) or sewer network, these legislations oblige water authorities governing communities to set a limit on pollutant loads diverted to the natural receiving water bodies and as such, to manage stormwater.

Urban stormwater poses numerous treats to living waters including erosion, sedimentation, flooding, temperature rise, dissolved oxygen depletion, nutrient enrichment, eutrophication, toxicity in the acute and accumulative pathways, reduced biodiversity and changes in communities (Marsalek 1998). Releases carry numerous pollutants and might exceed the loads represented by dry weather flow in terms of COD, suspended solids (TSS) and metals and might contain significant loads of ammonium (Kadlec and Wallace 2009). To tackle local and regional-scale water quality and quantity issues, stormwater best management practices (BMPs) are widely used to mitigate or avoid the listed problems to the maximum feasible extent through techniques, measures and structural controls (Muthukrishnan et al. 2006). BMPs are usually centralized although the advantages of distributed BMPs are acknowledged and an emerging trend can be observed in their implementation (Loperfido et al. 2014). This work focuses on vertical flow constructed wetland systems for combined sewer overflow treatment (CSO CWs) in the French practice. (Similar systems treating waters from separate sewer outlets (SSO) are touched only because the software developed linked to this thesis has a function of hydraulics optimization for them.) CSO CWs are applied as centralized systems between the point of overflow and the receiving water. They might be advantageous if the urban area is already developed and does not



allow the application of dispersed BMPs. Furthermore, CSO CWs can be integrated into a decentralized network of distributed BMPs too.

Stormwater is collected by combined sewers in about 25% of the lines (SoeS 2011) and the rest of the network length is separate sewer. The excessive flows generated by storm runoff are often released directly into the living waters as combined sewer overflow (CSO). To comply with EU Water Framework Directive (2000/60/EC) and the French legislations, pollution due to sewer overflow has to be managed. Furthermore, Article 4 of Urban Waste Water Treatment Directive (91/271/EEC) obliges the member states of the European Union to “ensure that urban waste water entering collecting systems shall before discharge be subject to secondary treatment or equivalent treatment”. Article R.2224-11 of the *Code Général des Collectivités Territoriales* states that “all waters entering a wastewater sewer, except unusual situation, have to be treated before to reach the waterbody”. Consequently, CSOs have to be treated before reaching the waterbody. Target pollutants are the same as those in sewage entering WWTP, so treatment should focus on TSS, COD and NH<sub>4</sub>-N/TKN. Flow control is needed as well for erosion prevention. Vertical flow wetlands like CSO CWs are claimed to offer advantages in terms of treatment performance (Mungasavalli and Viraraghavan 2006). They are proven efficient for various types of wastewaters like domestic, industrial, food etc. (Kadlec and Wallace 2009). When correctly designed, they combine filtration, physico-chemical processes including biodegradation and a hydraulic buffer effect. They are therefore capable to eliminate a wide range of particulate and dissolved pollutants (Uhl and Dittmer 2005).

A series of projects were started at IRSTEA (formerly known as Cemagref; Institut national de recherche en sciences et technologies pour l'environnement et l'agriculture, a public research institute in France focusing on land management issues such as water resources and agricultural technology) in order to optimize the design, operation and performance of CSO CWs. The first of them was the SEGTEUP project (Fournel 2012) which aimed to develop an optimized system derived from the German standards. The German VF CW system consists of a combined sewer overflow tank (CST) and a so-called '*Retentionsbodenfilter*' (retention soil filter, RSF) which are applied serially in this order, widely in the country. The experiences from RSFs (Uhl and Dittmer 2005) and the experiences from the French system for sewage treatment (Molle et al. 2005) were united to set up nine pilot scale filter beds (20 m<sup>2</sup> each, planted by *Phragmites australis*). These had different filter media and filter depth. The large-scale pilots were receiving controlled feedings enabling to study the performance of different system configurations over time. In summary, SEGTEUP aimed to develop an optimized concept which excludes the need of the tank (CST) in latter full scale projects.

As the follow-up of SEGTEUP, a new project was brought into action in a cooperation of several public and private stakeholders. The ADEPTE project (*Aide au dimensionnement pour la gestion des eaux pluviales par traitement extensif* – Supporting the dimensioning of extensive urban stormwater management systems) was born under the aegis of the National Biodiversity Strategy (*Strategie Nationale pour la Biodiversite 2011-2020*). The objective of the project was to lay down the design and operation guidelines of CWs for urban stormwater treatment. The ultimate project output was the design-support software Orage. The tool was to be made openly available from 2017 for both the public and private sector with the intention to simplify site-specific scaling and material selection of new CSO CWs (and SSO CWs) just as to aid dissemination. The research had been done at four full-scale wetlands located at three different climate regions of France:

- I. Marcy l'Etoile (CSO): Located close to Lyon at semi-continental climate and treating CSO, this wetland received pollutant loads with the highest variability. An intensive monitoring

(including online probes) had been carried out. This was the very first vertical flow CSO CW in France and pioneer in many aspects in a broader sense as well. Monitoring results from this site formed the base of the presented thesis work.

- II. Leuville-sur-Orge/Saint Germain les Arpajon (SSO): Located south of Paris this site is representative for oceanic-transitional climate.
- III. Moulins les Metz (SSO): this site represents the semi-continental transitional climate, located south of Luxembourg.
- IV. Périgny (SSO): horizontal flow wetland in oceanic climate.

This thesis deals with the design-support modelling of CSO CWs and introduces the research done at the Marcy l'Etoile site of the ADEPTE project. The main objectives of the work are:

- To verify an existing CW model package (HYDRUS /CW2D) in terms of applicability on CSO CWs (pilot scale). This first step helps to a better insight into CSO CWs. Due to their complexity CSO CWs were often considered as black-boxes. The deepened understanding is supposed to have value to achieve other research objectives with special emphasis on the development of a computational tool which i) is simple to use; ii) is built for CSO CWs and iii) is design-oriented (Orage).
- Create the framework of a design-support computational tool (Orage) which helps the scaling and material selection of CSO CWs. The first step is to formulate a numerical core model which works with time series of inflows and concentrations and calculates effluent qualities. The second step is the formulation of an iterative shell. The shell calls the core repetitively whilst searching for the ideal material (meaning low-cost) and the smallest filter area still effective in terms of hydraulics and pollutant removal. The tool should offer support for SSO CWs – optimization of hydraulics is satisfactory because effluent concentrations are low at SSO CWs anyway.
- Calibrate and verify the design-support tool based on scientific results from previous research and research at the Marcy l'Etoile site of the ADEPTE project. Report monitoring results of removal performance, hydraulics and nitrogen dynamics (adsorption – nitrification) of the Marcy l'Etoile site.
- Suggest improvements for the design and operation standards of the French concept of CSO CWs.

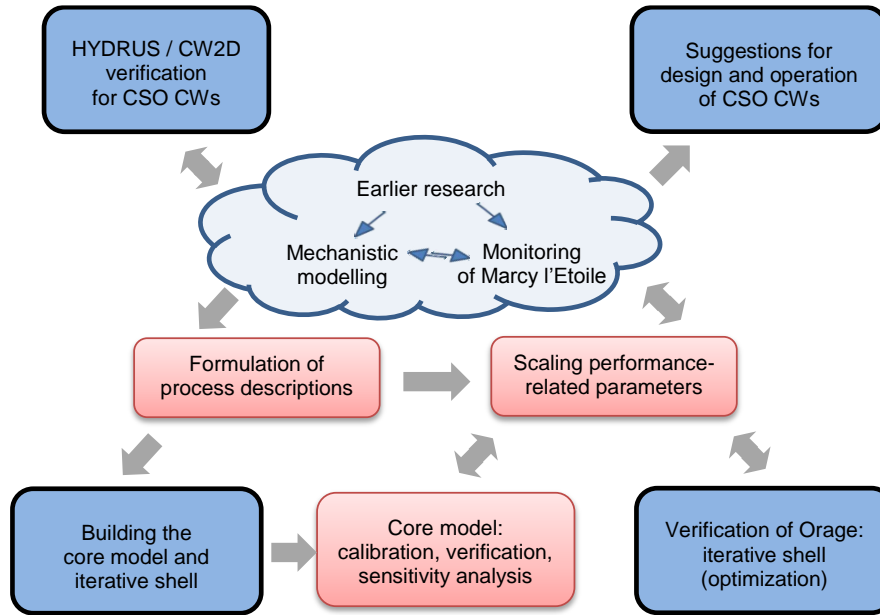


Fig. 1: Knowledge base and key steps towards the objectives (blue boxes). Arrows with two heads indicate where the process needed flexibility and allow two-directional exchange between steps.

The work is presented as a cumulative dissertation based on five manuscripts and is divided into four parts.

Part 1 (Chapter 2) is the general synthesis of the literature. The terminology and the traits of CSO CWs are introduced and the state of the art of modelling CSO CWs is discussed. The chapter gives a general overview of the broad context touched in this work (modelling and monitoring at full scale) to help the understanding of the work done and the outcomes obtained.

Part 2 (Chapter 3), titled ‘Setup of field experiments and model building’ is the chapter discussing the materials and methods of the field experiments. On the other hand, the steps and methods of model development, calibration and verification are summarized. These help to see the integrity of the work done on the key model components (core model and iterative shell) and the field monitoring (performance series and specific experiments). Although these were to be published as stand-alone articles, they have strong linkages due to the parallel nature of field research and model / program verification. The chapter is divided into two parts dealing with the on-site research and the third with modelling but always highlighting correlations by cross-references and practical examples.

Part 3 (Chapters 4-6) cumulates the articles born in the process of the thesis work. This part is divided into subchapters, each giving frame to and based on one manuscript. The summary of the context and then the closing thoughts help to string up the otherwise stand-alone works. Each article targets to add to the knowledge enumerated in the chapter ‘Synthesis of related literature’ and focuses more specifically on one or a few steps of the research (see Fig. 1).

Part 4 (Chapter 7) summarizes the main findings (‘Design proposals and final conclusions’). On the other hand it aims to give suggestions for design and operation of CSO CWs (see objectives). The new questions which have arisen during the research and model development are touched to propose directions for future research and the design-support software.

## 2 Synthesis of related literature

### 2.1 Terminology

Multiple definitions and descriptions exist in the scientific literature to resolve the term *wetlands* (e.g. Cowardin et al. 1985, Mitsch and Gosselink 2007, Kadlec and Wallace 2009). These definitions mention congruently several common traits of these semi-terrestrial land areas. Wetlands are saturated with water during part or all of the year and this has a deterministic effect on the soil properties and the vegetation they host. Wetlands are constructed at an increasing rate today all around the globe. A main driving force behind the spreading of constructed wetlands (CWs) is their use for wastewater treatment and any reference on CWs in this work is to be understood as CWs for the treatment of polluted water. These engineered systems are designed and constructed to utilize the natural processes which are related to microbial communities, plants and optionally the filter material which hosts the biota (Vymazal 2007).

CWs evolved in the recent decades and today, a wide range of design traits exist. According to hydraulic mode a CW can be surface flow (SF) or subsurface flow (SSF). According to the direction of the flow, SSF wetlands can be divided further into horizontal flow (HF) and vertical flow (VF). Wetland systems have a wide range of application from household sewage to wastewaters with special, often unique characteristics (Kadlec and Wallace 2009, Fonder and Headley 2013). Fig. 2 relates the types of constructed wetlands used for urban stormwater treatment according to the type of collection (sewer) and the direction of the flow. This work focuses on the French standard of VF CWs for combined sewer overflow treatment, referred to as CSO CWs. VF CWs for urban stormwater (i.e., from separated sewers) were touched only because the design-support tool Orage offers an optimization feature based on hydraulics.

STORMWATER TREATMENT			
	separate sewers	combined sewers	
CONSTRUCTED WETLANDS	SF	stormwater ponds retention ponds	FWS wetland (only as part of a treatment chain)*
	SSF	biofilters	CSO CWs
	VF	VF CWs for stormwater	RSFs**
HF	HFCWs for stormwater	-	

Fig. 2: Classification of constructed wetlands for stormwater treatment. \*: for the Italian system see Meyer et al. 2013; \*\*: for the German RSFs see Uhl and Dittmer 2005.

Stormwater is the water from precipitation events, often from heavy rainfalls which generate large volumes of runoff. The stormwater of urban areas (just as industrial or agricultural stormwater) is an environmental concern because it mobilizes and carries particulate and dissolved pollutants (Kadlec and Wallace 2009). In many communities, especially in European cities, a common sewer system collects sewage and urban runoffs. The wastewater treatment plants (WWTPs) at the endpoint of these networks are able to treat the dry weather loads or at most a few times higher flow (2-7 times in Germany, Uhl and Dittmer 2005). In France, the WWTP has to treat flow rates until a reference value, which enables to incorporate a part of the storm events. This

reference normally corresponds to the 95<sup>th</sup> percentile of flow rates at the treatment plant (based on a five year period). The rate is roughly around 2 to 3 times of the dry weather flows (article 2 de l'arrête du 21 juillet 2015, Ministry of Environment). Only pond systems and vertical flow constructed wetlands can accept higher hydraulic loads occurring during rain events (Molle et al. 2006, Arias et al. 2014). The capacity of the sewer pipes might be exceeded as well causing urban floods. In both practical cases, excess flow are bypassed and are rejected as combined sewer overflow (CSO). CSO is a source of pollutant and hydraulic shock to the often minor receiving waters. Releases from separated sewer systems are a similar concern due to solids, metals and high flow rates (Marsalek 1998). Urban stream syndrome is a generalized degradation of streams draining urban land compared to their former or natural state (Chocat et al., 1994; Walsh et al., 2005).

## 2.2 The characteristics of combined sewer overflow

The EU Water Framework Directive (WFD, EU directive 2000/60/EC) targets to improve the quality of the water bodies of the member states and has a dual approach. It calls for national regulations both for emission side (the quality of the released water) and for the immission (the quality of the receiving water). The quality of combined sewer overflow (CSO) is greatly affected by human activities. It has five main contamination sources:

- *Wet-weather atmospheric deposit*: condensation cores of the rain droplets are often atmospheric suspended pollutants which get back to land with the precipitation. During the process, other gaseous and non-gaseous contaminants are washed out, including nitrous oxides, carbon monoxide, sulphur dioxide, hydrocarbon vapours, trace metals and aerosols (Paren-Rouault and Boisson, 2007).
- *Urban washout*: Pavements and roads are the most important sources of suspended solids. Pollution of the urban runoff generated by precipitation events arrives to the sewer via three main processes (Gromaire 1998, Dechesne 2002): (1) continuous accumulation of materials during dry periods, (2) re-mobilization by the flows, (3) transportation into and through the sewer network.
- *Roof runoff*: the water from roofs is often the main source of Pb, Cu and Zn due to plumbing and other construction materials which are rich in these elements. Roof runoff is low in TSS.
- *Parasitic waters*: unaccounted groundwater intrusion to the sewer system.
- *Wastewater contribution* (specific for CSO): the arriving flow mixes with sewage and becomes rich in nitrogen and phosphorous compounds. The high flow speeds might also re-mobilize dry weather flow deposits and biofilms in the sewer network (Mourad, 2005).

The main contaminants can be arranged in three groups (Fournel 2012):

- *Solids*: the concentration of the carried solids can be described by a set of parameters. These include most commonly TSS (total suspended solids) and VSS (volatile suspended solids). Parameters describing organic pollution are largely dependent on the share of solid organic particles.
- *Organic pollution*: organic molecules are often biodegradable and yield nutrients as end-products. Organics are expressed in COD and BOD<sub>5</sub> or directly as TOC (total organic carbon), DOC (dissolved organic carbon) and VOC (volatile organic carbon). The organic pollution can be characterised by the COD/BOD<sub>5</sub> ratio which indicates biodegradability. Hardly biodegradable and toxic forms are polycyclic aromatic hydrocarbons (PAHs), pesticides and pharmaceutical compounds often grouped as organic micropollutants.

Furthermore, total COD is often separated into particulate COD (COD<sub>X</sub>) and dissolved COD (COD<sub>S</sub>) by filtration.

- *Mineral pollution*: nutrients can be described by the concentrations of total nitrogen (TN), organic nitrogen, ammonium-nitrogen (NH<sub>4</sub>-N), total Kjeldahl nitrogen (TKN), nitrate and nitrite (NO<sub>3</sub>-N, NO<sub>2</sub>-N) and phosphate (PO<sub>4</sub>-P). CSO can have significant heavy metal pollution (mainly Cu, Cd, Pb and Zn) and sometimes mineral de-icing salts (NaCl, CaCl<sub>2</sub>, KCl).

CSO is diluted compared to sewage regarding organics and nutrients expressed as COD, NH<sub>4</sub>-N and PO<sub>4</sub>-P. Still, flows rejected without treatment are one of the most important environmental concerns in Europe. The main effects of the pollutants in the releases are (based on Mitsch and Gosselink 2007):

- *TSS*: increasing turbidity in the receiving water, attaching in the gills of fish, forming deposits and shifting the benthic community, high organic content, most of the micropollutants travel with particulates.
- *Organics*: depletion of DO and shifting or destroying animal communities.
- *NH<sub>4</sub>-N*: this parameter is used to describe both ammonium- (NH<sub>4</sub>-N) and ammoniacal- (NH<sub>3</sub>-N) nitrogen. The proportion of NH<sub>3</sub>-N increases with higher pH and temperature. Ammonia is toxic to fish, amphibian and invertebrates. The substance causes bleeding gills and increases the transmissibility of the membranes of cells attacking the internal organs and even the skin of aquatic animals.
- *NO<sub>3</sub>-N*: causes eutrophication and algal blooms at increased concentrations. A shift in the trophic level of a water body can lead to ecological catastrophe.
- *PO<sub>4</sub>-P*: contributes to the eutrophication.
- *Heavy metals*: accumulation in the trophic cascade, acute toxicity.
- *PAHs*: possibility of acute toxicity on aquatic species, bioaccumulation.
- *Others*: The effect of many emerging pollutants and engineered molecules is often unknown and need further research.
- *Pathogens*: risk of human and animal health (CSO poses higher risk than SSO)

Incoming concentrations of most stormwater runoff parameters are time dependent due to the accumulation of dryfall on the catchment during the inter-event periods. At the beginning of the precipitation the accumulated materials are washed down. This entails pollutant loads are less linked to flow rates in time and makes sense to chart pollutant concentrations against time giving a *chemograph*. On chemographs it is often visible that rain events following a long deposition process are followed by a first flush of runoff which carries higher constituent concentrations than the runoff generated by the rest of the rain event. The first flush phenomenon is not observable though everywhere (Kadlec and Wallace 2009) and the constantly present dry weather flow makes the picture even more complex in the case of CSO.

Chemographs give an insight into single events which have high significance for research. However, statistics based on a large number of events and a large number of sites demanded the recent spreading of online probes, powerful computers and statistical software. The stochasticity of volumes and concentrations could not be easily followed intra-event. The flow-weighted mean called event mean concentration (EMC) was more apt to estimate the extent of pollution based on load series. EMCs of single events showed large differences but they indicated pollutant loads from CSO as well as descriptive statistics could be based on them for the comparison of different overflow sites. The value of EMC is calculated by Eq. 1:

$$EMC = \frac{\int QCdt}{\int Qdt} \quad 1)$$

where C is the instantaneous concentration [mg/L], Q is the instantaneous flow [m<sup>3</sup>/h] and t is the time [h].

Table 1 compares average CSO and SSO EMC values from multiple sites. It has to be stated for the interpretation that measured SSO and CSO qualities show high variability which is greatly dependent on the characteristics (slope, ratio of the sealed area, and return period of the rain events) of, and the material use at the watershed. The ranges are not representing minimum and maximum values but give a range of the average EMC values from multiple site-based statistics from the literature. It is generally true that CSO has higher concentrations of TSS, organics, nitrogen, phosphorous and coliforms. Stormwater wetlands treating SSO target in general the removal of solids, metals and PAHs or pathogens. The level of heavy metal pollution is greatly dependent on the material use and the presence of industry in the catchment, e.g. materials used for gutters and heavy industry in the case of both CSO and SSO treatment (Kadlec and Wallace 2009, Zgheib et al. 2012).

Table 1: Typical ranges of CSO and SSO concentrations. Values are average EMCs of multiple events and sites. Ranges represent the smallest and largest value found in the listed literature: a) Smullen et al. (1999); b) Kadlec and Wallace (2009); c) Fournel (2012); d) Sztruhár et al. (2002); e) Passerat et al. (2011); f) Zgheib et al. (2012) g) Schulz et al (1994); h) Gasperi et al. (2012). \*:TKN.

Parameter	Units	SSO [EMC]	CSO [EMC]
TSS	mg/L	78.4 <sup>a</sup> -106 <sup>f</sup>	85 <sup>c</sup> -430 <sup>d</sup>
BOD <sub>5</sub>	mg O <sub>2</sub> /L	14.1 <sup>a</sup>	35 <sup>c</sup> -135 <sup>h</sup>
COD <sub>tot</sub>	mg O <sub>2</sub> /L	52.8 <sup>a</sup> -89 <sup>f</sup>	99 <sup>c</sup> -445 <sup>d</sup>
TN	mg/L	2.4 <sup>a</sup>	3.6 <sup>c</sup> -16.8 <sup>d</sup>
NH <sub>4</sub> -N	mg/L	2.8 <sup>f</sup> *	2.0 <sup>c</sup> -9.9 <sup>h</sup>
TP	mg/L	0.3 <sup>a</sup> -0.9 <sup>f</sup>	1.3 <sup>c</sup> -3.5 <sup>h</sup>
Cu	µg/L	13.5 <sup>a</sup> -55.0 <sup>f</sup>	250 <sup>g</sup>
Pb	µg/L	27.0 <sup>f</sup> -67.5 <sup>a</sup>	250 <sup>g</sup>
Zn	µg/L	162 <sup>a</sup> -270 <sup>f</sup>	570 <sup>d</sup> -1020 <sup>g</sup>
Fecal coliforms	1000 CFU/ml	1.5 <sup>b</sup>	1.3 <sup>d</sup> -76 <sup>e</sup>

## 2.3 Legislative context

Legislations exist both at European and French national levels with a scope effecting stormwater wetlands directly or indirectly. The European Water Framework Directive (WFD; EU 2000/60/CE) is a framework for national and community water management policy. It defines categories for water quality based on hydromorphology, physicochemistry and biology for surface water and physicochemistry and quantity for ground water. It obliges the member states to make steps towards the targets of the framework via the national legislations. Good status has to be achieved for all waters, including the preservation of the status of those which already fulfil the criteria of calling it good. The WFD sets also quantitative thresholds on 41 priority substances or substance groups for discharges into surface waters. The WFD obliges member states to divide their territories into watersheds and create River Basin Management Plans for each, so not only to be encompassed into the national legislation but to take effect directly through more local executive bodies. The WFD was originally released with the deadline 2015 to achieve its goals. Later, the obligations were deferred to 2021 or even 2027 as assessments of the management plans have shown that reaching a good state of all water bodies needs a longer period.

The WFD is implemented in the French legislation by Act 2004-338 (October 2004) through the 'Water Management Scheme' (SDAGE - *Schéma Directeur d'Aménagement et de Gestion des Eaux*) at the level of the watersheds. At the local level, a 'Local Water Management Scheme' (SAGE - *Schéma d'Aménagement et de Gestion des Eaux*) is created and followed. Act 2006-1772 (December 2006) updates the French water policy framework by bringing in new objectives to those in WFD, in the perspective of this work notably by targeting the modernization of the organization and management of public water utilities including wastewater treatment. Although it is a common practice to release excessive flows originating from urban runoff which exceed the intake capacity of the municipal wastewater treatment plant (WWTP), these acts require the water authorities at the community level to limit direct release to natural waters.

From the dual emission/immission approach of WFD this work will focus on the discharge (emission). The water policies in France set the emission requirements for stormwater wetlands based on the receiving water body, considering the potential effects on the ecosystem of each. These include setting a limit on the overall effluent rate and the concentrations of TSS, total COD and NH<sub>4</sub>-N (total nitrogen and phosphorous limits are possible as well).

## 2.4 Vertical flow constructed wetlands for CSO treatment

### 2.4.1 Structural and operational traits of CSO CWs

Numerous BMPs exist for the treatment of urban stormwater. Centralized solutions are promising in Europe where urban and suburban areas are densely built and the historical tendency of building combined sewer networks often demands overflow point treatment of CSO. It is to mention that CSO CWs are ideally paired with decentralized solutions for infiltrating stormwater before reaching the sewer. An ultimate treatment goal was proposed by Geoff et al. (2016): the preservation or restoration of the receiving waters. The available practices should be looked at site-specifically and as complementary options rather than competitive. The present work focuses on the French standard of CSO CWs.

CSO CWs are usually installed after a single overflow structure of storm-generated flows. Their purpose is to mitigate environmental effects. The French system can be deployed as single



object for endpoint treatment due to its robustness. A classical CSO CW has different compartments which serve different functions. These compartments are, from top to bottom:

1. Storage basin: the detention space is for storing the arriving overflows which often arrive in a short period of time on the wetland. Satisfying treatment of this water is not possible in such a short time due to the nature of the physical-chemical processes taking place. The storage basin is often called retention room or layer as well. The term retention layer is originating from the conceptual models of these wetlands where it is represented as a layer indeed. Classical VF CWs lack this basin or if they have it represents a small volume for the storage of impulse-like loadings.
2. Deposit layer: the deposit layer is self-forming at operation. It does not affect treatment performance negatively with an optimized design but improves it. It is called also sludge blanket. Physical, chemical and biological removal processes take place as the water infiltrates and percolates vertically.
3. Filter layer: the filter material supports the growth of the biofilm and plants. Physical, chemical and biological removal processes take place as the water percolates vertically. Hosts a network of aeration pipes just above the drainage layer.
4. Drainage layer: contains the network of the drainage pipes and has a larger grain size as the filter layer does. The concentration of microorganisms decreases with depth and due to the smaller active surface this layer has little role in the treatment (Meyer 2011).

Flows arriving to CSO CWs are stochastic in terms of volumes, concentrations and return periods. System operation can be divided to intra-event (loaded) and inter-event (unloaded) periods. Dittmer (2006) described that these periods differ also in the dominant removal processes as well. Therefore, it is essential to discuss them separately. Fig. 3 shows the alternation of inter- and intra-event periods based on the water level in a filter. The characterization of the states and their dominant removal processes are described based on the similar German systems (Dittmer et al. 2005; Uhl and Dittmer 2005; Dittmer 2006; Dittmer and Schmitt 2011; Meyer 2011) and a summary is given below and in subchapter 2.4.2.

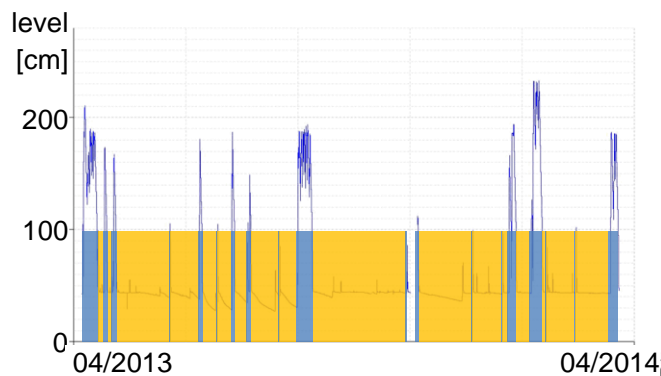


Fig. 3: Alternation of intra-event (blue) and inter-event (ochre) periods. The periods are well discernible based on the stage in the CSO CW (blue series).

Intra- and inter-event periods can be divided further into sub-categories according to hydraulics and stage as shown on Fig. 4. The duration of each state is exposed to the stochasticity of the loadings rates and return periods themselves.

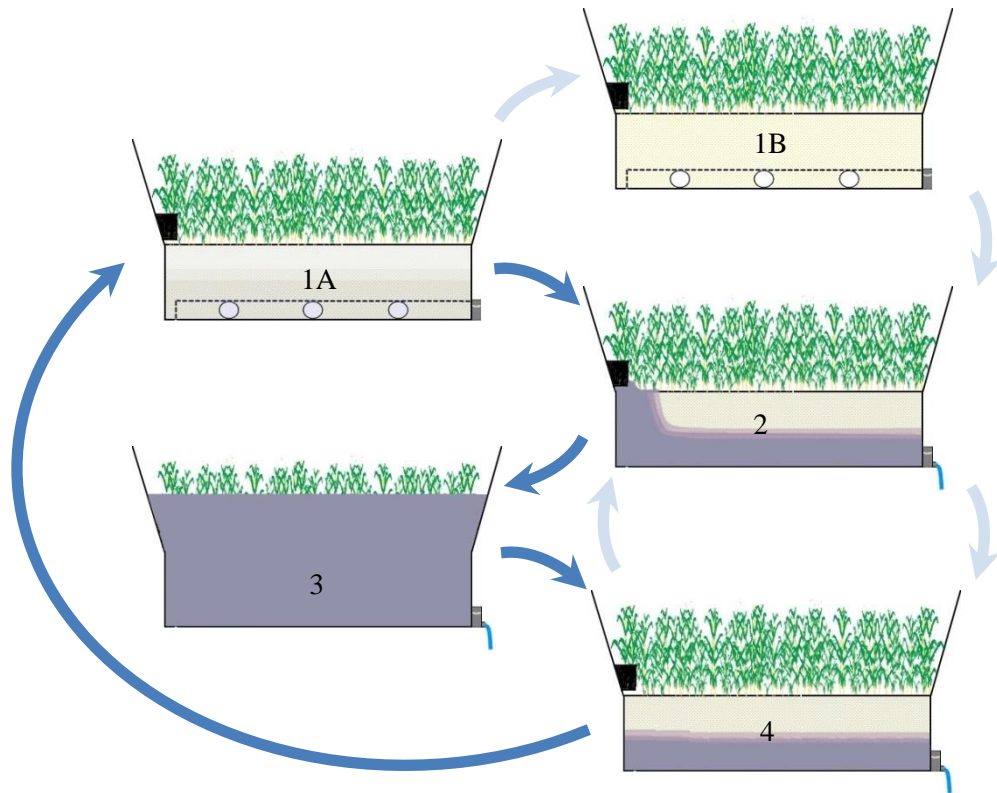


Fig. 4: The five states of a CSO CW. The classical alternation of intra- and inter-event periods can be broken down further as shown by stages 1A-1B and 2-4, respectively.

State 1A is the inter-event state of the filter in the classical sense. It establishes between two consecutive loadings and is the most durable. It is often referred to as “dry period” which is a misleading description. In fact, the filter stays moist after the gravity drainage of the water. The pores are filled with air and aerobic processes dominate, most importantly nitrification.

State 1B is the exact definition of a dry period. It might follow seldom the classical inter-event state. This condition is unwanted and occurs after extremely long periods without any load. There is a lack of some nutrient since long and the filter media has even dried out. This impacts negatively the ecosystem including the biofilm in the filter layer. If cracks occur on the deposits or in the filter, hydraulic short-circuits might decrease performance even further. Dittmer (2006) refers to lab-scale experiments in which biomass decreased after three weeks as well as COD removal decreased from 96 % to 74 % after three months without load. The effect might be more rapid in the case of open-air systems due to higher ET (evapotranspiration) rate. An impact on  $\text{NH}_4\text{-N}$  removal was not observed as it is removed by physical sorption during the loading. The occurrence of state 1B should be avoided, e.g. as proposed by Kadlec and Wallace (2009), by considering water sources for irrigation.

State 2 is normally a short period after the loading starts. It lasts ideally less than an hour; however, its duration depends on the difference of the inflow and the outflow rate. If the difference is small, this period might last long which is unwanted. The partial saturation of the filter means that only a share of the media is hosting removal processes and the percolation speed is high. This phenomenon is called short-circuiting. In comparison, the normal operation of the filter is close to

plug-flow (state 3) due to an outflow-limiting orifice (Dittmer 2006). Short-circuiting is expected to lead to a decrease of treatment performance.

The following state 3 is the longest of the intra-event states 2-4. It can last up to two days in the case of extreme precipitation events. Filter performance is the maximum due to the near plug-flow in the full volume of the filter. Seldom, for the smallest events, the water might stay below the surface of the filter so this state is absent or fleeting.

In state 4, the loading has stopped and the filter drains. The flow remains plug-flow. Aerobic processes start as air enters the pore space.

#### 2.4.2 Removal processes and efficiency

The treatment of stormwater in VF CWs is based on the interaction between the solid and liquid phase just as in any other SSF CWs. Water flow and solute transport have significant effect on the performance as it determines contact times between the pollutants and the inner pore surfaces. Though normally the particle size and the particle size distribution have the greatest effect on water flow and solute transport through the hydraulic properties (with special regards to conductivity) of the porous media, this is different in the case of CSO CWs. The outflow rate is limited at the outlet structure by an orifice. This orifice limits the percolation speed significantly compared the hydraulic conductivity of the used materials. The target range of velocities is 0.036-0.180 m<sup>3</sup>/m<sup>2</sup>/h or 0.01-0.05 L/s/m<sup>2</sup> (Meyer 2011). This ensures a uniform, near plug flow even in coarse media. The difference in the performance was measurable between the two ends of this range at column-scale where wall effects could get pronounced (Dittmer 2006).

Removal processes can be linked to the intra- or inter-event periods based on their dominant occurrence. The filter surface filters physically high amounts of solids in intra-event periods. Most solids are retained during and at the end of the ponding by the combined effect of filtration and sedimentation and by settling of the floating materials when ponding is over. The intrusion of the solids into the filter layer was less than 0.02 m in the case of German systems using a well-graded sand media of 0-4 mm (Dittmer 2006). The formation of the *sediment layer* is detectable even in the case of pre-settled water from CSO tanks but it is not pronounced for wetlands treating SSO (Zgheib et al. 2012). Sediments pose clogging risk when the system ages (or due to inappropriate design). On the other hand, sediment layers are rich in organics and small-particles and provide i) protection against drying, cold and erosion; ii) high adsorption capacity; iii) optimal environment for living organisms due to its water and nutrient contents; iv) surface distribution of inflows at short-circuiting in State 2 (Fig. 4) due to low conductivity.

The *filter layer* is the sole place of treatment until the sediment layer is formed. The sediment layer and the filter layer are going to be referred to as 'filter layer' in the following description. The filter layer takes a large share in the *filtration* processes of small particles. It was shown by Dittmer (2006) that particles below 5 µm and even flocculated colloids are removed. *Adsorption* takes place on the physical surfaces and the adsorption capacity is enhanced by the developing biofilm and surface sediments. Adsorption is the dominant process of NH<sub>4</sub>-N retention. Furthermore, uptake related to *biological activity* just as absorption into the biofilm might be responsible for the intra-event removal of dissolved COD (COD<sub>S</sub>). Intra-event removal processes are considered to be dominantly anaerobic and the operation is close to a regular SSF wetland. For a general description of these processes the reader is advised to rely on Kadlec and Wallace (2009). The specificity of pollutant removal in CSO CWs is to be sought rather in the alternation intra- and inter-event periods. After the filter is gravity-drained, air fills the pores and aerobic processes occur in the wet

environment. Nitrification is the most important process of the inter-event state. The previously adsorbed ammonium is transformed into nitrate through the aerobic pathway. The adsorption sites regenerate and NO<sub>3</sub>-N will be flushed out at the beginning of the next feeding. The wet and aerobic environment favours the mineralization of the organics with special regard on the solids lying or filtered out at the top of the filter (Dittmer et al. 2005, Uhl and Dittmer 2005, Meyer 2011, Dittmer and Schmitt 2011).

A conclusion from the alternation of intra- and inter-event removal processes is that although removal efficiency can be measured intra-event, removal happens also at the inter-event regeneration. EMC based removal efficiencies reported for a range of technologies are summarized in Table 2. (RSFs are CSO CW technology widely applied in Germany and are the closest to the French standard.) All values are derived from multiple measurements at multiple sites except for TOC for RSFs which is the average of multiple measurements at the RSF Kenten.

Table 2: Removal rates of different technologies for CSO and SSO treatment. Values are based on measured EMCs or the equivalent mass removal by event. Sources are a: EPA 1999a; b: EPA 1999b; c: Kadlec and Wallace (2009); d: EPA 1999c; e: Waldhoff 2008; f: Pinnekamp 2013; g: Frechen 2013.

Parameter	Sand filters <sup>a</sup>	Typical removal efficiency [%]		
		Bioretention <sup>b</sup>	FWS	RSFs
TSS	70	90	68 <sup>c</sup>	93 <sup>e</sup>
BOD <sub>5</sub>	70			
COD <sub>tot</sub>				86 <sup>e</sup>
TOC	48	90	34 <sup>d</sup>	62 <sup>f</sup>
TN <sub>S</sub>				
TN	21		30 <sup>c</sup>	
TKN	46	68-80		
NH <sub>4</sub> -N			31 <sup>c</sup>	83 <sup>e</sup>
NO <sub>3</sub> -N	0		45 <sup>c</sup>	
TP	33	70-83	41 <sup>c</sup>	80 <sup>e</sup>
Cu		93-98	49 <sup>c</sup>	78 <sup>g</sup>
Pb	45	93-98	74 <sup>c</sup>	64 <sup>&lt;g</sup>
Zn	45	93-98	60 <sup>c</sup>	62 <sup>&lt;g</sup>
Faecal coliforms	76	90	77 <sup>d</sup>	90 <sup>e</sup>

### 2.4.3 Overview of CSO CW practice in Europe

Meyer et al. (2013) overviewed CSO CWs comparing German, French and Italian approaches. The application of VF CWs for CSO started in Germany where the first installations dated to 1989. The first filters were built from natural soils thus CSO CWs were referred to as retention soil (RSFs, *Retentionsbodenfiltern*). Soil was later replaced by technical sands to delay clogging. Classical RSF systems receive water from a CSO tank storing runoff volumes up to 1.5-3.5 mm of rainfall. These tanks allow sedimentation before overflow due to their size. Their adverse effect is the extension of inter-event periods (less frequent overflows) and water stress of the wetland ecosystem.

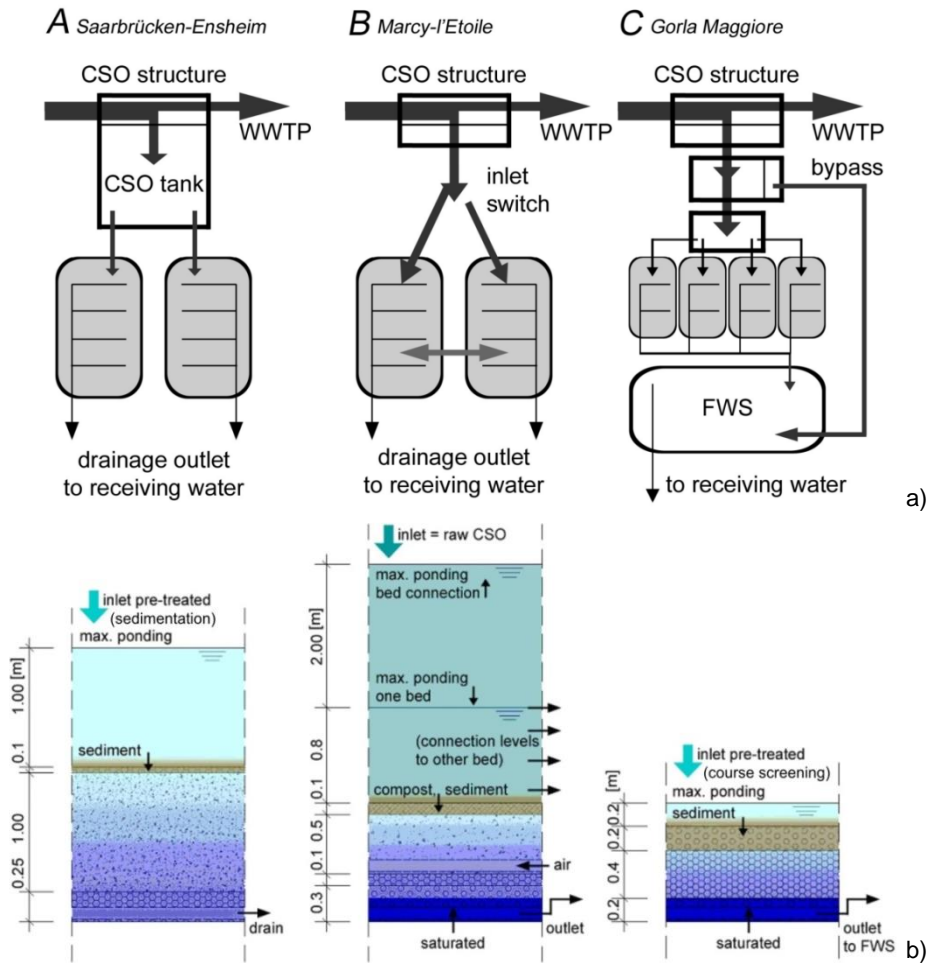


Fig. 5: The German, French and Italian wetland systems for CSO treatment. Panel a: overview of the treatment chain. Panel b: cross-section of the VF CW in the treatment chain.

The first German standard of RSFs was published in 2005 in the DWA Merkblatt 178 (DWA 2005). This standard had later a key role when creating the French and Italian concepts. Fig. 5: The German, French and Italian wetland systems for CSO treatment. Panel a: overview of the treatment chain. Panel b: cross-section of the VF CW in the treatment chain. compares the features and layering of the German, French and Italian CSO-systems. The wetland at Saarbrücken-Ensheim is representing just one of the several state-of-the art systems in Germany whilst the installation at Marcy l'Etoile and Gorla Maggiore are the pioneer full-scale systems. The fundamental difference is that the CSO tank has been excluded from the treatment chain. This means increased solid loads and more frequent loadings (Meyer et al. 2013). A detailed introduction of the French standard follows in the next chapter.

## 2.5 Numerical models of CSO CWs

### 2.5.1 General considerations

The treatment of combined sewer overflow (and stormwater in general) is characterized by the stochastic nature of rain events. As such, design approaches, which are commonly applied for wetlands treating sewage or other continuously available flows, are unsuitable for CSO CWs.

Numerical models were applied soon to understand CSO CWs better. Modelling seemed to be a challenging task just as design, again, due to the stochasticity of rain events and mainly due to its effect on removal efficiencies of the different pollutants. Models for the problem were used or developed with the following aims:

- iii) Mechanistic, process based models to have better insights into internal processes,
- iv) Design-support models to support and optimize site-specific design.

As stated in Meyer et al. (2015), all types of models are valuable, but some perform well when used for scientific purposes and others for engineering. Mechanistic models are often complex which carries great scientific value but encumbers practical applications by engineers.

### 2.5.2 Finite element modelling of CSO CWs

HYDRUS (© PC-Progress s.r.o.) is a model package to simulate variably-saturated flow, heat and solute transport in the porous media. It is a process-based tool which numerically solves Richards' equation and the convection-dispersion equation for heat and solute transport (Šimůnek et al., 2011). The tool was enabled to simulate pollutant removal in CWs with the release of the wetland module extension (Langergraber and Šimůnek, 2012). This offered two biokinetic models structured similarly as the Activated Sludge Models (ASM, Henze et al. 2000). Although the extension was not designed for event-driven wetlands, CW2D (Langergraber and Šimůnek, 2005) was tested for simulating of hydraulics and removal performance in CSO CWs.

Even if HYDRUS/CW2D was designated to work with continuous or frequent feeding patterns, the tool had nearly all sub-models necessary to describe the internal processes of CSO CWs. The exception was the particulate transport (filtration). Research pushed out the limits of CSO CW application progressively in Heinrichs et al. (2007; 2009), Meyer (2011) and then in Meyer et al. (2013) and effluent  $\text{NH}_4\text{-N}$  was fitted to measurements. Even so, a quasi-stable biomass could not be reached and this meant problems with the predictions on COD removal. Simulations showed the sign of unlimited biomass growth. Long term simulations failed to reproduce measured effluent concentration series for the pollutant. As COD and  $\text{NH}_4\text{-N}$  are both key pollutants, this left room for further investigation using HYDRUS/CW2D.

### 2.5.3 Design-support modelling of CSO CWs

Design-support models are simplified compared to process based finite-element models. Simplicity is expected to be correlated to practicability and therefore is an expectation rising from the engineering aim and the targeted users of these tools (Meyer et al 2015). The development of simplified tools targeting CSO CWs started almost at the same time when the first mechanistic model package (Langergraber and Šimůnek, 2005) was created for CWs in general.

There was one key lineage of design-support models for CSO treatment using vertical filters with well-documented evolution. The development was targeting the German Retention Soil Filters (*Retentionsbodenfiltern*). The first model was called RSF\_Disc. Its conceptual structure was created by Dittmer (2006) and was later implemented as an internal extension of an existing sewer simulation tool called KOSMO (Schmitt and Dittmer 2007). The concept and process equations were taken later as the basis of RSF\_Sim, implemented by Meyer (2011) and published in a cleared and advanced form in Meyer and Dittmer (2015). Effluent concentrations of  $\text{NH}_4\text{-N}$  were

successfully fitted to single events and medium term event series at full-scale by Tondera et al. (2013). RSF\_Sim is dedicated to support the scaling of RSFs.

Hydraulics is modelled by a tanks-in-series (TIS) model (Fig. 6). The wetland is represented by three tanks. From top to bottom these are: i) retention tank (ponding water); ii) process layer (subsurface water); iii) drainage layer (subsurface water). Such simplification of the otherwise complex hydraulics of any vertical subsurface flow wetlands was possible due to the outflow orifice. This feature limits the outflow rate and consequently the exchange rate between model compartments.

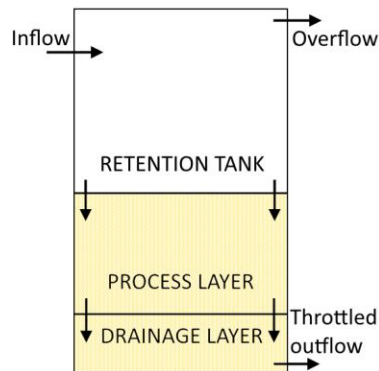


Fig. 6: Hydraulics in RSF\_Sim: TIS model (based on Meyer and Dittmer, 2015). The outflow structure comes with an orifice which throttles the flow. This feature is represented by a constant in the model, enabling a high level of simplification in the hydraulics, i.e. to model the system accurately as TIS.

Removal processes are modelled in the tank representing the process layer. Modelled pollutants are TSS, COD and  $\text{NH}_4\text{-N}$ . Dissolved and particulate COD fractions (COD\_S and COD\_X, respectively) are modelled separately. Process equations are based on the following principles:

- i) TSS and COD\_X are decreased to a constant background concentration in the effluent.
- ii) COD\_S is reduced by fixed removal efficiency, with the possibility to curb effluent values with a background concentration. A correlation factor is used to express performance drops after long dry periods.
- iii)  $\text{NH}_4\text{-N}$  removal is separated to intra-event adsorption and inter-event nitrification. Adsorption is expressed by a two-stage linear isotherm. Nitrification is dependent from the temperature and the adsorbed mass.

The modelled effluent series were fitted to  $\text{NH}_4\text{-N}$  concentrations of full-scale sites (Tondera et al. 2013, Meyer and Dittmer 2015). RSF\_Sim had been implemented in a MS Excel© table so the manual testing of different designs is needed for optimization. Finally, the tool is incompatible with the French standard. These reasons inspired the development of a new tool.



### 3 Setup of field experiments and model building

#### 3.1 Pioneer full-scale application of the French CSO CW: Marcy l'Etoile

##### 3.1.1 Wetland layout (Meyer et al. 2013, EPUR 2012)

The pioneer CSO CW was built in France in 2012 at a satellite town of Lyon called Marcy l'Etoile. It is the flagship and only CSO site in the ADEPTE project. The design load is 1160 m<sup>3</sup> which is the one year return flow what the site has to be able to detain and effectively treat. The watershed is 98 ha and the main dwelling type is single household. Dry weather flow was estimated to be equivalent to 9600 PE from the dwellings and industrial sources.

Fig. 7 shows the layout of the wetland. Discharged from the sewer [1], the flow continued towards the filter (F1 and F2) through a sand and grease trap [2] and the Venturi channel [3] allocated for inflow measurements. The wastewater loaded either filter bed 1 (F1, 253 m<sup>2</sup>) or 2 (F2, 245 m<sup>2</sup>), depending on the splitter [4] position. The kinetic energy of the incoming water was mitigated by gabions located below the inlet points [5] to avoid the remobilization of the filter material. The infiltrating water percolated through the porous media and was collected by a drain network distributed below the whole filter. Single bores limited the outflow rate on closed and exchangeable vertical pipes to 0.008 or 0.016 L/s/m<sup>2</sup> [6]. The vertical position of the orifices sets the level of the permanent saturation. Overflows can occur during extreme events through a trapezoid weir [7] located at the rim 2.1 m over the filter surface.

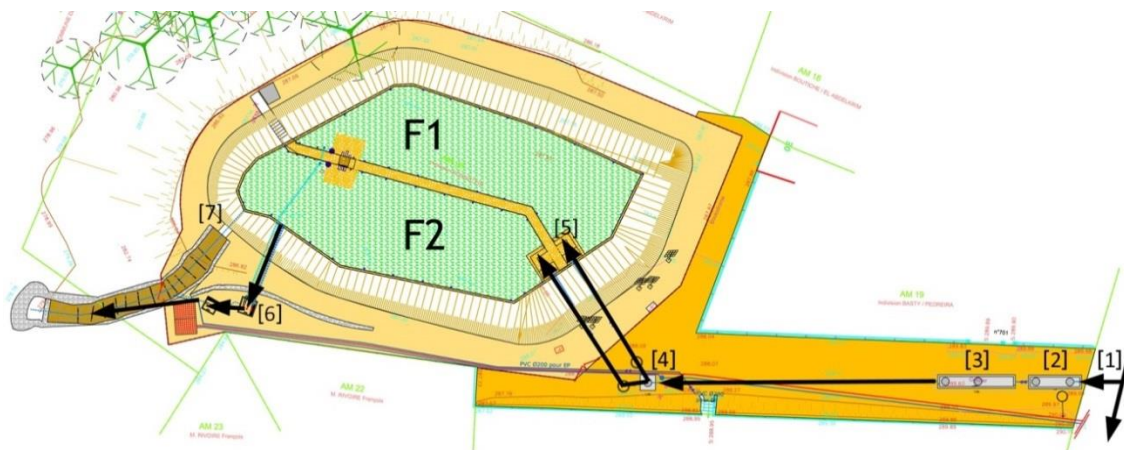


Fig. 7: The routing of flows towards, into and from the filter at Marcy l'Etoile. Point [1] marks the CSO structure and the green rectangles the two filters with the wall between them.

F1 and F2 have identical layer structures (Fig. 8). The drainage pipes run in 0.3 m of 10/20 mm gravel topped by 0.1 m 2/6 mm gravel. The aeration pipes run above the permanently saturated water layer. The permanent water helps to avoid water stress during long dry periods. The filtration layers are 0.6 m deep coarse media (F1: 0/4 mm; F2: 4.0/6.3 mm) in order to avoid clogging. The filter material is a mixture of fluvial sand (0.48 cm) and zeolite (0.12 cm, chabazite) in F1 whilst pozzolana in F2. Zeolite was used to increase NH<sub>4</sub>-N adsorption capacities; on the other hand, pozzolana was expected to have high adsorption capacity naturally. There is 0.1 m of compost on the top of the filters which was applied with the purpose to favour reed growth. Both filters are



planted with common reed (*Phragmites australis*) which had been grown to strength by the time of the experiments. Reed growth and stem movements caused by the wind help to keep the sludge blanket permeable.

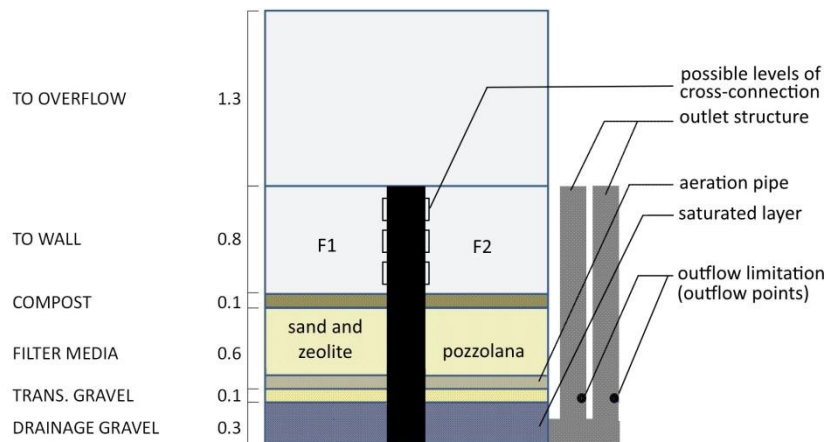


Fig. 8: Cross-section of the filter at Marcy l'Etoile. Units are given in metres.

### 3.1.2 Operation

The operation of the facility and its instruments can be divided into three phases based on the installed equipment and the characteristics of the water loaded on the filter:

- The first phase started in 2012. It lasted for a year and the filter received unknown loads of CSO. Overflows started to be dominated by industrial waters from a medical plant. This water was rejected when cleaning tanks, which were used to produce growth medium for bacteria. The industrial discharge was about 5-10 times the mean dry weather flow (about 50 m<sup>3</sup>/h), lasting for a few hours with a daily return. This first year was dedicated to the *establishment of the biological communities*, without measurements.
- The second phase started in 2013, with installing an adjustable weir to avoid daily loads. Level adjustments allowed generating a natural loading pattern. The weir was opened according to the forecasted storm events. Industrial flows still exceeded the volume of storm-originated flows, although there were a few, purely precipitation-triggered events caught as well. The period is going to be referred as *standard monitoring*.
- Additional equipment was installed for the third period which is going to be referred as *detailed monitoring* period. This period allowed the monitoring of outflows by filter side and with online probes. The feedings were artificially triggered by opening the weir. This means that in the majority of the cases stormwater was absent from the feedings. The phase served specific experiments like the tracer test, the measurement of adsorption capacities and the measurement of nitrification rate.

## 3.2 Monitoring targets and equipment

### 3.2.1 Monitoring of flows and water level

A weir was installed at the overflow point of the sewer at the start of the monitoring period in order to control feedings and create representative annual loads and time distribution of loading

events. Industrial releases represented a flow 5 to 10 times higher than the dry weather flow. The weir had to be adjusted to avoid daily feedings. On one hand, this meant small rain events were triggering feedings only if happening simultaneously with the industrial release. On the other, feedings could be artificially triggered by decreasing the weir to create extreme loads or to control the length of inter-event periods. The annual hydraulic loads are shown on Fig. 9 [ $\text{m}^3/\text{m}^2$ ]. Inflow volumes were registered in a Ventury channel based on water levels measured by an ultrasonic probe (Aqualyse Aqua Venturi® AV1000)

The water level was monitored using pressure probes (STS ATM.1ST/N/T) installed in each filter side. Measurements enabled to calculate the volumes inside or above the filter material. As such, the changes in the storage were known. Annex D introduces charts where water levels, inflow rates and hydraulic loads can be followed for the whole monitoring period.

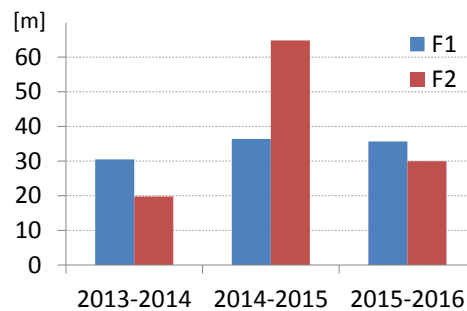


Fig. 9: Annual hydraulic loads on the filter sides. F1: sand (0.48 m) with zeolite (0.12 m); F2: 0.6 m pozzolana.

At the outlet, an inductive flow meter (Krohne Waterflux 3070) was installed to measure effluent rate from the system. For the period of the *intensive monitoring*, this device was used to calibrate the correlation (Fig. 10) between the outflow rate from the orifices and the pressure head in the outflow structures. The correlation enabled to record outflow rate by filter side adding a second pair of the same type of pressure probes in the outflow pipes. The pressure head – orifice flow correlation was calculated based on Bernoulli's law using Eq. 2, on a purely mathematical basis. The differences in the flow rate predicted by the two different methods were negligible.

$$Q = \mu_V \times A \times \sqrt{(2gh)} \quad 2)$$

where  $\mu_V$  is the discharge coefficient for the small and sharp edged orifice (0.61); A is the area of the orifice.

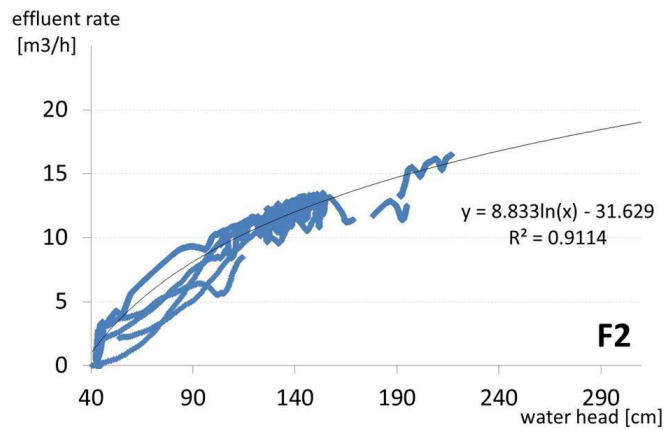


Fig. 10: Measured correlation of pressure head – orifice flow. Pressure probes were installed in the outflow structure.

### 3.2.2 Monitoring of pollutant concentrations

Automatic samplers (Lange Bühler 2000/1027) were installed for flow composite sampling and to record pollutographs at the inlet and the outlet. All samples were flow composite in this period (standard monitoring). Outlet samples were mixed water of the two filter sides at the outlet. A third sampler was added later and samples were taken by filter side from the 15<sup>th</sup> event on. The effluent was sampled time composite in this period (intensive monitoring), and the volumes which the samples were representative for were calculated with the orifice correlation.

The median inlet EMC at the site was comparable to typical CSO concentrations, although in the case of nutrients, it was slightly above them. Concentration values are summarized in Table 3 (repeating typical CSO values from Table 1).

Table 3: Inflow concentrations at Marcy l’Etoile. The values are compared to CSO concentrations from the following literature: c) Fournel (2012); d) Sztruhár et al. (2002); e) Passerat et al. (2011); g) Schulz et al (1994); h) Gasperi et al (2012). Values are average EMCs of multiple events and sites. Ranges represent the smallest and largest value found in the listed literature.

Parameter	Units	CSO [EMC]	Marcy l’Etoile [EMC]*
TSS	mg/L	85 <sup>c</sup> -430 <sup>d</sup>	220
BOD <sub>5</sub>	mg O <sub>2</sub> /L	35 <sup>c</sup> -135 <sup>h</sup>	76
COD <sub>tot</sub>	mg O <sub>2</sub> /L	99 <sup>c</sup> -445 <sup>d</sup>	220
TN	mg/L	3.6 <sup>c</sup> -16.8 <sup>d</sup>	
TKN	mg/L	22 <sup>h</sup>	21,6
NH <sub>4</sub> -N	mg/L	2.0 <sup>c</sup> -9.9 <sup>h</sup>	13,8
TP	mg/L	1.3 <sup>c</sup> -3.5 <sup>h</sup>	9,6
PO <sub>4</sub> -P			6,5
Cu	µg/L	250 <sup>g</sup>	32.5
Pb	µg/L	250 <sup>g</sup>	3.3
Zn	µg/L	570 <sup>d</sup> -1020 <sup>g</sup>	109
Fecal coliforms	1000 CFU/ml	1.3 <sup>d</sup> -76 <sup>e</sup>	

The sampling frequency was adjusted after the first results. Pollutographs allowed seeing the limits of the system. These were expected to occur as a drop in treatment performance during heavy loads, most importantly a breakthrough of NH<sub>4</sub>-N with the saturation of the adsorption sites. Water quality varied also at the beginning of an event. The volumes of the first samples were decreased to

record any first flush in the inflow or short-circuit effects and NO<sub>3</sub>-N washout at the outflow. Table 4 gives an overview of the sampling strategy. The samples were analysed for total suspended solids (TSS), total COD (COD<sub>tot</sub>), dissolved COD (COD<sub>S</sub>), NH<sub>4</sub>-N, NO<sub>3</sub>-N and PO<sub>4</sub>-P, following standards methods (APHA). In some cases, samples were analysed for TKN, BOD<sub>5</sub>, TP, TOC, DOC, and NO<sub>2</sub>-N as well.

Table 4: Mean volume covered by a composite sample, by event. The number of samples is given by filter side where the outflow has been sampled accordingly, e.g. 9+9 (sand and zeolite filter and pozzolana filter, respectively).

Event	Event volume [m <sup>3</sup> ]	Number of samples in/out	Composite samples represent in / out [m <sup>3</sup> ]	Event	Event volume [m <sup>3</sup> ]	Number of samples in/out	Composite samples represent in / out [m <sup>3</sup> ]
1	3000	-	-	17	491	2/6+7	246/38
2	300	2/6	150/50	18	448	3/9+8	149/26
3	280	5/4	56/70	19	793	1/14+14	793/28
4	300	5/4	60/75	20	747	2/8+8	374/47
5	2900	28/26	104/112	21	650	4/8+9	163/38
6	1200	1/6	1200/200	22	360	1/8+8	360/23
7	2800	10/18	280/156	23	742	1/10+10	742/37
8	1300	7/11	186/118	24	1321	4/9+9	330/73
9	537	4/14	134/38	25	1011	2/11+8	506/53
10	1020	4/6	255/170	26	1080	6/9+8	180/17
11	1665	9/16	185/104	27	1493	4/10+11	373/71
12	1380	6/11	230/125	28	1496	6/9+9	249/83
13	7500	16/23	469/326	29	1774	5/8+8	355/111
14	5600	13/23	431/243	30	3990	4/6+6	998/333
15	1607	7/9+9	229/89	31	6400	6/9+9	1067/356
16	290	1/5+5	290/29				

### 3.2.3 Targeting specific processes of filter functionality

Effluent samples were taken by filter side in the *intensive period of monitoring* (02.2015 – 05.2016). The monitoring goals included specific targets. These were anticipated to help to have a better insight in the system and to quantify phenomena otherwise difficult to measure. As such, above the standard monitoring of filter performance, this period included the experiments shortly outlined below. The description here focuses on an overview of technical aspects. A more detailed discussion can be found in the manuscript “Filling hydraulics and nitrogen dynamics in full-scale CSO CWs” (Pálffy et al. 2016a) of the subchapter “Performance and process dynamics of the first full-scale CSO CW in France”, presented later.

#### *Tracer test with multiple tracer injections*

The purpose of the experiment was to understand better the dilution effects at short-circuiting, with special regards to the evolution of the nominal detention time from an empty filter to filter saturation. To carry out the experiment, the outflow orifice of one filter side was blocked. This filter was filled to the top of the wall after closing all cross-connections and was used as a storage basin for the experiment. Only the drainage gravel was saturated in the other filter side at the beginning of the experiment.

A fluorimeter (GGUN-FL 932), calibrated with effluent from the site, was installed at the outlet structure. Then, water was pumped from the storage basin on the empty filter, ensuring a stable and low inflow rate and a slow, progressive saturation of the filter media. A fluorescein

solution was pumped to the inlet point using a peristaltic pump three times for a short period, to generate tracer spikes at the outflow. The concentration of these spikes was expected to be in inverse correlation with the saturation level (pressure head) at the time of the injection.

*Online monitoring of NH<sub>4</sub>-N and NO<sub>3</sub>-N in the effluent*

These pollutants were monitored by filter side using online probes (WTW Varion). For NH<sub>4</sub>-N, the purpose was to follow short-circuiting peaks in the effluent. The measurements were later analysed to see i) if there is NH<sub>4</sub>-N breakthrough due to short-circuiting; ii) to define the extent of this sort of short-circuiting effect; iii) if the extent is considerable, try to define alternative designs which might minimize the effect. Sampling frequency was one minute. The quality of probe measurements was ensured by taking composite samples simultaneously and analysing those at a certified laboratory. In ideal case, probe concentrations and lab results of grab samples had been identical (Eq. 3):

$$\int_{t_n}^{t_{n+1}} C dt, probe = C(n) \tag{3}$$

The actual shift was calculated based on linear regressions. Fig. 11 shows an example of the method done for both sides and for both pollutants by each event. Furthermore, three additional grab samples were thickened by NH<sub>4</sub>Cl and Ca(NO<sub>3</sub>)<sub>2</sub> to cover higher concentration ranges as well. The thickening was done at the beginning of each nitrification rate experiments (see below at the section “Load series with closed mass balances”).

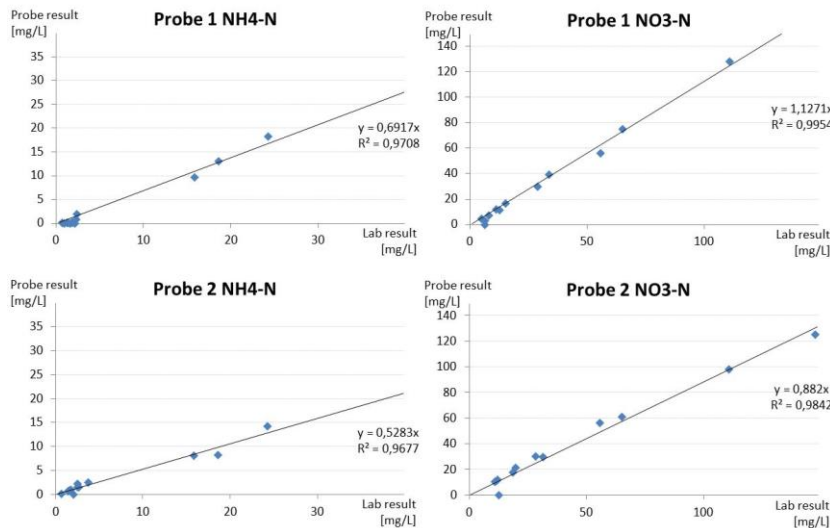


Fig. 11: Correlation of probe measurements and laboratory analysis. The correlations were set by event, based on the composite samples taken from the outflow and three grab samples thickened by NH<sub>4</sub>Cl and Ca(NO<sub>3</sub>)<sub>2</sub>.

*Measurement of water content in the porous media*

The water content of the porous media was monitored to visualize the spatial heterogeneity of the percolation at the beginning of events, i.e. until the saturation of the filter. Measurements were done with one minute sampling frequency along the longitudinal section of the pozzolana filter. It was assumed that the sludge blanket works against short-circuit effects by distributing inflows on a

larger filter surface before infiltration. On the other hand, the capillary effect was expected to support the plants and biomass with water in long dry periods, via a rise from the permanently saturated layer into the filter layer.

Time domain reflectometry (TDR) probes were used to monitor changes in the volumetric water content. The method is based on measuring the transit time of waves along a probe in the soil, based on the properties of electromagnetic waves. The measurement principle is based on the relationship of the water content and the dielectric constant. Fig. 12a shows one of the eighteen, 30 cm triple-wire TDR probes (six Campbell Scientific CS610 and twelve probes built in-house at UCL Belgium). For a more detailed description of the method or the design of triple-wire probes, the reader is advised to refer on Heimovaara (1993), Ledieu et al. (1986) and Topp et al. (1980). Due to the length limitation on the 50 Ohm coax cables, the related equipment was installed over the wall between the filters.

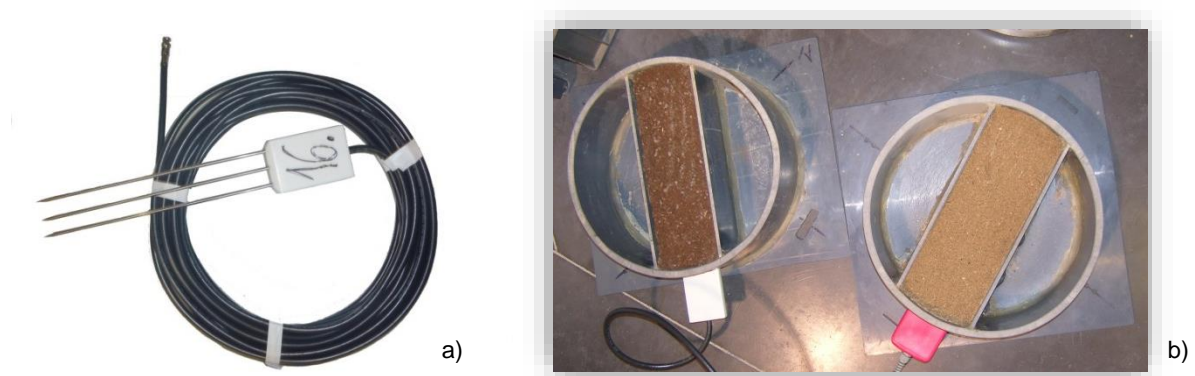


Fig. 12: Triple-wire TDR probe and in-house calibration (panel a and b, respectively). Note the two different filter materials on panel b: pozzolana (left) and sand and zeolite mixture in a ratio of 4:1 (right).

Although Topp's equation is a good estimation of the correlation between the permittivity and water content, the probes were calibrated in the lab for the sand and pozzolana used at Marcy l'Etoile (Fig. 12b). This might give better results because the materials were coarse. The same method was used as described by Fournel (2012) and the reader is advised to refer on that work for a detailed description of the calibration process. The measurements were done at ten known water content in five litres of material, repeated fifty times in a four second delay. The materials were then dried and wetted again to have three series of measurements. Fig. 13 shows the calibrated correlation between the relative dielectric constant and the volumetric water content. The apparent length and the offset of all probes were determined based on measurements repeated three times in air and water. As such, it was satisfactory to do calibration with one probe and make corrections later for each probe to diminish all differences in predicted water content originating from different lengths and offsets they have (Robinson et al. 2003).



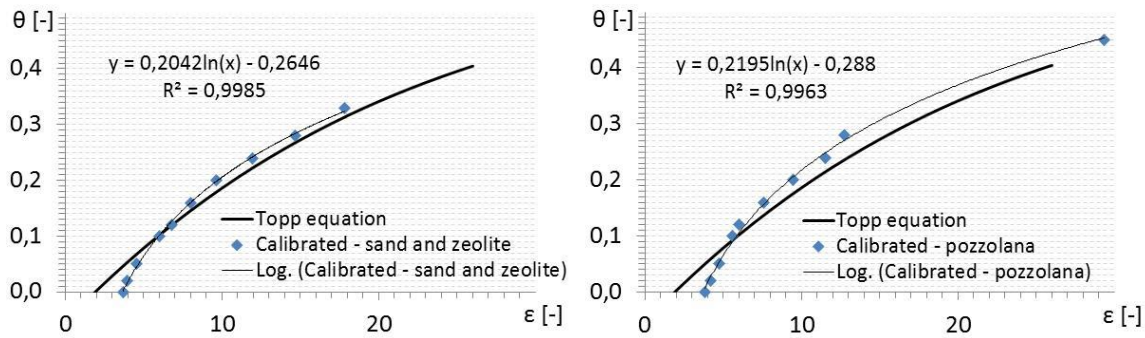


Fig. 13: Correlation of the dielectric constant ( $\epsilon$ ) and soil water content ( $\theta$ ) for the filter materials.

### *Load series with closed mass balances*

The purpose of setting up closed mass balances was to measure nitrification rate on the field scale. The weir at the overflow structure and the regular industrial release enabled to regulate loads and the duration of inter-event periods. Mass balances of  $\text{NH}_4\text{-N}$  and  $\text{NO}_3\text{-N}$  could be set based on measured in- and outflow volumes and concentrations for short event series. The experiments were repeated at summer, autumn and winter, to quantify the effects not only of the adsorbed mass but also the filter temperature on the nitrification rate. Two thermometers were installed in the filter media at 5 cm and 50 cm depth. The mean filter temperature of each inter-event period was calculated.

## 3.3 Model-based design toolkit: Orage

### 3.3.1 General purpose and structure

The design of event-driven wetlands like the ones treating stormwater is encumbered by the stochasticity of volumes, concentrations and return periods of flows. The goal of the toolkit Orage is to facilitate the design of CSO CWs, with support of VF CWs treating separate sewer outlet. Orage helps the selection of filter material and area as its standard feature and has a decision support function for sites where inflow series are unavailable.

The software is based on a numerical model in the core, but shaped into a design-support toolkit with a simplified (wizard-style) user interface. The programming was done by Megao Informatique based on the structure and approaches developed in the frames of this thesis work (see Annex A and Annex B). The handling of the model is automatized through an iterative shell which calls the core model repetitively. The automatization relies on i) design guidelines; ii) accounting for environmental factors like climate regions and seasons; iii) parameters fixed according to field measurements; iv) fix parameters associated with low model sensitivity; v) a low number of user-defined parameters vi) long-term input of flows and concentrations. Point ii), v) and vi) enable site-specific design. The goal is to enable water practitioners (engineers) to use the tool without special skills which are normally required for the numerical modelling of CWs, often decreasing practicability as discussed in Meyer et al. (2015).

As such, Orage consists of three major program elements (Fig. 14). For a more detailed layout, the reader is advised to refer on the Program overview in Annex A.

- i) The toolkit frame: user interface with data input, pre-processing, basic statistical analysis and charting features;
- ii) Iterative shell: the shell governs the automatic optimization and calls the core model repetitively with different materials, filter areas and for different pollutants (NH<sub>4</sub>-N, COD and TSS) to satisfy the concentrations thresholds (emission limits) whilst using the simplest material at the smallest possible filter area (in order of priority, respectively);
- iii) Core model: a design-support model running long-term simulations and returning a single variable (*Peak\_MA\_cc*) which is directly comparable to emission limits.

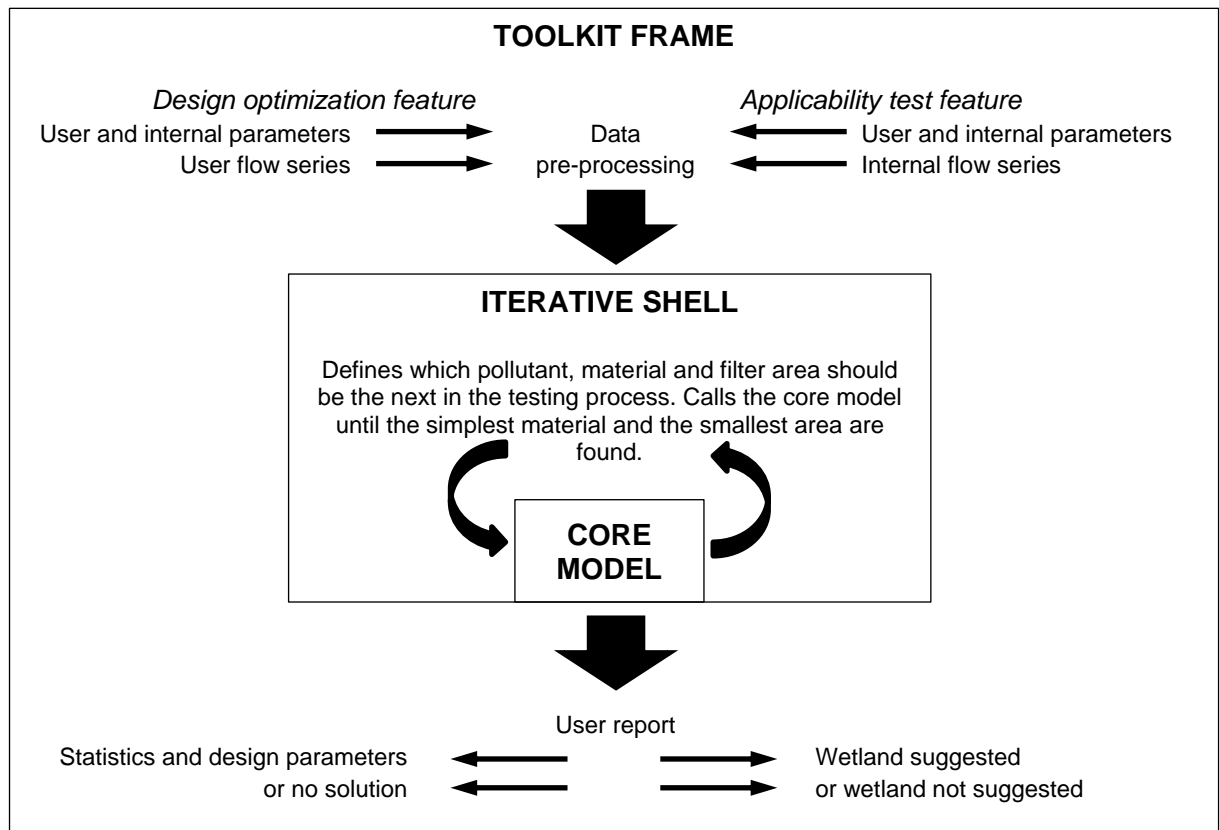


Fig. 14: The structure of Orage. The toolkit frame serves for input and output (user interface) as well as data pre-processing and analysis and relies on the iterative shell to call the core model repetitively until optimization is reached.



### 3.3.2 The toolkit frame

#### *Program features*

Orage offers two functions to help site-specific design. The standard function is the design-optimization feature, where the user input has to include own inflow series. The flow series are advised to be long term (up to several years) and have to include concentration data for the pollutant removal modelling. Measured overflow rates and concentrations and sewer model output are both satisfying. Calibrating sewer simulations using on-site data is recommended because a few measured events can enhance the accuracy of sewer models. Reliable and quality input data is essential to maximize the accuracy of Orage and its site-specific recommendations on the key design parameters like filter material and filter area.

The second feature of Orage is a decision-support function referred to as applicability test. If site-specific CSO or SSO data isn't available, neither measured nor simulated, decision makers can still rely on this function before opting for measurement campaigns or building the network in sewer models for simulations. The decision-support feature relies on 45 internal tables, each containing i) one year of simulated SSO flow series and ii) a dry weather flow pattern. Stormwater series cover the climate regions of mainland France (5 categories, Table 5).

Table 5: Climate regions in Orage

Climate region	Reference settlement
Mountain	Embrun
Atlantic temperate	Lille
Semi-continental	Metz
Mediterranean	Montélimar
Atlantic	Quimper

For each climate region, a range of land sealing categories can be selected, from 25% to 90% imperviousness (9 categories, Table 6). The sewer simulation tool CANOE (INSAVALOR and SOGREAH 1997) was used to create the internal tables, based on five years' of measured precipitation data (MeteoFrance), in one major town of each climate region. The year with the highest precipitation [mm] had been selected for the simulations. The user selects the region where the wetland is to be built and then estimates the imperviousness of the sewer's catchment. The estimation of the catchment's imperviousness is aided by land coverage categories, limiting the number of percentage values to select from. These selections enable to have input series with some wet-weather flow characteristics of the user's site, without site-specific user input. This specificity is increased later as described in the next heading dealing with input data.

## Setup of field experiments and model building

Table 6: Imperviousness category selection in Orage

Land coverage category	Percentage of impervious area
Scattered houses	25-40%
Residential areas	30-50%
Urbanized areas	50-75%
Industrial areas	50-80%
Commercial areas	70-90%
Streets and roads	70-90%
Selectable values	25%;30%;40%; 50%;60%;70%; 75%;80%;90%

### *Input data*

The input requirements are determined based on the software feature that is to be used. A summary is given in Table 7. If inflow series are provided, the data needs to be in a format where each row has inflow volume and pollutant concentrations representative for one time step of 6(-15) minutes.

Table 7: User input in Orage

Required user input	Software function	
	Design-support	Applicability test
Own inflow series	X	
Wetland type (CSO/SSO)	X	X
Available land area [m <sup>2</sup> ]	X	X
Climate region (5)	X	X
Catchment area [ha]		X
Imperviousness [%]		X
Population [PE]		(X)
Capacity of the combined sewer [m <sup>3</sup> /h]		(X)
Volume to be treated (design load) [m <sup>3</sup> ]	X	X
Legislative thresholds on emissions		
Allowed hydraulic load [m <sup>3</sup> /h]	X	X
NH <sub>4</sub> -N [mg/L]	X	X
COD [mg/L]	X	X
TSS [mg/L]	X	X

### *Data pre-processing*

Data pre-processing is depending from the inflow series which can be own dataset for the design-support function of the tool or internal tables for the decision-support function. The internal tables are re-arranged by additional pre-processing steps to scale flows and concentrations if necessary (see Data pre-processing in Annex A). These steps are carried out before the standard steps of pre-processing and are therefore discussed here first.

The standard catchment area of the internal tables is 50 ha. Therefore, stormwater flow rates are up- or downscaled to the user's catchment area based on simple linear correlation. Concentrations are unchanged and represent the higher end of the range found in the literature. If the wetland type is CSO, dry weather flow is scaled the same way as stormwater flow rates. The

standard flow follows the pattern of 2000 PE (Fig. 15) measured at the treatment plant of Challex, France.

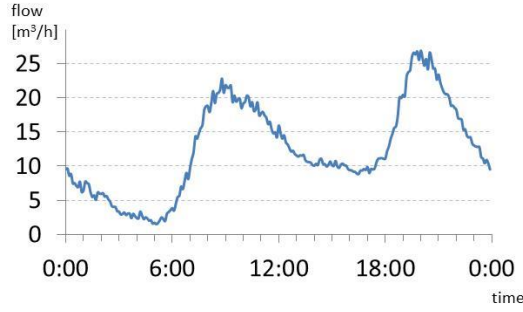


Fig. 15: Daily dry weather flow pattern for the decision support function (2000 PE).

After scaling the flows, concentrations are re-calculated assuming a perfect mixing. Source values are constant. High concentrations were selected for both the dry and wet weather flows to stay on the safe side. The selected values are summarized in Table 8 and represent event mean concentrations (EMCs).

Table 8: Quality of flows in the internal tables of Orage. As concentrations are variable, high concentrations were selected from the literature to stay on the safe side with the applicability test: h: Henze and Comeau (2008), a: Smullen et al. (1999); f: Zgheib et al. (2012).

Parameter	Low	Dry weather flow [mg/L] <sup>h</sup>			Orage	Stormwater [mg/L]		
		Low	Medium	High		Low	High	Orage
TSS	250	400	600	400	78.4 <sup>a</sup>	106 <sup>f</sup>	106	
COD	500	750	1200	900	52.8 <sup>a</sup>	89 <sup>f</sup>	89	
TKN	30	60	100		2.8 <sup>f</sup>			
NH4N	20	45	75	100			2.8	

The inflow rate and concentrations for CSO are re-calculated and a new table is generated according to the user's scenario. The overflow is based on a user specified value to limit the sewer flows down the overflow point as desired (e.g. the intake capacity of the wastewater treatment plant). An example can be seen on Fig. 16. Calculations are based on the following equations:

$$Sewer\_over_{t1} = \max(0; \frac{A_{catch}}{A_{unit\_catch}} \times Flows_{t1} + PE \times Unit\_dry_{t1} - Flow\_ret) \quad 4)$$

$$Sewer\_over\_cc_{t1} = \frac{\frac{A_{catch}}{A_{unit\_catch}} \times Flows_{t1} \times Flows\_cc + PE \times Unit\_dry_{t1} \times Dry\_std\_cc}{\frac{A_{catch}}{A_{unit\_catch}} \times Flows_{t1} + PE \times Unit\_dry_{t1}} \quad 5)$$

where  $Sewer\_over_{t1}$  is the overflow volume at the given time step;  $A_{catch}$  is the catchment area defined by the user;  $A_{unit\_catch}$  is 50 ha;  $Flows_{t1}$  is the flow of stormwater;  $PE$  is the population equivalent defined by the user;  $Unit\_dry_{t1}$  is the dry weather flow rate for one PE;  $Flow\_ret$  is the intake capacity of

the wastewater treatment plant. For Eq. 5),  $Sewer\_over\_cc_{t1}$  is the concentration of the overflows at the given time step and  $Flows\_cc$  is the stormwater concentration and  $Dry\_std\_cc$  is the sewage (dry weather) concentration for the given pollutant.

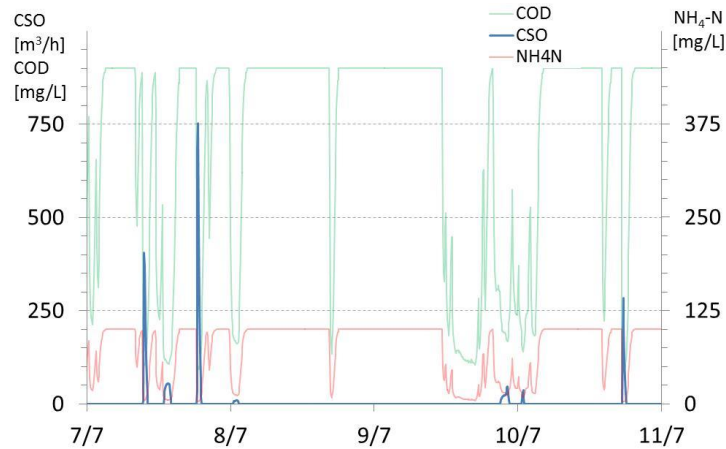


Fig. 16: An example of adjusted CSO flows and concentrations after data pre-processing (applicability test only). Note that concentrations got diluted at all seven overflows but also in cases when the precipitation was too little to generate CSO.

The steps discussed above generate a one-year long dataset scaled to the user's input scenario for the applicability test. Pre-processing steps from this point are identical for the two program modes. In the case of the applicability test, the data is always one year long so no data cropping is carried out. Contrary, because the user's input file is advised to be few to several years in length, the worst year is selected and cropped automatically. As such, the scaling of CSO CW is carried out based on one single year of data in both program modes.

The worst year is selected to encompass the five consecutive days which carry the highest  $NH_4-N$  load on the wetland of any. One year is selected around these days to have the highest annual volumetric load. Then, for both program modes, the data is re-structured to start the simulations after the longest dry period. This justifies that a high regeneration of the simulation domain is assumed as initial condition. Based on the longest dry period and the measured potential evapotranspiration (PET), the depth of the drainage layer is calculated as well. This depth will minimize the risk of drought stress in the filter where permanent water serves as a reservoir for the living organisms like plants and bacteria.

#### *Statistical analysis of in- and outflows and results*

Orange calls the iterative shell after data pre-processing is over. Based on simulation results, it reports statistics and design parameters listed below. Events are considered separate if there is at least 24 hours passing between them with no outflow.

Statistics on the input data:

- The five highest *NH<sub>4</sub>N* loads during any 5-day long period of the whole dataset<sup>1</sup>;
- Daily mass loads of the worst of such 5-day long periods<sup>2</sup>;
- Mass loads by event for the whole dataset (for each pollutant)<sup>3</sup>;
- Mass loads by event for the year selected for simulations (for each pollutant)<sup>3</sup>;
- Daily hydraulic loads of the whole dataset<sup>3</sup>;
- Daily hydraulic loads of the year selected for simulations<sup>3,4</sup>;

Statistics on the output (solution):

- *Peak\_MA\_cc* by event: all events<sup>3</sup>;
- *Peak\_MA\_cc* by event: events below the design load<sup>3</sup>;
- Hydraulic loads by event: all events<sup>3</sup>;
- Hydraulic loads by event: events below the design load<sup>3</sup>;

Proposed design parameters:

- Filter area [m<sup>2</sup>];
- Filter material (coarse sand, fine sand, pozzolana and sand with 0.07, 0.12 or 0.18 metres of zeolite);
- Filter depth [m];
- Highest expected ponding time [h];
- Annual hydraulic load [m];
- Required storage volume above the media [m<sup>3</sup>].

### 3.3.3 Iterative shell

The iterative shell is an automatic optimization algorithm which calls the core model repetitively. For a detailed description, the user is advised to rely on the corresponding manuscript in Chapter 5 and Annex A. Its purpose is to find the simplest filter material and then the smallest filter area with this material which satisfies all legislative thresholds (flow rate and concentrations). The toolkit frame submits the following parameters for the algorithm after pre-processing the data:

- i) Internal program parameters
- ii) User's input parameters
- iii) Flow series (user's input or re-scaled internal tables)

The core model returns one single value called *Peak\_MA\_cc* for the iterative shell at the end of each simulation. This value is similar to a flow-composite of the effluents at the worst event in the dataset. Comparing *Peak\_MA\_cc* values of known filter materials and areas enables the shell to find a solution where the tested design just satisfies the legislative thresholds on pollutant concentrations. This means both over- and underscaled filters will be ruled out.

---

<sup>1</sup> Ranking table

<sup>2</sup> Chart of minimum, average and maximum

<sup>3</sup> Box and whisker charts

<sup>4</sup> Column chart over one year

Optimization has the following steps:

- i) Hydraulic optimization: exclusion of excessively small and large filters. Small filters pose the risk of clogging. In large filters, the outflow rate limitation might never take effect, meaning most of the filter area is rarely or never utilized;
- ii) Optimization for  $NH_4N$  removal: selection of the simplest filter material and the smallest filter area which will keep effluent concentrations below the legislative thresholds. Orage has a database of  $NH_4-N$  adsorption isotherms: coarse sand, fine sand, pozzolana and sand and zeolite (mixtures or layered, with 0.07, 0.12 or 0.18 m zeolite in a filter depth fixed between 0.45 to 0.60 metres);
- iii) Single run to calculate COD removal performance;
- iv) (optional) Optimization for COD removal: further optimization of the filter area if necessary.
- v) (optional) Repeated optimization for  $NH_4N$  removal: further optimization of the filter area if necessary.
- vi) Single run for TSS removal to calculate removal performance.

### 3.3.4 Core model

#### *General considerations*

The iterative shell selects the filter area and the adsorption parameters for each simulation. These, and the user-defined internal parameters are imported into the core model. The model is calculating effluent rate and pollutant concentrations at each time step based on the inflow series and input parameters. The key output is one single variable by pollutant, *Peak\_MA\_cc* (see above).

The core simulates long-term series of hydraulics and removal performance in CSO CWs. This model is similar to an existing one, RSF\_Sim (Meyer and Dittmer 2015, Meyer 2011), but due to significant differences in hydraulics and other novelties, a new code had been built from scratch. The reader is advised to rely on the detailed information about model structure and process equations in the corresponding manuscript of Chapter 5, on Annex A (Core model) and on Annex B. Here, only a short summary is given in order to help the understanding of the core model's integration in Orage.

#### *Hydraulics*

Hydraulics is modelled by continuously stirred tank reactors in two parallel series (TIS) (Fig. 17) representing the twin filter sides of CSO CWs in France. The outflow orifice limits the outflow rate to a stable value and as such, justifies the simplification of filter hydraulics. Effluent rate has a constant upper threshold per unit surface. Because wetlands treating SSO are built with one filter basin, the model was created in a way that it works correctly when setting the area of the secondary filter and the cross-connection level to zero. Furthermore, due to the relative simplicity of a TIS model, short-circuiting is accounted for at pollutant removal calculations and not at hydraulics (short-circuiting is when infiltration and percolation are limited to the inlet zone).

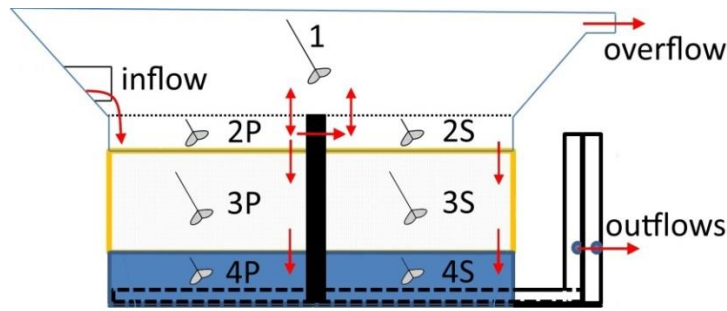


Fig. 17: The hydraulic model in Orage. Red arrows show possible flow directions. The numbered tanks are: 1: common basin; 2: reactors representing the volume from the filter to the wall; 3: process layers; 4: permanently saturated drainage layer. P: primary filter side; S: secondary filter side. The tanks of the secondary side have zero volumes and no flows if modelling single-sided filters (for SSO). If 2P and 2S are full, the inflow is distributed between tanks 1 and the empty space in 2P and 2S which is left by the constant outflow at every time step.

### Pollutant removal

*TSS* and *COD* removal is calculated when the water is leaving the process layer (exfiltration). A three-stage correlation is set between the process layer concentration and exfiltration concentration. Different removal efficiencies can be set up to consider the length of the inter-event periods and one freely chosen, temperature-dependent environmental effect of the preceding inter-event (Fig. 18). This might be the temperature itself but also potential evapotranspiration, which are dependent from the climate region and season. Parameters for *TSS* removal are calibrated to give a background concentration independently from inflow quality.

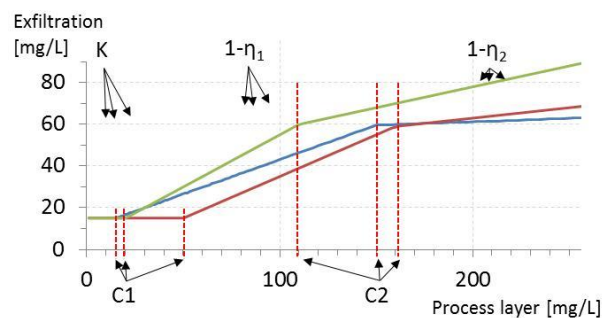


Fig. 18: Three examples of pollutant removal correlations for *COD* (uncalibrated). Correlations are dependent from the previous inter-event period and are defined by five parameters:  $K$ : background concentration,  $\eta_1$ : slope of the first stage,  $\eta_2$ : slope of the second stage,  $C_1$  and  $C_2$ : threshold concentrations between  $K$ ,  $\eta_1$  and  $\eta_2$ .

Ammonium removal is simulated as two-step process. Adsorption is calculated intra-event and nitrification inter-event. Adsorption isotherms are two-stage linear (defined by the first and second slope  $A_1$  and  $A_2$  which slopes are valid below and above the liquid phase concentration  $C_1$ , respectively). Equilibrium is instantaneous. The limited availability of adsorption sites at short-circuiting operation is considered. The domain is initiated with a completely regenerated drainage layer (background concentration) and a process layer with  $C_1/3$  [mg/L] in the liquid phase and the corresponding equilibrium concentration [mg/kg] in the solid phase.

Nitrification affects solid phase concentrations in the process layer and liquid phase concentrations in the drainage layer. Nitrification starts as soon as the water level in the process layer gets below the highest of the event, and in the drainage layer, as soon as the process layer is gravity-drained. The rate is function of the temperature and the adsorbed  $NH_4N$  mass and had been calibrated to field measurements.





## **4 Using process-based models to simulate CSO CWs**

## 4.1 Context and highlights

This paper discusses and targets to overcome the limitations of the process-based model package HYDRUS / CW2D for simulating lab-scale columns of CSO CWs. Earlier limitations were described in the papers Henrichs et al. 2007, 2009; Meyer 2011 and Meyer et al. 2013. Our work with HYDRUS / CW2D helped to display long-term purification tendencies and detailed wetland functions. This provided insights for the development of the core model of Orage which is partly a phenomenological model (phenomenological models are sometimes referred to as “simplified”). The work identified new limits for the applicability of HYDRUS / CW2D for CSO CWs which might help the development of the model itself or bring closer full-scale applications.

- We simulated combined sewer overflow constructed wetlands (CSO CWs) in HYDRUS/CW2D.
- Previous research showed strong limitations simulating CSO CWs in HYDRUS/CW2D.
- We calibrated biokinetic and other parameters using laboratory column experiments.
- We report quazi-stable biomass and a good fit for single loads and a load series.
- Former limitations were overcome and validation can continue with full scale.

Palfy TG, Molle P, Langergraber G, Troesch S, Gourdon R, Meyer D (2016): Simulation of constructed wetlands treating combined sewer overflow using HYDRUS / CW2D. *Ecol Eng* 87: 340-347. <http://dx.doi.org/10.1016/j.ecoleng.2015.11.048>; 0925-8574/ © 2015 Elsevier B.V.

## Full paper – Simulation of constructed wetlands treating combined sewer overflow using HYDRUS / CW2D

T.G. Pálffy<sup>a,b,c</sup>, P. Molle<sup>a</sup>, G. Langergraber<sup>d</sup>, S. Troesch<sup>b</sup>, R. Gourdon<sup>c</sup>, D. Meyer<sup>a</sup>

<sup>a</sup> IRSTEA Lyon, Freshwater systems, Ecology and Pollutions Research unit, 5 rue de la Doua - CS70077, 69626 Villeurbanne, France

<sup>b</sup> Epur Nature sarl, 153 Avenue Marechal Leclerc, 84510 Caumont sur Durance, France

<sup>c</sup> INSA Lyon, LGCIE DEEP Team, 20 av. A. Einstein, 69621 Villeurbanne cedex, France

<sup>d</sup> Institute of Sanitary Engineering and Water Pollution Control, University of Natural Resources and Applied Life Sciences (BOKU), Vienna, Austria

### Abstract

Constructed Wetland 2D (CW2D) is a biokinetic model describing microbial dynamics and transformation and degradation processes in subsurface flow constructed wetlands (CWs). The implementation of CW2D in HYDRUS (©PC Progress s.r.o.) was verified for application on CWs treating combined sewer overflow (CSO CWs). CSO CWs mitigate pollutant and hydraulic shock on receiving waters. Their loadings are stochastic in terms of periodicity, volume and quality. Their storage basin and outflow limitation causes cycles of saturated (intra-event) and unloaded (inter-event) states. The need for verification is due to this stochasticity. Key parameters to overcome the limitations identified by earlier studies were (1) biokinetic parameters, (2) fractionation of COD between readily and slowly biodegradable and inert forms and (3) adsorption of inert COD. With the new settings inoculation runs yielded stable biomass and domain conditions. These were successfully used as initial conditions for calibration and validation. Laboratory column experiments formed the basis of comparison, including single loads and a load series. The goodness of fit was quantified by an updated method. Good fit was reached to COD and NH<sub>4</sub>-N. Fitting to NO<sub>3</sub>-N was not a target; still, dynamics are discussed.

**Keywords:** combined sewer overflow, constructed wetland, CW2D, process-based model, biokinetics

**Software:** HYDRUS 2D/3D 2.03.0350 and HYDRUS Wetland Module ©PC Progress s.r.o. Patch provided to (i) simulate outflow rate limitation and (ii) avoid hung occurring at NH<sub>4</sub>N depletion in the domain.

**Abbreviations:** model parameters, variables and components are written in *italic*.

**E-mail addresses:** [tamas-gabor.palfy@irstea.fr](mailto:tamas-gabor.palfy@irstea.fr) (T.G. Pálffy), [pascal.molle@irstea.fr](mailto:pascal.molle@irstea.fr) (P. Molle), [guenter.langergraber@boku.ac.at](mailto:guenter.langergraber@boku.ac.at) (G. Langergraber), [remy.gourdon@insa-lyon.fr](mailto:remy.gourdon@insa-lyon.fr) (R. Gourdon), [meyer13@t-online.de](mailto:meyer13@t-online.de) (D. Meyer).



## **5 Orage: model-based and site-specific optimization of CSO CWs**

## 5.1 Context and highlights

The two manuscripts in this section titled “*Orage: a design-optimization modelling tool for CSO CWs*” demonstrate the software toolkit Orage. The toolkit has been developed for engineers to deal with the stochasticity of CSO flows and has three main components to enable practicable handling. The first is the core model, which is demonstrated, confirmed and tested in the first manuscript (subtitled “*core model*”). The second and third components are the iterative shell and the toolkit frame, which are explained, tested and optimized in the second manuscript (subtitled “*iterative shell*”).

Highlights of the first manuscript (core model):

- We developed a numerical model for dual-sided CSO constructed wetlands
- We demonstrate model functionality
- Calibration results to a single but extremely long load are shown
- We highlight model robustness via simulating event series and sensitivity analysis

Highlights of the second manuscript (iterative shell):

- We developed an optimization tool of wetlands treating combined sewer overflow
- We demonstrate its automatic optimization feature called the iterative shell
- Key parameters of the optimization process are fixed in a simulation experiment
- The iterative shell is confirmed and predictions are realistic
- NH<sub>4</sub>-N removal can be effective even at small filters where clogging might be a risk

Pálffy TG, Meyer D, Troesch S, Gourdon R, Olivier L, Molle P: Orage: a design optimization modelling tool for CSO CWs. Core model. Environ Model Softw, submitted.

## **Manuscript – Design optimization of CSO constructed wetlands: modelling filter performance.**

T.G. Pálffy<sup>\*a,b,c</sup>, D. Meyer<sup>a,b</sup>, S. Troesch<sup>b</sup>, R. Gourdon<sup>c</sup>, L. Olivier<sup>a</sup>, P. Molle<sup>a</sup>

<sup>a</sup>IRSTEA Lyon, Freshwater systems, Ecology and Pollution unit, 5 rue de la Doua - CS70077, 69626 Villeurbanne, France

<sup>b</sup>Epur Nature sarl, 153 av. Marechal Leclerc, 84510 Caumont sur Durance, France

<sup>c</sup>INSA Lyon, LGCIE DEEP Team, 20 av. A. Einstein, 69621 Villeurbanne Cedex, France

### **Abstract**

Constructed wetlands treating combined sewer overflow (CSO CWs) are variably saturated vertical flow filters in France, with outflow limitation and detention basins. By treating storm-generated flows, pollutants and flow peaks entering natural waters are reduced. Storm-generated flows are stochastic and therefore optimized CSO CW design requires a dynamic approach, i.e., a modelling software targeting engineers. Therefore a new tool called Orage was developed. Orage consists of a core model, an iterative shell and a user interface. It optimizes dimensions and materials of CSO CWs site-specifically, based on inflow series and a low number of input parameters. The core model simulates hydraulics and TSS, COD and NH<sub>4</sub>-N removal. Manual fitting of the core showed good results with a single load. The same parameters gave satisfying accuracy when simulating load series with closed material balance. Sensitivity analysis confirmed robustness and justified the coupling with the automatic shell algorithm.

**Keywords:** combined sewer overflow; constructed wetland; design-support modelling; dynamic design; stormwater treatment; Orage

**Software:** Orage alpha 0.6; developer: IRSTEA and MEGAO Informatique, France; contact: Remy Arnaud ([remi.arnaud@megao.com](mailto:remi.arnaud@megao.com)); availability: freeware, version 1.0 available online at [epnac.irstea.fr](http://epnac.irstea.fr) from 2017

**Abbreviations:** model parameters, variables and components are written in *italic*.

**E-mail addresses:** [tamas-gabor.palfy@irstea.fr](mailto:tamas-gabor.palfy@irstea.fr) (T.G. Pálffy), [meyer13@t-online.de](mailto:meyer13@t-online.de) (D. Meyer), [stephane.troesch@epurnature.fr](mailto:stephane.troesch@epurnature.fr) (S. Troesch), [remy.gourdon@insa-lyon.fr](mailto:remy.gourdon@insa-lyon.fr) (R. Gourdon), [laurie.olivier@irstea.fr](mailto:laurie.olivier@irstea.fr) (L. Olivier), [pascal.molle@irstea.fr](mailto:pascal.molle@irstea.fr) (P. Molle).

## 1. Introduction

### 1.1. CSO CWs and stormwater treatment

Urbanization impacts negatively the hydrology, physical-chemical properties and biota of surface- and groundwater without preventive actions. Water bodies are negatively impacted by untreated urban runoffs rejected as combined sewer overflow (CSO) or separate sewer outlet (SSO). Combined sewer networks accommodate high flow rates of stormwater mixed with domestic sewage. Overflow mechanisms are implemented to prevent overflowing of pipes and to limit downpipe flow rates to the capacity of the wastewater treatment plant. Unwanted peaks are discharged as CSO (Meyer et al. 2013) and are significant source of organics, nutrients, heavy metals and bacteria. In contrast, SSO is released end-of-pipe and has lower concentrations in organic matter and nutrient, but suspended solids, specific organic pollutants and heavy metals are a concern. Any flow peaks might erode and/or silt up stream habitat and change morphology. Urban stream syndrome is a generalized ecological degradation of streams draining urban land (Chocat et al. 1994, Walsh et al. 2005).

Constructed wetlands (CWs) for CSO treatment (CSO CWs) are being implemented or planned to be in several countries. In Europe, vertical downflow (VF) arrangements appeared promising (e.g. Meyer et al. 2013) after positive experiences with retention soil filters (RSFs) in Germany (Dittmer et al. 2016, Uhl and Dittmer 2005). The European Water Framework Directive (2000/60/EC) calls for a good quality of natural waters and the limitation and/or treatment of CSO will be mandatory in France. Among the different CW types (Fonder and Headley, 2013), those developed in France for end of pipe CSO treatment are vertical downflow arrangements with variable saturation and outflow rate limitation. In this paper, CSO CWs will be used to refer to the state of the art system in France, unless otherwise specified.

The loading characteristics of CSO CWs differ from CWs treating domestic wastewaters as the flows have stochastic periodicity, volume and quality. These systems have a detention basin above the filter material. Loadings saturate the porous media and cause ponding (intra-event state). Several hours might pass until the detained water is filtered, leaving through an orifice to limit outflow rate. After this, the pores in the filter media get filled with air again for several days (inter-event state) and might even dry out in extreme cases. Treatment processes can be attributed either to the intra-event or the inter-event environment by their dominant occurrence. Filtration, adsorption and anaerobic biodegradation take place during intra-event while aerobic bioprocesses, predominantly nitrification of adsorbed ammonia and organic matter biodegradation, dominate the inter-event phase (Dittmer et al. 2016, Dittmer and Schmitt 2011, Meyer 2011, Dittmer et al. 2005, Uhl and Dittmer 2005).

### 1.2. Design-support modelling of CSO CWs

Design optimization requires a dynamic approach due to the stochastic features of storm-generated flows. Some existing models match the complexity of the task. The process-based HYDRUS/CW2D (Langergraber and Šimůnek 2005) was validated at column-scale (Pálffy et al. 2015a, Meyer 2011, Henrichs et al. 2009, Henrichs et al. 2007), but it is considered too complex for design purposes (Meyer et al. 2015). Design-optimization model packages exist on the watershed scale. For example, a module of SUSTAIN (Lee et al. 2012) provides a generalized scheme of



process-based simulation of flow and pollutant transport for a handful of structural best management practices (BMP). However, CSO CW modelling requires including adsorption processes and outflow limitation features.

RSF\_Sim (Meyer and Dittmer 2015) is a design-oriented tool for retention soil filters (RSFs). It simulates full-scale, variably saturated vertical flow constructed wetlands with good accuracy (Meyer et Dittmer 2015, Tondera et al. 2013). Still, another tool has to be applied for design purposes in France due to some specificities in technical implementation (Meyer et al. 2013), such as the use of twin filter basins. Furthermore, RSF\_Sim is available in a table editor and as such, there is possibility to improve handling, data processing and automatization in general.

A new tool was therefore developed for CSO CWs, called Orage. Orage interpolates the optimal dimensions and material selection for plant design. The optimization is based on multi-year series of flows and pollutant concentrations. The tool offers practical handling via a user interface and by keeping the number of user-defined parameters low. Its core model simulates hydraulics and total suspended solids (*TSS*), chemical oxygen demand (*COD*) and ammonium-nitrogen (*NH4N*) removal. Several parameters are selected autonomously according to environmental factors such as regional climate, season or the length of the last inter-event period. The tool can scale single-basin stormwater wetlands as well which treat SSO but this function is in practice a hydraulic optimization since effluent concentrations of modelled pollutants stay at low concentration levels (Zgheib et al. 2012) anyway.

The objective of this paper is to 1) introduce the functionality and structure of the core model in Orage, 2) demonstrate its ability to simulate the operation of a real CSO CW which was implemented at Marcy l'Etoile (France) and monitored continuously, 3) define sensitive design parameters and thus justify the integration of the core model into an optimization algorithm where many parameters are fixed or selected from pre-defined tables.

## 2. Materials and methods

### 2.1. The concept of CSO CWs in France

CSO CWs are variably saturated vertical flow constructed wetlands treating combined sewer overflow. The current state of the art system in France (Fig. 25) is based on experiences from Germany (Dittmer and Schmitt, 2011; Frechen et al., 2006; Uhl and Dittmer 2005), from “French-design” CWs treating unsettled municipal wastewater (Molle et al. 2005) and pilot-scale research (Fournel 2012). Key considerations in the design of state of the art CSO CW systems are the following:

- i) Treating unsettled water facilitates sludge management. The twin filter sides allow sequential feeding. This means one side stays unloaded at regular events (small volumes). Both beds are fed in the case of bigger loads only. The primary filter is where the inlet flows; the secondary filter receives settled water through the primary if any. Alternation of filter priority allows longer inter-events in the secondary filter which favours mineralization of previously accumulated sludge and organics. This contributes to avoid clogging.
- ii) The permanently saturated bottom zone provides water to living organisms during dry periods and droughts.

- iii) There are aeration pipes above the saturated drainage layer, to increase aeration.
- iv) Zeolite might be mixed or layered with sand if higher ammonium-removal is needed;
- v) Compost is spread on the surface of the filter media to facilitate reed establishment in the start-up phase of the system.

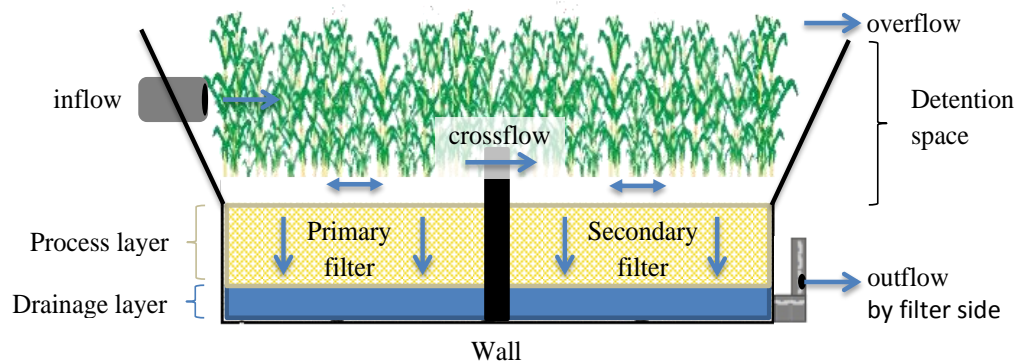


Fig. 25: Schematic cross-section and flows in CSO CWs.

An impervious liner is placed below the filter. Storm-generated flows enter the primary filter at the inflow point and fill the porous media. At the beginning of each loads, the infiltration and percolation are limited to the area close to the inlet. Pores saturate rapidly because the outflow is limited by a throttle orifice. Ponding follows in the detention space. The outflow limitation ensures then a fairly uniform flow (near plug-flow) and extends the detention time in the process layer, favouring pollutant removal.

An impermeable wall separates the filter sides. Crossflow occurs only if the water reaches the cross-connection pipe, making the secondary filter operational. In case of extreme storm events, overflows might occur. When the loading is over, the detained volume percolates through the filter progressively and the system empties.

The operating conditions described above allow CSO CWs to retain and / or degrade TSS, COD and  $\text{NH}_4\text{-N}$ , which would otherwise contaminate natural waters. The first stage of treatment is sedimentation and physical filtration in the top few centimetres of the filter (Dittmer 2006). The dominant processes for dissolved pollutants are anaerobic bacterial uptake of dissolved COD and adsorption of  $\text{NH}_4\text{-N}$ . These processes dominate during intra-event periods. During inter-event periods, however, the filter is drained, and the wet but aerated media favours nitrification and mineralization of organic solids (Dittmer and Schmitt 2011, Meyer 2011, Dittmer et al. 2005, Uhl and Dittmer 2005). The filters regenerate.

## 2.2. The core model of Orage

### 2.2.1. Development and novelty

The core model of Orage relies on knowledge from column experiments, pilots size and full scale plants and simulation studies with HYDRUS/CW2D (Pálffy et al. 2015a, Felmeden 2013, Fournel et al., 2013, Fournel, 2012, Dittmer and Schmitt 2011, Turković and Fuchs 2010, Heinrichs et al. 2007, 2009, Waldhoff 2008, Woźniak 2008, Woźniak et al. 2007, Dittmer 2006, Frechen et al. 2006, Dittmer et al. 2005). It is a time-step based numerical model where time series of CSO (or SSO) flows are imported. Measured flows and concentrations and simulation output of sewer modelling software like KOSIM, Mike Urban (SWMM and MOUSE engine) or CANOE (Schütze et al. 2002, INSAVALOR and SOGREAH 1997) can be used. Time steps are in the range of 6-15 minutes.

The core model of Orage is based on an existing model, RSF\_Sim (Meyer and Dittmer 2015, Meyer 2011). Aspects modified or added are: (1) a new hydraulic model which follows the same idea but ready to simulate both single- and twin-compartment filters; (2) the removal efficiency of total COD is concentration-dependent instead of limiting this to the dissolved fraction only and (3) the simulation of short-circuiting effects are built in as these decrease performance at commencing load. Furthermore, the core model selects parameters environmental-dependently (climate region, temperature, loads following a drought) and is integrated in an autonomous optimization code.

### 2.2.2. Hydraulics

The outflow orifice assures a stable and slow percolation (around  $0.02 \text{ l/s/m}^2$ ). Hydraulics in the core model is based on an outflow rate constant and continuously stirred tanks in two parallel series (Fig. 26). Flow- and transport equations are valid for single-sided filters if the area of the secondary side (F2) and the cross-connection level is zero. The core simulates short-circuiting at commencing load as discussed in subchapter 2.2.3.

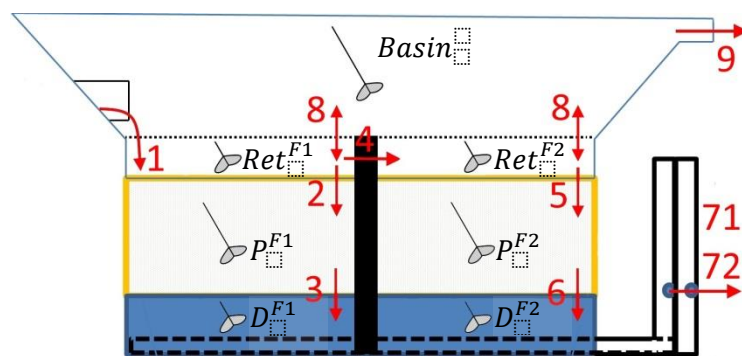


Fig. 26: The seven tanks and possible volumetric exchanges in the core model.

Volumes and concentrations of flow and storage are calculated at each time step ( $t1$ ) and are available from the preceding time step ( $t0$ ). The model space is discretized into seven tanks. The permanently saturated drainage layer is represented by  $D_{tx}^{F1}$  and  $D_{tx}^{F2}$  which have constant volume but concentrations may vary. The process layer is represented by  $P_{tx}^{F1}$  and  $P_{tx}^{F2}$  with volumes between the residual water and saturation. Removal processes are modelled in this layer. The

detention space is discretized into three tanks,  $Ret_{tx}^{F1}$ ,  $Ret_{tx}^{F2}$  and  $Basin_{tx}$ , and have volumes between zero and their maximum.

Flows occur after perfect mixing within the compartments. The inflow (1) arrives to the primary retention side  $Ret^{F1}$ . It infiltrates (2) to the primary process layer  $P^{F1}$ . Infiltration gets limited by the primary outflow orifice to match the outflow (71) when  $P^{F1}$  is full; otherwise the inflow (1) infiltrates instantaneously. Water percolates deeper (3) to the primary drainage layer  $D^{F1}$  and water leaves the filter, limited by (71). If the water in  $Ret^{F1}$  reaches the level of cross-connection, cross-flow (4) occurs. The cross-flow (4) for the secondary retention side  $Ret^{F2}$  is like the inflow (1) for the primary. Flows have an identical path: infiltration to  $P^{F2}$  (5) and percolation to  $D^{F2}$  (6) leads to a limited outflow (72). In case the water reaches the cross-connection level in  $Ret^{F2}$  as well, a common water level is established. Inflow (1) volumes are halved and distributed instantaneously; still,  $Ret^{F2}$  receives water through  $Ret^{F1}$  after complete mixing. If  $Ret^{F1}$  and  $Ret^{F2}$  are both full,  $Basin_{tx}$  starts to get filled. In this case, inflow (1) is distributed between the three compartments of the detention space.  $Ret^{F1}$  and  $Ret^{F2}$  has priority and receives equal volumes; the rest of the inflow (1) is added (8) to  $Basin_{tx}$  if there is any. Mixing happens independently by compartment. If  $Basin_{tx}$  is filled, overflow (9) is instantaneous. Detained volumes leave through (71) and (72). The calculation of flows, volumes and concentrations are detailed in Appendix A.

### 2.2.3. Pollutant removal

*COD* and *TSS* removal is calculated when water is leaving the process layer  $P^{Fx}$  (flows 3 and 6), based on empirical equations. These have been parameterized for *TSS* to yield a constant background value. In contrast, a true correlation was observed between inflow and outflow *COD*. Fournel (2012) suggested (1) a background constant for a diluted inflow, (2) a linear correlation at moderate concentrations and (3) a cap at high concentrations. A similar three-stage approach has been implemented in Orage with the possibility to use a second linear correlation instead of the cap. Process equations can be found in the subroutine ‘*V\_D\_Calc*’ of Appendix A.

Measured data showed a rather large variance. As such, using a single correlation rule could have led to weak designs unless performance was underestimated, which in itself reduces optimization efficiency. Meyer and Dittmer (2015) improved model predictions in *RSF\_Sim* taking into account the length of the preceding inter-event period (Fig. 27). Orage was enabled to automatically select parameters  $K$ ,  $CI$ ,  $Nu_1$ ,  $C2$ ,  $Nu_2$  depending on the inter-event duration, the season and the climate region. Dry and hot days were assumed to cause a drop in *COD* removal through bacterial starvation and drought. The procedure for the selection of the different parameter sets was implemented as follows:

1. Selection of a “climate-season” factor according to the season and the climate of the planned location of implementation;
2. Normalization of the duration of the preceding inter-event period (in days) based on this factor (a multiplier);
3. Selection of the corresponding inter-event period range (e.g. 2-8 days for 6.2 days)
4. Application of the set of parameters ( $K$ ,  $CI$ ,  $Nu_1$ ,  $C2$ ,  $Nu_2$ ) associated to this range. If this appears necessary, the parameters might be adjusted to distinguish between short-circuiting conditions or normal operation.

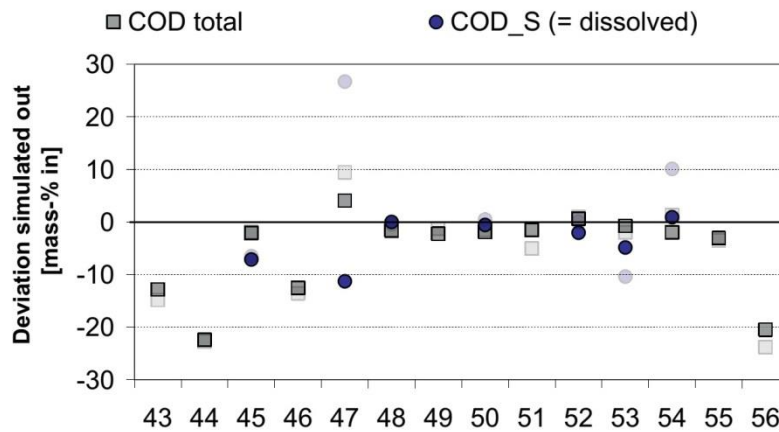


Fig. 27: Results in RSF\_Sim: mass removal percentage error can be decreased if considering the length of inter-event periods. Translucent symbols: error in predictions before; opaque symbols: after. Figure based on Meyer and Dittmer (2015).

The model accepts TKN (Total Kjeldahl Nitrogen) concentrations as input but handles it as  $NH_4-N$  (*component NH4N*). In reality, particulate nitrogen in TKN was found to be filtered, and then possibly accumulated in the sludge as organic nitrogen or ammonium after ammonification. Regarding the fate of TKN, releases were not detected in the full-scale CSO CW of Marcy L’Etoile.

$NH_4N$  removal is a two-step process, adsorption in the solid phase during loads and nitrification limited to the inter-event. Adsorption capacities in the material database represent 2-slope isotherms as shown in Fig. 28. The curve shows the instantaneous equilibrium between liquid and solid phase concentrations in the process layer  $P^{F,x}$ . It is a simplification of a Freundlich isotherm, having low mean absolute error (MAE) at the concentration range of stormwater and CSO (e.g. Sztuhár et al. 2002). It allows to express the state of equilibrium without solving a differential equation.

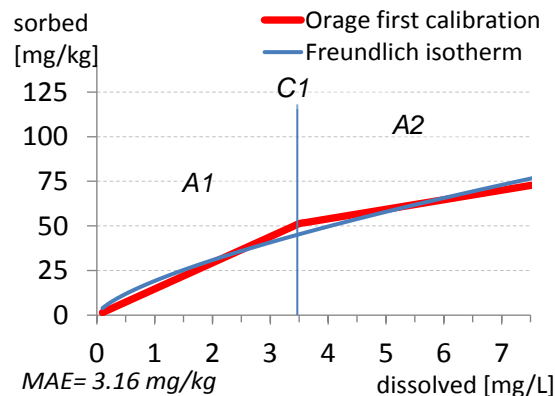


Fig. 28: Broken-stick isotherm and its parameters, compared to a Freundlich isotherm. A1: slope below threshold dissolved phase concentration C1; A2: decreased slope above C1.

Only the inlet zone of filters is water-contacted at the beginning of loads, which might last at low inflow rates. This short-circuiting mechanism was observed to lead to decreased performance (Pálffy et al. 2015b). Therefore, calculations differ until the water level is under a constant  $h_e$  (Fig. 29). If percolation is limited to the inlet zone, sorption capacity is limited as well. In this case,

passing water is mixed to the stored volume in  $P_{tx}^{Fx}$  after equilibrium concentrations are calculated separately for the infiltration zone only. The surface area of infiltration is estimated using Eq. (8) based on the inflow volume and Darcy's law. Mass of water-contacted media can then be estimated using Eq. (9):

$$A_{inf_{t1}^{Fx}} = \frac{F_{inf_{t1}^{Fx}}}{K(t1 - t0)} \quad (8)$$

$$M_{active_{t1}^{Fx}} = A_{inf_{t1}^{Fx}} \times d_{filt} \times rho_{media} \quad (9)$$

where  $A_{inf_{t1}^{Fx}}$ , the area of infiltration [ $m^2$ ];  $F_{inf_{t1}^{Fx}}$ , the infiltrating volume [ $m^3$ ];  $K$ , the infiltration [ $m$  per time step] through the organic deposit and compost on the top;  $M_{active_{t1}^{Fx}}$ , the mass of media [ $t$ ] in contact;  $d_{filt}$ , the depth of the filter layer and  $rho_{media}$ , the bulk density of the media [ $t/m^3$ ].

The adsorbed mass of  $NH4N$  is calculated for the overall mass of filter medium ( $NH4_{oldmass_{tx}^{Fx}}$ ) and the fraction stored in the short-circuiting zone ( $NH4_{infzonem_{tx}^{Fx}}$ ). The short-circuiting zone might saturate independently from the rest of the filter, allowing short-circuiting peaks to occur in the simulations. The infiltration area changes as a function of the infiltrating volume (inflow) at each time step (Fig. 29). If the infiltration area increases, the mass of sorbed  $NH4N$  is recalculated. If the infiltration area decreases, the total mass of sorbed  $NH4N$  is decreased proportionally ( $NH4_{oldmass_{tx}^{Fx}}$ ).

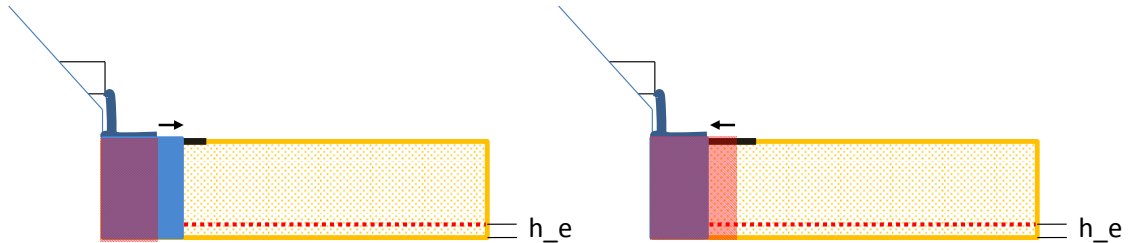


Fig. 29: Short-circuiting conditions with increasing (left) and decreasing (right) infiltration area. A potential value for  $h_e$  is shown.

Nitrification starts as soon as the filter layer begins to empty. The initial rate is linearly proportional to the emptied volume. Mass decrease is otherwise calculated according to Eq. 10, based on the work of Meyer and Dittmer (2015). The rate is the function of the mass in the solid phase and the mean seasonal temperature.  $NH4N$  in the drainage layer is solely in solution but nitrified anyway after the outflow ceases, down to a background concentration set to be the lowest EMC measured in the effluent of the full-scale site at Marcy-L'Etoile (1 mg/L).

$$NH4N(t + 1) = NH4N(t) \times e^{-d_{i,t}} \quad (10)$$

$$d_{i,t} = d_{i,t} \times e^{\frac{T-20}{Rc}}$$

where  $NH_4N(t)$  is the mass of  $NH_4N$  at time step  $t$ ,  $-d_{i,t}$  is a rate constant [1/time]. The second part of the equation corrects  $-d_{i,t}$  according to the temperature  $T$  [°C] and the temperature sensibility constant  $R_c$  [-]. Parameters are calibrated based on field measurements.

## 2.2.4. Shell integration

Orage was programmed to call the core model repetitively until the design is considered optimal. The iterative shell of Orage will be discussed in a second paper (Orage: a design optimization modelling tool for CSO CWs: Iterative shell). The connection between the core model and the iterative algorithm is discussed here.

The core model returns a single concentration value. This variable is called *Peak\_MA\_cc* (peak of moving average concentrations, mg/L). For small events with outflow duration under six hours, the value of *Peak\_MA\_cc* isn't recorded. If there is outflow at least for six hours but maximum for twenty-four hours, the maximum of the mean outflow concentrations, re-calculated at each time step, is selected. From twenty-four hours on, the average values are the moving average concentrations from the last twenty-four hour blocks, and the maximum might be updated based on these.

The tested design is acceptable if *Peak\_MA\_cc* is at the legislative threshold (within a tight tolerance range).

## 2.3. Calibration approach

### 2.3.1. First calibration to a single load

Calibration was based on flow and concentration series of data acquired from the full-scale CSO CW operated at Marcy l'Etoile, France (Pálffy et al. 2015b, Meyer et al. 2013). An extremely long event (event #14) was selected and parameters from the real site and RSF\_Sim standards (Meyer and Dittmer 2015) were used as base. The value of flow limitation was fine-tuned to fit water levels. *COD* parameters were then adjusted manually until a visually good fit was reached, without considering the effect of inter-events. Event #14 was a heavy load (156 g/m<sup>2</sup>) so  $NH_4N$  sorption was fitted to a real breakthrough curve. Nitrification rate parameters were set according to field measurements (Pálffy et al. 2016).

### 2.3.2. Confirming the calibrated parameters with event series

Event series were simulated without further parameter refinement. Four consecutive loads with closed material balance and short inter-event periods were modelled. Event #14 was added to see if preceding loads cause any changes in predictions. Table 1 summarizes the characteristics of the five events.

Table 13: Simulation series consisting of four consecutive loads (event #16-19) and event #14

Event #	Load [m]	Duration [h]	Preceding inter-event [d]
16	* 1.16	20.5	62.0
17	0.98	25.0	1.0
18	1.10	26.0	3.5
19	1.59	35.5	11.9
14	10.87	190.0	** (15.3)

\*: primary filter only; \*\*: arbitrarily selected

### 2.3.3. Assessment of model accuracy

Series of simulated *COD* and *NH4N* effluent concentrations were compared to experimental measurements. Accuracy was assessed by the following calculations:

- Difference of simulated 6/24h *Peak\_MA\_cc* compared to the measured: [mg/L], [%]
- Difference to measured mass removal: [%], [MAE %]
- Time weighted event mean concentrations (EMC): [MAE mg/L], [MAE %]
- Difference of total nitrified mass: [%]
- Difference in short-circuiting durations (for sensitivity analysis only),
- Time shift to measured *NH4N* breakthrough: [h]
- Goodness of fit:  $E_j$  (Ahnert et al. 2007).

The coefficient of efficiency ( $E_j$ ) was calculated with  $j=1$  to make it more sensitive to fitting inaccuracies (Ahnert et al. 2007). Composite samples covered various time intervals; this was counterbalanced by including time-weighting in the classical equation:

$$E_j = 1 - \frac{\sum_{i=1}^n |M_i t_i - \bar{E}_i t_i|^j}{\sum_{i=1}^n |M_i t_i - \bar{M} t_i|^j} \quad (11)$$

where  $M_i$  is the measured value for composite  $i$ ,  $\bar{E}_i$  is the average of simulated values coinciding with composite  $i$ ,  $\bar{M}$  is the time-weighted average of all measured values, and  $t_i$  is the time represented by composite  $i$ .

No classification ranges (i.e. good fit, bad fit) were proposed in Ahnert et al. (2007). It was suggested to apply other numerical methods simultaneously and to present charts for visual interpretation. If the value of  $E_j$  is below zero, either the arithmetic mean is a better predictor than the model or the measured values were too low or nearly constant (Pálffy and Langergraber 2014). The interpretation of  $E_j$  was aided by calculating the mean time-weighted deviation:

$$\overline{DEV} = \frac{\sum_{i=1}^n |M_i t_i - E_i t_i|}{t} \quad (12)$$



where  $t$  is the duration of the intra-event period on which the analysis is done.  $\overline{DEV}$  [mg/L] and  $\overline{DEV}$  [%] helps to decide if  $E_j$  indicates a poor fit or fails. The goodness of fit was considered weak if  $E_j$  indicated weak results with a value below 0.1 and  $\overline{DEV}$  seemed important.

### 2.3.4. Sensitivity analysis

Model sensitivity was tested using a one factor at a time (OAT) screening technique called the Morris method (Morris 1991), applied with the improvements of Campolongo et al. (2007). The method yielded two values describing the importance of each scrutinized model parameter. One was correlated to the overall influence ( $\mu_i^*$ ) on the output and the other to the non-linearity/interactions with other factors ( $\sigma_i$ ). The analysis was carried out separately on *COD* removal (number of parameters:  $k=16$ ) and on *NH4N* removal ( $k=21$ ) because the model did not allow to take into account interactions between the two pollutants and can be called on one pollutant at a time. Common parameters were those describing hydraulics and temperature dependence. Each model parameter  $x_i$  ( $i=1, \dots, k$ ) was varied within a pre-defined input range at four levels ( $p=4$ ), yielding  $N=160$  simulations for *COD* and  $N=220$  for *NH4N*. Input ranges were selected to be realistic for CSO CWs.

Values for  $\mu_i^*$  and  $\sigma_i$  were calculated based on the values of elementary effects (EE). Detailed description of the calculation were given by Morris (1991) and Campolongo et al. (2007). An EE was defined for each input vector  $\mathbf{x}$  consisting of  $k$  parameters, one changed at a time. For a given  $\mathbf{x}$ , the EE linked to the  $i$ th input factor is defined as:

$$d_i(x) = \frac{y(x_i, \dots, x_{i-1}, x_i + \Delta, x_{i+1}, \dots, x_k) - y(x)}{\Delta} \quad 13)$$

The basis of evaluation is often taken to be the arithmetic mean of model output, i.e.  $y(\mathbf{x}) = \text{EMC}(\mathbf{x})$ . For a more detailed outcome about model sensitivity and robustness, the analysis was done on all statistics listed in subchapter 2.3.3. As for goodness of fit, a single numerical had to be calculated from  $E_j$  and  $\overline{DEV}$ . Scores (1: worst) were derived based on arbitrarily selected ranges (Table 14). The final score was based on  $E_j$ : if the score for  $\overline{DEV}$  was the higher,  $E_j$  was increased by one, otherwise it was left unchanged. The arithmetic mean of six final scores (for five events, one by filter side) was defined as  $y(\mathbf{x})$ .

Table 14: Ranges for goodness of fit-based sensitivity analysis.

Score	Range for $E_j$ [-]	Range for $\overline{DEV}$ [mg/L]	
		<i>NH4N</i>	<i>COD</i>
1	$E_j < -1.5$	$2.00 < \overline{DEV}$	$15.0 < \overline{DEV}$
2	$-1.5 \leq E_j < -0.3$	$1.50 < \overline{DEV} \leq 2.00$	$12.0 < \overline{DEV} \leq 15.0$
3	$-0.3 \leq E_j < 0.1$	$1.25 < \overline{DEV} \leq 1.50$	$9.0 < \overline{DEV} \leq 12.0$
4	$0.1 \leq E_j < 0.5$	$0.75 < \overline{DEV} \leq 1.25$	$4.5 < \overline{DEV} \leq 9.0$
5	$0.5 \leq E_j$	$\overline{DEV} \leq 0.75$	$\overline{DEV} \leq 4.5$

The parameter ranges are listed in Annex C. A wide range was used on filter area  $A_{tot}$  (200 - 2000 m<sup>2</sup>), to focus the analysis on short-circuiting and to see if  $A_{tot}$  really has a minor effect on *COD* removal. Then, the analysis for *NH4N* was repeated, with a tighter range which was assumed to be hydrologically optimized (250-650 m<sup>2</sup>). Table 15 lists the short-circuiting times as the function of filter area.

Table 15: Short-circuiting times as the function of filter area at an outflow rate fixed to 0.108 m<sup>3</sup>/m<sup>2</sup>/h.

SA targeting short-circuiting		SA at hydrologically optimized areas	
filter area ( $A_{tot}$ )	short-circuiting time	filter area ( $A_{tot}$ )	short-circuiting time
290 m <sup>2</sup>	3%	270 m <sup>2</sup>	3%
830 m <sup>2</sup>	11%	390 m <sup>2</sup>	4%
1370 m <sup>2</sup>	43%	510 m <sup>2</sup>	6%
1910 m <sup>2</sup>	86%	630 m <sup>2</sup>	8%

### 3. Results and Discussion

#### 3.1. Calibration using a single event

The single run showed a good fit to measured hydraulics (Fig. 30) and outflow concentrations (Fig. 31). Water levels and ponding duration were also well predicted regardless the extreme length of the event. The existence of a constant outflow rate simplified indeed greatly the hydraulics of the system.

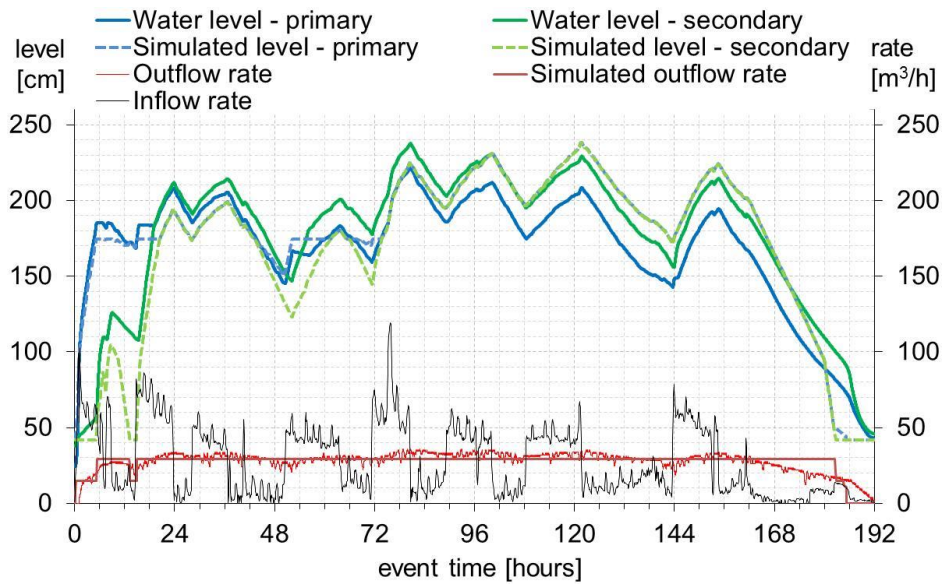


Fig. 30: Comparison chart of measured and simulated hydraulics of the single load (event #14). Water level is given by filter side, outflows are lumped.

The changes in COD were followed with a slight shift in time and with flattened amplitude, still well-fitted ( $E_j = -0.1$ , mean time weighted deviation: 7.5 mg/L).  $NH_4N$  was fitted excellently ( $E_j = 0.7$ , mean time weighted deviation: 1.2 mg/L). The time of predicted breakthrough showed a two hour delay which did not cause any visible shift on the chart.

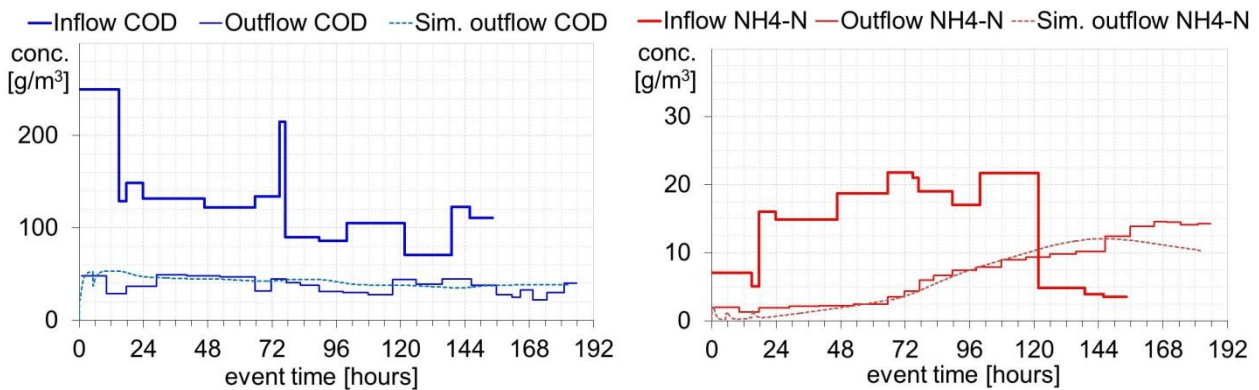


Fig. 31: Measured and simulated COD (left) and  $NH_4-N$  (right) concentrations of the single load (event #14).

Fitting  $NH_4N$  concentrations is crucial for a good design, especially after the breakthrough (see before 72 h event time on Fig. 31).

### 3.2. Event series

The fit between simulated and experimental effluent concentrations was between fairly good and good, with a score of 3.50 for  $COD$  and 3.33 for  $NH_4N$ . Results of statistical analysis are summarized in Table 16.

Table 16: Analysis of the model accuracy for the closed event series.

	<i>COD</i> :	<i>NH4N</i> :
Difference of simulated 6/24h <i>Peak_MA_cc</i> to measured:		
[mg/L]:	-18.9	-1.7
± [%]:	-26.9	-12.2
Difference to measured mass removal:		
± [%]:	-0.4	4.8
MAE [%]:	10.6	9.6
Time weighted EMC of the effluent:		
MAE [mg/L]:	6.9	1.4
MAE [%]:	8.8	33.5
Difference of total nitrified mass:		
[%]:	n/a	+15.8
Time shift to measured breakthrough (event #14 only):		
[hours]:	n/a	-0.1
Goodness of fit:		
$E_j$ [-]:	-0.64	-0.75
$\overline{DEV}$ [mg/L]:	8.4	1.5

Model predictions were satisfying for most of the events. Still, a gap of -26.9% for *COD Peak\_MA\_cc* was obtained, which should be improved because this variable will be used by the design-optimization algorithm. Fig. 32 shows intra-event concentrations at events #16-#19. The effluent concentrations of event #16 were underestimated by the model. The possible reasons for this observation were that 1) the samples for events #16 and #19 were taken from settled ponding water so input concentrations were lower than real inflow and 2) the dry period before event #16 was two month long and its possible impact on modelled performance had not been calibrated yet. Leaving away event #16 would have decreased the gap between the simulated and measured values down to -9.5%.

For *NH4N*, the event mean concentration had an average difference of 33.5% (MAE). However, expressed in concentrations, this difference is small.

Short-circuiting peaks were excessively large at events #17 and #18. A parameter ( $K2$ ) was set deliberately low to make short-circuit effects clearly visible.  $K2$  shall be fixed equal or just slightly lower to its counterpart used under normal operation in order to have smaller peaks. Lowering the initial short-circuiting peaks would result in a weaker goodness of fit value because  $NH4N$  concentrations were starting from close to zero. This can be counterbalanced by increasing the background concentration parameter higher. Event #14 was excluded from Fig. 32, because model predictions did not cause visually notable alternation compared to the single load (Fig. 31).

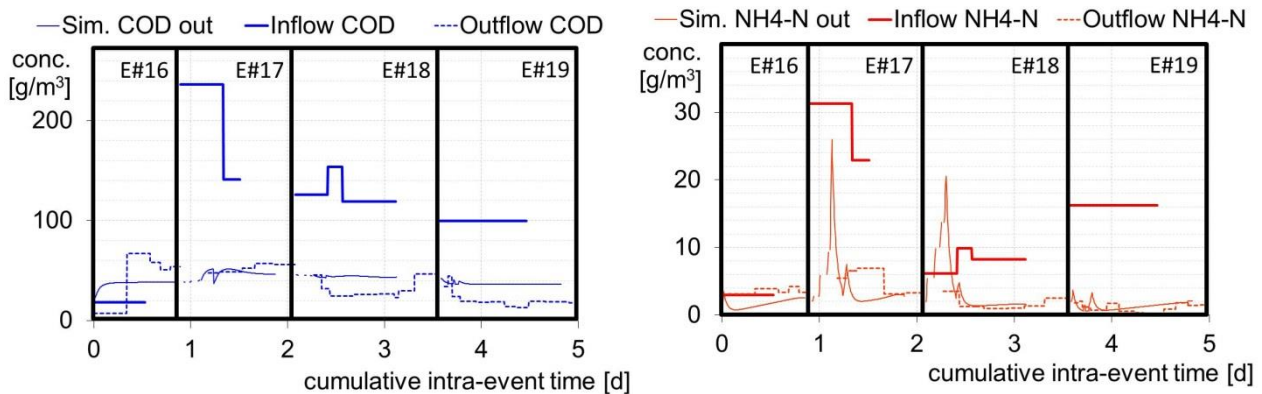


Fig. 32: Measured and simulated COD (left) and  $NH_4-N$  (right) concentrations of the event series (excluding event #14). Intra-event periods are cropped for better visibility. The short-circuiting constant (parameter  $K2$ ) was selected deliberately low to generate high  $NH_4N$  spikes and see functionality.

### 3.3. Sensitivity analysis

#### 3.3.1. SA of COD removal calculations

The sensitivity analysis on  $COD$  removal confirmed the importance of the performance parameters  $Nu_1$ ,  $C2$  and  $Nu_2$  for 6/24h  $Peak\_MA\_cc$  (Fig. 33). The model showed high sensitivity to the value of  $Nu_1$ . The other two performance parameters  $K$  and  $C1$  showed influence only at lower concentrations. Their effect was therefore small; inflow concentrations were too high to trigger background values in the effluent.

Model robustness had been confirmed as other parameters had little effect on simulations, especially on 6/24h *Peak\_MA\_cc*.

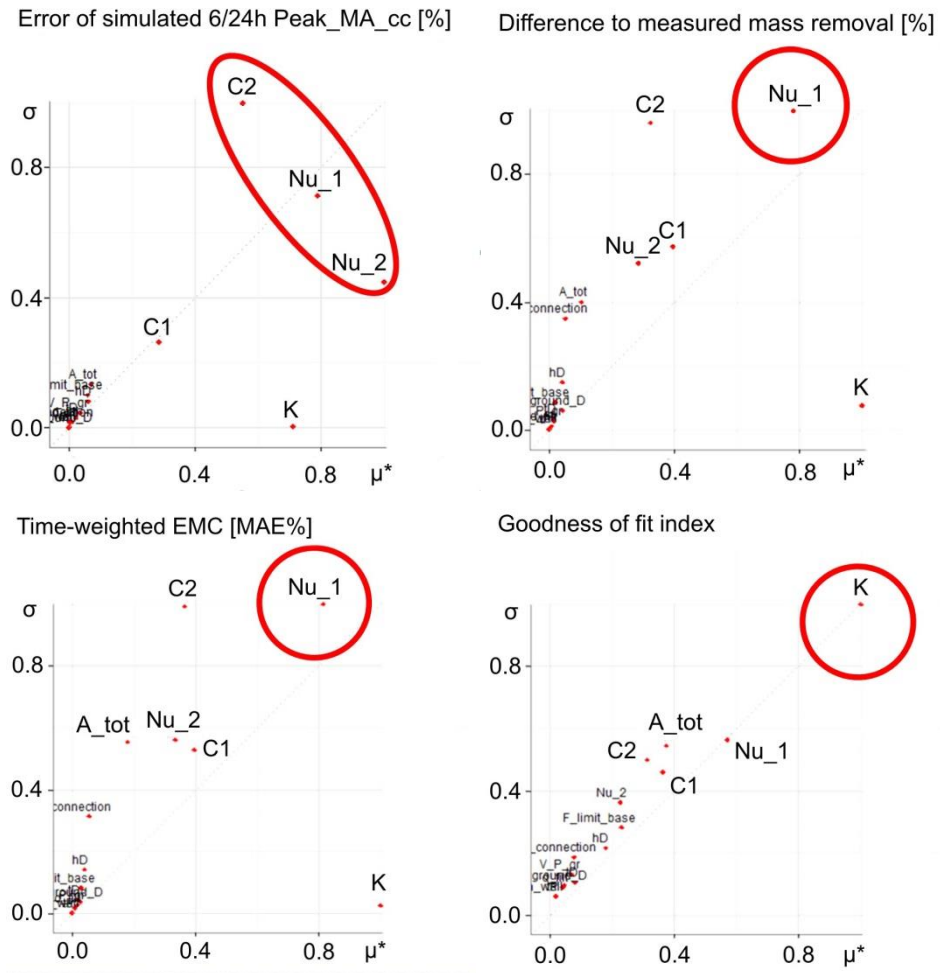


Fig. 33: Sensitivity analysis results for *COD*. Removal performance parameters  $K$ ,  $Nu_1$ ,  $C2$  and  $Nu_2$  had the most effect. The model was robust against all other parameters especially in the case of 6/24h *Peak\_MA\_cc*.

### 3.3.2. SA of $NH_4N$ removal calculations, with excessive short-circuiting durations

Wide parameter ranges were causing short-circuiting to be the dominant operation in the domain for almost all vectors ( $\mathbf{x}$ ) of the experiment. Ranges were tightened therefore in a second experiment to what physical research and design practice could justify. As such, one of the two analyses targeted performance at short-circuiting (wide ranges for area) and the other the classical operation with little short-circuiting (tight ranges for area).

The results at excessive short-circuiting durations (Fig. 34) highlighted significant parameters which determine short-circuiting duration, i.e., how long it takes until the water level fills up to the short-circuiting threshold depth  $h_e$ . These were 1)  $h_e$  itself [m], 2) the base outflow rate  $f_{limit\_base}$  [ $m^3/m^2/h$ ] and 3) the total filter area  $A_{tot}$  [in  $m^2$ ]. It can be anticipated that a bad combination of these hit performance badly. Parameters which describe adsorption capacities in the short-circuiting zone showed less importance ( $KI$ ,  $A1$ ,  $C1$ ). The total filter area ( $A_{tot}$ ) was the most significant of those parameters which are not going to be fixed.

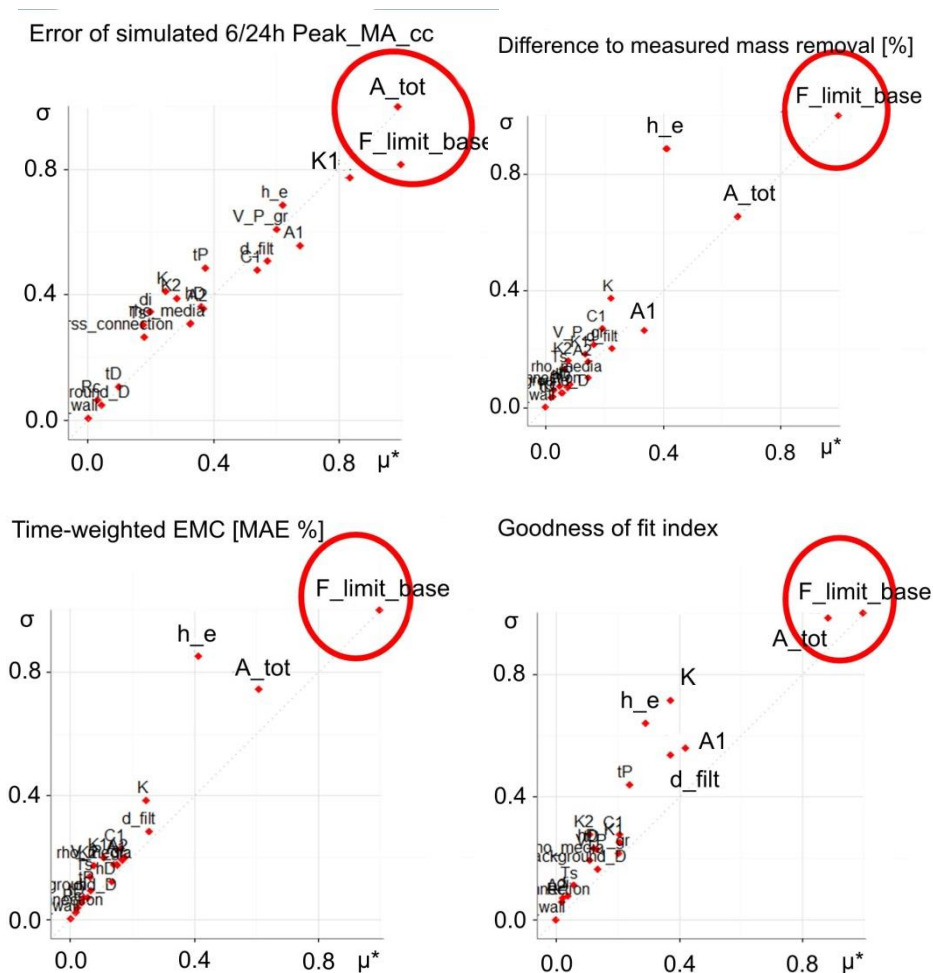


Fig. 34: Sensitivity analysis results for  $NH_4N$ : extreme short-circuiting durations in overscaled filters. Parameters impacting the longevity of short-circuiting ( $h_e$ ,  $F_{limit\_base}$  and  $A_{tot}$ ) had the most significant effect and adsorption capacities were less important.

### 3.3.3. SA of $NH_4N$ removal calculations, with normal short-circuiting durations

The range of the filter area ( $A_{tot}$ ) and the flow limitation ( $F_{limit\_base}$ ) were selected to give hydraulically consistent domains. Fig. 35 shows results with such input vectors ( $\mathbf{x}$ ).  $F_{limit\_base}$  was significant for the goodness of fit index, because at some vectors ( $\mathbf{x}$ ) the remaining short-circuiting peaks affected the fit even if the peaks themselves were fleeting.

Adsorption-related parameters were otherwise the most significant. These were 1) the material-specific adsorption capacity  $A1$  [ $m^3/kg$ ] and 2) the depth of the filter layer  $d_{filt}$  [m]. The depth of the filter, together with its area ( $A_{tot}$ ) determines the total mass [kg] of the media.  $A1$  can be calibrated to measurements, and  $A_{tot}$  is going to be optimized by the iterative shell of Orage.

It must be noted that  $d_{filt}$  is not a target of the optimization algorithms, and strong correlation was absent between treatment performance and filter depth (Fournel 2012). Meanwhile  $A_{tot}$ , on which the automatic optimization of Orage will be based, was deemed to be less significant by the SA. This is a weakpoint of the model where double thickness had the same effect on the virtual adsorption capacities as doubling filter area.

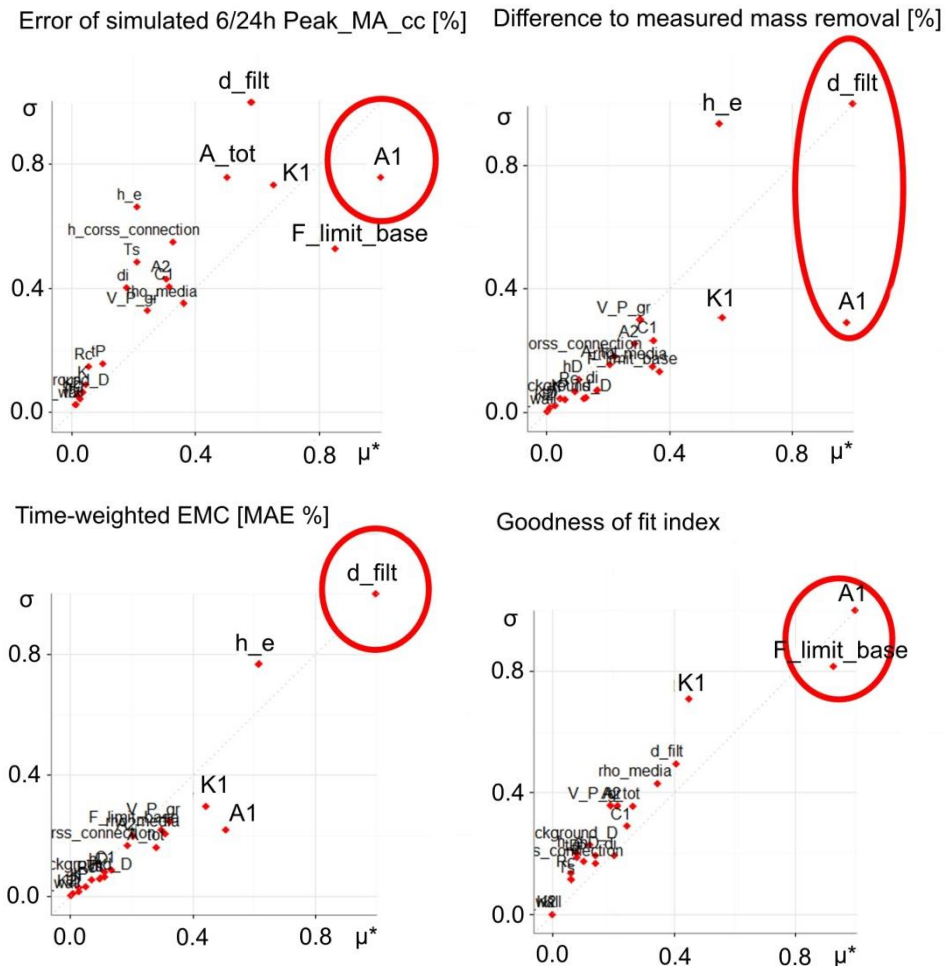


Fig. 35: Sensitivity analysis results for  $NH_4N$ : hydraulically optimized range for filter areas. Adsorption capacity ( $A1$ ) and the available mass of the material ( $d_{filt}$ ) were found to be the most significant.



## 4. Conclusions and Outlook

The core model of Orage was calibrated to a full-scale CSO CW (Marcy l'Etoile) treating unsettled water in twin basins. Manual calibration gave excellent goodness of fit to the single event even though hydraulic and pollutant loads were high. Then, a medium-term event series was simulated, consisting of five loads. The goodness of fit was moderate to good without changing parameters. The unloaded inter-event periods allowed the simulation domain to return to a stable condition which means background levels of water content and  $NH_4N$  in both the liquid and solid phases. As such, the core was proven to be capable to handle data series of any length and give acceptable predictions on effluent rates and pollutant concentrations. This is crucial for reliable design-support which will be based on long-term series.

Statistical analyses of measured and simulated effluent data confirmed model accuracy. The peak of moving average on effluent concentrations ( $Peak\_MA\_cc$ ) is a key variable. It is the connection between the core and the iterative shell which tests various designs (not presented here). Simulated  $Peak\_MA\_cc$  matched well measurements for  $NH_4N$  (error: -1.7 mg/L or -12.2%). The error was rather large for  $COD$  (-18.9 mg/L or -26.9%) due to one event which arrived after a warm and long inter-event and where ponding water was sampled instead of the inlet. Calibrating the effect of inter-event periods on  $COD$  removal should increase accuracy. Further calibration should follow focusing on the effect of unloaded periods on  $COD$  and heavy  $NH_4N$  loads.

The sensitivity analysis has proven model robustness. Most of the parameters can be safely fixed as these have little effect on the output within their realistic range. Parameters identified as significant are either fixed in design guidelines (e.g. percolation speed in the filter media  $F\_limit\_base$ ) or will need meticulous calibration ( $NH_4N$  adsorption parameters by material,  $COD$  removal parameters as the function of dry periods and temperature). The total filter area  $A\_tot$  was important for the simulated  $NH_4N$  removal. The analysis highlighted that filter depth  $d\_filt$  is important too. In the model, adsorption capacities are correlated with the mass of the filter media. In reality, the available organic matter plays a role as well (Fournel 2012).

The accuracy of the core model can be improved further. Modelling a diversity of full-scale sites would be beneficial, after enough sites are built to do so. This is especially true for parameters recorded in internal tables such as those responsible to select the climatic and inter-event effects for  $COD$  removal and the material database containing the adsorption isotherms.

The relatively simple process descriptions of Orage were proven to be satisfactory for modelling CSO CWs. The low number of input parameters will keep handling simple, without compromising the accuracy of predictions. The core is ready to be integrated in an autonomous iterative shell as it had shown accuracy and robustness.

## 5. Acknowledgements

The authors thank Jean-Marc Croumier the flexibility and patience in transferring our ideas into a computer program; the wastewater treatment team's engineers and technicians for their effort which supported field measurements; Nicolas Forquet for his advices and the script to generate parameter sets; Onema and RMC water authorities for their financial support.

Pálffy TG, Gourdon R, Meyer D, Troesch S, Molle P: Design optimization of CSO constructed wetlands: model-based optimization. Environ Model Softw, submitted.

## Manuscript – Design optimization of CSO constructed wetlands: model-based optimization

T.G. Pálffy<sup>\*a,b,c</sup>, R. Gourdon<sup>c</sup>, D. Meyer<sup>a,b</sup>, S. Troesch<sup>b</sup>, P. Molle<sup>a</sup>

<sup>a</sup>IRSTEA Lyon, Freshwater systems, Ecology and Pollution unit, 5 rue de la Doua - CS70077, 69626 Villeurbanne, France

<sup>b</sup>Epur Nature sarl, 153 av. Marechal Leclerc, 84510 Caumont sur Durance, France

<sup>c</sup>INSA Lyon, LGCIE DEEP Team, 20 av. A. Einstein, 69621 Villeurbanne Cedex, France

### Abstract

Constructed wetlands for combined sewer overflow treatment (CSO CWs) are variably saturated vertical flow filters in France. The design-support software Orage facilitates their design by optimizing filter area and material site-specifically, otherwise encumbered by the stochasticity of CSO volumes, concentrations and return periods. Optimization is based on measured or simulated inflow series and just a few input parameters. The iterative shell calls a core model repetitively. During the process, effluent flows and concentrations are simulated for several designs and compared to legislative thresholds. The shell was tested with measured and simulated inflows. Hydraulic optimization parameters were fixed and the optimization for pollutant removal is now more efficient. The optimization approach was verified using inflow and available land from a full-scale CSO CW, with different legislative thresholds. Zeolite-enriched media showed high NH<sub>4</sub>-N removal at hydraulic loads exceeding the recommendations of present guidelines, marking clogging as a potential limitation of compact filters.

**Keywords:** combined sewer overflow; constructed wetland; design-support modelling; dynamic design; Orage; stormwater treatment

**Software:** Orage alpha 0.8 developer interface; developer: IRSTEA and MEGAO Informatique, France; contact: Remy Arnaud (remi.arnaud@megao.com); availability: freeware, version 1.0 available online at [epnac.irstea.fr](http://epnac.irstea.fr) from 2017; disclaimer: Orage is not a substitute of engineering knowledge but a tool to facilitate decisions and design otherwise encumbered by the stochastic and site-specific nature of an engineering problem.

**Abbreviations:** model parameters, variables and components are written in *italic*.

**E-mail addresses:** [tamas-gabor.palfy@irstea.fr](mailto:tamas-gabor.palfy@irstea.fr) (T.G. Pálffy), [remy.gourdon@insa-lyon.fr](mailto:remy.gourdon@insa-lyon.fr) (R. Gourdon), [meyer13@t-online.de](mailto:meyer13@t-online.de) (D. Meyer), [stephane.troesch@epurnature.fr](mailto:stephane.troesch@epurnature.fr) (S. Troesch), [pascal.molle@irstea.fr](mailto:pascal.molle@irstea.fr) (P. Molle).

# 1. Constructed wetlands treating combined sewer overflow

## 1.1. Benefits

Urban stream syndrome is a generalized degradation of streams draining urban land compared to their natural state (Chocat et al., 1994; Walsh et al., 2005). These waters, which are ecosystems and natural resources, are negatively impacted by combined sewer overflows (CSO). Storm events trigger high flow rates of stormwater mixed with sewage in the combined sewer networks. If this rate exceeds the intake capacity of the wastewater treatment plant or what the pipe network can accommodate, the unwanted flow peak is discharged at CSO points (Meyer et al. 2013). These discharges are carrying pollutions in the form of organics, nutrients, heavy metals and bacteria. In contrast, separate sewer outlet (SSO) is released end-of-pipe and has lower concentrations but suspended solids, specific organic pollutants and heavy metals are still a concern. Both CSO and SSO<sup>5</sup> might cause flow peaks which erode and/or silt up stream habitat and change morphology.

Constructed wetlands for CSO treatment (CSO CWs) offer a solution to mitigate the impact of overflows. The term CSO CW was used here to refer to the state-of-the-art in France which is a vertical downflow arrangement. It was developed based on the retention soil filters in Germany (RSFs, *Retentionbodenfiltern*; Uhl and Dittmer 2005, Dittmer et al. 2016), the "French" constructed wetlands for domestic wastewater treatment (Molle et al., 2005) and pilot scale research (Fournel, 2012).

## 1.2. Specific features of CSO CWs

The feeding significantly differs from CWs treating domestic wastewater because CSO flows are stochastic in terms of volume, quality and return periods (Fig. 36). A detention basin over the filter is essential because feedings are flood-like. The basin is empty at the beginning of the events therefore Infiltration and subsequent percolation is limited to the inlet zone. This operational state is considered as short-circuiting. Decreases of NH<sub>4</sub>-N removal performance were reported (Pálffy et al. 2016a). However, pores saturate rapidly and ponding occurs which is considered the normal operational (intra-event state). The whole filter is water contacted and percolation is close to plug-flow. Performance are maximal. Low flow velocities are ensured by the mechanical outflow limitation (orifice) on the outlet structure.

Draining the detained water might take several hours. Once it is done, the pores get filled with air for several days (inter-event state) but stay wet which favours the metabolism of aerobic bacteria. Dominant removal processes differ in the anaerobic intra-event and aerobic inter-event state (Dittmer et al. 2005, Uhl and Dittmer 2005, Dittmer and Schmitt 2011, Meyer 2011, Dittmer et al. 2016). The system might be negatively impacted by long droughts due to the stress on its living organisms.

---

<sup>5</sup> This paper and the modelling tool Orage focuses on CSO-CWs but SSO is touched as well as Orage comes with a hydraulic optimization (scaling) support for SSO wetlands.

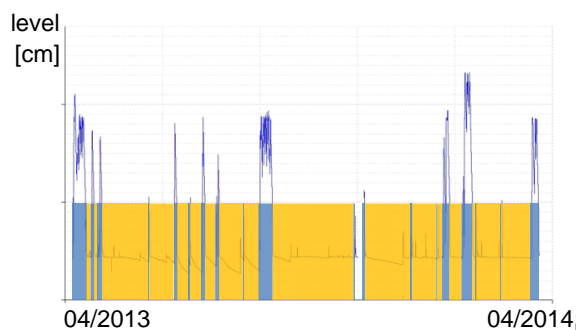


Fig. 36: Water levels in a full-scale CSO CW. Filter operation can be characterized by the stochastic alternation of intra-event (loaded; blue) and inter-event (unloaded, ochre) periods.

### 1.3. Design optimization and modelling

Storms generate stochastic load events (volumes, concentrations) alternated by inter-event periods with different length and temperature. The stochasticity demands a dynamic approach for design optimization which demand can be met by numerical models (Meyer et al., 2015).

Pálffy et al. (2016b) enumerated existing models. Although HYDRUS/CW2D (Langergraber and Šimůnek, 2005) had been calibrated for column scale CSO CWs (Pálffy et al., 2015a), less complexity would fit better engineering purposes (Meyer et al., 2015). On the other hand, the design-oriented model RSF\_Sim (Meyer and Dittmer, 2015) simulates German retention soil filters (RSFs) accurately even at full-scale. This tool was incompatible though with French standards due to the differences in technical implementation discussed in Meyer et al. (2013). Furthermore, HYDRUS/CW2D and RSF\_Sim would demand the manual iteration of different designs, leaving room for a simple and automated toolkit.

The design-support tool Orage has been created for the reasons mentioned above. The core model (Pálffy et al. 2016b) has been inspired by RSF\_Sim to simulate total suspended solids (TSS), chemical oxygen demand (COD) and ammonium-nitrogen ( $\text{NH}_4\text{-N}$ ) removal. Furthermore, Orage is capable to simulate both single- and twin-bed (standards for SSO and CSO in France, respectively) filters and to account for performance decrease at starting loads (short-circuiting). Although Orage was created for CSO CWs, it can help to scale filters treating SSO. This function is limited to a hydraulic optimization in practice because concentrations of  $\text{NH}_4\text{-N}$  and COD in SSO are low anyway and TSS is filtered out with high efficiency regardless inflow concentrations.

The core model works with long inflow datasets (a couple of years). Several parameters are selected automatically during the simulations according to environmental factors such as 1) the regional climate, 2) season and 3) the length of the preceding inter-event period. Furthermore, the core has been integrated into an iterative shell (automatic optimization algorithm) and a user interface to enhance practicability. After launching the optimization, the iterative shell calls the core model repetitively and optimizes the filter area and material.

The software offers a second, decision-support function. The “applicability test” can be used if inflow series are unavailable. The user will rely on one of the 45 internal inflow series (5 climate regions and 9 surface imperviousness categories), which are scaled linearly to the entered catchment area (base: 50 ha) and the PE value (base: 2000 PE). This function reports only 1) if a CSO CW is advisable, 2) if further investigation is proposed before design or 3) CSO CW is not advisable.

The iterative shell of Orage is described and confirmed in this paper using inflows from the existing full-scale site of Marcy l'Etoile. Furthermore, effluent  $\text{NH}_4\text{-N}$  concentrations are analysed in function of filter area and hydraulics and key model parameters are fixed to keep future designs hydraulically fit.

## 2. Methods

### 2.1. Automatized optimization of the iterative shell

#### 2.1.1. General outline

Orage is based on a numerical core model (Pálffy et al. 2016b) which simulates hydraulics (two tanks-in series in parallel) and pollutant removal ( $\text{NH}_4\text{-N}$ , COD and TSS). The core model is called repetitively by an optimization algorithm called the iterative shell. The target is a hydraulically sound design with the simplest material and smallest area (in order of priority). Limits on outflow rate and concentrations can be freely set for each simulation project. The program performs optimization on hydraulics,  $\text{NH}_4\text{-N}$  and COD removal (in order of priority). For the French standards of constructed wetlands treating combined sewer overflow, the reader is advised to refer on cross-section figures in Pálffy et al. (2016a) or Meyer et al. (2013).

#### 2.1.2. Hydraulics

The optimization of hydraulics precedes the optimization for pollutant removal. Its goal is to ensure the efficiency of the latter by determining the range of filter areas [ $A_{min}$ ;  $A_{max}$ ] which will be tested for pollutant removal. The hydraulic optimization is based on 1) the storage volume; 2) the allowed maximum of outflow rate and 3) the short-circuiting time (when percolation is limited to the inlet point), which correlate with filter area. The water authority provides data site-specifically which can be entered to limit point 1) and 2), whilst 3) is limited by an internal parameter as discussed later.

In the case of the maximum area ( $A_{max}$ ), user inputs set an initial limitation before optimization. These inputs are 1) the land area available for the construction and 2) the allowed maximum of outflow rate (because the release rate is linearly proportional to the area). However, these initial limitations might still allow excessively large domains. To filter out these, the dominance of short-circuiting operation over ponding is a good indicator. This is because the outflow rate in overscaled filters is high compared to the inflow rates. These domains never fill or do it slowly which is rendering a high ratio of short-circuiting time steps to all time steps. Therefore the hydraulic optimization decreases the limitation on  $A_{max}$  if necessary, until the ratio of short-circuiting time steps to normal time steps is acceptable (parameter *shortcut\_limit*, see the subchapter on the Refinement of the hydraulic optimization on page 79).

As for  $A_{min}$ , small designs might suffer from excessive hydraulic [ $\text{m}^3/\text{m}^2/\text{year}$ ] and solid [ $\text{kg}/\text{m}^2/\text{year}$ ] loads. Curbing  $A_{min}$  is necessary to avoid long intra-events and to decrease the risk of early clogging. The parameter  $h_{max}$  (maximum ponding depth over the filter area) helps to limit annual hydraulic loads in an indirect way. The wetland has to be able to accommodate a minimum volume fixed by the water authority and as such,  $h_{max}$  curbs  $A_{min}$  (Eq. 14) and therefore the annual hydraulic loads (Eq. 15) as well:

$$A_{min} = V_{design} / (h_{max} + h_P) \quad 14)$$

$$q = V / A_{min} \quad 15)$$

where  $A_{min}$  is the minimum filter area of the optimization range [ $m^2$ ];  $V_{design}$  is the volume which the wetland has to be able to accommodate [ $m^3$ ];  $h_{max}$  is the maximum allowed ponding depth [ $m$ ];  $h_P$  is the water column needed to fill the pore space [ $m$ ];  $q$  is the annual hydraulic load [ $m^3/m^2/year$ ];  $V$  is the total volume of wastewater arriving to the filter [ $m^3/year$ ].

The reader is advised to refer to subchapter 2.2 with regards to the parameter selection for *shortcut\_limit* and *h\_max*.

### 2.1.3. Pollutant removal

*The key variable of optimization: Peak\_MA\_cc*

The iterative shell calls the core model repetitively to perform the material selection and area optimization tasks. For each call, the model returns a single concentration value with the variable *Peak\_MA\_cc* (peak of moving average concentrations), which can be compared to the legislative thresholds. All loads on the CSO CW domain are considered for the calculation of *Peak\_MA\_cc*; however, events shorter than 6 hours (outflow) or where the inflow volume exceeds the one demanded for treatment ( $V_{design}$ ) are ignored. Events are considered to be a new event if there is at least 24 hours passed without outflow. Mean outflow concentrations are calculated at each time step of an event. Between 6 and 24 hours this mean is covering each previous time step since the event beginning (average). After 24 hours, only the last 24 hours are considered (moving average). When the event is over, the maximum of all records is selected (peak). This value is stored for each event. At the end of the simulation, the maximum of all stored values is identified (peak of peaks). This is the value of *Peak\_MA\_cc*, returned for the iterative shell during the optimization both for *NH4N* and *COD*.

*Optimization for ammonium-nitrogen (NH4N) removal*

The hydraulic optimization is followed by the optimization for  $NH_4-N$  removal (Fig. 37). More focus is given to this pollutant than for COD because optimization is nearly always necessary whilst for COD only in special cases. At first, the simplest material is identified which offers a solution with  $A_{max}$ . This is done based on an internal database which contains six adsorption isotherms, organized from the material with the weakest capacity to the one with the strongest. These were calibrated to pilot experiments (sand and gravel: Fournel, 2012) and the full-scale CSO CW at Marcy l'Etoile (pozzolana and zeolite-enriched media with 0.07, 0.12 or 0.18 m zeolite: Pálffy et al., 2016a,b). When *Peak\_MA\_cc* is at the legislative threshold or below, the material gets fixed before further optimization steps.

After fixing the material, the filter areas are minimized in the range [ $A_{min}$ ;  $A_{max}$ ] to still fulfil the legislative thresholds. Performance for  $A_{min}$  are calculated as the first step. If  $A_{min}$  is unsatisfying, the code assumes the linearity of *Peak\_MA\_cc* between the sufficient ( $A_{max}$ ) and insufficient ( $A_{min}$ ) filter areas. The core model is called again with the area where the linear

interpolation predicts  $Peak\_MA\_cc$  to equal the legislative limit. Simulations and linear interpolations are repeated until the simulation output is truly at the limit.

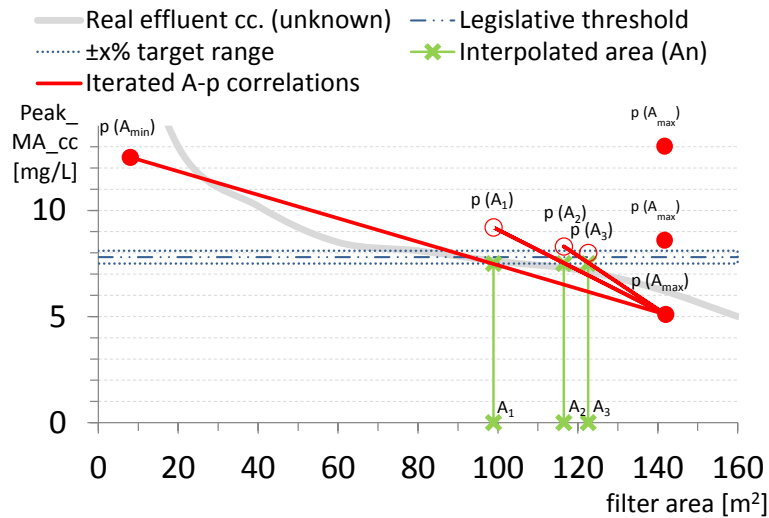


Fig. 37: Illustration of the optimization approach for  $NH_4N$ . The fictive steps were the following: 1) calling the core on three different materials from the database, until  $p(A_{max})$  gets below the target range (right); 2) a simulation showing that  $p(A_{min})$  would be unsatisfying (top left); 3) the first linear interpolation identifies  $A_1$  as a possible solution but calling the core with  $A_1$  shows that  $p(A_1)$  is above the tolerance range; so,  $A_1$  became the new  $A_{min}$ ; 4) the linear interpolation and simulation is repeated two more times ( $A_2$  and  $A_3$ ) –  $p(A_3)$  is found to be in the target range around the legislative threshold so it is accepted as solution.

#### Optimization for COD (COD) removal

After the domain is optimized for hydraulics and  $NH_4N$ , the core model is called to simulate COD removal. Optimization is necessary only if  $COD\ Peak\_MA\_cc$  is above the legislative threshold. Any optimization is carried out at a range defined by the hydraulic optimization (original  $A_{min}$ ) and the optimization result for  $NH_4N$  removal (updated  $A_{max}$ ). Otherwise, the result for  $NH_4N$  removal is kept as final solution.

Strong correlations were absent between filter area, materials and COD removal performance (Fournel 2012). However, it was shown that dry periods might lead to the starvation and drought stress of organisms responsible for the treatment of the soluble fraction. The effect was measured on dissolved COD removal (Meyer and Dittmer, 2015).

The core model was constructed accordingly: filter area and  $Peak\_MA\_cc$  do not have direct or significant correlation. However, indirectly (and oppositely to  $NH_4N$ ), a larger filter might mean lower performance. Large filters drain quicker and have longer inter-events. The core selects from multiple sets of COD removal parameters considering a potential performance drop after such periods. As such, a smaller simulation domain might perform slightly better in COD removal (lower  $Peak\_MA\_cc$ ). Therefore the linear interpolation approach for  $NH_4N$  is used for COD but assuming an inverse correlation of area and  $Peak\_MA\_cc$ .

#### Repeated optimization for ammonium-nitrogen ( $NH_4N$ ) removal

Any iteration for COD decreases filter area. However, the new  $A_{max}$  is known already to be smaller than the area which was necessary for  $NH_4N$  removal. Therefore, after any optimization on COD, the optimization routine of  $NH_4N$  has to be repeated. All areas satisfy COD within the new range; therefore, the second solution for  $NH_4N$  is final.

## 2.2. Refinement of the hydraulic optimization

### 2.2.1. General considerations

An almost monotonic correlation between filter area and *Peak\_MA\_cc* is vital for a successful optimization on pollutant removal. However, parameter interactions affect returned *Peak\_MA\_cc* values as well, especially for *NH4N* and at areas which are hydraulically unsound. This is because

- i. Short-circuiting might become dominant in excessively large filters (*Peak\_MA\_cc* up),
- ii. The old water in the permanently saturated drainage layer has a dilution effect which might be important in even larger filters (*Peak\_MA\_cc* down),
- iii. Excessively small filters mean shorter and less inter-events and therefore there is less time for nitrification (*Peak\_MA\_cc* up).

The optimization for pollutant removal might stop at a local minimum or fail to find a solution if the range of areas [*A\_min*; *A\_max*] is hydraulically not optimized, i.e., covers a wide range. Therefore, a hydraulic optimization is done before the optimization for *NH4N* and the range [*A\_min*; *A\_max*] is tightened as much as possible. This has to be done of course without excluding valuable areas for further optimization steps. The key parameters *h\_max* and *shortcut\_limit* were fixed in the described simulation study accordingly.

### 2.2.2. Optimization of key parameters *shortcut\_limit* and *h\_max*

A simulation study was carried out to optimize the parameter values of *shortcut\_limit* (maximum allowed ratio of short-circuiting time to total outflow time) and *h\_max* (maximum ponding depth over the filter area). Inflow *NH4N* concentrations were arbitrarily set to average 8.1 mg/L with a uniform distribution from 2.2 to 14.0 mg/L, following a randomized pattern. Inflows were the one year long internal datasets coming with Orage for its decision-support function. Flows represented 2 imperviousness categories (25% and 90%) and 5 climate regions (number of input series: 10) of the database. Then, for each input series separately, the 95<sup>th</sup> percentile of all event volumes was selected as the volume to be detained (*V\_design*).

Orage was forced to keep decreasing filter areas, which resulted in long series of simulations for each inflow dataset (10). Simulations were repeated on single and twin-compartment domains (number of simulation series: 20). The series of simulations enabled to plot *Peak\_MA\_cc* over a wide range of filter areas (i.e. ]*A\_min*; *A\_max*]). The annual hydraulic load [ $\text{m}^3/\text{m}^2$ ] and the actual ratio of short-circuiting time [%] were also known for each simulation. As such, rational values could be fixed for *shortcut\_limit* and *h\_max*. The steps were based on charts and statistics which helped to understand simulation domain (or CSO CW) behaviour from various aspects:

- i. Performance (*Peak\_MA\_cc*) in function of filter area,
- ii. Performance (*Peak\_MA\_cc*) in function of short-circuiting time,
- iii. Annual hydraulic load in function of short-circuiting time,
- iv. The correlation of *h\_max* with filter performance, helping to curb *A\_min* in an indirect way (explanation follows).

As for the last point, the analysis took multiple steps. The largest area was targeted where *Peak\_MA\_cc* is still over 90% of the average inlet concentration 8.1 mg/L (at 7.3 mg/L), as



illustrated by Fig. 38. Larger areas should be preserved for the optimization for  $NH_4N$  as the filter is getting big enough for efficient removal. Smaller areas should be excluded as these might be prone for clogging. As such, optimization for  $NH_4N$  should give better results without the range  $]0; A_{min}]$ . Parameter  $h_{max}$ , which is a fixed parameter in the tool, has a direct effect on  $A_{min}$  as shown by Eq. 14 earlier. To fix  $h_{max}$ , at first the area belonging to the 7.3 mg/L  $Peak\_MA\_cc$  was recorded from each simulation series (the optimal  $A_{min}$  of each). Then, ponding depths ( $h_{max}$ ) were calculated which were needed to store the design loads ( $V_{design}$ ) at these areas ( $N=20$ ). The maximum of all  $h_{max}$  was fixed as final value of the parameter. This is a compromise allowing to maximize all  $A_{min}$  in a way that the  $NH_4N$  removal optimization do not lose from the range where  $Peak\_MA\_cc$  undergoes the important changes.

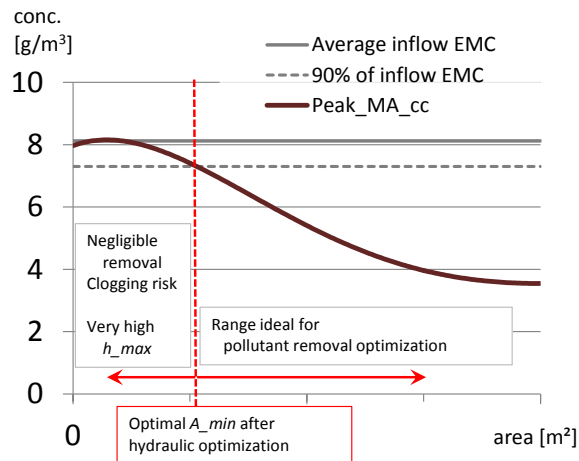


Fig. 38: Hydraulic optimization cuts small filter areas (illustration). Otherwise, even with negligible removal, such areas might have offered an unwanted solution at allowing legislative thresholds on  $NH_4-N$  concentrations. The parameter  $h_{max}$  plays a key role in determining  $A_{min}$  and therefore its value had to be fixed. It was done based on  $N=20$  simulation series (full  $Peak\_MA\_cc$  curves).

### 2.3. Verification of the iterative shell as whole

The optimization approach of Orage was verified using records from an existing CSO CW (Marcy l’Etoile, Pálffy et al. 2016a) monitored online. The input series was 1.5 years long. The loads were dominated by industrial releases. As such, inflow  $NH_4-N$  concentrations were slightly above the typical CSO (Sztuhár et al., 2002). The annual hydraulic load was around the design target of the real system (51.5 m<sup>3</sup>/yr). Fixed parameters (e.g. filter depth, wall height etc.) of the model were set to represent the geometry of the real site.

Verification took two steps. First, design criteria (e.g. concentration thresholds) were arbitrary selected to force numerous iterations. This helped to verify the  $COD$  and second  $NH_4N$  optimization steps which are rarely necessary (see subsections *Optimization for COD (COD) removal* and *Repeated optimization for ammonium-nitrogen ( $NH_4N$ ) removal* in subchapter 2.1.3 Pollutant removal). The design load (the maximum volume to be detained) and the available land of the real site (1160 m<sup>3</sup> and 500 m<sup>2</sup>, respectively) were kept for the process.

Then, the optimization for  $NH_4-N$  removal was scrutinized, by repeatedly scaling the site to satisfy pollutant thresholds ranging from 10 mg/L down to 4 mg/L with 1 mg/L steps. Furthermore, four simulations were run with the area fixed to that of the real site. This allowed seeing the best

achievable results by four materials already in the database. The propositions of the tool were compared to the real material and area of the filter at Marcy L'Etoile.

### 3. Results and discussion

#### 3.1. Parameter selection for hydraulic optimization

##### 3.1.1. Example for a complete *Peak\_MA\_cc* series

There were 20 complete *Peak\_MA\_cc* charts generated as discussed in subchapter 2.2.2. Although these charts were used for the parameter selection of hydraulic optimization, they serve as a true example for *NH4N Peak\_MA\_cc* evolution with the area. An example is Fig. 39. On this chart but also in other simulation series outputs in general (N=20), the following regions could be discretised: 1) filter areas with no treatment (plateau); 2) ideal optimization range [ $A_{min}$ ;  $A_{max}$ ] for *NH4N* removal; 3) range of excessive short-circuiting (higher concentrations); 4) dilution by the permanent water present at the beginning of loads. The vertical line marks the area where concentrations were the lowest.

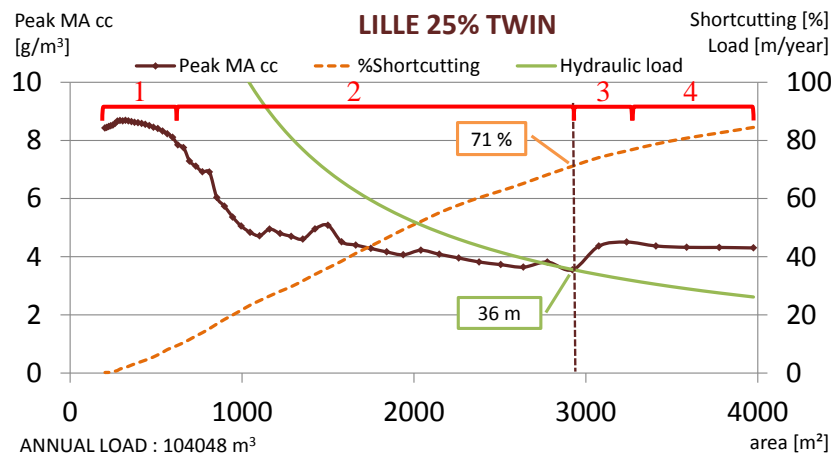


Fig. 39: Evolution of *Peak\_MA\_cc* (black line) in the function of filter area. Each point represents one simulation. Simulations can be separated into four distinctive regions: 1) small filter areas with no treatment and potential risk of clogging; 2) ideal optimization range; 3) range dominated by a concentration increase due to excessive short-circuiting; 4) range of excessive dilution by permanent water in the filter. Note how also the annual hydraulic load (continuous green line) and the share of short-circuiting time steps (orange dashed line) changes with the area.

The generated charts, including Fig. 39, verified that i) regions 3 and 4 are well discernible; ii) the hydraulic optimization is beneficial when targets to exclude regions 1,3 and 4; iii) *Peak\_MA\_cc* is almost monotonically decreasing with the area and this is an early justification of basing the optimization approach on linear interpolations.

##### 3.1.2. Allowed short-circuiting (*shortcut\_limit*)

The parameter is a record of the maximum allowed ratio of short-circuiting time steps to all time steps with outflow. It caps the maximum area ( $A_{max}$ ) before optimization on *NH4N* removal.

Fig. 40 shows *Peak\_MA\_cc* in function of short-circuiting, based on 20 simulation series. On one hand, the hydraulic optimization must avoid short-circuits to exclude large and therefore hydraulically unsound filters. Furthermore, it has to ensure that the valuable ranges for the *NH4N* optimization (left side of the series with the slope) are kept. Note that breakthrough of *NH4N* concentration gets pronounced under 50%-60% short-circuiting. Filters with higher short-circuiting ratio can be safely excluded.

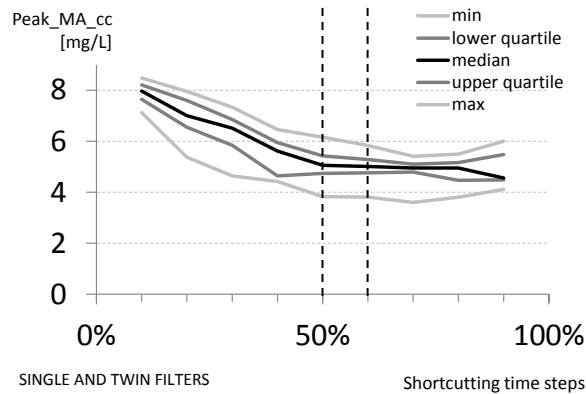


Fig. 40: *Peak\_MA\_cc* as the function of short-circuiting (N=20 simulation series).

To decide between the two values, the annual hydraulic load was to be analysed. This helped to avoid large filter areas where the load [ $\text{m}^3/\text{m}^2/\text{year}$ ] was too low to maintain a healthy wetland biota (underloaded filters). The annual hydraulic load is function of filter area just as short-circuiting; the nominal load might be too low for large filters. This would cause drought stress for certain designs. Present targets are 40 and 50 metres for CSO CWs but this has lately been increased. Hydraulic loads at 50% and 60% short-circuiting are shown by Fig. 41:

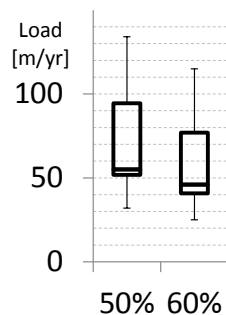


Fig. 41: Hydraulic load as the function of short-circuiting (N=20 simulation series). The flow pattern was typical SSO with loads from the internal inflow series of Orage. Whiskers mark 5<sup>th</sup> and 95<sup>th</sup> percentile.

Based on Fig. 41, the risk that Orage proposes underloaded filter designs is small both at 50% and 60% limit on short-circuiting time. However, it has to be kept in mind that the inflow series were from the simulation of separate sewer outlet (SSO). Contrary to CSO, even the shortest and smallest rains tend to generate loads on SSO wetlands, meaning higher annual load. As such, *shortcut\_limit* was fixed at 50% for now with the remark that it is an ideal value for SSO but a similar analysis should be done for CSO flow series as well. The value can be set separately and a lower tolerance might be beneficial.

### 3.1.3. Maximum ponding depth ( $h_{max}$ )

The value of  $h_{max}$  was fixed to 9.06 m (N=20). This was sufficient to store the design volume ( $V_{design}$ ) at filter areas where  $Peak_{MA_{cc}}$  was equal to 90% of the mean inlet concentration. The hydraulic load would average 150 m at these areas, with the distribution illustrated on Fig. 42:

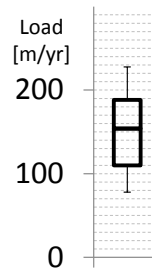


Fig. 42: Hydraulic load at  $A_{min}$  (N=20 simulation series). The flow pattern was typical SSO with loads from the internal inflow series of Orage. Whiskers mark 5th and 95th percentile.

Just as at the conclusion of the previous subchapter, it has to be kept in mind that simulation series on CSO would probably yield lower hydraulic loads.

## 3.2. Verification of the iterative shell

### 3.2.1. Verification of the iterative shell functions

Orage optimized material and area based on inflow series measured at Marcy l'Etoile. Simulations are marked on Fig. 43 in chronological order (series 1-3, arrow bases/heads). The process started with material selection and the optimization of area for  $NH_4-N$  (series 1). The fourth material was satisfactory, close to the 6 mg/L effluent threshold at  $A_{max}$ . An optimization for COD removal followed (series 2). The vertical arrows indicate the non-linearity of  $Peak_{MA_{cc}}$  which is specific for COD iterations. As this step decreased the filter area, a second optimization for  $NH_4-N$  removal (series 3) was called. A material with higher adsorption capacity was selected. Then, the necessary filter area was predicted to be smaller. Concentration-based optimization features were verified and the proposed area was realistic.

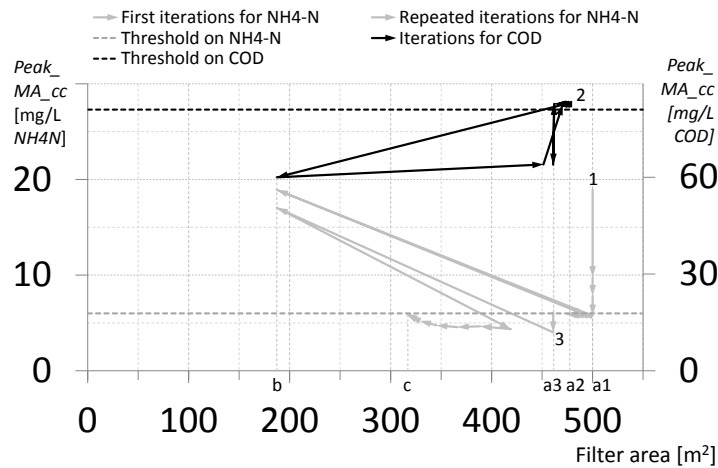


Fig. 43: Verification of the iterative shell of Orage. Each arrow base/head represents one of the thirty-six simulations. Series 1: first optimization for NH<sub>4</sub>-N removal; Series 2: optimization for COD removal; Series 3: final optimization for NH<sub>4</sub>-N removal. Areas: a1=500 m<sup>2</sup> (*A<sub>max</sub>*); a2=472 m<sup>2</sup> (solution of series 1); a3=461 m<sup>2</sup> (solution of series 2); b=187 m<sup>2</sup> (*A<sub>min</sub>*); c=315 m<sup>2</sup> (final solution of series 3).

Hydraulic optimization did not decrease initial *A<sub>max</sub>* before the optimization for pollutant removal. This is because land limitations were strict (500 m<sup>2</sup>).

### 3.2.2. Comparison of design proposals to the parameters of an existing CSO CW

Orage was used to run simulations with measured inflow series and the general design (except area and material) of the CSO CW at Marcy l’Etoile. The software predicted a strong dependency of NH<sub>4</sub>-N removal in the function of the applied material (Table 17). In a filter domain which had the same area as Marcy l’Etoile (500 m<sup>2</sup>), the following thresholds were predicted to be met:

Table 17: Predicted performance as the function of filter media. The filter design was otherwise identical to the full-scale CSO CW at Marcy l’Etoile.

Material	<i>Peak_MA_cc</i> [mg/L]
Coarse sand (S)	9.8
S + 0.07 m zeolite	7.8
S + 0.12 m zeolite	5.8
S + 0.18 m zeolite	3.9

Other simulations were run to test the capabilities of Orage from a user point of view. The experiment used program features which are available for the user in the final interface. This means low number of adjustable parameters and high reliance on the complete range of optimization features. Table 18 enumerates proposed designs based on the 1.5 years dataset. Materials and areas were identified by the iterative shell automatically.

Table 18: Proposed designs in function of effluent limits (filter depth: 0.6 metres). Input: 1.5 years measured data from the CSO CW at Marcy-L'Etoile and had high NH<sub>4</sub>-N concentrations (mean around 15 mg/L). S: adsorption calibrated to a sand 0-4 mm, d<sub>10</sub>: 0.43 mm; d<sub>60</sub>: 1.89 mm based on the work of Fournel (2012).

Limit NH <sub>4</sub> -N [mg/L]	Material	Area [m <sup>2</sup> ]
10.0	Coarse sand (S)	478
9.0	S + 0.07 m zeolite	331
8.0	S + 0.07 m zeolite	479
7.0	S + 0.12 m zeolite	334
6.0	S + 0.12 m zeolite	472
5.0	S + 0.18 m zeolite	333
4.0	S + 0.18 m zeolite	473

The feedings at the Marcy l'Etoile CSO CW are mostly of industrial origin with a quality similar to CSO. The feeding pattern and annual volumes were controlled in a way to represent the load pattern of real CSO sites. It is notable that concentrations of inlet NH<sub>4</sub>-N were above the typical CSO values.

With the material at Marcy (mixture 4:1, equivalent to 0.48 m sand + 0.12 m zeolite) and allowing legislative thresholds of 7.0 and 6.0 mg/L, the software predicted the need of filter areas of 334 m<sup>2</sup> and 472 m<sup>2</sup>, respectively. This means that a compact filter area (compared to the original 500 m<sup>2</sup>) should be satisfactory for pollutant removal even at high concentrations of NH<sub>4</sub>-N arriving to the filter.

## 4. Conclusions and possibilities

### 4.1. Fixing hydraulic parameters

The parameters *shortcut\_limit* (maximum short-circuiting allowed) and *h\_max* (maximum ponding depth over the simulated filter area) were fixed. The new values satisfied several simulations (N=20) and inflow series (N=10). This ensures that hydraulic optimization will work on a wide range of scenarios. This increases the efficiency of the succeeding optimization steps as well. The parameter *h\_max* is a virtual value, i.e., an internal parameter of Orage. Orage reports a different value, the necessary volume of the basin for detaining the volume which is demanded by the water authorities (*V\_design*). Selecting the maximum stage of the filter stays the task of the engineer. The high value of *h\_max* means the detention basin might need a larger area in practice than the filter surface because CSO systems should be implemented with much lower ponding depths (compact filters).

Full series of predicted outflow concentrations (*Peak\_MA\_cc*) were charted over a wide range of filter areas and several simulation series (e.g. Fig. 39). The charts show that adding 0.12 m of zeolite will allow the construction of compact filters due to the high adsorption capacity of this material compared to sand. High hydraulic loads (high solid load per unit surface) will be more of a concern in these than NH<sub>4</sub>-N loads. Rapid aging or filter clogging should be avoided when it comes to the design of compact filters. Further research will be needed to quantify tolerance and to prevent aging / clogging at high annual hydraulic loads (up to 250 m/year), by defining upper thresholds for organic loads and inorganic fines arriving on unit surface area.

### 4.2. Optimizations on pollutant removal

Full *Peak\_MA\_cc* charts helped to parameterize hydraulic optimization. These confirmed also the iterative approach of the optimization for NH<sub>4</sub>-N removal. Later, the verification of the iterative shell confirmed overall functionality. The tool was capable to optimize *Peak\_MA\_cc* to fixed legislative thresholds on concentration, considering both the *NH4N* and *COD* model constituents. Predictions on area and material were consistent and comparable to the real CSO CW at Marcy l'Etoile. The tool suggested sharply different designs in the function of the legislative thresholds.

Effluent concentration thresholds are advised to be set rigorously on NH<sub>4</sub>-N (between 3-5 mg/L) to benefit from the optimization feature of the software. An allowing threshold would lead to return *A\_min* as solution more often, meaning to support the design of CSO CWs which do not benefit from the capabilities what the state of the art CSO CW concept offers.

### 4.3. Remarks on software utilisation

Software accuracy can be increased further. The present values of *shortcut\_limit* and *h\_max* are rather allowing. It is advised to revise them in the future with identical simulation approach but based on measured flows and separately for SSO and CSO. It is also advised to refine material properties and removal rate constants based on a range of sites built in the future. The first sites scaled with the tool should be intensively monitored. The feedback would be important to maximize the precision of the optimization.

The practical use of Orage can be encouraged with the present calibration but with caution. Orage is not a substitute of engineering knowledge but a tool to facilitate decisions and design otherwise encumbered by the stochastic and site-specific nature of an engineering problem.

## 5. Acknowledgements

The authors thank Jean-Marc Croumier the flexibility and patience in transferring our ideas into a computer program; Dirk Esser for his advice on realistic ponding depths; Onema and RMC water authorities for their financial support.



## 5.2 Key findings of the two manuscripts in this section

The core model of Orage has gone through a wide range of tests, including visual and statistical evaluation of goodness of fit. The model has been confirmed and proven to be robust by the sensitivity analysis and by the simulation of event series using parameters which were otherwise calibrated only to a single event. Model accuracy was moderate to good. Accuracy will be further improved by further calibration to field measurements.

Accuracy and robustness are two important factors for reliable design optimization. It has been shown that the integration of the core model into an automatized iterative shell is justified due to its reliability.

As for the iterative shell, parameters of the hydraulic optimization were fixed using internal SSO input series with  $\text{NH}_4\text{-N}$  concentrations typical for CSO. This means hydraulic loads for CSO would be lower with the same maximum ponding depth ( $h_{max}$ ) (smaller risk of clogging at  $A_{min}$ ). Even so, when building compact filters (i.e., where the net filter area is smaller than the total basin area), technical measures should be considered to minimize clogging risks. Building compact filters is possible based on the simulation results, without compromising  $\text{NH}_4\text{-N}$  removal performance. However, further research will be needed to quantify tolerance and to prevent aging / clogging at high annual hydraulic loads (up to 250 m/year), by defining upper thresholds for organic loads and inorganic fines arriving on unit surface area.

On the side of overscaled filters, the parameters of the hydraulic optimization were fixed to be rather allowing (the range [ $A_{min}$ ;  $A_{max}$ ] is wide on the side of  $A_{max}$ ), and therefore further adjustments would enable better efficiency in the future. This can be done based on real CSO inflow data. As an overall conclusion, the iterative shell has been confirmed and verified by comparing its suggestions to the design of a full-scale CSO site at Marcy l'Etoile. Industrial application is encouraged.



## **6 Performance and process dynamics of the first full-scale CSO CW in France**

## 6.1 Context and highlights

The experimental site at Marcy l'Etoile was the first full-scale CSO CW built and evaluated in France. Flows and water quality have been intensively monitored using automatic samplers and online probes, for a period of three years. Two events were sampled for micropollutants (metals and PAHs) as well. This enabled the evaluation of filter performance in terms of pollutant removal. Additionally, medium-term campaigns targeted specific processes inside the filter, one by one. These processes were i) filter hydraulics at commencing load; ii) nitrogen dynamics and iii) sludge accumulation. Results are introduced in two manuscripts belonging to this section, titled "*Filling hydraulics and nitrogen dynamics in a full-scale CSO CW*" and "*Efficiency of a full-scale CSO CW for major- and micropollutants*". Some of the scrutinized processes were known from earlier works. Still, quantification was essential even in those cases to calibrate the core model of Orage.

Highlights of the manuscript dealing with hydraulics and nitrogen dynamics:

- We introduce experiments targeting process dynamics of a full-scale CSO CW
- Filling hydraulics is visualized inside the longitudinal section of the filter
- Adsorption capacities are quantified for pozzolana and a sand and zeolite mixture
- Nitrification rate and nitrate flush are analysed in-depth and an equation is fitted
- We give proposals for the improvement of design as well as for future research

Highlights of the manuscript dealing with removal performance and solid accumulation:

- The first full-scale CSO CW in France has been intensively monitored
- We analyze efficiency on major pollutants based on a high number of events
- The depth of sludge is mapped and sludge is analysed for metals and PAHs;
- COD removal is analyzed by multiple linear regression with environmental factors
- Understanding micropollutant behaviour in the system needed more detailed research

Pálffy TG, Gourdon R, Meyer D, Troesch S, Olivier L, Molle P: Filling hydraulics and nitrogen dynamics in full-scale CSO CWs. Manuscript ready for submission.

## Manuscript – Filling hydraulics and nitrogen dynamics in full-scale CSO CWs

T.G. Pálffy<sup>\*a,b,c</sup>, R. Gourdon<sup>c</sup>, D. Meyer<sup>a,b</sup>, S. Troesch<sup>b</sup>, L. Olivier<sup>a</sup>, P. Molle<sup>a</sup>

<sup>a</sup>IRSTEA Lyon, Freshwater systems, Ecology and Pollution unit, 5 rue de la Doua - CS70077, 69626 Villeurbanne, France

<sup>b</sup>Epur Nature sarl, 153 av. Marechal Leclerc, 84510 Caumont sur Durance, France

<sup>c</sup>INSA Lyon, LGCIE DEEP Team, 20 av. A. Einstein, 69621 Villeurbanne Cedex, France

### Abstract

According to French standards, constructed wetlands treating combined sewer overflow (CSO CWs) are vertical flow filters with detention basin and outflow limitation. Their purpose is to treat rapid loads of wastewater with stochastic volumes, concentrations and periodicity. The first full-scale CSO CW has been monitored at Marcy l'Etoile for three years, involving online equipment. It provided in-depth understanding of hydraulics and nitrogen dynamics. The saturation of the filter media was visualized along the longitudinal section of the filter to follow hydraulics in the fill stage. Tracer tests showed short-circuiting effects weakening as the filter saturated, which tallied with decreasing NH<sub>4</sub>-N concentrations in the outflow. Adverse short-circuiting effects can be diminished by minimizing fill time of the media. As for nitrogen dynamics, adsorption capacities showed no difference in the two filter sides, one with a sand-zeolite mixture (4:1) and the other with pozzolana. An equation was fitted to temperature and adsorbed NH<sub>4</sub>-N mass measurements to calculate inter-event nitrification. The rate was found to double with every 5.7 °C. The results helped to calibrate the design-support software Orage. Finally, the analysis of the NO<sub>3</sub> N washouts highlighted the possibility of a second filter stage for denitrification.

**Keywords:** adsorption capacity, combined sewer overflow, constructed wetland, short-circuiting, nitrification rate, Orage

**E-mail addresses:** [tamas-gabor.palfy@irstea.fr](mailto:tamas-gabor.palfy@irstea.fr) (T.G. Pálffy), [remy.gourdon@insa-lyon.fr](mailto:remy.gourdon@insa-lyon.fr) (R. Gourdon), [meyer13@t-online.de](mailto:meyer13@t-online.de) (D. Meyer), [stephane.troesch@epurnature.fr](mailto:stephane.troesch@epurnature.fr) (S. Troesch), [laurie.olivier@irstea.fr](mailto:laurie.olivier@irstea.fr) (L. Olivier), [pascal.molle@irstea.fr](mailto:pascal.molle@irstea.fr) (P. Molle).

## 1. Introduction

### 1.1. CSO treatment with vertical flow systems

Constructed wetlands for combined sewer overflow treatment (CSO CWs) are vertical flow filters with detention basin and fixed outflow rate. Because feedings are triggered by intense precipitation events, loads are stochastic in terms of volumes, concentrations and return periods. Water arrives if sewer flows exceed what the wastewater treatment plant or the pipe itself can accommodate (Meyer et al. 2013). Treating this water instead of direct rejection protects natural waters against pollutants and disadvantageous changes of streambed morphology. As such, CSO CWs mitigate the so-called urban stream syndrome which is the generalized degradation of stream habitats draining urban land (Chocat et al. 1994; Walsh et al. 2005).

The pattern of hydraulic operation differs from CWs treating sewage. As outlet flow limitation is lower than infiltration capacity, loadings saturate the porous media from the bottom at first and then cause ponding in the detention basin above it. The ponding might reach significant depth at voluminous events (intra-event state). The infiltration and subsequent treatment of the detained water may take several hours according to the small diameter of the orifice limiting the outflow. The coarse filter material helps to avoid clogging and outflow limitation avoids hasty passage and too short biofilm contact. When ponding is over, air penetrates the pores again. The filter layer gets gravity drained and rests unloaded for several days (inter-event state). Then, aerobic processes dominate. Filter design should seek a way to avoid drought stress on wetland biota as beds might dry out in extremely long and warm inter-events. The regeneration in the unloaded period enables to treat another load rapidly and efficiently (Dittmer et al. 2005; Uhl and Dittmer 2005, Dittmer and Schmitt 2011; Meyer 2011;).

CSO CWs typically target to remove water quality constituents TSS, COD and  $\text{NH}_4\text{-N}$ . The treatment starts with sedimentation and physical filtration in the top few centimetres (Dittmer 2006). The dominant processes are filtration of organic and inorganic solids, anaerobic bacterial uptake of dissolved COD and  $\text{NH}_4\text{-N}$  adsorption. In contrast, the still wet but air-filled media favours nitrification and the mineralization of organics in the inter-event period (Dittmer et al. 2005; Uhl and Dittmer 2005; Dittmer and Schmitt 2011; Meyer 2011).

### 1.2. The standard of CSO CWs in France

CSO treatment will be mandatory in France in accordance with the goals set in the European Water Framework Directive (2000/60/EC). Vertical downflow arrangements (Fonder and Headley 2013) were applied or desired in European countries as stand-alone stage or as an element of a treatment chain (Meyer et al. 2013). The first positive experiences came from retention soil filters (RSFs or Retentionsbodenfiltern) in Germany (Uhl and Dittmer 2005; Dittmer 2006). We refer with the term CSO CW to the French state of the art (Fig. 44) unless otherwise specified.

Performance and process dynamics  
of the first full-scale CSO CW in France

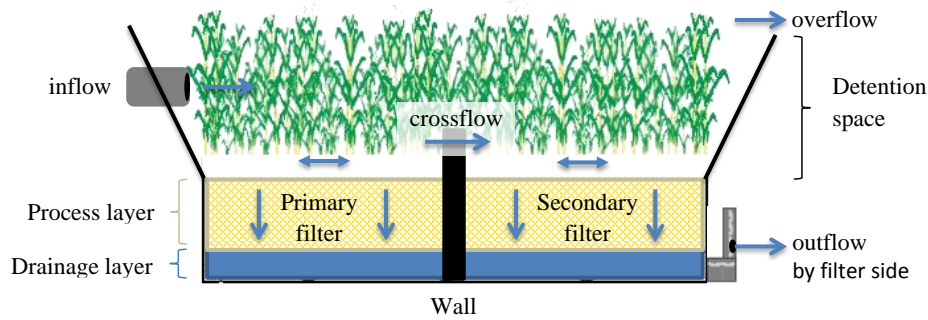


Fig. 44: CSO CWs in France come with twin filter sides and permanently saturated drainage layer.

Standards in France were based on experiences from Germany (Uhl and Dittmer 2005; Frechen et al. 2006; Dittmer and Schmitt 2011), from pilot-scale studies on a range of filter materials and filter depths (Fournel 2012) and on “French-design” CWs which treat unsettled municipal wastewater (Molle et al. 2005). The traits of CSO CWs are:

- i) Treating unsettled water facilitates sludge management. To protect the system against early clogging, feeding priority is alternated between the twin filter sides. The secondary side receives settled water from the primary side and at large events only. As such, longer inter-events and low solid loads favour sludge mineralization on the secondary side.
- ii) the permanently saturated drainage layer on the bottom saves water for living organisms to any drought;
- iii) aeration pipes are laid above the drainage layer. Placing them in the process layer is assumed to improve aeration;
- iv) zeolite is added to the filter media if higher ammonium-removal is needed;
- v) a thin compost cover facilitates reed establishment.

The first full-scale CSO CW site was built at Marcy l’Etoile (France). Table 19 summarizes the general characteristics of the wetland. The combined sewer drains mostly residential area and the wetland was designed to accommodate flow volumes with one year return period. As an industrial release is present in the sewer, a weir has been installed at the overflow point. The regular adjustment of this weir enabled to mimic the stochasticity of feedings without rain. Concentration ranges were comparable to unsettled CSO (Sztruhár et al. 2002; Fournel 2012), with NH<sub>4</sub>-N concentrations at the upper end of the range (median EMC: 13.8 mg/L).

## Performance and process dynamics of the first full-scale CSO CW in France

Table 19: General characteristics of the CSO CW at Marcy l'Etoile

Parameter	Unit	Value
Catchment area	[ha]	98
Detention capacity	[m <sup>3</sup> ]	1160
Nominal hydraulic load	[m/year]	50
Filter surface	[m <sup>2</sup> ]	500
Target outflow rate	[l/s/m <sup>2</sup> ]	0.016
Population equivalent	p.e.	9200

The filter layers are shown on Fig. 45. One filter side was filled with a mixture of 48 cm sand and 12 cm zeolite (4:1) whilst the other with pozzolana. The filter had about three years of startup operation before the nitrogen dynamic assessments.

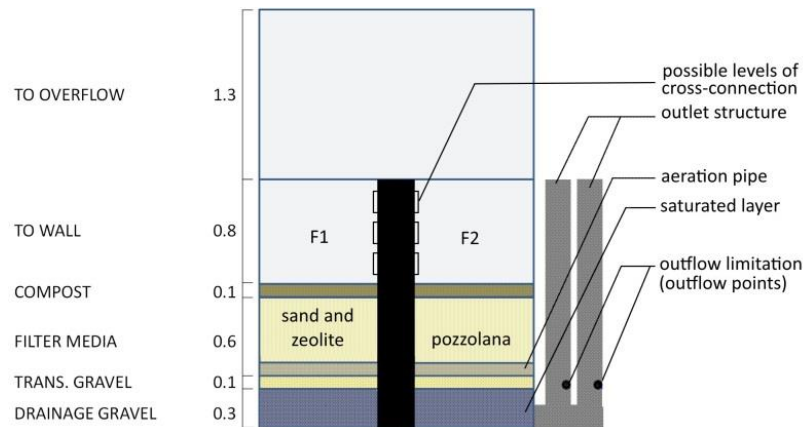


Fig. 45: Cross-section and internal structure of the CSO CW at Marcy l'Etoile, France.

## 2. Materials and Methods

### 2.1. Monitoring of flows and concentrations

Flow measurements and sampling were automatic. Inflow rates were registered based on an ultrasonic probe over a Venturi channel. At the outlet structure, the orifice allowed to use pressure probes and a calibrated correlation of the outflow rate with the pressure head.

Flow composite samples were taken at the inlet. The outlet was sampled time composite as orifice flows were stable. Inlet and outlet samplings had a mean volume of 326 m<sup>3</sup> and 60 m<sup>3</sup>, respectively. Samples were analysed for TSS, total and filtered COD, NH<sub>4</sub>-N, NO<sub>3</sub>-N and PO<sub>4</sub>-P. Two online probes (WTW Varion) were placed in the outlet structures to monitor NH<sub>4</sub>-N and NO<sub>3</sub>-N concentrations with a sampling rate of one minute. Loads averaged 735 m<sup>3</sup> for nitrification rate tests and 4800 m<sup>3</sup> for adsorption capacity tests.



## 2.2. Water content and wetting front

Plug flow is assumed through the porous filter media after it is saturated by water. In contrast, a wetting front can be assumed at commencing load meaning a partial utilisation of the filter at the proximity of the inlet point. If percolation is limited to the inlet zone, biofilm contact and adsorption capacities are limited as well. The phenomenon is referred to as short-circuiting and decreases performance.

To visualize it, changes in the volumetric water content were followed by measurements. Time domain reflectometry (TDR: Topp et al. 1980; Ledieu et al. 1986) was used with a sampling rate of one minute. A network of eighteen probes (30 cm, triple wire, CS610 or built in-house at UCL Belgium) was installed as shown on Fig. 46. The probe density was higher to improve resolution near the inlet. The probes were calibrated for the two filter materials of Marcy l'Etoile following the method of Fournel (2012). The installation disturbed the media so the first measurements started after loading 25% of the annual target volume.

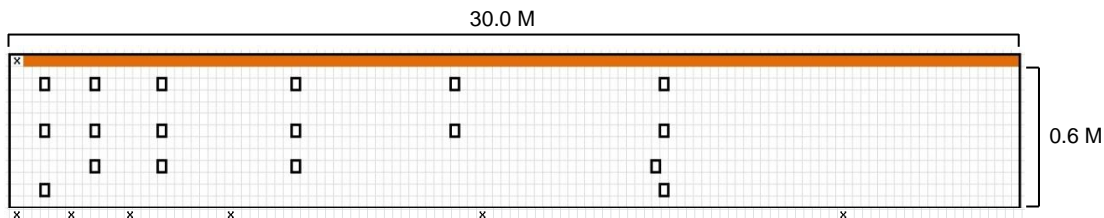


Fig. 46: Position of the eighteen TDR probes along the longitudinal filter section (cells are 5 cm vertically and 25 cm horizontally). Framed cells represent the probes. Squares filled with 'x' represent extra points where the water content was known to be saturated during loading (drainage layer and inlet point at the top). The brown strip marks the compost and sludge cover.

Data had been imported in MS Excel and associated with cells to represent the longitudinal section. Inverse distance weighting (IDW: Shepard 1968) was used for multivariate interpolation with the known scattered set of points. IDW was carried out with the parameters summarized in Table 20. Colouring was then rendered and a macro enabled to visualize the saturation and the drainage of the filter with one minute detail.

Table 20: Parameters at the multivariate interpolation of volumetric water content for inverse distance weighting.

Parameter	Value
Power parameter $p$ [-]	5.0
Horizontal search neighbourhood [m]	15.0
Vertical search neighbourhood [m]	0.4
Number of cells	1027
Number of cells with TDR measurements	18
Number of auxiliary data cells at the filter bottom	6
Number of auxiliary data cells at the filter top	1

### 2.3. Tracer test and evidence of short-circuiting

The saturated drainage layer was assumed to mitigate short-circuiting by dilution. Once the load starts, the water get in contact with more and more adsorption sites until filter saturation is reached, thus improving ammonium adsorption. Dilution with water already present and adsorption will work together against concentration breakthrough caused by short-circuiting and short detention times. A tracer test with multiple tracer pulses had been carried out to see the effect of dilution.

A fluorometer (GGUN-FL 932) was calibrated using outflow from the site and registered outlet concentration on a minute time step. One filter side was used as a storage basin after blocking its outlet. Then, a pump delivered flow to the filter in operation at a low rate ( $11.5 \text{ m}^3/\text{h}$ ) to reach saturation in 4.5 hours. Fluorescein impulses (uranine) were injected into the inflow (duration: 6.2 minute, target concentration:  $0.8 \text{ g/m}^3$ ), using a peristaltic pump at the start of the load and 1.5 hours and 3 hours later. When the process layer had been saturated, the filter was flooded by opening knife gate valves on the cross-connection pipes between the two filter sides. Flooding lasted nearly for three days to ensure high tracer recovery.

Results from the tracer experiment had been indirectly compared to ammonia short-circuiting measurements during normal events. The short-circuiting effect on ammonia removal has been monitored by online nitrogen probes placed at the outlet. Short-circuiting peaks of  $\text{NH}_4\text{-N}$  (Fig. 47) were analysed ( $N=20$ ). Their base was taken to be the minimum concentration within three hours before (0% breakthrough). A complete breakthrough was when the top of the peak equalled to the inflow concentration (100% breakthrough). The breakthroughs were normalized by expressing them as percentage of the complete breakthrough.

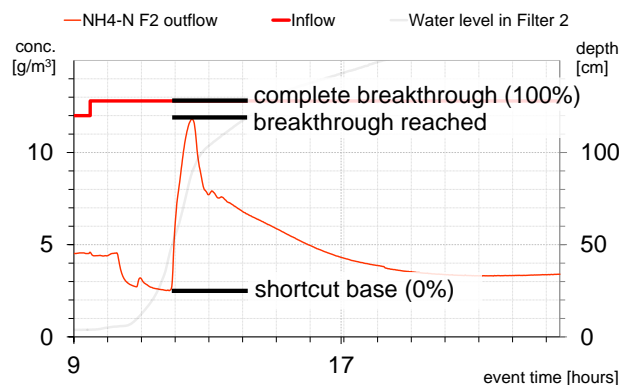


Fig. 47: Normalization of short-circuiting peaks. A breakthrough would be complete if the effluent concentration was equal to the inflow concentration. By the time the saturation is complete (filter surface at 100 cm level) the peak was always over just like on this example representing the strongest observed peak.

### 2.4. Quantification of ammonium adsorption capacity

Regular industrial releases enabled to generate extremely long feedings by leaving the weir at the overflow point open. High  $\text{NH}_4\text{-N}$  loads were assumed to saturate adsorption sites and make breakthrough observable (Uhl and Dittmer 2005; Woźniak 2008; Fournel 2012; Meyer and Dittmer 2015). Two events were created. A perfect mixing and a uniform load of  $\text{NH}_4\text{-N}$  were assumed on the two filter sides with water levels above the wall separating these. One event was sampled from the mixed effluent and one other was monitored by filter side. Table 21 summarizes the load characteristics. Events were preceded by at least two weeks of inter-event to allow filter regeneration. For the event where the filter sides were compared, the same initial state could be assumed in the two filter sides because the event was preceded by a load followed by a long inter-

event to have complete regeneration. Retained  $\text{NH}_4\text{-N}$  masses were calculated based on the mass balance. The mass of  $\text{NH}_4\text{-N}$  in the infiltrating wastewater was divided between the two filters based on a simulation in Orage (Pálffy et al. 2016). It was assumed that all  $\text{NH}_4\text{-N}$  removal in the intra-event is due to adsorption.

Table 21: Overload events at Marcy l'Etoile

Event	Preceding inter-event [days]	Duration [days]	Load [m]	Load [g $\text{NH}_4\text{-N}/\text{m}^2$ ]
E14	14	7.7	11.11	156.4
E30	25	5.5	8.02	114.6

## 2.5. Quantification of the nitrification rate at field scale

The long regeneration time prior to nitrification rate experiments allowed assuming that residual  $\text{NH}_4\text{-N}$  in the filter is negligible. Then, inflow and outflow masses had been recorded for four consecutive events (Table 22). The adsorbed  $\text{NH}_4\text{-N}$  mass was estimated for the beginning of each inter-event period. A part of this adsorbed mass was nitrified and flushed out as  $\text{NO}_3\text{-N}$  at the following load. The mass of the flushed nitrate was divided by the duration of the inter-event to get the nitrification rate. Atmospheric exchange and alternative pathways like anammox were ignored. Denitrification lacks organic carbon and anoxic environment.

The rate was assumed to be dependent from the temperature and the concentration of the pollutant in the adsorbed phase. Soil thermometers were placed in the filter media at 5 and 50 cm depth. The experiments were repeated in three different seasons and mean inter-event temperatures were used (Table 22). Finally, 16 (from the simulation tool RSF\_Sim, Meyer and Dittmer 2015) were fitted to the nine measurements. The outcomes were used to calibrate the design-support modelling software Orage (Pálffy et al. 2016).

$$\text{NH4N}(t + 1) = \text{NH4N}(t) \times e^{-d_{i,t}} \quad (16)$$

$$d_{i,t} = d_{i,t} \times e^{\frac{T-20}{Rc}}$$

where  $\text{NH4N}(t)$  is the mass of  $\text{NH4N}$  (model component for  $\text{NH}_4\text{-N}$ ) at time step  $t$ ,  $d_{i,t}$  is a rate constant [1/time]. The second line of the equation corrects  $d_{i,t}$  according to the temperature  $T$  [°C] and the temperature sensibility constant  $Rc$  [-].

Performance and process dynamics  
of the first full-scale CSO CW in France

Table 22: Inter-events of the three nitrification rate campaigns (rest periods before the loads).

Experiment no., Season	Event no.	Inter-event [days]	Filter temp. [°C]
#1 Spring	E16	(60)	
	E17	1.0	17.5
	E18	3.5	21.9
	E19	11.9	18.7
#2 Summer	E20	(12)	
	E21	7.2	23.4
	E22	6.0	26.5
	E23	4.8	24.7
#3 Winter	E25	(36)	
	E26	3.2	10.7
	E27	2.9	13.6
	E28	4.6	12.7

## 2.6. Nitrate flush

Adsorbed  $\text{NH}_4\text{-N}$  was observed to be nitrified in the inter-event periods under aerobic conditions and nitrate to be flushed out early with the next load (Uhl and Dittmer 2005). This caused a concentration peak of  $\text{NO}_3\text{-N}$  at the beginning of each load at Marcy l'Etoile as well. After the peak, nitrate concentrations in the effluent settled to match the influent. The peaks allowed assigning hydraulic loads [in  $\text{m}^3/\text{m}^2$ ] which are required to flush out nitrate. Although nitrate flush is less harmful for receiving waters than ammonia it is still a concern because it might contribute to harmful algal blooms and was found to shift algal communities (Walsh et al., 2005).

## 3. Results and Discussion

### 3.1. Hydraulic short-circuits

The filling until saturation can be followed on Fig. 48 in twenty minute steps (Fig. 48a-g). The proximity of the inlet was wet before loading which is probably the effect of the locally present sludge blanket (Fig. 48a). Soon after the loading started (b), the wetting front reached the permanently saturated layer (c). Short-circuiting was strong because infiltration was limited to the proximity of the feeding point. As such, the outflow limitation couldn't take effect and the percolation rate was limited by the conductivity of the sludge blanket. This can be assumed from the unsaturated nature of flow (Fig. 48c and d). Water retention times are in the range of an hour instead of the 16 hours which is normal after saturation (results from tracer experiments, Fig. 49). From this moment on, the wetting front extended horizontally and the filter media is filled from bottom to top at the same time (Fig. 48d-f). The whole filter is saturated finally (Fig. 48g) and ponding occurs. The filling took 90 minutes in this experiment but for other events it had often been more rapid.

## Performance and process dynamics of the first full-scale CSO CW in France

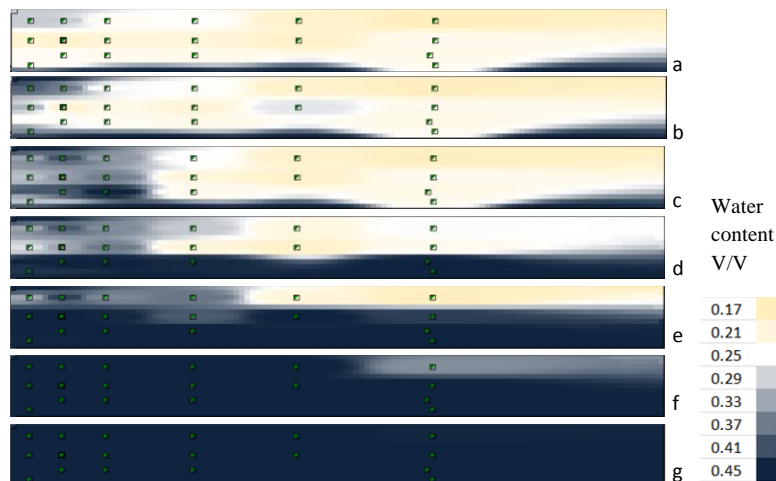


Fig. 48: The short-circuiting phenomena of CSO CWs. When loads begin, the flow is limited close to the inlet point (panels b to d; top left). With increasing water level, more filter media gets water-contacted (panels e-f) until saturation is reached (panel g). This latest ensures maximized performance and is considered as normal operation (near plug-flow).

The tracer experiment targeted the same phenomena. Tracer recovery rate was 90.1%. The fluorescein impulses generated two distinctive peaks and one plateau in the concentration curve of the effluent (Fig. 49).

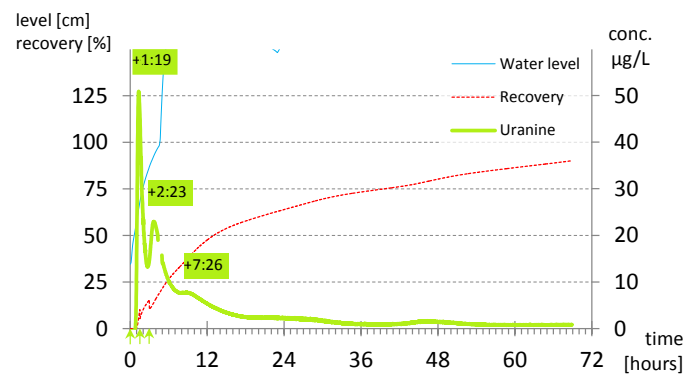


Fig. 49: Tracer concentration (uranine) at the outlet. The arrows near the origin mark tracer injections. The boxes at the peaks write the delay [in hours] since the corresponding injection. The water level reached the filter surface at 100 cm.

The arrival of the tracer peaks to the effluent gained more delay with the increasing pressure head. The first peak occurred in 79 minutes after injection which was the nominal detention time at the beginning of the experiment. Water arrived to a filter where only the permanently saturated drainage layer was saturated (level at 35 cm). The detention time rose later to 143 minutes at 68 cm and 446 minutes at 87 cm. An increase of the detention time favours removal process. TDR and tracer test results helped to anticipate the evolution of short-circuiting with regards to  $\text{NH}_4\text{-N}$  removal performance. Adsorption and mixing with the pore water can be anticipated to decrease  $\text{NH}_4\text{-N}$  breakthrough together as well as longer contact times work to aid biofilm to remove dissolved pollutants in general.

The measurements of online nitrogen probes tallied with tracer test results for all observations. Fig. 50 shows the correlation between the pressure head at commencing load (the initial depth of the saturated layer) and the peak of the breakthrough which was reached during short-circuiting. The permanently saturated drainage layer mitigates the short-circuiting effect by keeping effluent concentrations low. Breakthrough of  $\text{NH}_4\text{-N}$  concentrations above 40 to 50 cm pressure head was considered unimportant because there was little room left for further improvement.

## Performance and process dynamics of the first full-scale CSO CW in France

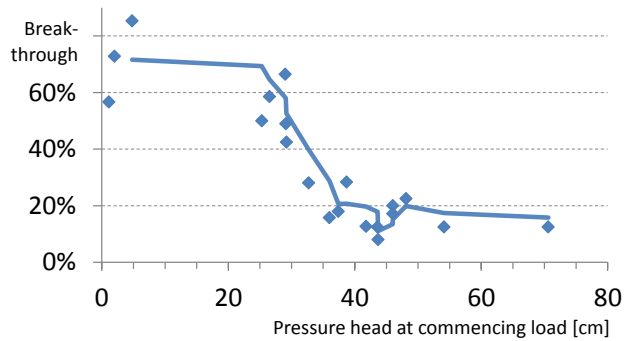


Fig. 50: The strength of  $\text{NH}_4\text{-N}$  breakthrough due to short-circuiting in the function of pressure head at commencing load. The blue series represent the three period moving average. Based on the visual interpretation of the trend, there is little room for further deterioration or improvement below 25 cm and above 45 cm, respectively.

### 3.2. Nitrogen dynamics

#### 3.2.1. Adsorption capacities

The breakthrough test served to evaluate  $\text{NH}_4\text{-N}$  adsorption capacity and showed a large potential for mass removal for the two filter sides together (E14, Fig. 51). Breakthrough started after filtering  $1850 \text{ m}^3$  which is the volume of the five years' event. It corresponds to an adsorption of  $46.5 \text{ g NH}_4\text{-N/m}^2$ . Mean inlet concentration was  $12.5 \text{ g/m}^3$ . Effluent concentrations before breakthrough were slightly above those observed in systems in Germany (e.g. Meyer and Dittmer, 2015). As for the rest of the load, effluent concentrations rose progressively. Retained mass was  $80.6 \text{ g NH}_4\text{-N/m}^2$  and inlet EMC was  $16.0 \text{ g/m}^3$  for the whole event.

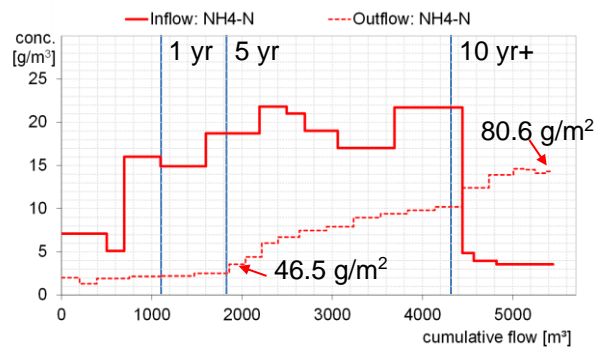


Fig. 51: Breakthrough curve and adsorption capacities based on both filter sides (E14).

There were no notable differences between the two filter sides despite of the different filter media (E30, Fig. 52). Breakthrough occurred after retaining  $36.4 \text{ g/m}^2$  and  $39.5 \text{ g/m}^2$  in the primary (sand+zeolite mixture, 4:1) and secondary (pozzolana) filter side, respectively. This corresponds to an infiltrated volume of  $1680 \text{ m}^3$ , which is somewhat below the load with five years return. The mean inlet concentration was about  $17.5 \text{ mg/L}$  until the breakthrough. For the whole event, inlet EMC was  $14 \text{ mg/L}$ . The retained mass was  $54.7 \text{ g/m}^2$  and  $54.8 \text{ g/m}^2$  in the primary and in the secondary filter, respectively. This corresponds to a mass removal of 52% in sand+zeolite mixture and 54% in the pozzolana filter (adsorbed mass:  $69.1 \text{ g/t}$  and  $102.0 \text{ g/t}$ , respectively).

## Performance and process dynamics of the first full-scale CSO CW in France

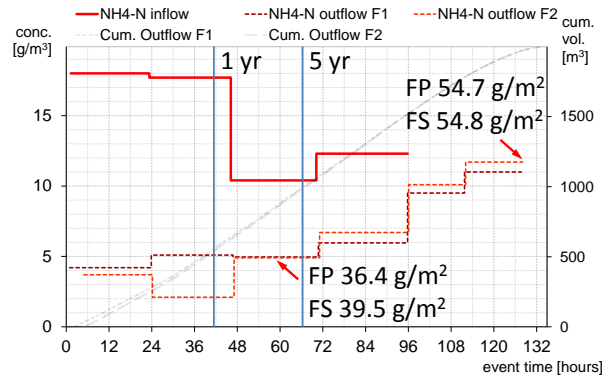


Fig. 52: Breakthrough curve and adsorption capacities by filter side (E30). FP: primary filter side; FS: secondary filter side.

The breakthrough events E14 and E30 were used to calibrate the design-support tool Orage. The improvement in the adsorption capacity due to zeolite was calculated by comparing the capacities of Marcy l'Etoile (4:1 sand and zeolite mixture, equivalent to 0.48 m sand and 0.12 m zeolite) to pilot-scale experiments with 0.6 metres of pure sand (Fournel, 2012). This enabled to estimate adsorption capacities for sand-zeolite mixtures containing 7 cm and 18 cm of zeolite as well, based on a correlation which was expected to be linear between the improvement of the adsorption capacities with the depth of zeolite. Adsorption isotherms belonging to all three zeolite depths were included in the material database of Orage.

### 3.2.2. Nitrification

The nitrification rate was determined based on closed mass balances calculated for four consecutive loads (Fig. 53). The experiment was repeated in three seasons to calibrate the impact of filter temperature. The cumulative adsorbed ( $\text{NH}_4\text{-N}$ ) and released ( $\text{NO}_3\text{-N}$ ) masses can be followed on the three panels of Fig. 53. During the spring campaign (Fig. 53, top panel), nitrification seems to be incomplete but according to the length of the last dry period, it was likely complete. At summer, the warm temperature led notably quicker to complete regeneration. The winter rate was biased towards soil temperatures normally observable at spring due to the mild weather and the temperature of the industrial flow. Even so, with lower temperature, the regeneration was significantly slower.

## Performance and process dynamics of the first full-scale CSO CW in France

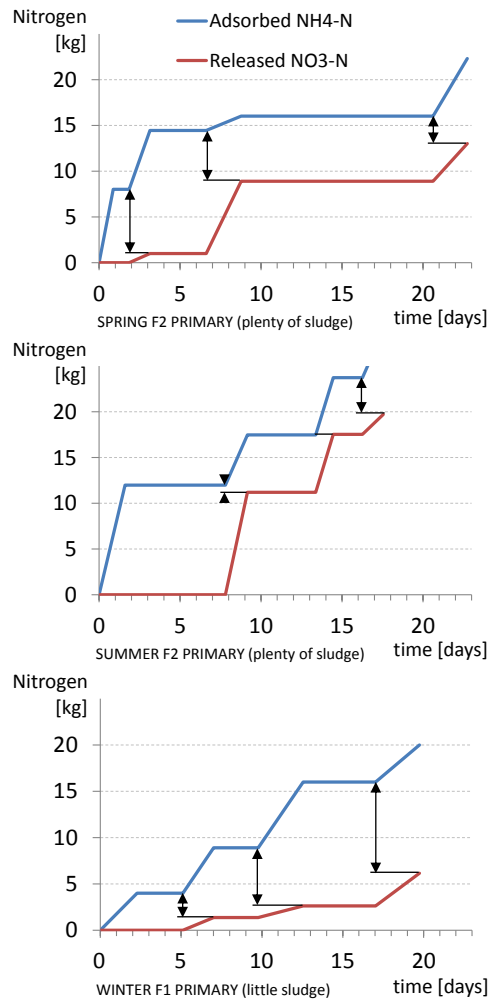


Fig. 53: Cumulative masses of adsorbed nitrogen ( $\text{NH}_4\text{-N}$ ) and released nitrogen ( $\text{NO}_3\text{-N}$ ). The arrows mark the residual mass in the filter at the end of each inter-event. Intra-event increments are linear interpolations based on the beginning and end of events.

The results were used to fit Eq. (16 (subchapter 2.5) as shown on Fig. 54, with  $d_{i,t} = 0.0077/\text{h}$  and  $R_c = 8.229\text{ }^\circ\text{C}$ . The simulated decrease in the adsorbed mass and the nitrification rate were marked from the beginning to the end of the nine inter-events as a section. This was possible by setting the initial adsorbed mass according to the measured and fixing the temperature at the measured average. The mean rate in time equalled to the rate when the mass decrease is fifty per cent of the inter-event total. The measured mean rate was placed in the space as well and the coefficient of efficiency was calculated on the mean nitrification rate. Simulations based on the calibrated Eq. (16 predicted the measured rate with good accuracy ( $R^2=0.93$ ).



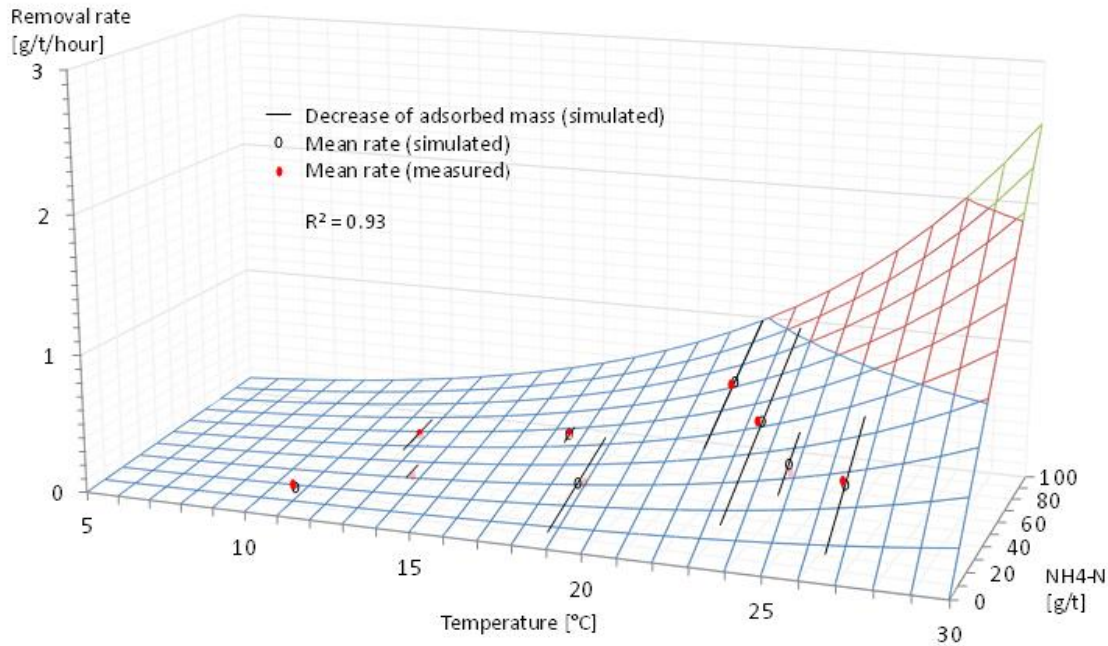


Fig. 54: Nitrification rate as function of temperature and adsorbed mass. The surface given by Eq. 1 was fitted to field measurements (red points). The equation was used to simulate nitrification (straight black sections for the nine inter-events) based on the measured adsorbed mass (higher end) at the mean of inter-event temperatures. The means of simulated rates were marked by the black points.

Nitrification rate was found to double with every 5.7 °C. As a rule of thumb, filter regeneration took around half a week at summer, around one week at spring and at least two weeks in winter even at mild filter temperatures.

NO<sub>3</sub>-N was flushed out at the beginning of the loads after each inter-event. The hydraulic load until complete flush was often small compared to the event total [in m<sup>3</sup>/m<sup>2</sup>]. Fig. 55 shows the completeness of the flush in terms of mass as the function of the load (N=19 events). Catching the first meter of water on a regular basis would mean catching most of the released nitrogen. The results highlight that designing a second stage (denitrification step) after the classical CSO CWs and targeting complete nitrogen elimination worth further consideration.

## Performance and process dynamics of the first full-scale CSO CW in France

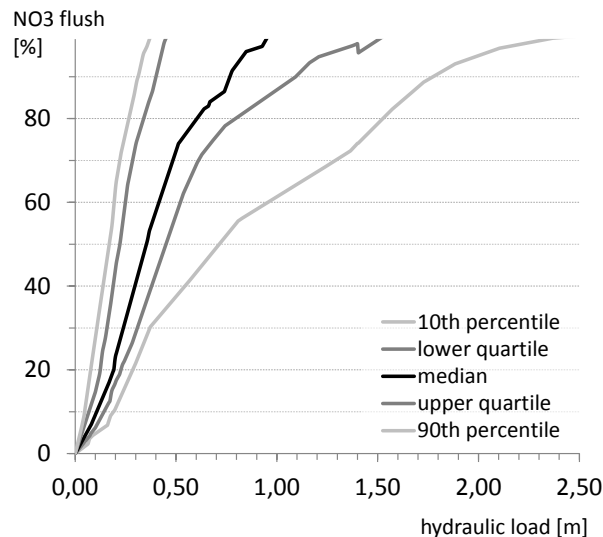


Fig. 55: Completeness of the nitrate flush as the function of the hydraulic load for N=19 flush peaks. For the interpretation, the median event needed about 0.95 metres of load until the flush was complete.

## 4. Conclusions and proposals for future research and development

A range of approaches was applied to target filter hydraulics at commencing load. It was shown that short-circuits can cause important breakthroughs when the water level at the bottom of the filter is low due to the partial utilization of the filter limited to the area at the proximity of the inlet point. Low and lasting inflow rates could exacerbate this phenomenon and cause lastingly high  $\text{NH}_4\text{-N}$  concentrations on the effluent side without actually depleting the adsorption capacities of the whole filter. It is advised to implement changes in design which minimize short-circuiting duration and peak concentration:

- i) A dual orifice system can minimize short-circuiting duration by speeding up the filling of the process layer. The diameter of the current orifice can be decreased and a second orifice can be added just at the level of the top of the filter layer. This ensures rapid filling and grants a rapid drainage of the ponding water (most of the detained volumes) at the same effluent rate which the systems are calibrated for today.
- ii) Keeping a permanently saturated water layer decreases the peak concentrations occurring at short-circuiting and therefore it is advised.
- iii) The sludge blanket has a beneficial effect as it extends the infiltration area by decreasing the hydraulic conductivity of the filter surface. The inlet point is advised to be placed at the centre of the filter which allows the concentric spreading of the sludge blanket and also helps to avoid wall effects. Large filters might benefit from multiple inlet points when fed by raw wastewater. The settled cross-connection water is advised to be led to an inlet point to benefit from the sludge blanket created by the raw water.

The amendment of 0.12 m of zeolite to 0.48 m of sand delayed  $\text{NH}_4\text{-N}$  breakthrough until mass loads got extreme. Pure pozzolana and sand-zeolite mixtures showed the same capacities. Media with high adsorption capacities could enable to decrease the active filter area whilst maintaining the detention volume; however, increased hydraulic loads [ $\text{m}^3/\text{m}^2$ ] and increased TSS load might be a concern. Clogging and sludge distribution has to be reconsidered when trying to develop more compact systems. Another issue might be cold temperatures at which the incomplete

inter-event regenerations might lead to a multi-event, progressive saturation of the otherwise excessively available adsorption sites.

This can be a target of future research because filter regeneration (nitrification) was found to be strongly correlated to filter temperatures. Instead of the general rule that biochemical reaction halves with each 10 °C (e.g. Russel 2006), rate halved with each 5.7°C. Filters at climates with cold and rainy winter might benefit the most from advanced materials as under such climates the media should be able to store NH<sub>4</sub>-N from several consecutive events.

Nitrate flush could be captured for a second stage by collecting approximately the first 0.5-1.0 m of the loads. As such, complete nitrogen removal might be addressed whilst keeping the areal demand realistic.

Aside the direct conclusions, the results helped also to parameterize the design-support software Orage. The core model relies on field measurements for defining 1) the threshold water level between short-circuiting and normal operation during simulations, 2) the adsorption isotherms of pozzolana and zeolite-enriched materials in the material database and 3) the nitrification rate in the inter-event periods of the simulations.

## 5. Acknowledgements

The authors thank Nicolas Forquet, Jérémie Aubert and Mélissa Gérodolle for the help with technical installations. Thanks Onema and RMC water authorities for their financial support

Pálffy TG, Gerodolle M, Gourdon R, Meyer D, Troesch S, Molle P: Filling hydraulics and nitrogen dynamics in full-scale CSO CWs. Manuscript ready for submission.

## **Manuscript – Efficiency of a full-scale CSO CW for major- and micropollutants**

T.G. Pálffy<sup>\*a,b,c</sup>, M. Gerodolle<sup>a</sup>, R. Gourdon<sup>c</sup>, D. Meyer<sup>a,b</sup>, S. Troesch<sup>b</sup>, P. Molle<sup>a</sup>

<sup>a</sup>IRSTEA Lyon, Freshwater systems, Ecology and Pollution unit, 5 rue de la Doua - CS70077, 69626 Villeurbanne, France

<sup>b</sup>Epur Nature sarl, 153 av. Marechal Leclerc, 84510 Caumont sur Durance, France

<sup>c</sup>INSA Lyon, LGCIE DEEP Team, 20 av. A. Einstein, 69621 Villeurbanne Cedex, France

### **Abstract**

The performance of a vertical flow constructed wetland for combined sewer overflow treatment has been evaluated. The full-scale site has been monitored for three years for major pollutants and two load events for micropollutants (metals and PAHs) were sampled as well. Performance were predominantly high (97% for TSS, 80% for COD, 72% for NH<sub>4</sub>-N), even if several loads were extremely voluminous pushing the filter to its limits. Two filter materials (4:1 mixture of sand with zeolite and pure pozzolana) showed similar treatment performance. Furthermore, environmental factors were correlated with COD removal efficiency. The greatest influencers of COD removal efficiency were the inlet dissolved COD concentrations and the duration and potential evapotranspiration of the previous inter-event period. Furthermore, sludge was analysed for quality and a sludge depth map was created. The map and calculations of the changes in sludge volume helped to understand solid accumulation dynamics.

**Keywords:** CSO CW, constructed wetland, combined sewer overflow, micropollutant removal, sludge blanket

**E-mail addresses:** [tamas-gabor.palfy@irstea.fr](mailto:tamas-gabor.palfy@irstea.fr) (T.G. Pálffy), [remy.gourdon@insa-lyon.fr](mailto:remy.gourdon@insa-lyon.fr) (R. Gourdon), [melissa.gerodolle@irstea.fr](mailto:melissa.gerodolle@irstea.fr) (M. Gerodolle), [meyer13@t-online.de](mailto:meyer13@t-online.de) (D. Meyer), [stephane.troesch@epurnature.fr](mailto:stephane.troesch@epurnature.fr) (S. Troesch), [pascal.molle@irstea.fr](mailto:pascal.molle@irstea.fr) (P. Molle).

## 1. Introduction

Urbanization greatly impacts waters via increasing flood risks and pollution. The increased volumes of storm-generated runoffs cause hydraulic shocks on small streams and flush pollutants from urbanized areas, including dry weather deposits and also atmospheric pollution (Chocat et al. 1994; Walsh et al. 2005). The mitigation of the impacts became not only an environmental but also a regulatory and social concern. Decision makers and stakeholders face a challenge to achieve a good ecological status of waters defined in the European Water Framework Directive (2000/60/CE).

Urban runoff and sewage are often collected in combined sewers and might mix with parasitic waters as well. Also called urban wet weather effluents, these waters are the source of physical, chemical and ecological degradation of the natural environment (Angerville 2009). The pathway of the pollution is via the overflow mechanism (combined sewer overflow, CSO) which is implemented to limit flows according to the transport capacity of the sewer network or the capacity of the wastewater treatment plant under. Pollutant concentrations in CSO are comparable or greater to sewage regarding metals and total suspended solids (Dembele et al. 2009). Furthermore, single events have a shock-effect on the receiving streams due to the carried organics and ammonia.

To deal with these problems, municipalities are required to implement management strategies. Common solutions are tanks for settling and storage or network separation (Dittmer 2006), but economic implications are often major and benefits often partial. Consequently, there is a real development need for alternatives such as constructed wetlands.

Constructed wetlands for combined sewer overflow treatment (CSO CWs) are cost-efficient and reduce negative impacts by buffering hydraulic loads, filtering suspended solids, and retaining a large proportion of organics and nutrients (Uhl and Dittmer 2005; Frechen et al. 2006; Dittmer and Schmitt 2011).

CSO CWs in France were developed based on experiences from the German retention soil filters (vertical flow filters treating CSO tank overflows, Uhl and Dittmer 2005) and from “French design” CWs treating municipal wastewater (Molle et al. 2005). The new technology has several innovations such as: (i) the coarser media allows feeding without pre-treatment (eliminating the CSO tank and sludge management); (ii) the presence of a permanently saturated layer at the bottom mitigates water stress during extended dry periods; (iii) aeration pipes are at an elevated position above the permanently saturated layer; (iv) zeolite is present in the filter media if high ammonium removal is needed and (v) the wetland is separated into two twin filter sides, enabling alternated operation and quicker regeneration of the secondary side (mineralization of organics) (Meyer et al. 2013).

The full-scale facility at Marcy l’Etoile is the first having these innovations. The main goal of this study was to assess performance of the system according to three criteria: filter hydraulics, treatment efficiency (major pollutants and micropollutants) and pollutant accumulation and retention in the sludge. Another aspect was to understand the impact of environmental factors on the removal, for example, that of the temperature, the length of the inter-event (unloaded) periods, etc. The final aim was, subsequently, to provide data for the optimization of CSO CWs by testing system limitations.

## 2. Materials and Methods

### 2.1. The studied CSO CW

Fig. 56 shows the layout of the full-scale CSO CW at Marcy l'Etoile. Discharged from the sewer [1], the flow reaches the filter through a 20 m<sup>3</sup> sand and grease trap [2] and a Venturi channel [3]. The wastewater is loaded on the primary filter which can be selected to be F1 (253 m<sup>2</sup>) and F2 (245 m<sup>2</sup>) by a splitter [4]. The kinetic energy of the water is mitigated by gabions below the inlet points [5] to avoid the remobilization of the filter material. The filter media in the two sides differs for research purposes: F1 has a 4:1 mixture of sand and zeolite (expressed in depth for the filter: 0.48 m and 0.12 m, respectively) and F2 has pozzolana (Fig. 57). The infiltrated water is collected by a drain network. The detention time in the media is regulated via two outflow orifices which are the single effluent points at both sides [6]. Their vertical position sets permanent saturation at the drainage layer. Extreme events might cause overflows through a trapezoid weir [7] at the rim of the 2.1 m deep basin.

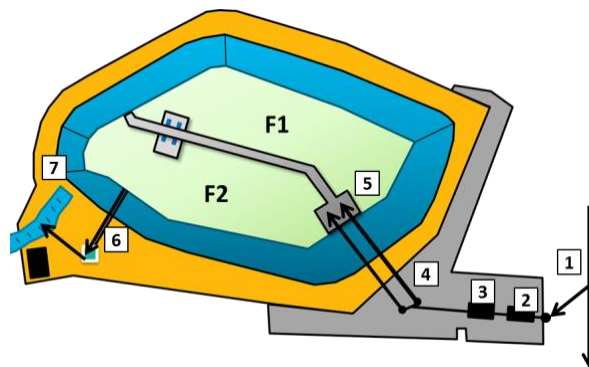


Fig. 56: The layout of the CSO CW at Marcy l'Etoile.

The design load is the event volume which the CSO CW has to be able to detain and treat. It was set by the water authorities to 1160 m<sup>3</sup>, which equals 2.3 m<sup>3</sup>/m<sup>2</sup> (or 2.3 m). The annual target of hydraulic load was 40 m. Some events of the presented experiments were particularly big to see system limits.

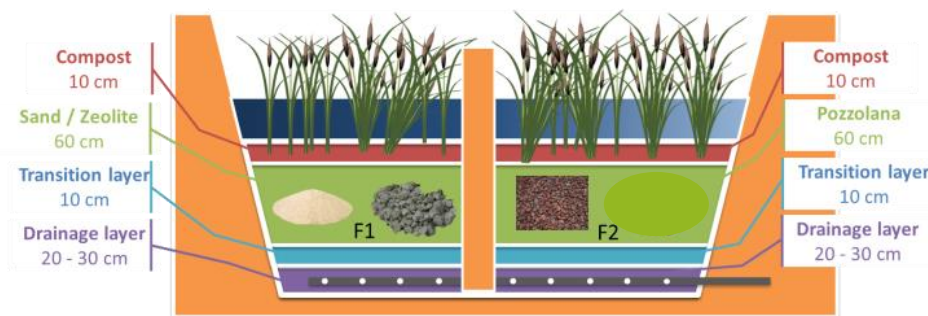


Fig. 57: Cross-section of the CSO CW at Marcy l'Etoile. Note the different filter materials in F1 and F2 (sand and zeolite and pozzolana, respectively)

## 2.2. Monitoring campaign

### 2.2.1. Campaign overview

The site at Marcy l'Etoile started operation in 2012. The results presented in this article are based on a three years' campaign which lasted from spring 2013 to spring 2016. Thirty-one loading events, some exceptionally big to test system limits, were monitored to gain information on performance. Feedings were manually induced, taking advantage of the frequent and high-rate industrial releases in the sewer. In some cases, urban storm water was present in the flows as well. The two filters were alternated seldom to track potential clogging effects (Fig. 58).

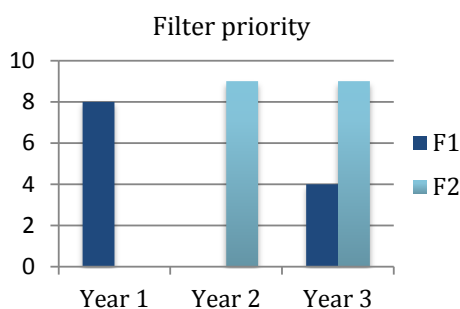


Fig. 58: Number of events by filter side priority

### 2.2.2. Hydraulic monitoring

Four probes were set up to measure piezometric water level in each filter sides and in each outlet structure. Furthermore, flow rates were measured by:

- ultrasonic probe (Aqualyse AquaVenturi, 1000 m<sup>3</sup>/h) in a Venturi channel at the inlet;
- inductive flow meter (Krohne Waterflux 3070) and later by a calibrated pressure head - orifice flow correlation for each filter sides.

### 2.2.3. Major pollutants monitoring

Three automatic samplers were installed. Samples were flow composite at the inlet. At the outlet, filter sides were sampled time composite because the flow rate was nearly constant. Furthermore, two online probes (WTW Varion) were placed in the outlet structure to monitor NH<sub>4</sub>-N and NO<sub>3</sub>-N concentrations. Some events were sampled only for global effluent quality, i.e. mixed water from the two filter sides. The major pollutants have been studied in 30 campaigns. The sampling frequency was adjusted based on the first results. Samples were analysed for total suspended solids (TSS), total COD (COD<sub>tot</sub>), dissolved COD (COD<sub>S</sub>), NH<sub>4</sub>-N, NO<sub>3</sub>-N and PO<sub>4</sub>-P following standards methods (APHA). Performance were compared according to filter side priority and material.

Many factors might impact removal performance, e.g. the load of the previous event or environmental factors. In the case of NH<sub>4</sub>-N and PO<sub>4</sub>-P, mechanisms are well understood. These are i) adsorption and nitrification and ii) progressive saturation of adsorption sites, for the two

pollutants, respectively. However, removal of COD in CSO CWs receiving unsettled flows hasn't been analyzed before. To find the factors of COD removal, a PCA has been carried out, followed by the creation of a multivariable linear model to reach quantitative predictions which deal with factor interactions.

The selected parameters for the PCA were: i) total COD load of the previous event, ii) the duration of the preceding inter-event, iii) potential evapotranspiration (PET) during the inter-event, iv) the soil and air temperature of the inter-event, v) the inflow for the considered event, vi) COD concentrations.

#### 2.2.4. Micropollutants monitoring

The methods of Choubert et al. (2011) were followed. Outflows were sampled by filter side to see differences in efficiency. Each automatic sampler was equipped with a single 16L glass container. Sampling tubes were changed to stiff Teflon (polytetrafluoroethylene) tubes.

Three sampling campaigns were realized, two day long each. Two of these sampled the start of two events whilst the third sampled the end of the second one. Both events represented extreme loads. Samples were analysed for 25 metals (ICP-MS) and 18 PAHs (HPLC). Removal rate was defined if inlet concentration was over five times the quantification limit (QL). Where concentrations did not reach the QL at the outlet, removal efficiency was calculated using 50% of QL.

#### 2.2.5. Monitoring of sludge depth and micropollutants

The sampling followed the protocol described in EPNAC (2014). Sampling points were set along three diagonals every two metres, yielding around 30 points by side (Fig. 59).

One campaign targeted sludge quality. Samples were taken using a glass jar, removing all sludge down to the compost at each point. Then, the jar was emptied in a glass bowl. The sludge was mixed with a stainless spoon separately by side.

Sludge depth distribution and changes were recorded after two events. Measurements were done six days after the end of intra-events, each bringing extreme solid loads. Loads were separated by a one month inter-event. Depths were interpolated for the whole surface using the software Q-Gis® for inverse distance weighting (IDW, power parameter P=6).

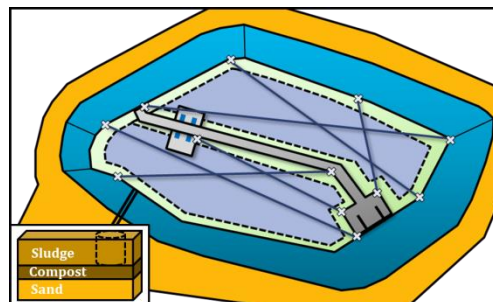


Fig. 59: Sludge sampling paths. Note that compost was avoided to be taken with the samples (bottom left corner).



### 3. Results

#### 3.1. Hydraulic loads

The twin filter sides were alternated irregularly and they received slightly different hydraulic loads, as shown on Table 23.

Table 23: Hydraulic loads by filter side at the CSO CW at Marcy l'Etoile. S: side with sand and zeolite; P: side with pozzolana.

		Year 1		Year 2		Year 3	
Events sampled		8		9		14	
Filter material		S	P	S	P	S	P
Hydraulic load by event [m]	Mean	1.8	1.3	1.5	2.7	1.4	1.6
	Min	0.6	0.0	0.0	0.5	0.0	0.6
	Max	3.3	3.0	5.4	9.7	5.7	5.9
	SD	1.2	1.2	1.8	3.0	1.4	1.5
Annual load [m]		24.7		37.9		41.4	

The filter received about 62% of the design load in the first year of monitoring (Fig. 60). This was an undershot which can change mass removal compared to a year when the filter receives the design load. However, the low load was caused by one single unloaded period so an important effect is unlikely. In the following two years, loads were closely corresponding to the cumulated design load.

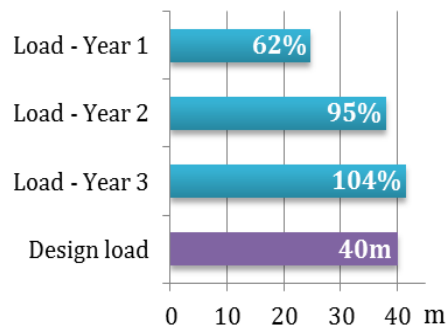


Fig. 60: Annual hydraulic loads in the monitoring period.

#### 3.2. Major pollutants

##### 3.2.1. Global performance of the whole filter

Hydraulic and pollutant loads were stochastic which is normal for CSO. Performance were determined based on the mass removal for major pollutants (Fig. 61): TSS, total, dissolved and particulate COD (COD\_tot, COD\_S and COD\_X, respectively), and ammonium nitrogen (NH<sub>4</sub>-N). Nitrate nitrogen (NO<sub>3</sub>-N) and phosphate (PO<sub>4</sub>-P) were also studied although these are not amongst the targeted substances by current design.

Performance and process dynamics  
of the first full-scale CSO CW in France

**TSS:** High and stable removal rates were obtained (96% with SD=2.9) and outlet concentrations

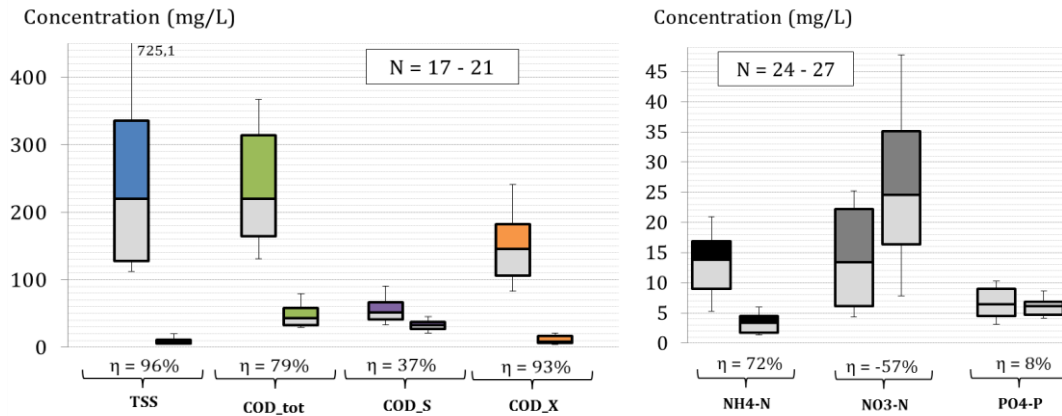


Fig. 61: In-and outlet EMCs and mass removal performances ( $\eta$ ) for the major pollutants. Whiskers represent the 10<sup>th</sup> and 90<sup>th</sup> percentile. N: number of events.

stayed around 10 mg/L. This result is consistent with other studies, e.g. Dittmer (2006), Amaral et al. (2013).

**COD:** The removal rate of 79% was slightly lower than that experienced at CWs with CSO tank (90%, Masi et al. 2016). Filtration was a dominant removal process and as such, higher inflow concentrations improved efficiencies (see also section 3.2.4). Meanwhile, low inlet concentrations led to low removal – an outlet background concentration had already been described by Dittmer and Schmitt (2011), as the metabolic residue and inert COD from sediment mineralization. Furthermore, when separating the dissolved phase (COD\_S) from particulate phase (COD\_X), it can be seen that dissolved COD removal is less efficient (37% on average) which is congruent with experiences with the German RSFs (42%).

**NH<sub>4</sub>-N:** Inflow concentrations were expected up to 9.9 mg/L for CSO (Gasperi et al., 2012). Measurements showed sometimes higher values (13.8 mg/L EMC<sub>in</sub>) because the industrial release contained slightly higher loads than typical stormwater. Removal performance were generally high (>71%), even when this represent all loads including many above the design volume (1160 m<sup>3</sup>) which the wetland has to be able to treat.

**NO<sub>3</sub>-N:** Removal was not an aim. Measurements helped to follow nitrogen-related processes. Inlet concentrations were high due to the industrial discharges. The effluent peaks at the outlet were the flush of nitrified ammonium. There was no sign of de-nitrification.

**PO<sub>4</sub>-P:** Removal was negligible (8%) and often negative. However, total phosphorous was sampled as well for a low number of events and organic phosphorus accumulated in the sludge via filtration. Total phosphorous removal ranged around 45-75% (N=2) in the second year of the analysis, with outflow concentrations below quantification limit.

### 3.2.2. Filter side comparison

When focusing on filter priority, it can be concluded that the primary filter receives most of the solids. Sedimentation proves to be an important factor when comparing inflow with water at the cross-connection point. Even if both sides received near the same hydraulic loads, water on the secondary one had only about 15% of inlet TSS concentration. This means that the classical differentiation of hydraulic loads by filter side is not a good predictor of aging-related processes, unless the filters have been regularly alternated and a long-term analysis is done.

Filter sides were compared also focusing on the two filter materials (Fig. 62). Differences were anticipated in dissolved pollutant removal due to different adsorption capacities and environments for biofilm development. Performance were determined for the sand and zeolite mixture (ratio: 4:1, relative depth: 0.48 m and 0.12 m) and pozzolana (0.6 m). However, both for events below and above design load, the two filters performed well ( $p\_value = 0.42$ , Student test). Pozzolana is a natural material and might show differences in adsorption capacities depending on the region of origin. However, it has to be highlighted that the relative thickness of the effective media for  $NH_4-N$  adsorption was 0.12 m zeolite against 0.60 m pozzolana. Pozzolana might offer a competitive alternative to sand and zeolite mixtures in certain cases (when available locally).

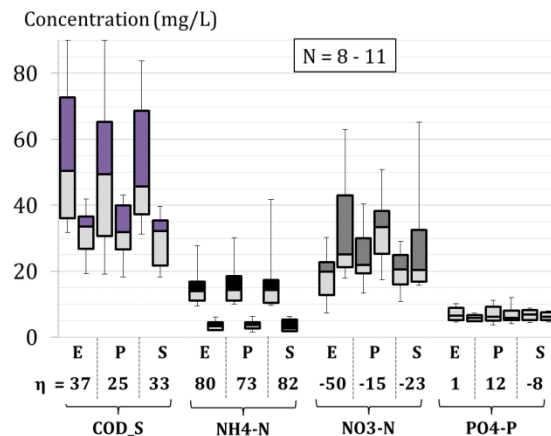


Fig. 62: In-and outlet EMCs and mass removal performance ( $\eta$ ) for dissolved pollutants. E: entire filter, P: pozzolana filter side, S: sand filter side, N: number of events.

### 3.2.3. Performance below and above the design load

For solids and organics, mass removal performance are the same with  $p\_value = 0.51$  (Fig. 63). An exception is the dissolved fraction of organics (COD\_S) where performance drop is apparent.

In the case of nutrients, which represent the dissolved fractions just like COD\_S, extreme loads impacted performance of events with high inflow volumes (Fig. 64). Median mass removal for  $NH_4-N$  and  $PO_4-P$  was lowering by 23% and 14% for ammonium and phosphorous, respectively.

## Performance and process dynamics of the first full-scale CSO CW in France

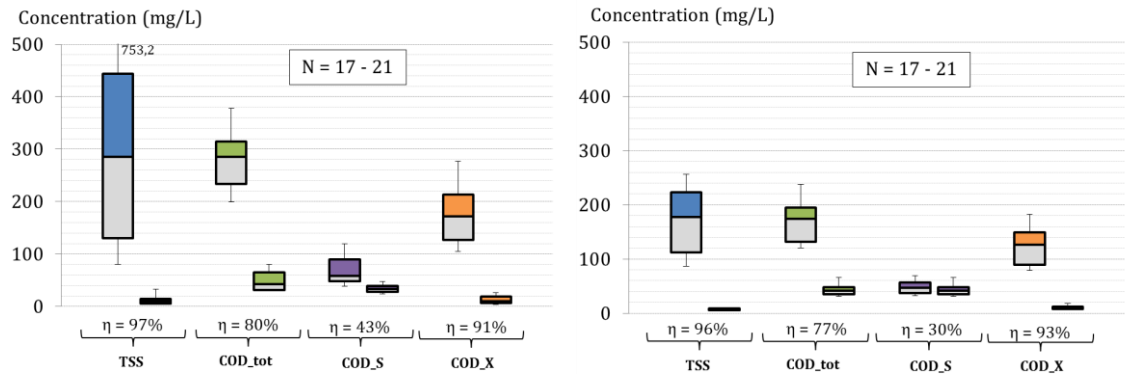


Fig. 63: In-and outlet EMCs and mass removal performances ( $\eta$ ) for solids and organics by load. Left: events below, and right, events above the design load (2.3 m). N: number of events.

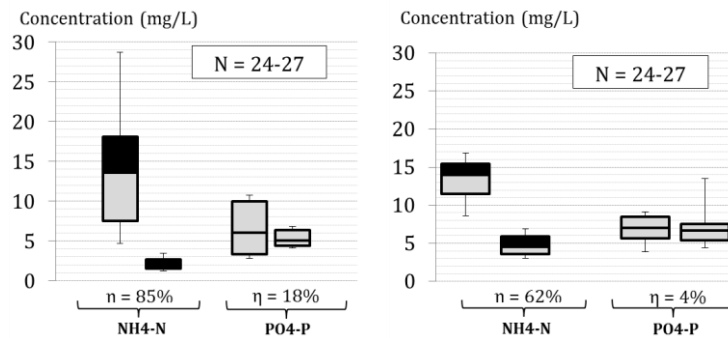


Fig. 64: In-and outlet EMCs and mass removal performances ( $\eta$ ) for nutrients by load. Left: events below, and right, events above the design load (2.3 m). N: number of events.

### 3.2.4. Influential factors for performance

Environmental conditions affect biomass both inter- and intra-event. The PCA visualized the variability of COD removal according to several parameters as shown by Fig. 65. The plane defined by F1 and F2 explained 62.5% of the total variance in the dataset. The duration and the cumulative PET of the inter-event as well as the inlet COD<sub>S</sub> concentration had a positive correlation with outlet total COD concentration. A multiple linear regression was set (Eq. 17), leading to a fit shown on Fig. 66.

Performance and process dynamics  
of the first full-scale CSO CW in France

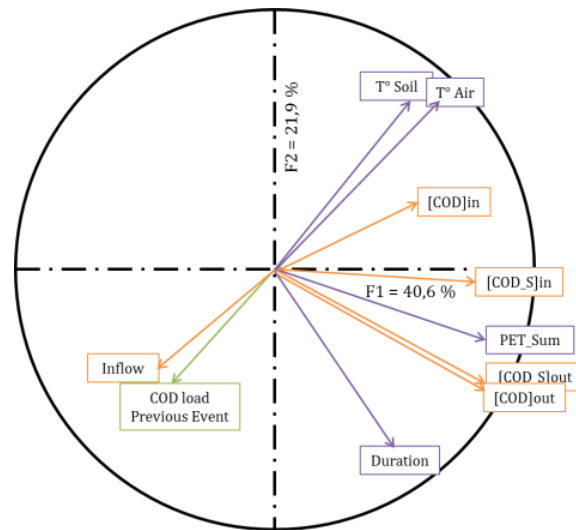


Fig. 65: Result of the PCA on COD removal (N=24).

$$[COD_{out}] = 0,19Duration + 0,21[COD_S]in + 0,10PET + 23,56 \quad 17)$$

, where *Duration* is the length of the inter-event expressed in days and *PET* is the cumulative value of PET in millimetres for the whole inter-event.

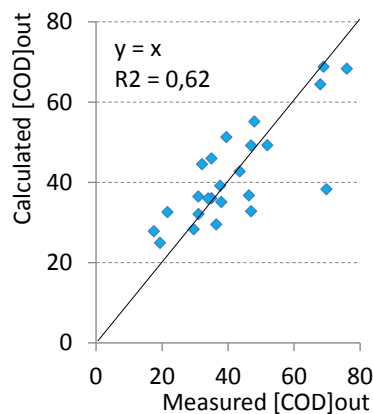


Fig. 66: Predictions in function of measured effluent COD concentrations.

### 3.3. Micropollutants

#### 3.3.1. Metals

Twenty-five metals were studied in the dissolved and particulate phases (Table 24). Of these, cadmium, nickel and lead are “priority substances” by the EU Water Framework Directive (2000/60/EC). An Environmental Quality Standard (EQS) is defined for them as a concentration in the receiving water which should be abided after discharge (immission). Concentrations are 0.08-0.25 µg/L, 4 µg/L and 1.2 µg/L for Cd, Ni and Pb, respectively.

Performance and process dynamics  
of the first full-scale CSO CW in France

Table 24: Inlet metal concentrations at Marcy l'Etoile. Metal concentrations under the quantification limit: "-".

	Dissolved (µg/L)		Particulate (µg/L)		Dissolved (µg/L)		Particulate (µg/L)		
	Mean	SD	Mean	SD	Mean	SD	Mean	SD	
Li	-	-	8.3	0.7	Rb	-	-	7.7	1.9
B	-	-	73.6	8.0	Sr	94.6	66.4	205.5	12.0
Al	424.7	302.9	12.2	-	Mo	-	-	1.1	0.2
Ti	14.3	-	2.0	-	Sb	-	-	0.3	0.1
V	-	-	0.9	0.2	Ba	46.2	30.0	15.7	4.3
Cr	4.2	3.6	0.9	0.1	Pb	2.6	-	0.7	0.1
Mn	14.2	12.9	17.2	6.5	U	-	-	1.0	0.3
Fe	394.8	247.5	63.6	9.3	Se	-	-	-	-
Co	-	-	0.4	0.1	Ag	-	-	-	-
Ni	-	-	5.6	5.9	Sn	-	-	-	-
Cu	24.7	19.3	7.8	2.4	Ti	-	-	-	-
Zn	54.4	44.7	54.6	13.0	Cd	-	-	-	-
As	-	-	2.2	0.6					

In storm-generated flows (third campaign, end of the feeding), most metals were bound with particles. This is in accordance with Dembele et al. (2009), who found particulate forms representing 55-85% of total from a similar residential catchment. In comparison with a wet weather discharge study covering explicitly urbanized areas (Becouze-Lareure et al. 2016), metal concentrations were low. Concerning removal efficiency (Table 25), four compounds have good performance both at the beginning and at the end of the event: Al, Ti, Cr and Ba. For five others (Mn, Fe, Cu, Zn, Sr), release was observed at the beginning of the feeding whilst removal efficiencies were improved and some of them even exceed 90% after extreme load volumes passing the filter. Priority substances (Ni and Pb) were not quantified at the beginning of the event. The explanation of system behaviour will need further research focusing on the detailed composite sampling of regular loads, with pH and possibly redox measurements.

Table 25: Overall removal efficiencies for metals.

	12-Apr		13-Apr		26-May		27-May		31-May		1-Jun	
	F1	F2	F1	F2	F1	F2	F1	F2	F1	F2	F1	F2
Al	65	39	95	91	98	75	99	64	94	92	99	94
Ti	46		89	91	64	60						
Cr	78	76	84	84			91	89	96	96	97	97
Mn	-1729	-376	-1054	-207	-779	-631	-1220	-662	3	-25	12	36
Fe	-205	-83	-2	36	-69	4	-198	-36	57	87	26	86
Ni											96	97
Cu	3	-60	-5	12	64	-22	66	-22	94	89	96	93
Zn	-80		-11	-36	-42	-12	29	-47	68	59	79	71
Sr	4	-16	-23	-6	-24	-90	-3	18	61	61	36	45
Ba	61	100	68	75	85	78	79	93	93	95	90	93
Pb									65	56	65	57

### 3.3.2. Polycyclic Aromatic Hydrocarbons (PAHs)

PAHs primarily exist adsorbed to soil particles due to their chemical properties (Prabhukumar and Pagilla 2010). Mean total PAH concentration was about 1.3 µg/L, mostly bound to particulates. This is lower than concentrations found in highway runoff, reported to be 3-5 µg/L by Terzakis (2008) and similar residential area runoff, reported to be 1.2 µg/L by Ruban (2005). Compounds are listed in Table 26. PAHs were above five times the quantification limit only for three pollutants. Removal efficiencies were calculated only for these and were high as shown by Fig. 67.

Table 26: Outlet PAH concentrations at Marcy l'Etoile.

Performance and process dynamics  
of the first full-scale CSO CW in France

PAH	conc. [µg/L]	PAH	conc. [µg/L]
Acenaphthene	0.011	Indeno(1,2,3-cd)pyrene	0.006
Benzo(a) anthracene	0.028	Naphthalene	0.034
Benzo(a) pyrene	0.002	Benzo(g,h,i) perylene	0.006
Benzo(b) fluoranthene	0.006	Chrysene	0.010
Fluoranthene	0.013	Phenanthrene	0.018
Fluorene	0.011	Pyrene	0.013

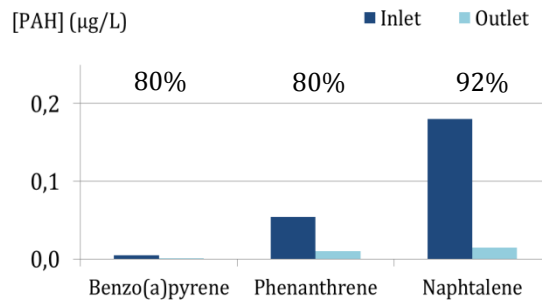


Fig. 67: In- and outlet concentrations and removal efficiencies for PAHs. The concentration of other compounds was too close to the quantification limit to calculate removal performances.

Seven PAHs are considered as priority substances in the Water Framework Directive (WFD) (Table 27). Many high-molecular-weight PAHs (benzo (b) fluoranthene, benzo (a) pyrene, benzo (k) fluoranthene, benzo (g,h,i) perylene) are known or suspected carcinogens, and many low-molecular-weight PAHs (naphthalene, anthracene: high solubility and volatility) are acutely toxic to aquatic organisms (Smith et al. 2000). None of these seven substances exceeded their EQS, not even in the effluent water.

Table 27: Priority substances and EQS values in the European Water Framework Directive.

PAH	EQS (µg/L)
Naphthalene	130
Anthracene	0.1
Fluoranthene	0.12
Benzo(b)fluoranthene	0.017
Benzo(k)fluoranthene	0.017
Benzo(a)pyrene	0.27
Benzo(g,h,i)perylene	0.0082



### 3.4. Sludge

#### 3.4.1. Sludge blanket

The 1st campaign followed 3 years of operation with filter priority alternations, during which F1 and F2 received 82.5 m and 102.3 m of water, respectively. Sludge maps (Fig. 68) show inhomogeneous distribution: sludge is thicker close to the inlet and absent from the other end of the filter.

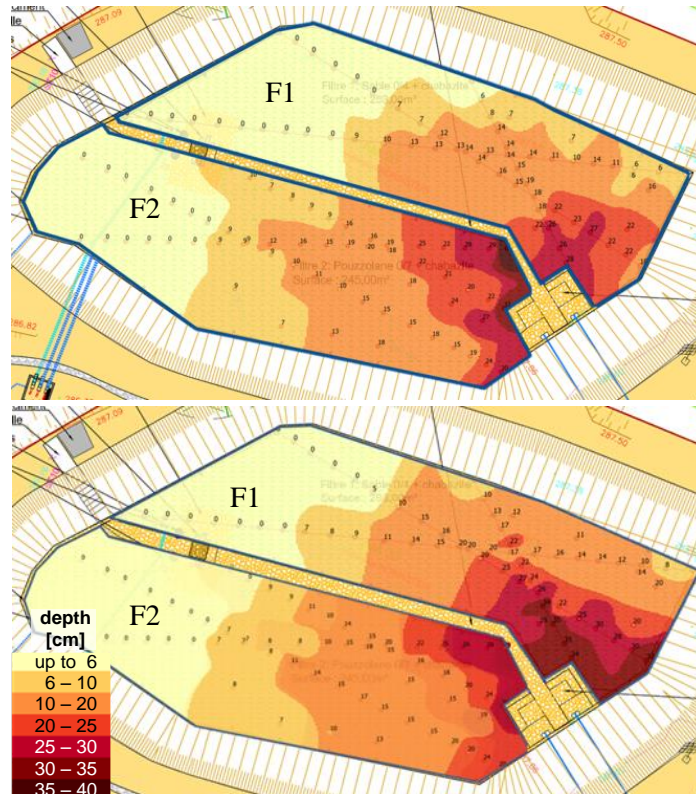


Fig. 68: Sludge blanket map after three years of operation. Above and below: after heavy loads ( $8 \text{ m}^3/\text{m}^2$  and  $12 \text{ m}^3/\text{m}^2$ ) separated by a one-month inter-event.

The accumulated sludge volume after 3 years was  $24 \text{ m}^3$  for F1 and  $26 \text{ m}^3$  for F2 (Fig. 69). If the sludge was uniformly distributed, this would correspond to  $3.2 \text{ cm}/\text{year}$  of accumulation over F1 and  $3.5 \text{ cm}/\text{year}$  for F2. The values correspond to about  $0.35 \text{ mm}$  of sludge for  $1 \text{ m}$  of hydraulic load.

The change of sludge volume between the two campaigns explains short term functioning with regards on filter priority and regeneration. The imposed load on the whole filter was extremely high:  $12 \text{ m}$  of water, corresponding to around six months of normal operation. However, settled water carries only about 15% of TSS, therefore solid load is equivalent to what a single sided-filter had received from about  $22 \text{ m}$  of hydraulic load for F1 (primary side, inlet flow) and only  $2 \text{ m}$  for F2 (secondary side, cross-connection flow only). The increase of sludge over F1 was  $4.8 \text{ m}^3$ . By contrast, sludge volume decreased over F2 by  $2.1 \text{ m}^3$ .



Performance and process dynamics  
of the first full-scale CSO CW in France

Concerning distribution, sludge settled in a semi-circle: more concentrated close to the inlet, less near the middle of the filter. Close to F1 inlet, sludge depth grew by 21%.

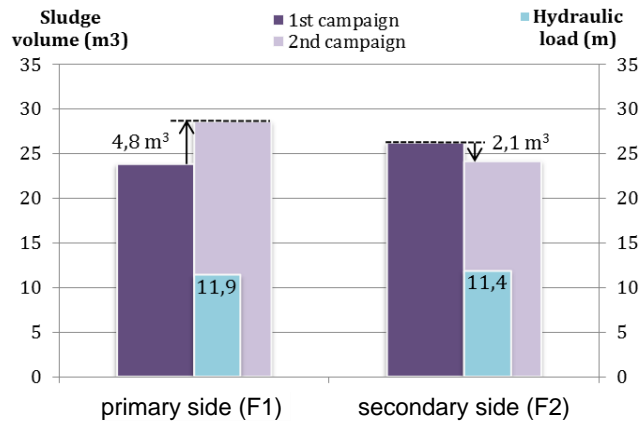


Fig. 69: Changes in the sludge volume after a heavy load. The change is the integrated effect of a long inter-event period (1 month, decomposition) and the load (about 12 m<sup>3</sup>/m<sup>2</sup>, accumulation).

### 3.4.2. Dry and organic matter (OM) content

To better understand sludge accumulation and decomposition dynamic, dry- and volatile matter contents are crucial parameters. Sludge sampling imposed an idea about mineralization on a mature filter. Fig. 70 shows that sludge on F1 contained more water than F2 and had higher volatile matter content (6 days after the 8 m<sup>3</sup>/m<sup>2</sup> load). This is consistent with previous observations: inlet water contains an important amount of fresh organic matter (OM) which settles quickly on F1, but the secondary filter (F2) wears a more mature blanket.

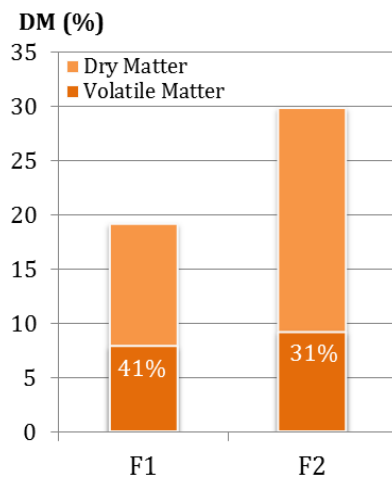


Fig. 70: Dry and volatile organic matter content of the sludge.

According to Molle et al. (2004), sludge mineralization is governed by drying and the OM content which is degradable. OM in the sludge of mature CWs treating municipal wastewater is between 30 and 50 %. At Marcy l'Etoile, this value ranged around 30-40%.

### 3.4.3. Sludge and micropollutants

Samples were analysed for metals and PAHs. Concerning PAHs, 11 of the 18 analyzed substances were detected (Fig. 71). Except of naphthalene, PAHs are very hydrophobic: their solubility in water is low. On the other hand, their alcohol/water coefficients ( $K_{ow}$ ) are relatively high, indicating a potential for adsorption on suspended matter and, consequently, their presence in any sludge.

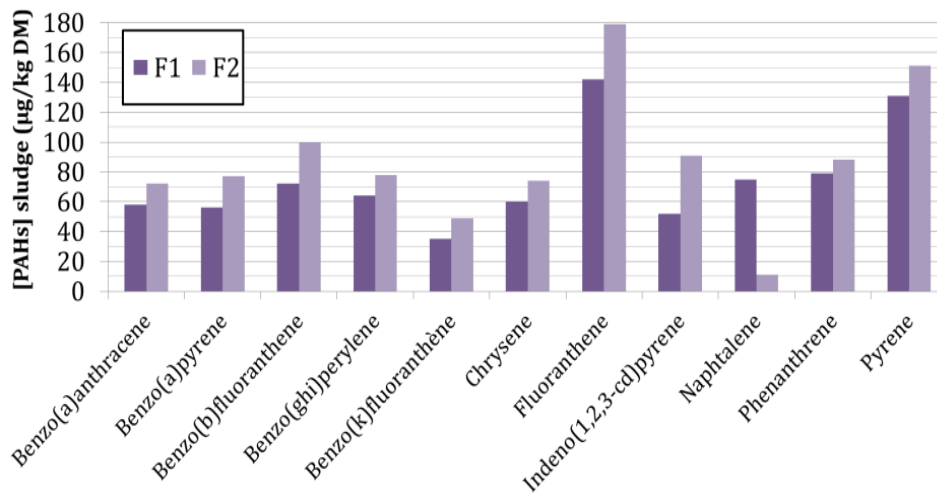


Fig. 71: PAHs in the sludge of Marcy l'Etoile

For metals, 25 substances were analysed (Fig. 72). Rb, Sb, Se, Tl and U remained below the detection limit.

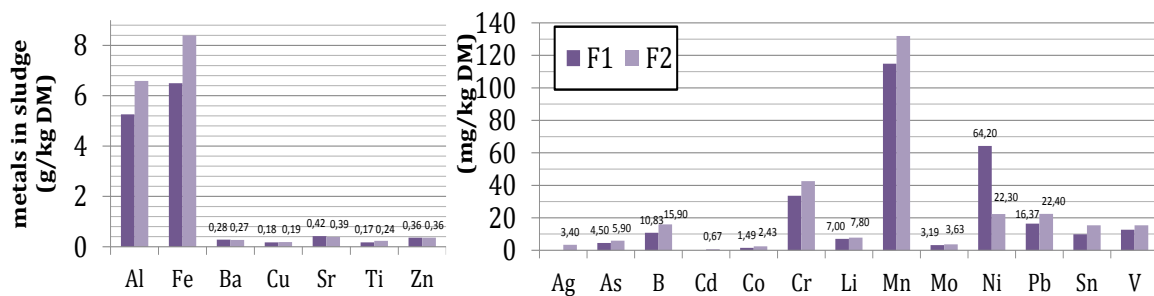


Fig. 72: Metals in the sludge of Marcy l'Etoile

Compared to the thresholds posed by the French regulation concerning wastewater sludge recovery (Table 28), sludge at Marcy l'Etoile could be used for manuring or composting. However, it is important to keep in mind that most of the flow the filter received during its operation was dominated by industrial flows instead of real stormwater; therefore, no general conclusion is drawn here about the safety of the use of CSO CW sludge in agricultural practice.

## Performance and process dynamics of the first full-scale CSO CW in France

Table 28: French regulation for 3 PAHs and 6 metals concerning sludge recovery compared to the values found at Marcy l'Etoile.

Water quality constituent	Limit values (mg/kg DM)	Mean values (mg/kg DM)
Fluoranthene	5.0	0.20
Benzo(b)fluoranthene	2.5	0.09
Benzo(a)pyrene	2.0	0.07
Cd	10	0.67
Cr	1000	38.1
Cu	1000	181.6
Ni	200	43.3
Pb	800	19.4
Zn	3000	361.5
Cr + Cu + Ni + Zn	4000	643.9

### 4. Conclusions and outlook

CSO CWs perform well and have proven to be robust in removing major pollutants. Mass removal performance for events below the design load (1160 m<sup>3</sup> or 2.3 m) were 97% for TSS, 80% for COD and 85% for NH<sub>4</sub>-N. Performance drops were observed only in the case of extreme events representing a volume with a return period over two years (about 12 m hydraulic load). However, as inter-event regeneration and intra-event removal processes cannot be separated, it is important to keep in mind that pollutant loads have to be in balance with the time available for regeneration. Otherwise filters will be prone to premature aging (clogging) and might perform below expectations.

The comparison of the filter sides with different filter materials showed identically good removal efficiency for the sand and zeolite mixture (4:1, with a relative depth of 0.12 m for zeolite and 0.48 of sand) and natural pozzolana (0.60 m). Pozzolana offers an alternative to sand and zeolite mixture. In terms of filter priority, sludge accumulation was prominent close to the inlet of the primary filter. Sludge was absent at the cross connection (far from the inlet point). This means the cross-connection can be placed just over the filter surface if its location is far from the inlet. A low cross-connection level might enable frequent feeding on the secondary side and avoiding drought stress on it, without compromising its regeneration.

The analysis of COD removal performance confirms dependency on environmental parameters and on the concentration of the dissolved fraction in the inlet. Total outlet COD concentration can be calculated from dissolved inlet COD, inter-event duration and PET and a constant background concentration. The reliability of this method was mediocre, with the coefficient of determination explaining the variability with an  $R^2=0.62$ . The method is valid for event mean concentrations, and as such, leaves room for future studies considering a potential evolution intra-event as well as analyses based on a larger population number. The equation can be taken into account at the step of CSO CW dimensioning.

It was shown that the technology removes effectively several micropollutants as well, both from the group of PAHs (benzo(a)pyrene, phenanthrene, naphthalene) and metals (Al, Ti, Cr and Ba). For Mn, Fe, Cu, Zn and Sr, higher outlet concentrations were observed at the beginning of the feedings. This might indicate the release of metals after solid mineralization in the inter-event periods. However, due to the low number of the analysed samples (N=2-6) and the nature of the

Performance and process dynamics  
of the first full-scale CSO CW in France

inflows (often an industrial release substituted the surface runoff part), a deeper conclusion needs further research. Focus should be given on detailed composite sampling of regular loads, with pH and possibly redox measurements.

## 6.2 Key findings of the two manuscripts in this section

The analysis of process dynamics and the performance of the first full-scale CSO CW helped to confirm and parameterize the design-support software Orage.

Hydraulic short-circuits were shown to cause important  $\text{NH}_4\text{-N}$  breakthroughs. This might be an issue at long inflows with low rate (e.g. during long rain events or into oversized filters). A partial utilization of the filter might cause concentration breakthrough even in wetlands with robust adsorption capacity. This can be more a risk in the case of oversized filters. A plausible symptom could be reed growing strong only at the inlet zone. The negative effects of short-circuiting are or could be mitigated by:

- a) Permanent water layer at the filter's bottom
- b) Application of a dual orifice system (smaller orifice at the permanent water level, larger orifice a few centimetres below the filter surface)
- c) Efforts to maximize the area of the sludge blanket at the inlet and to divert cross-connection water back on it.

The sand and zeolite mixture (4:1) and pozzolana were both effective in  $\text{NH}_4\text{-N}$  removal at 0.6 metres filter depth (i.e., 0.12 m of zeolite compared to 0.60 metres of pozzolana). The application of materials with high adsorption capacity will enable further decrease in filter area. In the case of smaller areas, however, annual solid loads might become a concern. Further research is necessary to know more about filter aging and clogging. Another issue in small filters could be the progressive saturation of the adsorption sites at cold temperatures and rainy weather. Several loads might eventually saturate the adsorption capacities due to the low nitrification rate in the inter-event periods. Orage accounts for the phenomena.

As a final conclusion about nitrogen dynamics, nitrate is flushed out with roughly one meter of load. De-nitrification could be reached in a second stage in theory, catching only this flush instead of all event effluent. This would decrease the footprint of the stage.

As for filter performance, CSO CWs offer a robust solution for removing major pollutants. Mass removal performance for events below the design load (2.3 m) were 97% for TSS, 80% for COD and 85% for  $\text{NH}_4\text{-N}$ . Performance drops were observed only in the case of extreme events representing a volume with a return period over two years (about 12 m load). Natural pozzolana can be a good alternative to a sand and zeolite mixture (if locally available). Total outlet COD concentration can be calculated from dissolved inlet COD, inter-event duration and PET and a constant background concentration ( $R^2=0.62$ ). It was shown that the technology removes effectively several micropollutants as well, both from the group of PAHs (benzo(a)pyrene, phenanthrene, naphthalene) and some metals (Al, Ti, Cr and Ba). A deeper conclusion needs further research. Focus should be given on detailed composite sampling of regular loads, with pH and possibly redox measurements.

Sludge accumulation was prominent close to the inlet of the primary filter. Contrary, sludge was absent far from the inlet point. This means the cross-connection can be placed just over the filter surface if its location is far from the inlet which helps to avoid drought stress on the secondary filter.

## 7 Design proposals and final conclusions

### 7.1 Proposals for design practice

#### 7.1.1 Minimizing hydraulic short-circuits

Following filling hydraulics by a range of experiments gave insight into the operation of CSO CWs at the beginning of the loads. These experiments have proven the existence of short-circuiting which refers to the partial utilization of the filter limited to the inlet zone. The phenomenon is fleeting in most of the cases. Even so, in certain hydraulic conditions (i.e. low and lasting inflow rate or oversized filters), it might be responsible for considerable performance drops, especially for  $\text{NH}_4\text{-N}$ . Short-circuiting is proposed to be addressed by design the following ways:

The outlet structure can be modified to have two orifices instead of one. This could decrease filling times, and at the same time, preserve the time needed to drain large volumes from the system. This latter is crucial for maximizing the length of inter-event periods for filter regeneration. The orifice which is used in present design could be decreased in diameter in a way to provide only a fraction of the targeted outflow rate. This would ensure a rapid filling, minimizing the duration of short-circuiting. The second orifice could be positioned in level with the filter surface. The outflow from the two orifices would ensure the same outflow rate [ $\text{L/s/m}^2$ ] as targeted in today's designs. Only the water stored in the porous media would take longer to be drained. This volume is a small fraction of the total stored volumes (e.g. a 60 cm filter has about 20 cm of water at  $\theta=0.33$ ). A proposed ratio of the drainage rate is 1:2 from the lower and upper orifice at a ponding depth of one meter, respectively (around +2.5 hours drainage time). Dual orifice might speed up nitrate flush as well due to longer contact times at the beginning of the event.

Another way to minimize short-circuiting effect is having a permanently saturated drainage layer at the bottom of the filter. This permanent water was shown to effectively work against concentration breakthroughs, i.e., effluent concentration peaks, via mixing. It carries also the possibility to mitigate unfavourable drought effects in long inter-event periods. The effect was observed also in Orage during test runs. The tool was calibrated to offer at least 0.3 metres of saturated drainage layer below the process layer, and might propose up to 0.4 metres depth for data series with extremely arid climatic conditions.

#### 7.1.2 Inlet distribution

Short-circuiting was targeted by various experiments at Marcy l'Etoile. Still, there were only a few hints how to optimize the feeding distributions in order to avoid short-circuits. Placing a single inlet point at the filter side is unfavourable because it might favour wall effect. It led also to an uneven sludge distribution. The deposits were thick at the inlet point and absent from the further side of the filter. Deposit depth showed a concentric decrease starting from the inlet. Therefore, point-like inlets are advised to be placed in the centre of the filter to maximize the surface of the sludge blanket.

The use of several inlet points (e.g. H feeding with an overhead system) is preferable for both small and large filters, at least the same density as the filter at Marcy l'Etoile had (one point per

250 m<sup>2</sup>). This allows an even distribution of the sludge which works against short-circuiting. The infiltration rate is limited by the hydraulic conductivity of the deposits until the filter is saturated, leading to an unsaturated flow below the infiltration area. Feeding from trenches along the long sides of the filters is a third option applied in practice in Germany; however, its effect on short-circuits is unknown (e.g. potentially high wall effect, heavier solids limited close to the wall).

### 7.1.3 Cross-connection structure

Cross-connection carries settled water from one filter side to the other. Solids (TSS) arriving on the secondary filter side were below 15% of the inlet concentration (N=3). This means the sludge blanket was absent at the cross-connection points at Marcy. Therefore short-circuit effects were not mitigated by the surface distribution of the water. To benefit from the sludge, the cross-connection water could be carried and fed to the inlet point where the sludge blanket is the thickest.

It is important to avoid features which decrease the effective depth of the filter layer both at the cross-connection and the inlet points. At Marcy l'Etoile, gabions were used to absorb the kinetic energy of the inflow. It prevented the re-mobilization of the filter media but the rock cages were sunken 30 cm into the filter material, meaning that the effective depth of the filter at these points was halved. Such practice favours hydraulic short-circuits. It is advised to keep such structures on the surface or use a liner underneath to avoid adverse effects.

Filter side alternation should provide longer inter-events in the secondary filter for sludge mineralization. However, feeding frequency is rather difficult to control and in the case of a series of events with small volume, the secondary side might suffer from drought if it stays dry. As cross-connection waters carry low amounts of sludge, frequent feeding itself should not perturb regeneration but protect the secondary side from drought. Therefore it is advised to place cross-connection reasonably low, close to the surface of the filter. Meanwhile the wall height between the primary and secondary sides should ensure sedimentation in the primary side. The height at Marcy l'Etoile was found to be satisfactory (h=80 cm).

### 7.1.4 Overflows

Overflows are naturally low in solids because they occur only at extreme events. Furthermore, sedimentation led to lower concentrations at Marcy in the case of the particulate quality constituents TSS, the corresponding COD fraction, TKN and TP. An overflow through a porous media (e.g. gravel) might maximize solid and floating material removal.

## 7.2 Conclusions and Outlook

### 7.2.1 Process-based modelling of CSO CWs

HYDRUS / CW2D was capable to simulate CSO column performance for COD and NH<sub>4</sub>-N removal in the short and medium term. Previous limitations could be overcome and biomass growth reached a quasi-stable state and no initial peak of COD was observed. Validation of HYDRUS / CW2D on full-scale systems can follow. The tool can be potentially applied for design purposes but needs trained professionals and a high number of simulations, i.e. working hours. The re-calibration

of some parameters will be necessary, keeping in mind that the French system receives unsettled water contrary to the columns.

### 7.2.2 Orage in practice

The core model of Orage has proven to be robust and the automatic optimization process has been verified. The iterative shell gave realistic proposals when re-scaling an existing site (Marcy l'Etoile). The precision of the tool can be increased based on field scale data from full-scale sites, by refining parameter calibration. Ideally, these sites should be monitored intensively and scaled based on the propositions of Orage. It might help to refine parameters i) of filter materials, ii) in internal tables describing COD removal performance and their environment-dependency and iii) the hydraulic optimization process. It would allow also the direct comparison of predicted and measured performance from sites receiving real CSO. Orage should be handled as a tool to facilitate decisions and design and not as a substitute of engineering companies or consulting firms.

### 7.2.3 Filter performance and compact filters

Removal efficiencies of targeted pollutants were 97% for TSS, 80% for COD and 85% for  $\text{NH}_4\text{-N}$  for events below the design load ( $2.3 \text{ m}^3/\text{m}^2$ ,  $N=19$ ). Both pozzolana and the 4:1 mixture of sand and zeolite have showed a high capacity of  $\text{NH}_4\text{-N}$  retention. Other major pollutants had little correlation with the filter area in earlier pilot-scale research. According to the field adsorption capacities measured at Marcy l'Etoile, filters could serve a detention basin exceeding their net surface area two or three times. However, this would increase the annual hydraulic load to levels which are not seen in today's practice. This involves the risk of premature clogging. Future experiments are advised to focus on the effect of excessive annual hydraulic (and correlated solid) loads and on engineering solutions to keep most of the solids in the sewer even if feeding with raw wastewater. The testing range of annual hydraulic loads advised for studies could range up to  $250 \text{ m}^3/\text{m}^2/\text{year}$ .

The regeneration of the filters was slower than expected in cold temperatures. Nitrification rate doubled with each  $5.7 \text{ }^\circ\text{C}$ . This means that adsorption capacities at cold climates have to satisfy a series of loads, possibly the whole winter. This is the second aspect next to clogging which might limit the compaction of the net filter surface. Orage accounts for a progressive saturation of the filter when proposing filter material and area.

Total outlet COD concentration can be calculated from dissolved inlet COD, inter-event duration and PET and a constant background concentration ( $R^2=0.62$ ). This is valid for event mean concentrations; experiments of the future might target to explain inter-event dynamics in the function of environmental factors in the inter-events.

It was shown that CSO CWs remove effectively several micropollutants as well, both from the group of PAHs (benzo(a)pyrene, phenanthrene, naphthalene) and some metals (Al, Ti, Cr and Ba). A deeper conclusion needs further research. Focus should be given on detailed composite sampling of regular loads, with pH and possibly redox measurements.



#### **7.2.4 Second stage for denitrification**

It has been shown how the nitrate flush is related to the load passing through the filter. Most of the nitrate is flushed out at the beginning of the events with the first meter of load. Therefore, capturing exclusively the first meter of load of each event would be satisfactory to target total nitrogen removal at the scale of any treated rain event. However, this poses the question of the carbon source and an associated water residence time in a second treatment stage to guarantee a TN removal performance. This has to be studied in the future. Confirmation of this one meter load to be caught, directs towards compact filters (with the use of zeolite or other advanced materials in the present design) to keep the low footprint of the overall system.

## 8 Acknowledgements

Many thanks to Daniel Meyer who headhunted me, taught me and advised me generously, to my supervisors Pascal Molle and Rémy Gourdon for their profound support, for Stéphane Troesch for being the best boss ever, and to Zoltán Gribovszki at the University of West Hungary who first introduced me constructed wetlands. Thanks to Vanessa Aburegiaba and Barbara at IRSTEA for their tremendous help, for Corinne Brosse and LAMA staff in general for being so flexible towards our stochastic sampling practice, for Nicolas Forquet for his practical help with instrumentation and scripts, Laurie Olivier for helping the project enthusiastically even after her internship was over. Many thanks to Delphine Bouillet and David Sanahuja for lodging me in the first months. Thanks to Jean-Marc Croumier for being so flexible and insightful with the programming of Orage.

Thanks to Ania Morvannou, Boram Kim, Sylvain Michel, Jérémie Aubert, Vincent Bourgeois, Clément Cretoiller, Olivier Garcia and Didier Coupet for helping with practical work. Thanks for the software CANOE, the field trips and the events to the laboratory LGCIE. Thanks to the internship students Laurie Olivier and Mélissa Gerodolle who gave essential support.

Thanks to the CIFRE scholarship partners: to the Ministère de l'Éducation Nationale, de l'Enseignement Supérieur et de la Recherche and Epur Nature sarl for funding my PhD, to IRSTEA for hosting me and for INSA Lyon for coordinating my curricula. Thanks to ONEMA and water authorities for supporting financially the ADEPTE project and thus many of the research activities related to this thesis.

Thanks to my family and my friends for all their support.

## Acknowledgements

## 9 References

- Ahnert M, Blumensaat F, Langergraber G, Alex J, Woerner D, Frehmann T, Halft N, Hobus I, Plattes M, Spring V, Winkler S (2007): Goodness-of-fit measures for numerical modelling in urban water management – a summary to support practical applications. Poster presented at the 10th IWA Specialised Conference on Design, Operation and Economics of large Wastewater Treatment Plants, Vienna, Austria, pp. 69-72. URL: [http://www.hsgsim.org/downloads/Ahnert-et-al\\_LWWTP07\\_paper.pdf](http://www.hsgsim.org/downloads/Ahnert-et-al_LWWTP07_paper.pdf), (accessed: 31 July 2014).
- Alaphilippe G, Bois JS, Carchano T, Chanseau JP, Chartier A, Hess C, Jauffred L, Liénard A, Luttiau A, Malamaire G, Molle P, Mercoiret L, Philippe R, Ragainne N, Saint Laurent G, Vincent J, Wepierre N (2011): *Protocole de prélèvement, d'échantillonnage, et d'analyse des boues de Filtres Plantés de Roseaux (FPR) en vue de leur valorisation par épandage agricole*. (Sample taking, handling and analysis protocol of sludge in constructed wetlands with regards to their agricultural potential.). Research report, IRSTEA and ONEMA, Lyon, France. [http://epnac.irstea.fr/wp-content/uploads/2013/02/2011\\_Onema-Cemagref\\_Protocole-pr%C3%A9l%C3%A8vement-LSPR.pdf](http://epnac.irstea.fr/wp-content/uploads/2013/02/2011_Onema-Cemagref_Protocole-pr%C3%A9l%C3%A8vement-LSPR.pdf), accessed 02.09.2016 [in French].
- Amaral R, Ferreira F, Galvao A, Matos JS (2013): Constructed wetlands for combined sewer overflow treatment in a Mediterranean country, Portugal. *Wat. Sci. Tech.* 67(12) :2739-2745. DOI: 10.2166/wst.2013.180
- Angerville R (2009): *Evaluation des risques écotoxicologiques liés au déversement de rejets Urbains par Temps de Pluie (RUTP) dans les cours d'eau : Application à une ville française et à une ville haïtienne*. (Evaluation of ecotoxicology risks of urban wet weather flows posed on water courses : case studies of a French and a Haitian settlement.). PhD thesis, INSA of Lyon. <https://tel.archives-ouvertes.fr/tel-00446988/document>, accessed 02.09.2016 [in French].
- Arias L, Bertrand-Krajewski JL, Molle P (2014): Simplified hydraulic model of French vertical-flow constructed wetlands. *Wat. Sci. Tech.* 70(5): 909-916.
- Becouze-Lareure C, Dembélé A, Coquery M, Cren-Olivé C, Barillon B, Bertrand-Krajewski JL (2016): Source characterization and loads of metals and pesticides in urban wet weather discharges. *Urban Water J.* 13(6): 600-617. DOI: 10.1080/1573062X.2015.1011670
- Campolongo F, Cariboni J, Saltelli A (2007): An effective screening design for sensitivity analysis of large models. *Environ Model Softw* 22: 1509-1518.
- Chocat B, Cathelain M, Mares A, Mouchel JM (1994): Pollution caused by urban stormwater: impacts on receiving waters [in French] – La pollution due aux rejets urbains de temps de pluie : impacts sur les milieux récepteurs. *La Houille Blanche*, 1-2: 97-105.
- Choubert JM, Martin-Ruel S, Budzinski H, Miège C, Esperanza M, Lagarrigue C, Coquery M (2011): Limiting the emissions of micro-pollutants: what efficiency can we expect from wastewater treatment plants? *Wat. Sci. Tech.* 63(1): 57-65. DOI: 10.2166/wst.2011.009.
- Cowardin LM, Carter V, Golet FC, Laroe ET (1985): *Classification of wetlands and deep water habitats of the united states*. Washington D.C., U.S. Fish and Wildlife Service.
- Dechesne M (2002): Understanding and modelling the operation of urban stormwater infiltrations basins for the assessment of technical and environmental performance over the long term [in

- French] – Connaissance et modélisation du fonctionnement des bassins d’infiltration d’eaux de ruissellement urbain pour l’évaluation des performances techniques et environnementales sur le long terme. PhD thesis at INSA Lyon. URL: <http://theses.insa-lyon.fr/publication/2002ISAL0097/these.pdf>, (accessed: 4 August 2016).
- Dembélé A, Becouze C, Bertrand-Krajewski JL, Cren-Olivé C, Barillon B, Coquery M (2009): Quantification des polluants prioritaires dans les rejets urbains de temps de pluie – Les premiers résultats du projet de recherche ESPRIT mené sur deux bassins versants. *Techniques Sciences Méthodes*, 2009/4: pp. 60-76.
- Dittmer U (2006): Retention and transformation processes of carbon and nitrogen compounds in retention soil filters for CSO treatment [in German] – *Prozesse des Rückhaltes und Umsatzes von Kohlenstoff- und Stickstoffverbindungen in Retentionsbodenfiltern zur Mischwasserbehandlung*. PhD thesis, Kaiserslautern Technical University. Schriftenreihe des Fachgebiets Siedlungswasserwirtschaft der Technischen Universität Kaiserslautern, Volume 23. URL (English abstract): <http://nbn-resolving.de/urn/resolver.pl?urn:nbn:de:hbz:386-kluedo-20509>, (accessed: 4 August 2016).
- Dittmer U, Meyer D, Langergraber G (2005): Simulation of a subsurface vertical flow constructed wetland for CSO treatment. *Wat Sci Tech* 51(9): 225-232.
- Dittmer U, Meyer D, Tondera K, Lambert B, Fuchs S (2016): Treatment of CSO in Retention Soil Filters – lessons learned from 25 years of research and practice. Proceedings of 9th Novatech conference on Urban Water planning and technologies for sustainable management. Graie and INSA, Lyon, France.
- Dittmer U, Schmitt TG (2011): Purification processes in biofilter systems for CSO treatment. Proceedings of the 12<sup>th</sup> International Conference on Urban Drainage, Porto Alegre, Brazil. URL: <https://web.sbe.hw.ac.uk/staffprofiles/bdgsa/temp/12th%20ICUD/PDF/PAP005473.pdf>, (accessed: 4 August 2016)
- EPUR (2012): Design documentation of Marcy l’Etoile [in French] – *Livrable final et plan de recolement*. Epur Nature, Caumont-sur-Durance, France.
- EU 2000/60/EC: Directive 2000/60/EC of the European Parliament and of the Council establishing a framework for the Community action in the field of water policy. URL: [http://ec.europa.eu/environment/water/water-framework/index\\_en.html](http://ec.europa.eu/environment/water/water-framework/index_en.html), (accessed on 12/01/2015).
- Felmeden J (2013): Retention of the phosphorous in combined sewer overflows using retention soil filters [in German] – Phosphorrückhalt in der Mischwasserbehandlung durch Retentionsbodenfilter-Anlagen. PhD thesis, Department of Sanitary and Environmental Engineering, University of Kassel, publication No. 33. URL: <http://www.uni-kassel.de/upress/online/frei/978-3-89958-610-7.volltext.frei.pdf>, (accessed: 4 August 2016).
- Fonder N, Headley T (2013): The taxonomy of treatment wetlands: a proposed classification and nomenclature system. *Ecol Eng* 51: 203-211.
- Fournel J (2012): *Extensive systems for the management and treatment of urban runoffs in rainy weather* [in English] – *Systemes extensifs de gestion et de traitement des eaux urbaines de temps de pluie*. PhD thesis, Université de Montpellier II, Sciences et Techniques du Languedoc. URL:

- <http://www.biu-montpellier.fr/florabium/jsp/nnt.jsp?nnt=2012MON20111>, (accessed 14.06.2016).
- Fournel J, Forquet N, Molle P, Grasmick A (2013): Modelling constructed wetlands with variably saturated vertical subsurface-flow for urban stormwater treatment. *Ecol Eng* 55: 1-8.
- Frechen FB (2013): RSFs in Hessen – supplementary research on the retention of phosphorous and heavy metals [in German] – Retentionsbodenfilter (RBF) in Hessen – Ergänzungsuntersuchungen zum Phosphor- und Schwermetallrückhalt. PhD thesis, Schriftenreihe des Fachgebietes Siedlungswasserwirtschaft der Universität Kassel. Volume 35. URL: <http://www.uni-kassel.de/upress/online/frei/978-3-86219-666-1.volltext.frei.pdf>, (accessed: 4 August 2016).
- Frechen FB, Schier W, Felmeden J (2006): The plant-covered retention soil filter (RSF): the mechanical and biological combined sewer overflow (CSO) treatment. *Plant. Eng. Life Sci.* 6(1): 74-79.
- Gasperi J, Zgheib S, Cladière M, Rocher V, Moilleron R, Chebbo G (2012): Priority pollutants in urban stormwater: Part 2 – Case of combined sewers. *Water Res.* 46: 6693-6703.
- Gromaire MC (1998): Urban wet weather pollution in combined sewer networks. Characteristics and origins [in French] – *La pollution des eaux pluviales urbaines en réseau d'assainissement unitaire – caractéristiques et origines*, Ecole Nationale des Ponts et Chaussées, Paris. URL: <https://tel.archives-ouvertes.fr/tel-00005596/document>, (accessed : 4 August 2016).
- Heimovaara T (1993): Design of triple wire time domain reflectometry probes in practice and theory. *Soil Sci Soc Am J*, 57: 1410-1417.
- Henrichs M, Langergraber G, Uhl M (2007): Modelling of organic matter degradation in constructed wetlands for treatment of combined sewer overflow. *Sci Tot Env* 380: 196-209.
- Henrichs M, Welked A, Uhl M (2009): Modelling of biofilters for ammonium reduction in combined sewer overflow. *Wat Sci Tech* 60(3): 825-831.
- Henze M, Gujer W, Mino T, Loosdrecht M (ed.) (2000): *Activated sludge models ASM1, ASM2, ASM2d and ASM3*. IWA Publishing: London, UK.
- INSAVALOR and SOGREAH (1997): CANOE, a urban hydrology software, design and evaluation of sewage networks, simulation of rain events, flows and water quality. User's manual [in French] – *CANOE, logiciel d'hydrologie urbaine, conception et évaluation de réseaux d'assainissement, simulation des pluies, des écoulements et de la qualité des eaux. Manuel de l'utilisateur*.
- Kadlec RH, Wallace SD (2009): *Treatment wetlands (2nd ed.)*. Boca Raton, CRC Press.
- Langergraber G, Šimůnek J (2005): Modeling variably-saturated water flow and multi-component reactive transport in constructed wetlands. *Vadose Zone J.* 4(4):924-938.
- Langergraber G (2001): *Development of a simulation tool for subsurface flow constructed wetlands*. PhD thesis, Institute of Sanitary Engineering and Water Pollution Control, University of Natural Resources and Life Sciences, Vienna, Austria. URL (abstract):

- [https://zidapps.boku.ac.at/abstracts/search\\_abstract.php?paID=3&paLIST=0&paSID=2817](https://zidapps.boku.ac.at/abstracts/search_abstract.php?paID=3&paLIST=0&paSID=2817), (accessed: 4 August 2016).
- Langergraber G, Šimůnek J (2012): *HYDRUS Wetland Module Manual, Version 2. Hydrus Software Series 4*. Department of Environmental Sciences, University of California Riverside: Riverside, California, USA.
- Ledieu J, de Ridder P, de Clerck P, Dautrebande S (1986): A method of measuring soil water content by time domain reflectometry. *J Hydrol* 88: 319-328.
- Lee JG, Selvakumar A, Alvi K, Riverson J, Zhen JX, Shoemaker L, Lai F (2012): A watershed-scale design optimization model for stormwater best management practices. *Environ Model Softw* 37: 6-18.
- Loperfido JV, Noe GB, Jarnagin ST, Hogan DM (2014): Effects of distributed and centralized best management practices and land cover on urban stream hydrology at the catchment scale. *J Hydrol* 519: 2584-2595.
- Marsalek J (1998): Challenges in urban drainage. In: *Hydroinformatic tools for planning, design, operation and rehabilitation of sewer systems*, Environment NAS (ed.), Kluwer Academic Publishers, Dordrecht/Boston/London, pp. 1-23.
- Masi F, Rizzo A, Bresciani R, Conte G (2016): Constructed wetland for combined sewer overflow treatment: ecosystem services at Gorla Maggiore, Italy. *Ecol. Eng.*, in press.
- Meyer D (2011): Modelling and simulation of constructed wetlands for combined sewer overflow treatment [in German]. – *Modellierung und Simulation von Retentionsbodenfiltern zur weitergehenden Mischwasserbehandlung*. PhD dissertation, Kaiserslautern Technical University. Schriftenreihe des Fachgebiets Siedlungswasserwirtschaft der Technischen Universität Kaiserslautern. Volume 31. URL: [https://kluedo.ub.uni-kl.de/files/2843/Dissertation\\_Daniel\\_Meyer\\_online.pdf](https://kluedo.ub.uni-kl.de/files/2843/Dissertation_Daniel_Meyer_online.pdf), (accessed: 4 August 2016).
- Meyer D, Chazarenc F, Claveau-Mallet D, Dittmer U, Forquet N, Molle P, Morvannou A, Pálffy TG, Petitjean A, Rizzo A, Campà RS, Scholz M, Soric A, Langergraber G (2015): Modelling constructed wetlands: scopes and aims – a comparative review. *Ecol Eng* 80: 205-213.
- Meyer D, Dittmer U (2015): RSF\_Sim – a simulation tool to support the design of constructed wetlands for combined sewer overflow treatment. *Ecol Eng* 80:198-204.
- Meyer D, Molle P, Esser D, Troesch S, Masi F, Dittmer U (2013): Constructed wetlands for combined sewer overflow treatment – comparison of German, French and Italian approaches. *Water* 5(1): 1-12.
- Meyer D, Schmitt TG, Woźniak R, Sommer T, Hagen H (2008): Results of long-term pollution-load simulations of lab-scale constructed wetlands for CSO treatment. In: *Proceedings of the 11<sup>th</sup> International Conference on Wetland Systems for Water Pollution Control*, pp 790-796, Indore, India.
- Mitsch WJ, Gosselink JG (2007): *Wetlands (4th ed.)*. New Jersey, Wiley & Sons.
- Molle P, Liénard A, Boutin C, Merlin G, Iwema A (2005): How to treat raw sewage with constructed wetlands: an overview of the French systems. *Wat Sci Tech* 51(9): 11-21.

- Molle P, Liénard A, Grasmick A, Iwema A (2006): Effect of reeds and feeding operations on hydraulic behavior of vertical flow constructed wetlands under hydraulic overloads. *Water Res.* 4(3): 606-612.
- Morris MD (1991): Factorial sampling plans for preliminary computational experiments. *Technometrics* 33(2): 161-174.
- Moss B (2010): *Ecology of freshwater (4th ed.)*. Wiley-Blackwell, Hong Kong.
- Mourad M (2005): Modelling the quality of urban runoff: sensibility on experimental data and practical relevance [in French] – *Modélisation de la qualité des rejets urbains de temps de pluie: sensibilité aux données expérimentales et adéquation aux besoins opérationnels*. INSA Lyon, Lyon. URL: <http://docinsa.insa-lyon.fr/these/2005/mourad/these.pdf>, (accessed: 4 August 2016).
- Mungasavalli DP, Viraghavan T (2006): Constructed wetlands for stormwater management: a review. *Fresen Environ Bull* 15: 1363-1372.
- Muthukrishnan S, Madge B, Selvakumar A (2006): The use of best management practices (BMPs) in urban watersheds – executive summary. In: Field R, Tafuri AN, Muthukrishnan S, Madge Acquistio BA, Selvakumar A (ed.): *The use of best management practices (BMPs) in urban watersheds*. DEStech Publication Inc, Lancaster, PA, pp 13-70.
- Pálffy T. G., Langergraber G. (2014). The verification of the Constructed Wetland Model No. 1 implementation in HYDRUS using column experiment data. *Ecol. Eng.* 68: 105-115.
- Pálffy TG, Gourdon R, Meyer D, Troesch S, Olivier L, Molle P (2016a): Filling hydraulics and nitrogen dynamics in full-scale CSO CWs. *Ecol. Eng.*, submitted.
- Pálffy TG, Meyer D, Troesch S, Gourdon R, Olivier L, Molle P (2016b): Orage: a design optimization modelling tool for CSO CWs. Core model. *Environ. Model. Softw.*, submitted.
- Parent-Rouault C, Boisson JC (2007): Impacts des rejets urbains de temps de pluie (RUTP) sur les milieux aquatiques: état des connaissances. *Revue des sciences de l'eau. Journal of Water Science* 20: 229-239.
- Passerat J, Outtara NK, Mouchel JM, Rocher V, Servais P (2011): Impact of an intense combined sewer overflow event on the microbiological water quality of the Seine River. *Water Res* 45(2): 893-903.
- Pinnekamp J (2013): Optimization of the operation of RSFs treating combined sewer overflow [in German] – *Betriebsoptimierung von Retentionsbodenfiltern im Mischsystem*. Closing research report, Ministry for Climate Protection, Environment, Agriculture, Conservation and Consumer Protection of the State of North Rhine-Westphalia, Germany. [http://www.lanuv.nrw.de/wasser/abwasser/forschung/pdf/Abschlussbericht\\_Retentionsbodenfilter.pdf](http://www.lanuv.nrw.de/wasser/abwasser/forschung/pdf/Abschlussbericht_Retentionsbodenfilter.pdf), (accessed 03 February 2015).
- Prabhukumar G, Pagilla K. (2010): Polycyclic aromatic hydrocarbons in urban runoff-sources, sinks and treatment. Review of the Illinois Institute of Technology. <http://drscw.org/dissolvedoxygen/DPAH1.pdf>, accessed: 02.09.2016



## References

- Robinson DA, Schaap M, Jones SB, Friedman SP and Gardner CMK (2003): Considerations for improving the accuracy of permittivity measurement using time domain reflectometry: air-water calibration, effects of cable length. *Soil Sci Soc Am J*, 67: 62-70.
- Rousseau DPL, Horton D, Vanrolleghem PA, de Pauw N (2005): Impact of operational maintenance on the asset life of storm reed beds. *Wat Sci Tech* 51(9): 243-250.
- Ruban V, Larrarte F, Berthier M, Raimbault G (2005): Quantitative and qualitative hydrologic balance for a suburban watershed with a separate sewer system (Nantes, France). *Wat. Sci. Tech.* 51(2): 231-238.
- Russel DL (2006): *Practical wastewater treatment*. Wiley, New Jersey, USA.
- Samsó R, Garcia J (2013): BIO\_PORE, a mathematical model to simulate biofilm growth and water quality improvement in porous media: Application and calibration for constructed wetlands. *Ecol Eng* 54: 116-127.
- Schmitt TG, Dittmer U (2007): Long term simulation study of Retention Soil Filters for CSO treatment [in German] – Simulationsstudie zum Langzeitverhalten von Retentionsbodenfiltern zur weitergehenden Mischwasserbehandlung. *GWF Wasser und Abwasser* 11/2007:793-800.
- Schulz W, Brechenmacher M, Wirth H (1994): Combined sewer overflow from the city area of Munich. *Sci Tot Env* 146/147: 493-498.
- Schütze MR, Butler D, Beck B (2002): *Modelling, simulation and control of urban wastewater systems*. Springer, London, p. 285.
- Shepard D (1968): A two-dimensional interpolation function for irregularly-spaced data. Proceedings of the 1968 23<sup>rd</sup> ACM national conference, pp. 517-524.
- Šimůnek, J; van Genuchten, MTh; Šejna, M (2011): *The HYDRUS software package for simulating the two- and three-dimensional movement of water, heat, and multiple solutes in variably-saturated media*. Technical Manual, version 2.0. PC Progress: Prague, Czech Republic.
- Smith JA, Sievers M, Huang S, Yu SL (2000): Occurrence and phase distribution of polycyclic aromatic hydrocarbons in urban storm-water runoff. *Wat. Sci. Tech.* 42(3-4): 383-388.
- Smullen JT, Shallcross AL, Cave AK (1999): Updating the U.S. nationwide urban runoff quality data base. *Wat Sci Tech* 39(12): 9-16.
- SOeS (2011): The sanitation services in France: key figures of 2008 [in French] – Le service d'assainissement en France: principales données 2008. Chiffres et statistiques 210: 8 p.
- Sztruhár D, Sokáč M, Holienčín A, Markovič A (2002): Comprehensive assessment of combined sewer overflows in Slovakia. *Urban Water* 4(3): 237-243.
- Terzakis S, Fountoulakis MS, Georgaki I, Albantakis D, Sabathianakis I, Karathanasis AD, Kalogerakis N, Manios T (2008): Constructed wetland treating highway runoff in the central Mediterranean region. *Chemosphere* 72(2): 141-149.
- Tondera K, Meyer D, Pinnekamp J (2013): Calibrating a simulation tool for constructed wetlands for combined sewer overflow treatment with field data. *Proceedings of the 5th International Symposium on Wetland Pollutant Dynamics and Control (WETPOL)*, Ecole des Mines de

## References

- Nantes and GEPEA, Nantes, France. URL: <http://web.emn.fr/x-dsee/wetpol2013/index.php?page=book-of-abstracts>, (accessed: 21 July 2016).
- Topp GC, Davis JL, Annan P (1980): Electromagnetic determination of soil water content: measurements in coaxial transmission lines. *Water Resour Res* 16(3): 574-582.
- Turković R, Fuchs S (2010): Oxygen transport and consumption in wastewater percolated sand-filters. Proceedings of 12<sup>th</sup> International Conference on Wetland Systems for Water Pollution Control, Venice, Italy.
- Uhl M, Dittmer U (2005): Constructed wetlands for CSO treatment: an overview of practice and research in Germany. *Wat Sci Tech* 51(9): 23-30.
- UN (2014): *World urbanization prospects: the 2014 revision, highlights (ST/ESA/SER.A/352)*. United Nations Department of Economic and Social Affairs, Population Division.
- United States Environmental Protection Agency (EPA) (1999a): Storm water technology fact sheet: sand filters. Office of Water Washington, D.C. EPA 832-F-99-007. URL: [http://water.epa.gov/scitech/wastetech/upload/2002\\_06\\_28\\_mtb\\_sandfltr.pdf](http://water.epa.gov/scitech/wastetech/upload/2002_06_28_mtb_sandfltr.pdf), (accessed: 3 February 2015).
- United States Environmental Protection Agency (EPA) (1999b): Storm water technology fact sheet: bioretention. Office of Water Washington, D.C. EPA 832-F-99-012. URL: [http://water.epa.gov/scitech/wastetech/upload/2002\\_06\\_28\\_mtb\\_biortn.pdf](http://water.epa.gov/scitech/wastetech/upload/2002_06_28_mtb_biortn.pdf), (accessed: 3 February 2015).
- United States Environmental Protection Agency (EPA) (1999c): Storm water technology fact sheet: storm water wetlands. Office of Water Washington, D.C. EPA 832-F-99-025. [http://water.epa.gov/scitech/wastetech/upload/2007\\_05\\_29\\_mtb\\_wetlands.pdf](http://water.epa.gov/scitech/wastetech/upload/2007_05_29_mtb_wetlands.pdf), (accessed: 3 February 2015).
- Vietz G, Rutherford ID, Fletcher TD, Walsh CJ (2016): Thinking outside the channel: Challenges and opportunities for protection and restoration of stream morphology in urbanizing catchments. *Landscape Urban Plan* 145: 34-44.
- Vymazal J (2007): Removal of nutrients in various types of constructed wetlands. *Sci Tot Env* 380(1-3): 48-65.
- Waldhoff A (2008): Sanitation of combined sewer in retention soil filters (RSFs) [in German] – *Hygienisierung von Mischwasser in Retentionsbodenfiltern (RBF)*. PhD thesis, Department of Sanitary and Environmental Engineering, University of Kassel, publication No. 30. URL: <http://www.uni-kassel.de/upress/online/frei/978-3-89958-606-0.volltext.frei.pdf>, (accessed: 4 August 2016).
- Walsh CJ, Roy AH, Feminella JW, Cottingham PD, Groffman PM, Morgan II RP (2005): The urban stream syndrome: current knowledge and the search for a cure. *J N Am Benthol Soc* 24(3): 706-723.
- Woźniak R (2008): Determination of load limits on filter substrates of constructed wetlands for combined sewer overflow treatment [in German] – *Ermittlung von Belastungsgrenzen an Bodensubstraten zur weitergehenden Mischwasserbehandlung in Retentionsbodenfiltern*. PhD thesis at the Department of Architecture/Regional Development and Environmental

## References

- Planning/Civil Engineering at TU Kaiserslautern, Schriftenreihe Band 24. URL: [https://kluedo.ub.uni-kl.de/files/1948/Diss\\_Wozniak\\_SIWAWI.pdf](https://kluedo.ub.uni-kl.de/files/1948/Diss_Wozniak_SIWAWI.pdf), (accessed: 4 August 2016).
- Woźniak R, Dittmer U, Welker A (2007): Interaction of oxygen concentration and retention of pollutants in vertical flow constructed wetlands for CSO treatment. *Wat Sci Tech* 56(3): 31-38.
- Zgheib S, Moilleron R, Chebbo G (2012): Priority pollutants in urban stormwater: Part 1 – Case of separate storm sewers. *Water Res.* 46: 6683-6692.

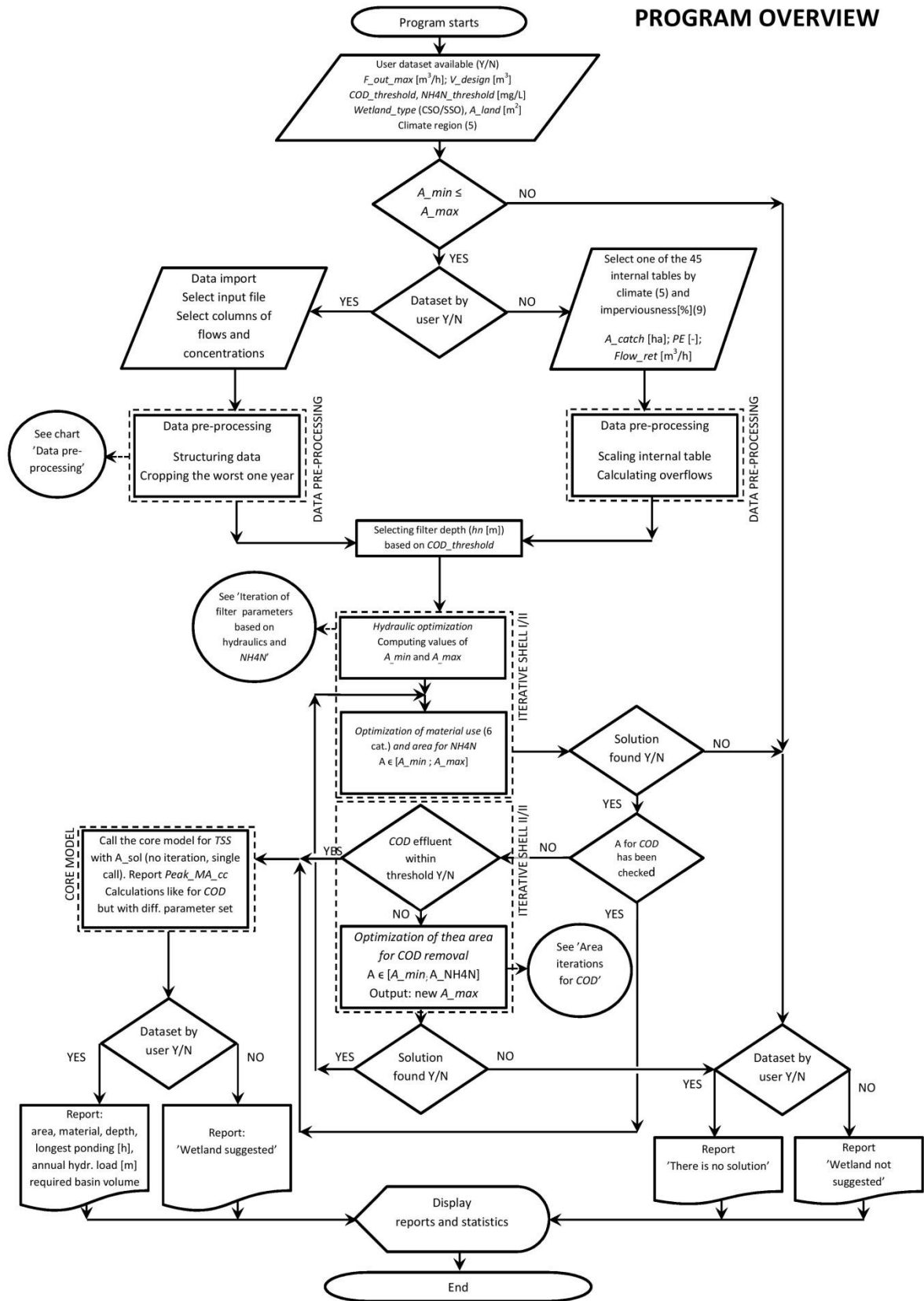
## **Annexes**



**Annex A:**  
Flow charts

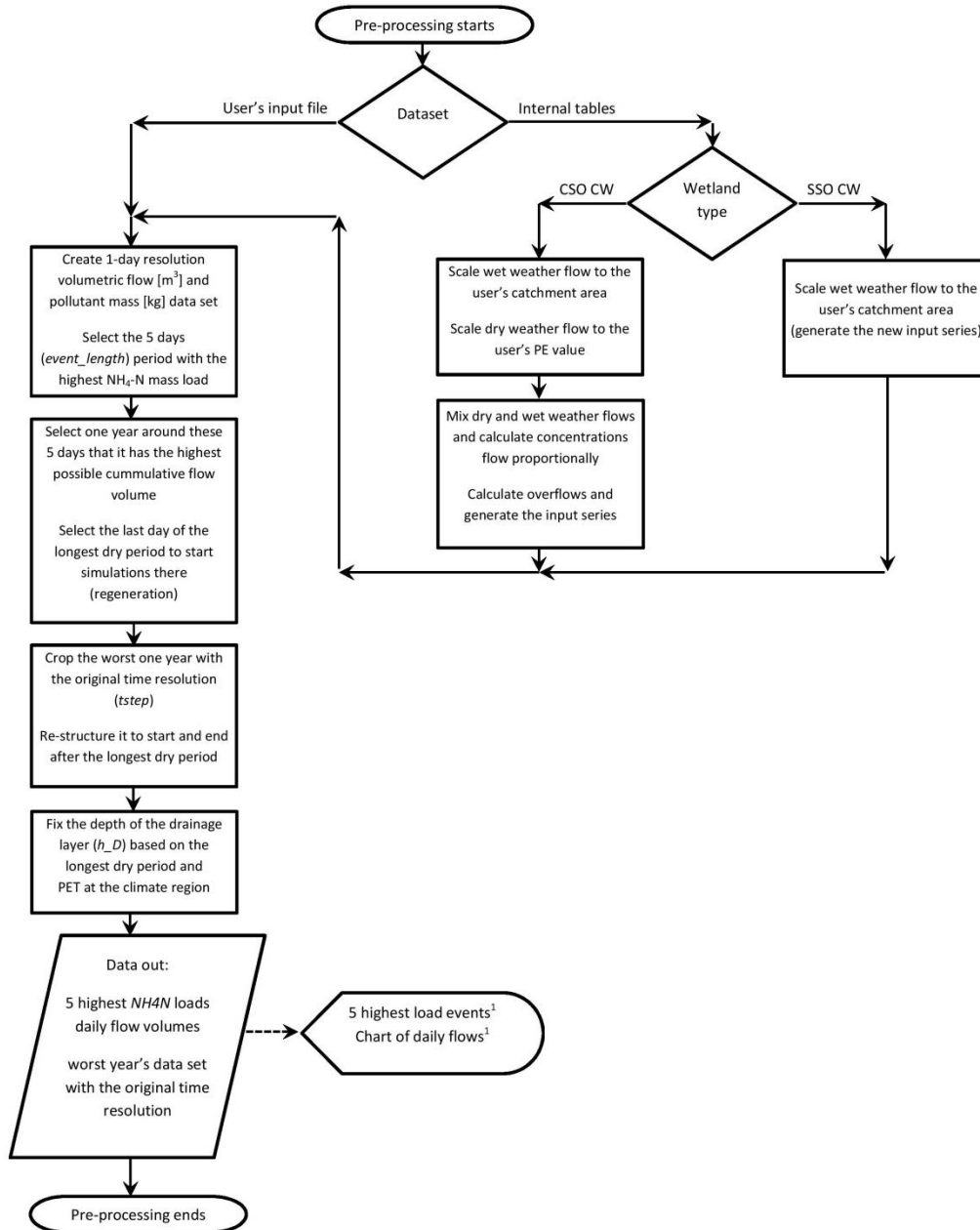


PROGRAM OVERVIEW



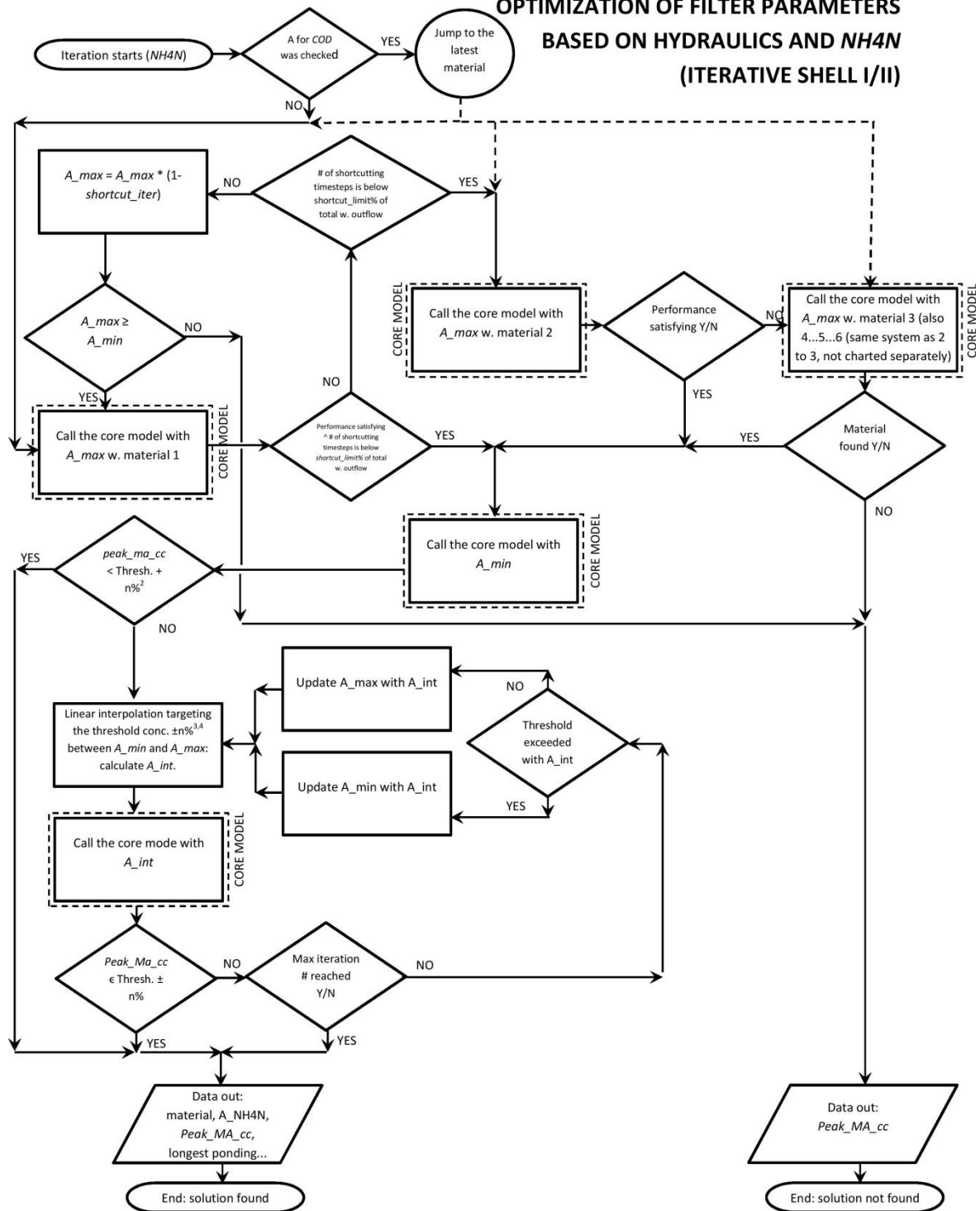


## DATA PRE-PROCESSING



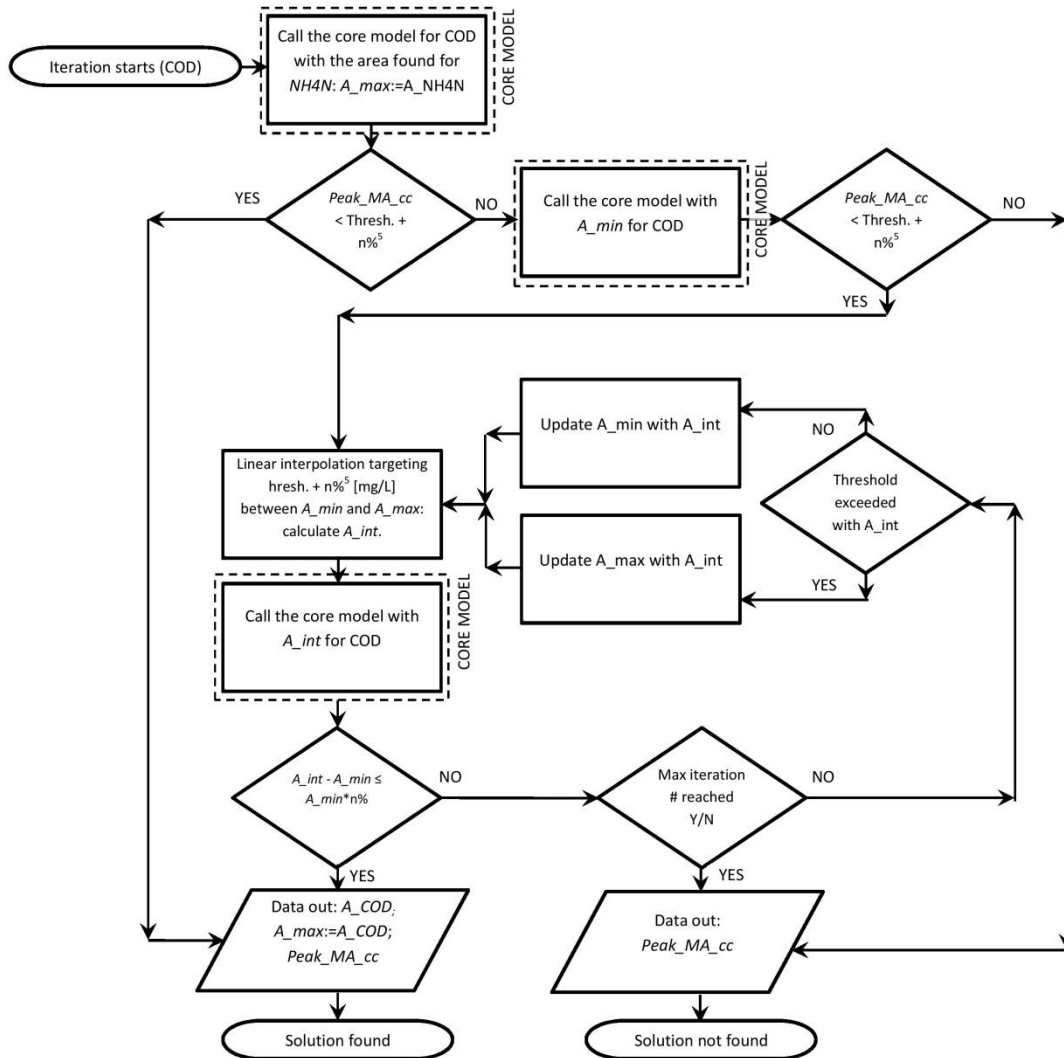
<sup>1</sup>: Display in tabular format: date (beginning and end); NH<sub>4</sub>-N mass [kg]; average volume per day [m<sup>3</sup>]; falling in the selected year [Y/N]. Shown with the user reports; see program overview.

**OPTIMIZATION OF FILTER PARAMETERS  
BASED ON HYDRAULICS AND NH4N  
(ITERATIVE SHELL I/II)**



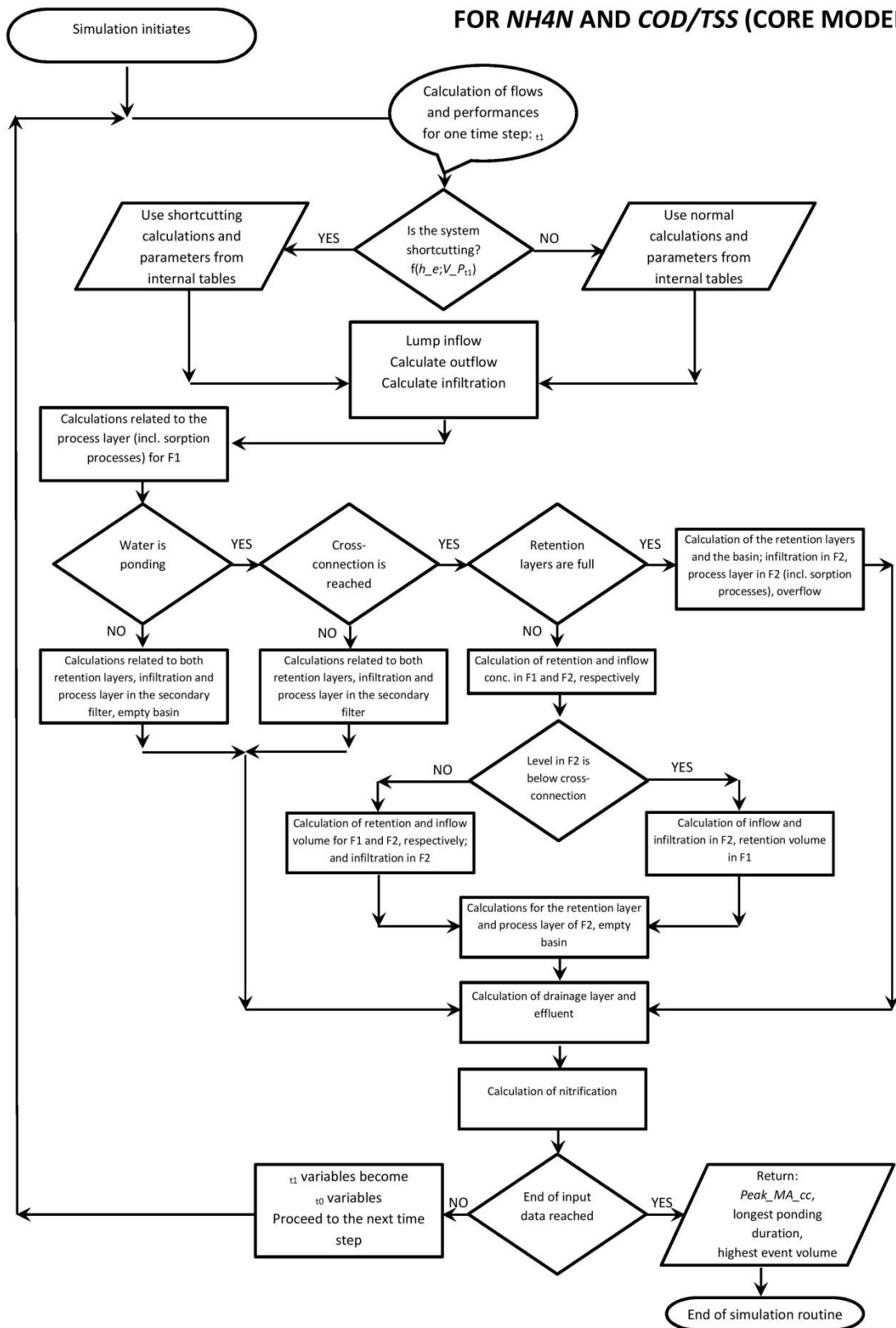
<sup>2</sup> NH4N\_threshold + band\_NH4N  
<sup>3</sup> NH4N\_threshold + band\_NH4N for the first iteration  
<sup>4</sup> NH4N\_threshold ± band\_NH4N; target the opposite side of the band to find the optimal area quicker.

**AREA ITERATIONS FOR COD  
(ITERATIVE SHELL II/II)**



<sup>5</sup> COD\_threshold + band\_COD

**CALCULATION OF PERFORMANCES  
FOR NH<sub>4</sub>N AND COD/TSS (CORE MODEL)**





**Annex B:**  
Algorithm of the core model



The core is called for one pollutant (TSS, COD or NH4N) at a time and calculations are repeated at each time step (t1). Environment-dependent parameters are refreshed based on internal tables before each time step to match the operational mode and the season. The reader is advised to refer on Fig. 26 for interpretation.

### Section I: Subroutines

#### SUBROUTINE Lump\_Inflow\_Ret (Fx)

// lumping the volume in the retention compartment ( $Ret_{t1}^{Fx}$ ) and the inflow (F1) if their total is less than the available pore volume in the process layer.

$$\text{IF } 0 < F_{in_{t1}^{Fx}} + V_{Ret_{t0}^{Fx}} < V_{P_{max}^{Fx}} - V_{P_{t0}^{Fx}}$$

$$F_{in_{cc_{t1}^{Fx}}} = (F_{in_{mass_{t1}^{Fx}} + V_{Ret_{mass_{t0}^{Fx}}}) / (F_{in_{t1}^{Fx}} + V_{Ret_{t0}^{Fx}})$$

$$F_{in_{t1}^{Fx}} = F_{in_{t1}^{Fx}} + V_{Ret_{t0}^{Fx}}$$

$$V_{Ret_{t0}^{Fx}} = 0$$

$$V_{Ret_{cc_{t0}^{Fx}}} = 0$$

END IF

END SUB

#### SUBROUTINE V\_P\_Calc (Fx, pollutant)

// calculating concentrations in the liquid phase (all pollutants) and in the solid phase (sorbed NH4N) of the process layer ( $P_{t1}^{Fx}$ ).

$$V_{P_{t1}^{Fx}} = V_{P_{t0}^{Fx}} - F_{out_{t1}^{Fx}} + F_{inf_{t1}^{Fx}}$$

IF pollutant  $\neq$  NH4N

// calculations for COD and TSS: instantaneous mixing:

$$V_{P_{conc_{t1}^{Fx}}} = \frac{V_{P_{mass_{t0}^{Fx}} - F_{exf_{mass_{t1}^{Fx}} + F_{inf_{mass_{t1}^{Fx}}}}}{V_{P_{t1}^{Fx}}}$$

ELSE

// calculations for NH4N: instantaneous mixing and sorption:

$$\text{IF } V_{P_{t1}^{Fx}} < V_e \wedge V_{P_{t1}^{Fx}} < V_{P_{max}^{Fx}} - F_{inf_{t1}^{Fx}} \quad // \text{shortcutting operation mode}$$

$$A_{inf_{t1}^{Fx}} = \frac{F_{inf_{t1}^{Fx}}}{K(t1 - t0)}$$

$$M_{active_{t1}^{Fx}} = A_{inf_{t1}^{Fx}} \times d_{filt} \times rho_{media}$$

$$\text{IF } A_{inf_{t0}^{Fx}} = 0$$



$$NH4\_infzonem_{t0.5}^{Fx} = \frac{A\_inf_{t1}^{Fx}}{A^{Fx} \times NH4\_oldmass_{t0}^{Fx} + F\_inf\_mass_{t1}^{Fx}}$$

ELSE

$$\begin{aligned} NH4\_infzonem_{t0.5}^{Fx} &= \frac{\min(A\_inf_{t1}^{Fx}; A\_inf_{t0}^{Fx})}{A\_inf_{t0}^{Fx}} \times NH4\_infzonem_{t0}^{Fx} \\ &+ \frac{A\_inf_{t1}^{Fx} - A\_inf_{t0}^{Fx} + ABS(A\_inf_{t1}^{Fx} - A\_inf_{t0}^{Fx})}{2A^{Fx}} \times NH4\_oldmass_{t0}^{Fx} \\ &+ F\_inf\_mass_{t1}^{Fx} \end{aligned}$$

END IF

IF  $F\_inf_{t1}^{Fx} = 0$ 

$$F\_inf\_cc_{t1}^{Fx} = 0$$

ELSE

// normal operation mode

$$\text{IF } \frac{NH4\_infzonem_{t0.5}^{Fx}}{F\_inf_{t1}^{Fx} + K2 \times A1 \times M\_active_{t1}^{Fx}} \leq C1$$

$$F\_inf\_cc_{t1}^{Fx} = \frac{NH4\_infzonem_{t0.5}^{Fx}}{F\_inf_{t1}^{Fx} + K2 \times A1 \times M\_active_{t1}^{Fx}}$$

ELSE

$$F\_inf\_cc_{t1}^{Fx} = \frac{NH4\_infzonem_{t0.5}^{Fx} - S1 \times M\_active_{t1}^{Fx} \times K2}{F\_inf_{t1}^{Fx} + K2 \times A2 \times M\_active_{t1}^{Fx}}$$

END IF

END IF

$$NH4\_infzonem_{t1}^{Fx} = NH4\_infzonem_{t0.5}^{Fx} - F\_inf\_mass_{t1}^{Fx}$$

IF  $A\_inf_{t0}^{Fx} = 0$ 

$$\begin{aligned} NH4\_oldmass_{t1}^{Fx} &= NH4\_oldmass_{t0}^{Fx} - \frac{A\_inf_{t1}^{Fx}}{A\_Fx} \times NH4\_oldmass_{t0}^{Fx} \\ &+ NH4\_infzonem_{t1}^{Fx} \end{aligned}$$

ELSE

$$\begin{aligned}
& NH4\_oldmass_{t1}^{Fx} \\
&= NH4\_oldmass_{t0}^{Fx} - \frac{A\_inf_{t1}^{Fx} - A\_inf_{t0}^{Fx} + ABS(A\_inf_{t1}^{Fx} - A\_inf_{t0}^{Fx})}{2A^{Fx}} \\
&\times NH4\_oldmass_{t0}^{Fx} + \frac{A\_inf_{t0}^{Fx} - A\_inf_{t1}^{Fx} + ABS(A\_inf_{t0}^{Fx} - A\_inf_{t1}^{Fx})}{2A\_inf_{t0}^{Fx}} \\
&\times NH4\_infzonem_{t0}^{Fx} + NH4\_infzonem_{t1}^{Fx} - NH4\_infzonem_{t0}^{Fx}
\end{aligned}$$

END IF

END IF

$$V\_P\_conc_{t1}^{F1} = \frac{V\_P\_mass_{t0}^{Fx} - F\_exf\_mass_{t1}^{Fx} + F\_inf\_mass_{t1}^{Fx}}{V\_P_{t1}^{Fx}}$$

ELSE

$$\begin{aligned}
V\_P\_conc_{t0.5}^{Fx} &= V\_P\_conc_{t1}^{Fx} \\
V\_P\_mass_{t0.5}^{Fx} &= V\_P\_conc_{t0.5}^{Fx} \times V\_P_{t1}^{Fx}
\end{aligned}$$

$$\text{IF } \frac{V\_P\_mass_{t0.5}^{Fx} + NH4\_oldmass_{t0}^{Fx}}{V\_Pmax^{Fx} + K1 \times A1 \times M\_tot^{Fx}} \leq C1$$

$$V\_P\_conc_{t1}^{Fx} = \frac{V\_P\_mass_{t0.5}^{Fx} + NH4\_oldmass_{t0}^{Fx}}{V\_Pmax^{Fx} + K1 \times A1 \times M\_tot^{Fx}}$$

ELSE

$$V\_P\_conc_{t1}^{Fx} = \frac{V\_P\_mass_{t0.5}^{Fx} + NH4\_oldmass_{t0}^{Fx} - S1 \times M\_tot^{Fx} \times K1}{V\_Pmax^{Fx} + K1 \times A2 \times M\_tot^{Fx}}$$

END IF

$$NH4\_oldmass_{t1}^{Fx} = NH4\_oldmass_{t0}^{Fx} + V\_P\_mass_{t0.5}^{Fx} - V\_P\_mass_{t1}^{Fx}$$

END IF

END IF

END SUB

### SUBROUTINE *V\_D\_Calc (Fx, pollutant)*

*// calculating the concentration of the exfiltration (flows 3 and 6 on Fig. 26) and the concentration in the drainage layer. COD removal is calculated when the water leaves the process layer ( $P_{t1}^{Fx}$ ).*

IF pollutant = NH4N

$$\begin{aligned}
F\_exf\_mass_{t1}^{F1} &= F\_out_{t1}^{F1} \times V\_P\_conc_{t0}^{F1} \\
F\_exf\_mass_{t1}^{F2} &= F\_out_{t1}^{F2} \times V\_P\_conc_{t0}^{F2} \\
V\_D\_conc_{t1}^{Fx} &= (V\_D\_mass_{t0}^{Fx} - F\_out\_mass_{t1}^{Fx} + F\_exf\_mass_{t1}^{Fx}) / V\_D^{Fx}
\end{aligned}$$

ELSE

IF  $V\_P\_conc_{t0}^{Fx} \leq C1$ 

$$COD\_exf\_cc_{t1}^{Fx} = K$$

ELSE IF  $C1 < V\_P\_conc_{t0}^{Fx} < C2$ 

$$COD\_exf\_cc_{t1}^{Fx} = K + (V\_P\_conc_{t0}^{Fx} - C1) \times (1 - \eta_1)$$

ELSE

$$COD\_exf\_cc_{t1}^{Fx} = K + (C2 - C1) \times (1 - \eta_1) + (V\_P\_conc_{t0}^{Fx} - C2) \times (1 - \eta_2)$$

END IF

 $V\_D\_conc_{t1}^{Fx}$ 

$$= \frac{(V\_D\_mass_{t0}^{Fx} - F\_out\_mass_{t1}^{Fx} + COD\_exf\_cc_{t1}^{Fx} \times COD\_exf\_cc_{t1}^{Fx})}{V\_D^{Fx}}$$

END IF

END SUB

**SUBROUTINE** Nitrification (Fx)

*// calculating nitrification: the mass of NH4N which is remaining in the solid phase of the process layer. The concentration of the residual water content stays unchanged until the next load when the equilibrium is calculated again for the whole filter. However, the liquid phase of the drainage layer is nitrified directly:*

IF  $F\_in_{t1}^{Fx} > minflow$ 

$$V\_P\_E_{max}^{Fx} = \max(V\_P_{t1}^{Fx}; V\_P\_E_{max}^{Fx})$$

ELSE IF  $F\_in_{t1}^{Fx} \leq minflow$  AND  $V\_P_{t1}^{Fx} \leq V\_P\_grav + minflow$ 

$$V\_P\_E_{max}^{Fx} = 0$$

END IF

IF  $V\_P_{t1}^{Fx} > V\_P\_grav + minflow$ 

$$NH4\_oldmass_{t1}^{Fx} = \left(1 - \frac{V\_P_{t1}^{Fx}}{V\_P\_E_{max}^{Fx}}\right) \times NH4\_oldmass_{t1}^{Fx} \times e^{-di \times e^{\frac{Ts-20}{Rc}}} + \frac{V\_P_{t1}^{Fx}}{V\_P\_E_{max}^{Fx}} \times NH4\_oldmass_{t1}^{Fx}$$

ELSE

$$NH4\_oldmass_{t1}^{Fx} = NH4\_oldmass_{t1}^{Fx} \times e^{-di \times e^{\frac{Ts-20}{Rc}}}$$

$$V\_D\_conc_{t1}^{Fx} = \max(V\_D\_conc_{t1}^{Fx} \times e^{-di \times e^{\frac{Ts-20}{Rc}}}; NH4\_background\_D)$$

END IF  
END SUB

## Section II: Core

CALL *Lump\_Inflow\_Ret* (F1)  
CALL *Lump\_Inflow\_Ret* (F2)

*// outflow volumes and concentrations (71) and (72):*

$$\begin{aligned} F_{out_{t1}}^{F1} &= \min(F_{limit} \times A^{F1}; V_{P_{t0}}^{F1} - V_{P_{grav}}) \\ F_{out_{cc_{t1}}^{F2}} &= V_{D_{conc_{t0}}^{F2}} \\ F_{out_{t1}}^{F2} &= \min(F_{limit} \times A^{F2}; V_{P_{t0}}^{F2} - V_{P_{grav}}) \\ F_{out_{cc_{t1}}^{F2}} &= V_{D_{conc_{t0}}^{F2}} \end{aligned}$$

*// infiltration volume and concentration F1 (2):*

IF  $V_{Ret_{t0}}^{F1} > 0$

$$\begin{aligned} F_{inf_{t1}}^{F1} &= \min(F_{limit} \times A^{F1}; V_{Ret_{t0}}^{F1}) \\ F_{inf_{cc_{t1}}^{F1}} &= V_{Ret_{cc_{t0}}^{F1}} \end{aligned}$$

END IF

IF  $V_{Ret_{t0}}^{F1} = 0$

$$\begin{aligned} F_{inf_{t1}}^{F1} &= \min(F_{in_{t1}}^{F1}; V_{P_{max}}^{F1} - V_{P_{t0}}^{F1}) \\ F_{inf_{cc_{t1}}^{F1}} &= F_{in_{cc_{t1}}^{F1}} \end{aligned}$$

END IF

*// process layer volume and concentration F1:  $P_{t1}^{F1}$ , incl. sorption calculations:*

CALL *V\_P\_Calc*(F1, pollutant)

*// volumes, flows and concentrations above the media (F1) and in the secondary filter side  
// case A: water is ponding but below the level of the cross-connection; calculation for  $Ret_{t1}^{F1}$  only:*

IF  $0 < V_{Ret_{t0}}^{F1} \leq V_{cross\_connection} - F_{in_{t1}}^{F1}$

$$\begin{aligned} V_{Ret_{t1}}^{F1} &= V_{Ret_{t0}}^{F1} - F_{inf_{t1}}^{F1} + F_{in_{t1}}^{F1} \\ V_{Ret_{cc_{t1}}^{F1}} &= \frac{V_{Ret_{mass_{t0}}^{F1}} - F_{inf_{mass_{t1}}^{F1}} + F_{in_{mass_{t1}}^{F1}}}{V_{Ret_{t1}}^{F1}} \end{aligned}$$

IF  $V_{Ret_{t0}}^{F2} > 0$

$$F_{inf_{t1}}^{F2} = \min(F_{limit} \times A^{F2}; V_{Ret_{t0}}^{F2})$$

ELSE

$$F_{inf_{t1}}^{F2} = V_{Ret_{t0}}^{F2}$$

END IF

$F\_inf\_cc_{t1}^{F2} = V\_Ret\_cc_{t0}^{F2}$   
 CALL  $V\_P\_Calc (F2, pollutant)$

END IF

*// case B: there is no ponding at all:*

IF  $V\_Ret_{t0}^{F1} = 0$

$V\_Ret_{t1}^{F1} = F\_in_{t1}^{F1} - F\_inf_{t1}^{F1}$   
 $V\_Ret\_cc_{t1}^{F1} = F\_in\_cc_{t1}^{F1}$   
 $F\_inf_{t1}^{F2} = V\_Ret_{t0}^{F2}$   
 $F\_inf\_cc_{t1}^{F2} = V\_Ret\_cc_{t0}^{F2}$   
 $V\_Ret_{t1}^{F2} = 0$   
 $V\_Ret\_cc_{t1}^{F2} = 0$   
 $V\_basin_{t1} = 0$   
 CALL  $V\_P\_Calc (F2, pollutant)$

END IF

*// case C: water is ponding and there is cross-flow (4, Fig. 26), i.e. F2 is in operation:*

IF  $V\_Ret_{t0}^{F1} > V\_cross\_connection - F\_in_{t1}^{F1}$

*// there is cross-flow (4) but the retention layers  $Ret_{t1}^{Fx}$  are not full:*

IF [ $V\_Ret_{t0}^{F1} + V\_Ret_{t0}^{F2} + F\_in_{t1}^{F1} + V\_basin_{t0}$   
 $\leq Vmax\_Ret^{F1} + Vmax\_Ret^{F2} + V\_Pmax^{F2} - F\_limit \times A^{F2} - V\_P_{t0}^{F2}$ ]  
 $\vee [(V\_Ret_{t0}^{F1} + V\_Ret_{t0}^{F2} + F\_in_{t1}^{F1} + V\_basin_{t0}$   
 $> Vmax\_Ret^{F1} + Vmax\_Ret^{F2} + V\_Pmax^{F2} - F\_limit \times A^{F2} - V\_P_{t0}^{F2})$   
 $\wedge (V\_Ret_{t0}^{F2} < V\_cross\_connection)]$

$$V\_Ret\_cc_{t1}^{F1} = \frac{V\_Ret\_mass_{t0}^{F1} - F\_inf\_mass_{t1}^{F1} + F\_in\_mass_{t1}^{F1} + V\_basin\_mass_{t0}}{V\_Ret_{t0}^{F1} - F\_inf_{t1}^{F1} + F\_in_{t1}^{F1} + V\_basin_{t0}}$$

$$F\_in\_cc_{t1}^{F2} = V\_Ret\_cc_{t1}^{F1}$$

*// the water level in the secondary filter is below the cross-connection:*

IF  $V\_Ret_{t0}^{F1} + F\_in_{t1}^{F1} + V\_basin_{t0} - V\_cross\_connection + V\_Ret_{t0}^{F2}$   
 $\leq V\_cross\_connection + V\_Pmax^{F2} - F\_limit \times A^{F2} - V\_P_{t0}^{F2} + F\_out_{t1}^{F2}$

$V\_Ret_{t1}^{F1} = V\_cross\_connection - F\_inf_{t1}^{F1}$   
 $F\_in_{t1}^{F2} = V\_Ret_{t0}^{F1} + F\_in_{t1}^{F1} + V\_basin_{t0} - V\_cross\_connection$   
 CALL  $Lump\_Inflow\_Ret (F2)$

IF  $V\_Ret_{t0}^{F2} > 0$

$F\_inf_{t1}^{F2} = \min(F\_limit \times A^{F2}; V\_Ret_{t0}^{F2})$   
 $F\_inf\_cc_{t1}^{F2} = V\_Ret\_cc_{t0}^{F2}$

ELSE

$F\_inf_{t1}^{F2} = \min(F\_in_{t1}^{F2}; V\_Pmax^{F2} - V\_P_{t0}^{F2} - F\_limit \times A^{F2} + F\_out_{t1}^{F2})$   
 $F\_inf\_cc_{t1}^{F2} = F\_in\_cc_{t1}^{F2}$

END IF

*// the water level in the primary and secondary filter is above the cross-connection:*

ELSE

$$F\_inf_{t1}^{F2} = V\_Pmax^{F2} - V\_P_{t0}^{F2} - F\_limit \times A^{F2} + F\_out_{t1}^{F2}$$

$$IF V\_Ret_{t0}^{F2} > 0$$

$$F\_inf\_cc_{t1}^{F2} = V\_Ret\_cc_{t0}^{F2}$$

ELSE

$$F\_inf\_cc_{t1}^{F2} = F\_in\_cc_{t1}^{F2}$$

END IF

$$\begin{aligned} V\_above\_connection &= F\_in_{t1}^{F1} + V\_basin_{t0} \\ &+ \max(0; V\_Ret_{t0}^{F1} - V\_cross\_connection + F\_out_{t1}^{F1}) \\ &+ \max(0; V\_Ret_{t0}^{F2} - V\_cross\_connection + F\_limit \times A^{F2}) \\ &- \max(0; V\_cross\_connection - F\_out_{t1}^{F1} - V\_Ret_{t0}^{F1}) \\ &- \max(0; V\_cross\_connection - F\_limit \times A^{F2} - V\_Ret_{t0}^{F2}) \\ &- F\_inf_{t1}^{F2} + F\_limit \times A^{F2} \end{aligned}$$

$$\begin{aligned} V\_Ret_{t1}^{F1} &= V\_cross\_connection - F\_out_{t1}^{F1} \\ &+ V\_above\_connection \times A^{F1} / A\_tot - F\_inf_{t1}^{F1} \end{aligned}$$

$$\begin{aligned} F\_in_{t1}^{F2} &= F\_inf_{t1}^{F2} - F\_limit \times A^{F2} \\ &+ \max(0; V\_cross\_connection - F\_limit \times A^{F2} - V\_Ret_{t0}^{F2}) \\ &+ V\_above\_connection \times A^{F2} / A\_tot \\ &- \max(0; V\_Ret_{t0}^{F2} - V\_cross\_connection + F\_limit \times A^{F2}) \end{aligned}$$

END IF

$$V\_Ret_{t1}^{F2} = V\_Ret_{t0}^{F2} - F\_inf_{t1}^{F2} + F\_in_{t1}^{F2}$$

$$IF V\_Ret_{t1}^{F2} = 0$$

$$V\_Ret\_cc_{t1}^{F2} = 0$$

ELSE

$$V\_Ret\_cc_{t1}^{F2} = (V\_Ret\_mass_{t0}^{F2} - F\_inf\_mass_{t1}^{F2} + F\_in\_mass_{t1}^{F2}) / V\_Ret_{t0}^{F2}$$

END IF

CALL V\_P\_Calc (F2, pollutant)

$$V\_basin_{t1} = 0$$

$$V\_basin\_cc_{t1} = 0$$

*// the retention layers Ret\_{t1}^{Fx} are full and Basin\_{t1} gets loaded; overflow possible:*

ELSE

$$V\_Ret_{t1}^{F1} = Vmax\_Ret^{F1} - F\_out_{t1}^{F1}$$

$$V\_Ret_{t1}^{F2} = Vmax\_Ret^{F2} - F\_out_{t1}^{F2}$$

$$V\_basin_{t1} = V\_basin_{t0} - Vmax\_Ret^{F1} + V\_Ret_{t0}^{F1} - Vmax\_Ret^{F2} + V\_Ret_{t0}^{F2} + F\_in_{t1}^{F1}$$

$$Massfrom\_Overload_{t1}^{F1} = \max(0; V\_Ret_{t0}^{F1} - Vmax\_Ret^{F1}) \times V\_Ret\_cc_{t1}^{F1}$$

$$Massfrom\_Inflow_{t1}^{F1} = \min[\max(0; Vmax\_Ret^{F1} - V\_Ret_{t0}^{F1}); F\_in_{t1}^{F1} \times A^{F1}/A\_tot] \times F\_in\_cc_{t1}^{F1}$$

$$Massfrom\_Basin_{t1}^{F1} = \min\{\max[Vmax\_Ret^{F1} - V\_Ret_{t0}^{F1}] - \min[\max(0; Vmax\_Ret^{F1} - V\_Ret_{t0}^{F1}); F\_in_{t1}^{F1} \times A^{F1}/A\_tot]; V\_basin_{t0} \times A^{F1}/A\_tot\} \times V\_basin\_cc_{t0}$$

$$V\_Ret\_cc_{t1}^{F1} = (V\_Ret\_mass_{t0}^{F1} - F\_inf\_mass_{t1}^{F1} + Massfrom\_Inflow_{t1}^{F1} + Massfrom\_Basin_{t1}^{F1} - Massfrom\_Overload_{t1}^{F1})/V\_Ret_{t1}^{F1}$$

$$F\_inf_{t1}^{F2} = F\_limit \times A^{F2}$$

$$F\_inf\_cc_{t1}^{F2} = V\_Ret\_cc_{t0}^{F2}$$

CALL V\_P\_Calc (F2, pollutant)

$$Massfrom\_Overload_{t1}^{F2} = \max(0; V\_Ret_{t0}^{F2} - Vmax\_Ret^{F2}) \times V\_Ret\_cc_{t1}^{F2}$$

$$Massfrom\_Inflow_{t1}^{F2} = \min[\max(0; Vmax\_Ret^{F2} - V\_Ret_{t0}^{F2}); F\_in_{t1}^{F2} \times A^{F2}/A\_tot] \times F\_in\_cc_{t1}^{F2}$$

$$Massfrom\_Basin_{t1}^{F2} = \min\{\max[Vmax\_Ret^{F2} - V\_Ret_{t0}^{F2}] - \min[\max(0; Vmax\_Ret^{F2} - V\_Ret_{t0}^{F2}); F\_in_{t1}^{F2} \times A^{F2}/A\_tot]; V\_basin_{t0} \times A^{F2}/A\_tot\} \times V\_basin\_cc_{t0}$$

$$V\_Ret\_cc_{t1}^{F2} = (V\_Ret\_mass_{t0}^{F2} - F\_inf\_mass_{t1}^{F2} + Massfrom\_Inflow_{t1}^{F2} + Massfrom\_Basin_{t1}^{F2} - Massfrom\_Overload_{t1}^{F2})/V\_Ret_{t1}^{F2}$$

$$V\_Basin\_cc_{t1} = (V\_basin\_mass_{t1} - Massfrom\_Basin_{t1}^{F1} - Massfrom\_Basin_{t1}^{F2} - Massfrom\_Inflow_{t1}^{F1} - Massfrom\_Inflow_{t1}^{F2} + F\_in\_mass_{t1}^{F1})/V\_basin_{t1}$$

IF V\_Basin\_{t1} > Vmax\_basin

$$F\_Over_{t1} = V\_Basin_{t1} - Vmax\_basin$$

$$F\_Over\_cc_{t1} = V\_basin\_cc_{t1}$$

$$V\_Over_{t1} = V\_Over_{t0} + F\_over_{t1}$$

$$V\_Over\_mass_{t1} = V\_Over\_mass_{t0} + F\_Over_{t1} \times F\_Over\_cc_{t1}$$

$$V\_Basin_{t1} = Vmax\_basin$$

END IF

END IF

END IF

*// drainage layer concentrations, COD removal:*

CALL V\_D\_Calc (F1, pollutant)

CALL V\_D\_Calc (F2, pollutant)

*// concentration of the effluent after outflow from the two filter sides 71 and 72 is mixed:*

$$F_{effluent_{t1}} = F_{out_{t1}^{F1}} + F_{out_{t1}^{F2}}$$

$$F_{effluent_{cc_{t1}}} = (F_{out_{t1}^{F1}} \times F_{out_{cc_{t1}}^{F1}} + F_{out_{t1}^{F2}} \times F_{out_{cc_{t1}}^{F2}}) / F_{effluent_{t1}}$$

// nitrification when the process layer  $P_{t1}^{F_x}$  releases water:

CALL Nitrification (F1)

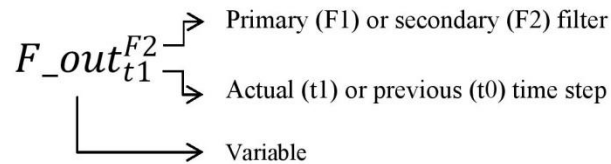
CALL Nitrification (F2)

// the peak value of the dynamic moving average called Peak\_MA\_cc is updated here at the end of the time step.

// t0 values are updated by the current t1 values

### Section III: Description of parameters and variables

Notation of parameters and variables:



List of parameters:

$A$ : filter area, [m<sup>2</sup>]

$A_{tot}$ : total filter area, [m<sup>2</sup>]

$A1$ : slope of the first stage in the broken stick adsorption isotherm, [m<sup>3</sup>/kg]

$C1$  (COD): threshold concentration to select  $K$  or  $Nu_1$ , [g/m<sup>3</sup>]

$C1$  (NH<sub>4</sub>N): threshold concentration to select  $A1$  or  $A2$ , [g/m<sup>3</sup>]

$C2$  (COD): threshold concentration to select  $Nu_1$  or  $Nu_2$ , [g/m<sup>3</sup>]

$D_{filt}$ : filter depth, [m]

$-d_i$ : nitrification rate constant, [1/dt]

$F_{limit}$ : outflow limitation, [m<sup>3</sup>/h]

$K$  (COD): background COD concentration, [g/m<sup>3</sup>]

$K(t1-t0)$ : infiltration in unit time step (based on the hydraulic conductivity), [m/dt]

$K1$ : adsorption capacity constant for NH<sub>4</sub>N at normal operation, [-]

$K2$ : adsorption capacity constant for NH<sub>4</sub>N at normal operation, [-]

$Minflow$ : minimum inflow rate which is accounted for, [m<sup>3</sup>/h]

$NH4\_background\_D$ : background concentration of NH<sub>4</sub>N in the drainage layer where nitrification stops

$Rc$ : rate sensibility of nitrification to scale temperature dependency of the process, [°C]

$Rho\_media$ : bulk density of the filter media, [t/m<sup>3</sup>]

$S1$ : Y-axis intersection of  $A2$ , [mg/kg]

$Ts$ : seasonal mean temperature, [°C]

$V_{cross\_connection}$ : cross connection level, [m]

$V_D$ : volume of water in the drainage layer, [m<sup>3</sup>]

$V_e$ : volume of water in the process layer below which shortcutting is assumed, [m<sup>3</sup>]

$V_{Pmax}$ : maximum (or pore) volume in the process layer, [m<sup>3</sup>]

$V_{max\_basin}$ : maximum volume in the common basin, [m<sup>3</sup>]

$V_{max\_Ret}$ : maximum volume in the retention compartment, [m<sup>3</sup>]

$Nu_1$  (correctly  $\eta1$ ): slope of the COD removal isotherm between  $C1$  and  $C2$  [-]

$Nu_2$  (correctly  $\eta2$ ): slope of the COD removal isotherm above  $C2$  [-]



## List of variables:

$A_{inf}$ : surface area of infiltration at shortcutting mode, [m<sup>2</sup>]  
 $COD_{exf\_cc}$ : exfiltration concentration from the process layer if pollutant is *COD*, [g/m<sup>3</sup>]  
 $F_{exf\_mass}$ : exfiltration mass from the process layer, [g/m<sup>3</sup>]  
 $F_{in}$ : inflow volume to  $F^1$  or crossflow volume to  $F^2$ , [m<sup>3</sup>]  
 $F_{in\_cc}$ : concentration of  $F_{in}$ , [g/m<sup>3</sup>]  
 $F_{in\_mass}$ : mass of  $F_{in}$ , [g]  
 $F_{inf}$ : infiltration volume, [m<sup>3</sup>]  
 $F_{inf\_cc}$ : concentration of  $F_{inf}$ , [g/m<sup>3</sup>]  
 $F_{inf\_mass}$ : mass of  $F_{inf}$ , [g]  
 $F_{out}$ : outflow volume, [m<sup>3</sup>]  
 $F_{out\_cc}$ : concentration of  $F_{out}$ , [g/m<sup>3</sup>]  
 $F_{out\_mass}$ : mass of  $F_{out}$ , [g]  
 $F_{Over}$ : overflow, [m<sup>3</sup>]  
 $F_{Over\_cc}$ : concentration of  $F_{Over}$ , [g/m<sup>3</sup>]  
 $M_{active}$ : mass of the filter media in active contact with the infiltrating water at shortcutting, [t]  
 $NH4_{infzorem}$ : mass of *NH4N* adsorbed in  $M_{active}$ , [g]  
 $NH4_{oldmass}$ : mass of *NH4N* adsorbed in the total filter mass, [g]  
 $V_{basin}$ : volume of water in the basin, [m<sup>3</sup>]  
 $V_{basin\_cc}$ : concentration for  $V_{basin}$ , [g/m<sup>3</sup>]  
 $V_{basin\_mass}$ : mass in  $V_{basin}$ , [g]  
 $V_{D\_conc}$ : concentration for  $V_{D}$ , [g/m<sup>3</sup>]  
 $V_{D\_mass}$ : mass in  $V_{D}$ , [g]  
 $V_{Over}$ : cumulative volume of overflow, [m<sup>3</sup>]  
 $V_{Over\_mass}$ : mass in  $V_{Over}$ , [g]  
 $V_{P}$ : volume of water in the process layer, [m<sup>3</sup>]  
 $V_{P\_conc}$ : concentration for  $V_{P}$ , [g/m<sup>3</sup>]  
 $V_{P\_E}$ : maximum water volume reached in the process layer during the ongoing event, [m<sup>3</sup>]  
 $V_{P\_grav}$ : residual water volume in the process layer after gravity drainage, [m<sup>3</sup>]  
 $V_{P\_mass}$ : mass in  $V_{P}$ , [g]  
 $V_{Ret}$ : water volume in the retention compartment, [m<sup>3</sup>]  
 $V_{Ret\_cc}$ : concentration for  $V_{Ret}$ , [g/m<sup>3</sup>]  
 $V_{Ret\_mass}$ : mass in  $V_{Ret}$ , [g]

**Annex C:**  
Parameter ranges of the sensitivity analysis



Ranges were discretized to four values ( $p=4$ ), the upper and lower 5% were excluded.

## COD

Parameter	Description	Unit	Range min	Range max
$F_{limit\_base}$	Flow limitation	$m^3/m^2/h$	0.018	0.18
$V_{P\_gr}$	Residual water content	$m^3/m^3$	0.01	0.16
$hD$	Drainage layer depth	m	0.1	0.5
$tD$	Drainage layer porosity	$m^3/m^3$	0.2	0.4
$tP$	Process layer porosity	$m^3/m^3$	0.2	0.4
$A_{tot}$	Total area	$m^2$	200	2000
$h_{wall}$	Level from the filter to the top of the wall	m	0.7	1.2
$h_{cross\_connection}$	Level from the filter to the cross-connection	m	0.1	0.6
$Nu_1$	Removal performance for COD	%	0.1	0.99
$Nu_2$	Removal performance for COD	%	0.1	0.99
$C1$	Threshold between $K$ and $Nu_1$	$g/m^3$	1	70
$C2$	Threshold between $Nu_1$ and $Nu_2$	$g/m^3$	70	200
$K$	Background COD concentration in the effluent	$g/m^3$	1	70
$Ts$	Seasonal mean temperature	$^{\circ}C$	5	25
$COD_{background\_D}$	Background COD concentration	$g/m^3$	0	80

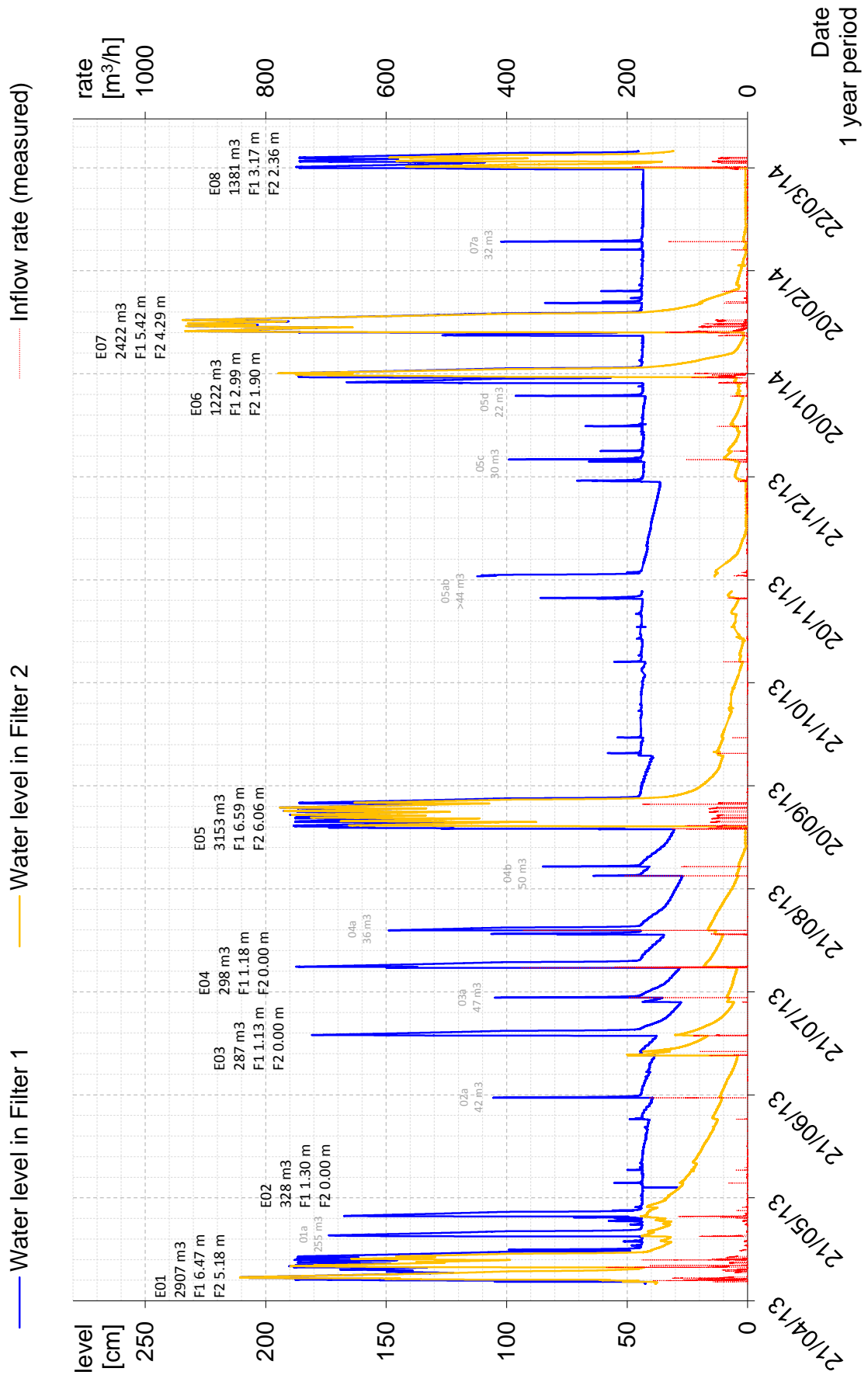
## NH4N

Parameter	Description	Unit	Range min	Range max
$F_{limit\_base}$	Flow limitation	$m^3/m^2/h$	0.024	0.108
$V_{P\_gr}$	Residual water content	$m^3/m^3$	0.01	0.16
$hD$	Drainage layer depth	m	0.1	0.5
$tD$	Drainage layer porosity	$m^3/m^3$	0.2	0.4
$tP$	Process layer porosity	$m^3/m^3$	0.2	0.4
$A_{tot}$	Total area: first analysis	$m^2$	200	2000
	Total area: second analysis		250	650
$h_{wall}$	Level from the filter to the top of the wall	m	0.7	1.2
$h_{cross\_connection}$	Level from the filter to the cross-connection	m	0.1	0.6
$h_e$	Short-circuiting threshold water level	m	0.15	0.3
$K$	Hydraulic conductivity	m/h	1.8	18
$d_{filt}$	Filter depth	m	0.3	0.6
$Rho_{media}$	Bulk density	$g/m^3$	1	1.75
$K1$	Constant of NH4N adsorption for plug-flow	-	0.35	1
$K2$	Constant of NH4N adsorption for short-circuiting	-	0.35	1
$A1$	Slope of the adsorption isotherm	$m^3/g$	5	100
$A2$	Slope of the adsorption isotherm	$m^3/g$	1	20
$C1$	Threshold between $A1$ and $A2$	$g/m^3$	0.5	5
$di$	Nitrification rate coefficient	-	0.00001	0.025
$Ts$	Seasonal mean temperature	$^{\circ}C$	5	25
$NH4_{background\_D}$	Background NH4N concentration	$g/m^3$	0	5
$Rc$	Rate sensibility	$^{\circ}C$	3.6	28.86

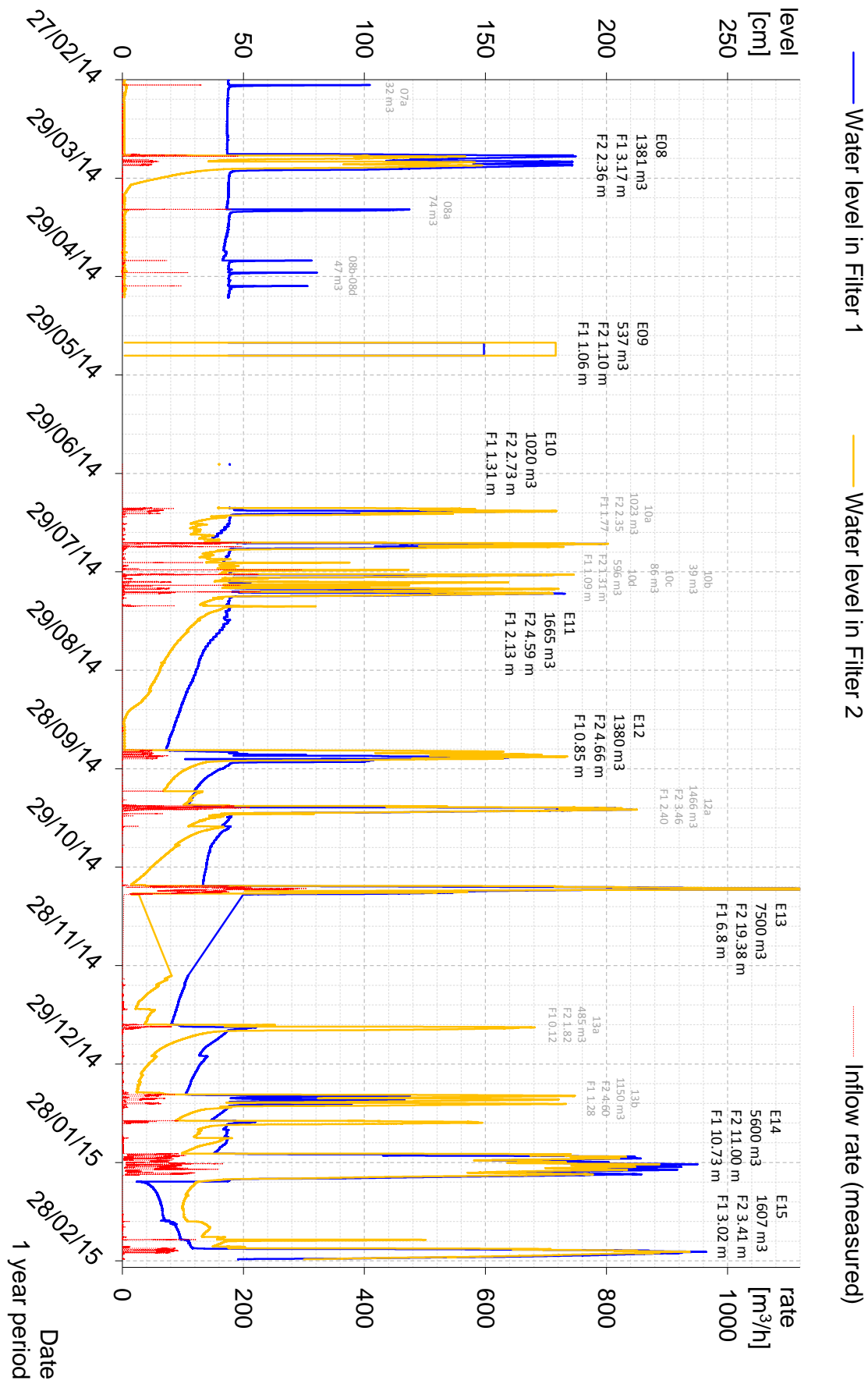


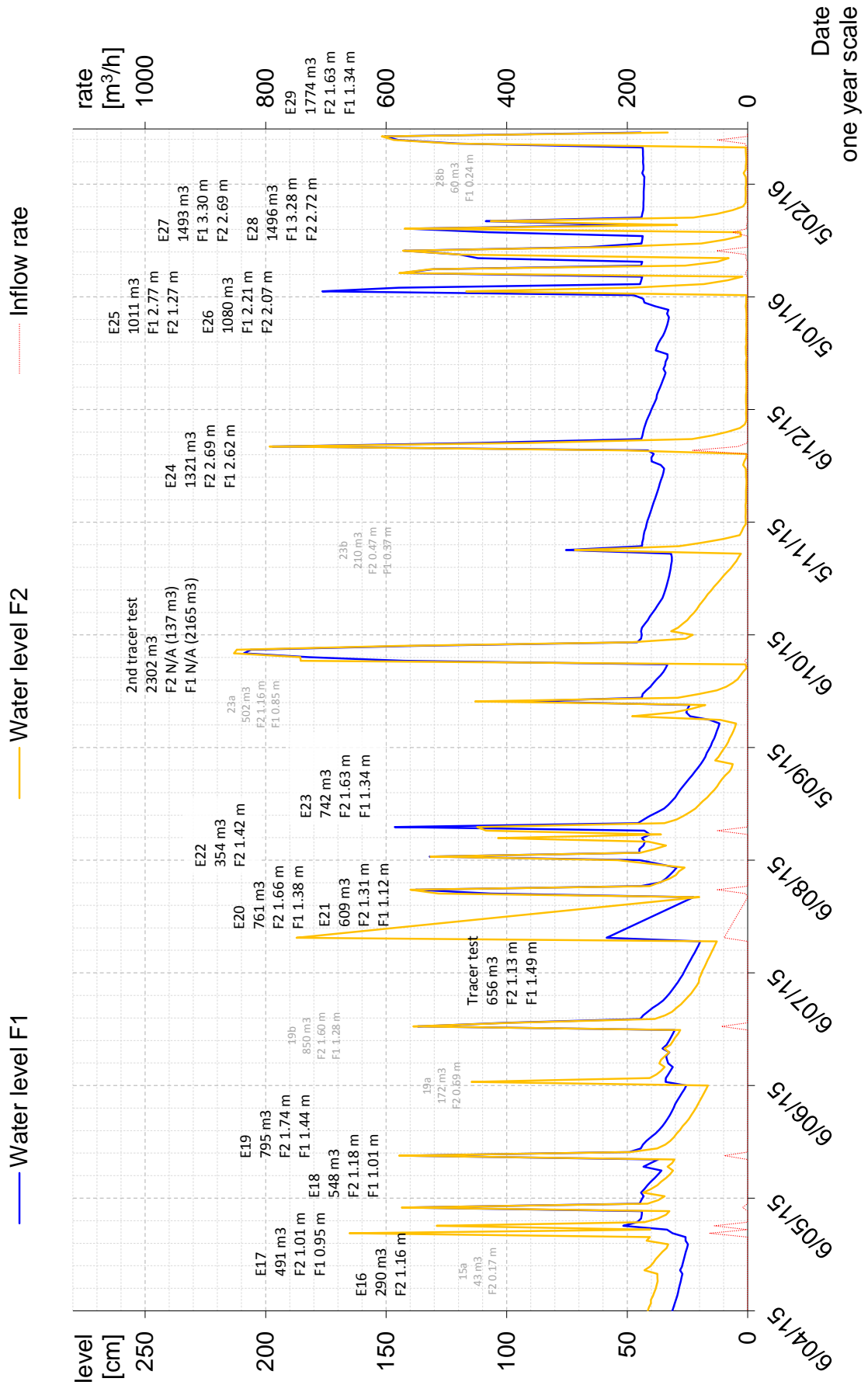
**Annex D:**  
Overview of load events at Marcy l'Etoile













## Research output of the author

Publications written during the PhD studies are written in black.

### Conference presentations

- Pálffy TG, Gourdon R, Troesch S, Molle P: Hydrology and NH<sub>4</sub>-N removal in a CW treating combined sewer overflow. Oral presentation, 15th IWA Specialist Conference on Wetland Systems for Water Pollution Control. IWA/Gdansk University of Technology. Gdansk, Poland, 2016.
- Pálffy TG, Meyer D, Gourdon R, Troesch S, Molle P: Orage: a dynamic design tool for CWs treating combined sewer overflow. Oral presentation, 15th IWA Specialist Conference on Wetland Systems for Water Pollution Control. IWA/Gdansk University of Technology. Gdansk, Poland, 2016.
- Pálffy TG, Gourdon R, Troesch S, Molle P, Meyer D: Orage: design-support modelling of vertical flow CSO CWs. 9th NOVATECH. Planning & technologies for sustainable urban management. Oral presentation, Graie and INSA Lyon, Lyon, France, 2016.
- Pálffy TG, Meyer D, Troesch S, Gourdon R, Molle P: Planted detentive filters [\*CWs] treating combined sewer overflow. Oral presentation, UNESCO EcoHydrology' 2015. UNESCO, IRSTEA, ISA, Lyon 1. Lyon, France, 2015.
- Pálffy TG, Gourdon R, Troesch S, Molle P, Meyer D: Simulation of PDFs [\*CWs] treating urban stormwater. Oral presentation, 6th WETPOL International Symposium on Wetland Pollutant Dynamics and Control. Constructed Wetland Association, York, United Kingdom, 2015.
- Pálffy TG, Meyer D, Stéphane T, Gourdon R, Molle P: Performance of a full-scale CW treating unsettled CSO. Oral presentation, 6th WETPOL International Symposium on Wetland Pollutant Dynamics and Control. Constructed Wetland Association, York, United Kingdom, 2015.
- Pálffy TG, Molle P, Gourdon R, Troesch S, Meyer D: HYDRUS/CW2D simulation of CWs treating Combined Sewer Overflow. Oral presentation, 14th IWA Specialist Conference on Wetland Systems for Water Pollution Control. IWA and Tongji University, Shanghai, China, 2014.
- Pálffy TG, Molle P, Gourdon R, Troesch S, Meyer D: HYDRUS/CW2D simulation of CWs treating Combined Sewer Overflow. Ecotechnologies for the treatment of variable wastewater and stormwater flows. Oral presentation, International workshop, RWTH Aachen University and NIWA, New Zealand. Aachen, Germany, 2014.
- Pálffy TG, Gribovszki Z, Langergraber G: Numerical simulation of the treatment performance of a horizontal flow constructed wetland for polishing SBR effluent. Oral presentation, 5th WETPOL International Symposium on

Wetland Pollutant Dynamics and Control. Ecole des Mines de Nantes and GEPEA, Nantes, France, 2013.

Pálffy TG, Langergraber G: Simulation of constructed wetland microcosms using the HYDRUS wetland module. Oral presentation, 5th WETPOL International Symposium on Wetland Pollutant Dynamics and Control. Ecole des Mines de Nantes and GEPEA, Nantes, France, 2013.

## Publications

Pálffy TG, Meyer D, Troesch S, Gourdon R, Olivier L, Molle P: Orage: a design-optimization modelling tool for CSO CWs. Core model. (submitted)

Pálffy TG, Gourdon R, Meyer D, Troesch S, Molle P: Orage: a design-optimization modelling tool for CSO CWs. Iterative shell. (submitted)

Pálffy TG, Gourdon R, Meyer D, Troesch S, Olivier L, Molle P: Filling hydraulics and nitrogen dynamics in full-scale CSO CWs. (submitted)

Pálffy TG, Gerodolle M, Gourdon R, Meyer D, Troesch S, Molle P: Performance assessment of a vertical flow constructed wetland treating unsettled CSO. (submitted)

Pálffy TG, Molle P, Langergraber G, Troesch S, Gourdon R, Meyer D (2016): Simulation of constructed wetlands treating combined sewer overflow using HYDRUS/CW2D. *Ecol. Eng.* 87: 340-347.

Pálffy TG, Gribovszki Z, Langergraber G (2015): Design-support and performance estimation using HYDRUS/CW2D: A horizontal flow constructed wetland for polishing SBR effluent. *Water Sci. Technol.* 71(7): 965-970.

Pálffy TG, Langergraber G (2014): The verification of the Constructed Wetland Model No. 1 implementation in HYDRUS using column experiment data. *Ecol. Eng.* 68: 105-115.

Rizzo A, Pálffy TG, Schreiber C, Tondera K, Forquet N: Modelling under varying flows. - In: Tondera K, Chazarenc F, Tanner CC (ed): *Ecotechnologies for the treatment of variable wastewater and stormwater flows* (in edition).

Meyer D, Chazarenc F, Claveau-Mallet D, Dittmer U, Forquet N, Molle P, Morvannou A, Pálffy TG, Petitjean A, Rizzo A, Campà RS, Scholz M, Soric A, Langergraber G (2015): Modelling constructed wetlands: scopes and aims – a comparative review. *Ecol. Eng.* 80:205-213.



